UNIVERSIDADE FEDERAL DO RIO GRANDE DO SUL

INSTITUTO DE CIÊNCIAS BÁSICAS DA SAÚDE

PROGRAMA DE PÓS-GRADUAÇÃO EM CIÊNCIAS BIOLÓGICAS: BIOQUÍMICA

EFEITO DO DITELURETO DE DIFENILA SOBRE AS CÉLULAS NEURAIS DE RATOS JOVENS: VIAS DE SINALIZAÇÃO, HOMEOSTASE DO CITOESQUELETO E NEURODEGENERAÇÃO

Luana Heimfarth

Porto Alegre

2012

UNIVERSIDADE FEDERAL DO RIO GRANDE DO SUL

INSTITUTO DE CIÊNCIAS BÁSICAS DA SAÚDE

PROGRAMA DE PÓS-GRADUAÇÃO EM CIÊNCIAS BIOLÓGICAS: BIOQUÍMICA

EFEITO DO DITELURETO DE DIFENILA SOBRE AS CÉLULAS NEURAIS DE RATOS JOVENS: VIAS DE SINALIZAÇÃO, HOMEOSTASE DO CITOESQUELETO E NEURODEGENERAÇÃO

Luana Heimfarth

Orientadora: Profa. Dra. Regina Pessoa Pureur

Co-orientador: Prof. Dr. João Batista Teixeira da Rocha

Tese apresentada ao programa de Pós-Graduação em Ciências Biológicas-Bioquímica da Universidade Federal do Rio Grande do Sul, como requisito parcial à obtenção do grau de Doutor em Bioquímica.

Porto Alegre

2012

"A dúvida é o principio da sabedoria."

"O começo de todas as ciências é o espanto de

as coisas serem o que são"

Aristóteles

AGRADECIMENTOS

À Regina pela amizade, orientação e dedicação, que foram fundamentais para a realização desse trabalho.

Ao João, pela ajuda durante a realização desse trabalho.

À Samanta pelo apoio e companheirismo de todas as horas.

À Karina, a Natália, Paula pelos bons momentos e risadas de todos os dias

À Priscila, Helen, Tita, Carolina, Carol, Cíntia e Dani pela amizade.

À Jú pela amizade e companheirismo de muitos anos. Obrigada por me ouvir quando eu mais precisava.

Aos bolsistas de iniciação científica Fernanda, Bárbara, Rônan, Ângela, Luíza, Luísa pela amizade, apoio e dedicação nesse tempo que trabalhamos juntos.

Aos colegas e amigos do departamento de bioquímica pelas conversas e risadas.

Aos meus amigos de Novo Hamburgo, que me alegraram e compartilharam bons momentos da minha vida.

Aos amigos da faculdade de Farmácia.

Aos meus tios e primos, que de alguma maneira contribuíram para o meu crescimento pessoal.

A todos os colegas, professores e funcionários do Departamento de Bioquímica que de alguma forma me ajudaram a desenvolver esse trabalho.

Ao CNPq pela bolsa concedida.

Finalmento, agradeço com todo o meu carinho àqueles que desde o ínício de minha vida sempre estiveram comigo, me apoiando, ensinando e não me deixando desistir no primeiro obstáculo: meu pai Celso, minha mãe Carmen e meus irmãos Tales e Tobias. Obrigada por tudo, eu não seria o que sou hoje sem o apoio, amizade e amor de vocês.

ÍNDICE

PARTE I

RESUMO..... **2**

ABSTRACT..... **4**

LISTA DE ABREVIATURAS..... **6**

LISTA DE FIGURAS E TABELAS..... **8**

1. INTRODUÇÃO..... **9**

1.1. Telúrio..... **9**

1.1.1. Ditelureto de difenila..... **10**

1.2. Citoesqueleto..... **13**

1.2.1. Filamentos Intermediários..... **15**

1.2.1.1 Neurofilamentos..... **17**

1.2.1.2 Proteína Glial Fibrilar Ácida..... **18**

1.2.1.3 Vimentina..... **20**

1.3. Fosforilação de proteínas do citoesqueleto..... **21**

1.4. Sinalização celular..... **26**

1.4.1. Cálcio..... **26**

1.4.2. Sistema Glutamatérgico..... **28**

1.4.2.1. Receptores glutamatérgicos ionotrópicos..... **29**

1.4.2.2. Receptores glutamatérgicos ionotrópicos..... **30**

1.4.3. Via das quinases ativadas por mitógenos..... **30**

2. OBJETIVO..... **33**

2.1. Objetivos gerais..... **33**

2.2. Objetivos específicos..... **33**

3. MATERIAIS E MÉTODOS..... **36**

PARTE II

4. ARTIGOS CIENTÍFICOS …… **37**

Capítulo 1: *In vivo* treatment with diphenyl ditelluride induces neurodegeneration in striatum of young rats: implications of MAPK and Akt pathways……. **38**

Capítulo 2: Disrupted cytoskeletal homeostasis, astrogliosis and apoptotic cell death in the cerebellum of young rats injected with diphenyl ditelluride…… **79**

Capítulo 3: Exposure of young rats to diphenyl ditelluride during lactation affects the homeostasis of the cytoskeleton of neural cells of both striatum and cerebellum…… **130**

Resultados adicionais: Efeito da transmissão vertical do ditelureto do difenila sobre o citoesqueleto, MAPK e PKA do córtex cerebral e hipocampo de ratos jovens..... **176**

Capítulo 4: Diphenyl ditelluride induces hypophosphorylation of intermediate filaments through modulation of DARPP-32-dependent pathways in cerebral cortex of young rats…….. **214**

Capítulo 5: Cross-talk among intracellular signaling pathways mediates the diphenyl ditelluride actions on the hippocampal cytoskeleton of young rats…… **229**

PARTE III

5. DISCUSSÃO..... **242**

5.1. Modelo 1: Efeito *in vivo* da administração subcutânea do $(PhTe)_2$ sobre o citoequeleto de ratos jovens..... **244**

5.2. Modelo 2: Efeito do $(PhTe)_2$ transmitido verticalmente (através do leite materno) sobre o citoequeleto de ratos jovens..... **254**

5.3. Modelo 3: Efeitos *in vitro* do ditelureto de fenila sobre o citoequeleto de ratos jovens..... **262**

5.4. Efeito do tipo de exposição ao $(PhTe)_2$ sobre a fosforilação dos FIs neuronais e gliais em diferentes estruturas cerebrais..... **274**

6. CONCLUSÃO..... **278**

6.1. Conclusão geral..... **278**

6.2. Conclusão específica..... **278**

8. PERSPECTIVAS..... **281**

9. REFERÊNCIAS BIBLIOGRÁFICAS..... **282**

PARTE I

RESUMO

O telúrio é um elemento raro usado como componente industrial de muitas ligas. Estudos *in vivo* e *in vitro* demonstraram que compostos orgânicos do telúrio são neurotóxicos, entre eles podemos destacar o ditelureto de difenila [$(PhTe)_2$]. Os efeitos provocados por esse organotelureto nos diferentes sistemas são importantes, no entanto, os observados no SNC são particularmente marcantes. Relatos têm demonstrado que o $(PhTe)_2$ pode causar alterações no estado de fosforilação dos filamentos intermediários (FIs) neuronais e gliais, sendo os neurônios e astrócitos importantes alvos desse neurotoxicante. Considerando que o citoesqueleto é um importante alvo de neurotoxinas, nosso trabalho estudou o efeito do $(PhTe)_2$ sobre alguns parâmetros bioquímicos do citoesqueleto neural. Ratos submetidos a uma injeção subcutânea de $(PhTe)_2$ apresentaram alteração na fosforilação e/ou expressão das subunidades dos neurofilamentos (NF-H, NF-M e NF-L), da GFAP e da vimentina, bem como ativação das vias das MAPK e da PKA. Essas modificações são dependentes da estrutura estudada (cerebelo ou estriado) e da idade do animal. Além disso, uma única administração de $(PhTe)_2$ em ratos jovens provocou morte neuronal e astrogliose. Quando o $(PhTe)_2$ é administrado nas ratas mães durante os primeiros 14 dias de lactação verificamos que ocorre uma modificação no sistema fosforilante associado aos FIs nos filhotes, novamente de uma maneira estrutura (córtex cerebral, hipocampo, estrido ou cerebelo) e idade dependente. Além disso, verificou-se que esse organocalcogênio injetado nas ratas mães também age sobre as vias das MAPK e da PKA. Estudos in vitro mostraram que esse composto orgânico do telúrio causa hipofosforilação dos FIs neuronais e gliais no córtex cerebral. Esse efeito é mediado por alteração homeostase do cálcio e do glutamato, bem como pela inibição da PKA,

alteração da fosforilação da proteína DARPP-32(Thr34) e ativação da PP1. No hipocampo temos uma ativação dos receptores glutamatérgicos ionotrópicos e metabotrópicos, acarretando uma alteração na homeostase do cálcio e ativação da PKC, PKCaMII e via das MAPK, conduzindo a um aumento de fosforilação dos FIs neuronais e gliais. Nossos resultados mostraram, portanto, que o $(PhTe)_2$ altera a homeostase do citoesqueleto cerebral e que essa modificação é dependente do desenvolvimento do animal, da estrutura cerebral estudada, bem como da maneira de contato com esse neurotoxicante. Além disso, verificou-se o envolvimento de várias vias de sinalização nas ações desencadeadas pelo composto orgânico do telúrio sobre os FIs, estando elas muitas vezes interligadas. Esses resultados podem contribuir para o melhor entendimento dos mecanismos envolvidos em uma intoxicação com compostos de telúrio, sendo que o desequilíbrio do citoesqueleto pode estar associado à neurotoxicidade desse organotelureto.

ABSTRACT

Tellurium is a rare element used as a component of many industrial alloys. In vivo and in vitro studies have demonstrated that organic tellurium compounds are neurotoxic. We can highlight the organic coumpoud diphenyl ditelluride [$(PhTe)_2$]. The effects caused by this organoteluride in different systems are important, however, the effects observed in the CNS are particularly striking. Reports have shown that $(PhTe)_2$ can induces changes in the phosphorylation state of neuronal and glial intermediate filaments (IFs). The neurons and astrocytes are important targets of this neurotoxin. Considering that the cytoskeleton is an important target for neurotoxins, the aim of the present study was studied the effect of $(PhTe)_2$ on some biochemical parameters of the neural cytoskeleton. Rats treated with a single subcutaneous (s.c.) injection of $(PhTe)_2$ showed changes in the phosphorylation and / or expression of neurofilament subunit (NF-H, NF-M and NF-L), GFAP and vimentin, as well as activation of the MAPK pathway and PKA. These changes are dependent on the structure studied (cerebellum or striatum) and age of the animal. Furthermore, a single administration $(PhTe)_2$ in young rats caused neuronal death and astrogliosis. When $(PhTe)_2$ is administered in dams during the first 14 days of lactation we observed a change in the phosphorylating system associated with IFs in pups. This effect is dependent of the structure studied and the developmental stages of the pups. Furthermore, it was found that $(PhTe)_2$ is administered in dams during the first 14 days of lactation also acts on the MAPK pathway and in the PKA. In vitro studies showed that the organic tellurium causes hipophosphorylation of the neuronal and glial IFs proteins in the cerebral cortex. This effect is mediated by change in calcium and glutamate homeostasis, inhibition of PKA, desphosphorylation of the protein DARPP-32 (Thr34) and activation of PP1. In the

hippocampus have an activation of ionotropic and metabotropic glutamatergic receptors, causing an alteration in calcium homeostasis and activation of PKC, PKCaMII and MAPK pathway, leading to increased phosphorylation of neuronal and glial IFs. The results of this work showed that the (PhTe)2 changes cytoskeletal homeostasis in brain. This modification is dependent of the animal development, the brain structure studied, as well as the way of contact with the neurotoxin. Moreover, there is the involvement of different signaling pathways in the action of (PhTe)2 and they are often interconnected. These results may contribute to a better understanding of mechanisms involved in intoxication with tellurium compounds. The imbalance of the cytoskeleton may be associated with neurotoxicity of this organochalcogenide.

LISTA DE ABREVIATURAS

AMPc	Adenosina 5`-monofosfato ciclíco
AMPA	(R,S)α-amino-3-hydroxy-5-methyl-4-isoxazolepropionate
CCVD	Canal de cálcio voltagem dependente
CDK5	Proteína quinase dependente de ciclina 5
DARPP32	Fosfoproteína regulada por Dopamina e AMP cíclico
ERK1/2	Quinase regulada por sinal extracellular 1/2
FI	Filamento Intermediário
GFAP	Proteína Glial Fibrilar Ácida
(H_2Te)	Telureto de hidrogênio
iGluR	Receptor glutamatérgico ionotrópico
ip	Intraperitoneal
IP_3	Inositol-1,4,5-trifosfato
KA	Cainato
JNK	c-Jun amino-terminal quinase
MAPK	Quinases ativadas por mitógeno
MF	Microfilamento
mGluR	Receptor glutamatérgico metabotrópico
MT	Microtúbulo
NeuN	Proteína nuclear específica de neurônios
NF	Neurofilamento

NF-H	Subunidade protéica de 200 kDa dos neurofilamentos
NF-L	Subunidade protéica de 68 kDa dos neurofilamentos
NF-M	Subunidade protéica de 150 kDa dos neurofilamentos
NMDA	N-methil-D-aspartato
$(PhSe)_2$	Disseleneto de Difenila
(PhTe)2	Ditelureto de Difenila
Pi	Iodeto de propídeo
PKA	Proteína quinase A
PKC	Proteína quinase C
PKCaMII	Proteína quinase dependente de cálcio e calmodulina II
PLC	Fosfolipase C
PP1	Proteína fosfatase 1
PP2a	Proteína fosfatase 2a
PP2b	Proteína fosfatase 2b
RE	Retículo endoplasmático
RNAm	Ácido ribonucleico mensageiro
Ry	Receptor rianoidina
SNC	Sistema Nervoso Central
SNP	Sistema Nervoso Periférico
sc	Subcutânea
vim	Vimentina

LISTA DE FIGURAS E TABELAS

Figura 1	Estrutura do ditelureto de difenila.....	**11**
Figura 2	Representação esquemática dos constituintes do citoesqueleto	**14**
Figura 3	Representação esquemática da estrutura da subunidade de um FI	**15**
Figura 4	Classificação e ocorrência dos FIs humanos.....	**16**
Figura 5	Processos celulares que ocorrem no cérebro nos quais a GFAP desempenha um papel importante.....	**19**
Figura 6	Representação esquemática do sistema de fosforilação de proteínas e alguns dos agentes regulatórios.....	**22**
Figura 7	Esquema mostrando a fosforilação das subunidades dos NFs (NF-L, NF-M e NF-H) realizada por várias proteínas quinases nas regiões amino- e carboxi-terminal.....	**24**
Figura 8	Sítios fosforilados PKA, PKC, PKCaMII na região amino-terminal da vimentina.....	**25**
Figura 9	Representação esquemática de diversas funções celulares mediadas pelo cálcio.....	**27**
Figura 10	Cascata de sinalização conduzindo a ativação das MAPK.....	**31**
Figura 11	Efeito do $(PhTe)_2$ administrado subcutaneamente em ratos de 15 dias sobre a fosforilação dos FIs gliais e neuronais 3 dias após o contato com a droga.....	**245**
Figura 12	Padrões dos maiores tipos de oscilações das concentrações intracelulares de cálcio.....	**266**
Figura 13	Figura representativa da ativação/inibição da DARPP-32.....	**268**
Tabela 1	Efeito administração subcutânea de $(PhTe)_2$ em ratos de 15 dias sobre a fosforilação dos FIs neuronais e gliais em diferentes estruturas cerebrais 3 ou 6 dias após a injeção.....	**274**
Tabela 2	Efeito da administração subcutânea de $(PhTe)_2$ nas mães durante os primeiros 14 dias de lactação (P0-P13) sobre a fosforilação dos FIs neuronais e gliais em diferentes estruturas cerebrais nos os filhotes de 15, 21, 30 ou 45 dias de idade.....	**275**
Tabela 3	Efeito do tratamento *in vitro* $(PhTe)_2$ sobre a fosforilação dos FIs neuronais e gliais no córtex cerebral e hipocampo de animais de 9, 15 e 21 dias de idade.....	**276**

1. INTRODUÇÃO

1.1. TELÚRIO

O telúrio pertence ao grupo XVI da tabela periódica, ou seja é um calcogênio assim como o oxigênio, enxofre, selênio e polônio. Esse elemento foi descoberto em 1782 pelo químico Frans-Joseph Mueller von Reichenstein, que estava estudando um minério contendo ouro (Cooper, 1971). O telúrio é um elemento raro, não essencial e em muitos casos tóxico. Pouco é conhecido a respeito da toxicidade do telúrio nos humanos, provavelmente porque o contato com compostos contendo essa substância são raros (Ba *et al.*, 2010). As características clínicas de uma toxicidade aguda ao telúrio incluem gosto metálico, náuseas, vômito, mucosa oral e pele escura e odor de alho (Yarema and Curry, 2005).

Compostos de telúrio são usados ou produzidos em processos industriais, por exemplo, na produção de aço e no refino eletrolítico de metais pesados. Esse elemento é empregado também na manufatura de semicondutores, na indústria de componentes eletrônicos, síntese de fármacos e explosivos, na vulcanização da borracha, em lubrificantes sólidos, na petroquímica, entre outros (Clayton e Clayton, 1981; Taylor, 1996). Além disso, estudos têm demonstrado que futuramente compostos de telúrio poderão ser utilizados no estudo de proteínas e enzimas, como biomarcadores (na forma de CdTe fluorescente) e serem agentes de antibióticos e de drogas contra o câncer (Ba *et al.*, 2010; Sredni, 2011).

O telúrio é ocasionalmente encontrado na forma nativa, mas na maioria das vezes está na forma de telureto de ouro, a calaverita, ou combinado com outros metais. Ele existe na forma elementar (Te^0), inorgânica (por exemplo o TeO_2) e orgânica (por

exemplo o ditelureto de difenila) (Cooper, 1971). A toxicidade deste calcogênio está associada ao composto específico, ou seja, depende da forma química em que esse elemento é encontrado, inorgânica ou orgânica, e em alguns casos depende também do estado de oxidação. Isso pode ocorrer devido às diferentes propriedades farmacológicas e farmacocinéticas desses compostos e de seus metabólitos dentro do corpo humano (Ba et al., 2010). Embora o telúrio seja considerado um metalóide tóxico, alguns organoteluretos podem agir como imunomoduladores, drogas anti-tumorais (Engman *et al.*, 2000; Engman 2003), bem como antioxidantes (Rossato *et al.*, 2002; Savegnago *et al.*, 2006).

Tanto as formas orgânicas quanto as inorgânicas do telúrio são tóxicas para o SNC de roedores (Maciel *et al.*, 2000; Nogueira *et al.*, 2001; Widy-Tyszkiewicz *et al.*, 2002). Além disso, é descrito que a forma metálica desse composto pode causar lipofuccinose cerebral em ratos adultos (Duckett and White, 1974). Compostos de telúrio inibem a enzima escaleno monooxigenase, inibindo, portanto, a síntese de colesterol e provocando uma desmielinização transitória do sistema nervoso periférico. Isso provavelmente ocorre, pois esses compostos interagem com os resíduos cisteinil das proteínas (Laden e Porter, 2001)

1.1.1. DITELURETO DE DIFENILA

O ditelureto de difenila [$(PhTe)_2$] é um composto orgânico do elemento telúrio, cuja fórmula está representada na Figura 1. Há estudos mostrando que essa substância é capaz de alterar a funcionalidade de vários sistemas fisiológicos, como o sistema nervoso central (Heimfarth et al., 2008; Souza et al, 2011; Stangherlin et al., 2009), hematológico (Borges *et al.*, 2007; Schiar *et al.*, 2007), pulmonar (Pinton *et al.*, 2011b).,

2011), renal e hepático (Borges et al., 2007; Meotti et al., 2003), bem como afetar o desenvolvimento embrionário e fetal (Roman *et al.*, 2007).

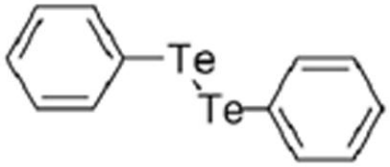

Ditelureto de difenila

Figura 1: Estrutura do ditelureto de difenila. Adaptado de Borges *et al.*, 2005.

Os efeitos neurotóxicos deste organotelureto são bem descritos na literatura. O $(PhTe)_2$ causa efeitos tóxicos marcantes ao SNC de roedores tanto após uma exposição aguda ou prolongada, quanto, quando injetado por via subcutânea ou intraperitoneal (Maciel et al., 2000; Meotti et al., 2003; Nogueira et al., 2001). Relatos têm demonstrado que ele pode modificar a funcionalidade do sistema glutamatérgico *in vivo* e *in vitro*, sendo capaz de alterar a homeostase do glutamato. Essa alteração do sistema glutamatérgico é dependente da idade do animal (Nogueira *et al.*, 2001; Souza *et al.*, 2010). Além disso, a exposição vertical, ou seja, através do leite materno a esse composto pode causar mudanças neurocomportamentais e danos cognitivos na prole (Stangherlin *et al.*, 2006; Stangherlin *et al.*, 2009). Segundo Maciel *et al.*, 2000, o tratamento de camundongos com $(PhTe)_2$ revelou alterações histológicas acentuadas no cérebro. Estudos *in vitro* com esse composto mostraram que ele é capaz de afetar a atividade de enzimas importantes para o funcionamento do SNC, como a Na^+, K^+ - ATPase cerebral, que é inibida por ele de maneira dependente da concentração (Borges *et al.*, 2005). Os danos neurotóxicos causados pelo $(PhTe)_2$ podem estar relacionados,

pelo menos em parte, com alterações na função dos canais de cálcio, ou seja, por mudanças na homeostase desse importante segundo mensageiro celular (Moretto *et al.*, 2007). Em relação ao sistema fosforilante associado ao citoesqueleto, esse organocalcogênio induz um aumento da atividade *in vitro* de quinases que levam à hiperfosforilação de proteínas do citoesqueleto em fatias de córtex cerebral de ratos jovens (Funchal et al., 2006; Moretto et al., 2005).

O $(PhTe)_2$ pode causar danos oxidativos no tecido pulmonar, levando a uma provável toxicidade ao sistema respiratório (Pinton *et al.*, 2011b). Além disso, afeta a as enzimas aspartato aminotransferase (AST) e alanina aminotransferase (ALT), bem como aumenta os níveis de creatinina sérica, caracterizando dano hepático e renal respectivamente (Meotti *et al.*, 2003). Schiar et al. (2007) demonstraram que esse organocalcogênio afeta o sistema hematológico, pois causa hemólise dos eritrócitos. Além disso, há relatos de leucocitose, com presença de células mononucleares atípicas em ratos tratados com $(PhTe)_2$ (Borges *et al.*, 2007).

O átomo de telúrio presente em compostos orgânicos é facilmente oxidado, o que torna estas substâncias aptas a agirem como antioxidantes, portanto, compostos orgânicos de telúrio, provavelmente, são capazes de proteger proteínas e lipídios contra o estresse oxidativo em vários sistemas (Kanski *et al.*, 2001). O $(PhTe)_2$ reduz a peroxidação lipídica induzida por cloreto férrico e oxalato (Pinton et al., 2011a; Puntel et al., 2007). Além disso, diminui a carbonilação de proteínas induzida por nitroprussiato de sódio, bem como pode agir como *scavanger* de radicais livres (Pinton *et al.*, 2011a), mostrando assim que essa droga apresenta propriedades antioxidantes. Entretanto, devido as suas características tóxicas, o risco-benefício desse composto não é compensador.

O citoesqueleto cerebral é uma importante estrutura celular que tem sua organização e dinâmica alteradas por neurotoxinas, entre elas o $(PhTe)_2$. Esse composto modifica a funcionalidade do citoesqueleto cerebral, causando efeitos neurotóxicos ao sistema (Heimfarth *et al.*, 2008).

1.2. CITOESQUELETO

Para que as células funcionem adequadamente elas devem se organizar no espaço, interagir mecanicamente com o ambiente ao seu redor, apresentar uma conformação correta, ser fisicamente robustas e estar estruturadas de forma adequada internamente. Muitas células devem também ser capazes de modificar sua forma e migrar para outros locais. Além disso, toda a célula deve ser capaz de reorganizar seus componentes internos como decorrência dos processos de crescimento, divisão e/ou adaptação à mudança no ambiente. Todas essas funções estruturais e mecânicas apresentam-se altamente desenvolvidas em células eucarióticas, sendo dependentes de um extraordinário sistema de filamentos denominado citoesqueleto (Alberts et al., 2008).

As proteínas do citoesqueleto têm papel fundamental na criação e manutenção da forma celular de neurônios e astrócitos, participam da manutenção do calibre axonal, bem como do transporte de organelas e substâncias envolvidas na transmissão sináptica (Kirkpatrick e Brady, 1999; Ackerley *et al.*, 2000). Essa rede proteica é um importante alvo para mecanismos de transmissão de sinais a partir de receptores de membrana plasmática, levando a uma resposta celular apropriada. Além disso, está envolvida na organização e reorganização dos receptores de membrana, sendo essencial para os mecanismos de reconhecimento celular (Carraway, 2000), bem como para a modulação

da viabilidade celular através do processo de apoptose (Ndozangue-Touriguine *et al.*, 2008).

As diferentes atividades do citoesqueleto dependem de três tipos de filamentos proteicos: filamentos de actina ou microfilamentos (MF), microtúbulos (MT) e filamentos intermediários (FI) (Figura 2). Cada tipo é formado pela polimerização de monômeros específicos (Carraway, 2000; Alberts et al., 2008). Os três tipos de filamentos do citoesqueleto são conectados entre si e suas funções são coordenadas, permitindo a participação em inúmeras atividades celulares em conjunto com diversas proteínas acessórias (Bear et al., 2002; Alberts et al., 2008).

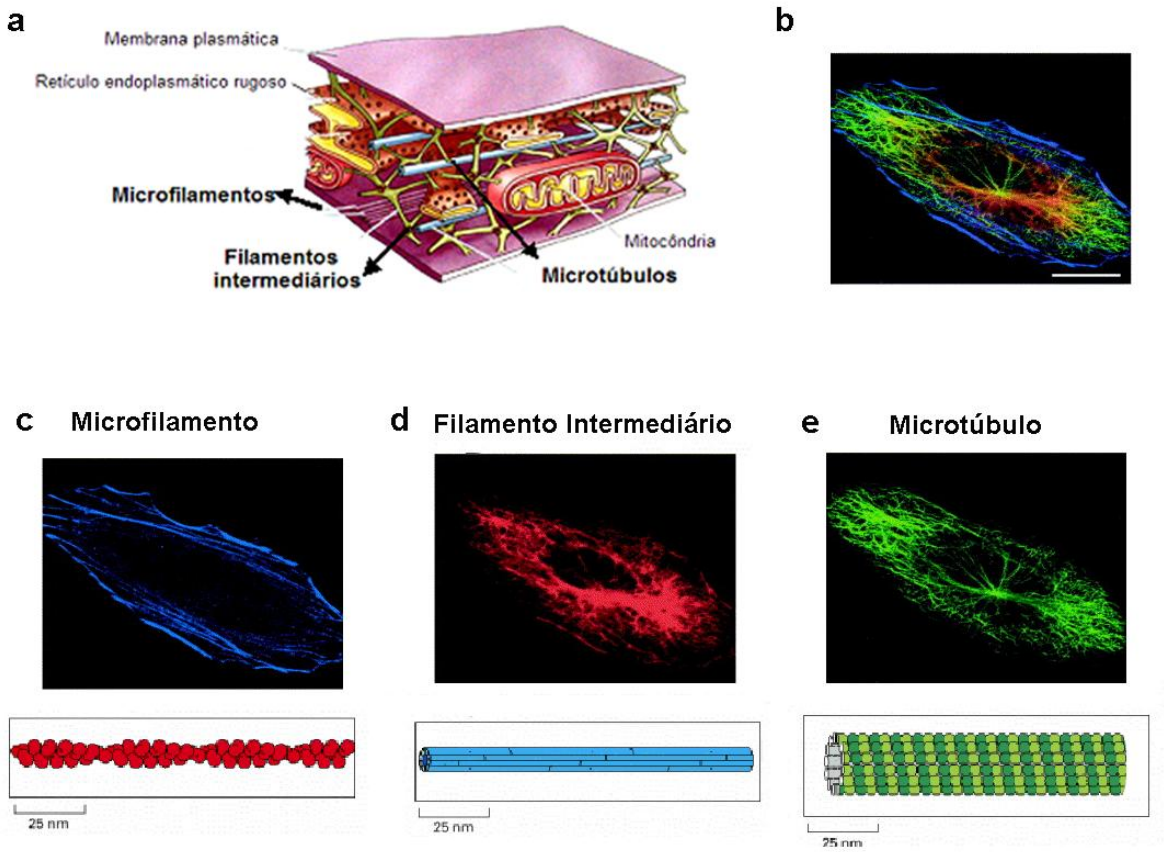

Figura 2. Representação esquemática dos constituintes do citoesqueleto (a, b). Faloidina marcando microfilamentos (azul) (b,c), anti-queratina 8/queratina 18 para visualizar os filamentos intermediários (vermelho) (b,d), anti-tubulina para marcar

microtúbulo (verde) (b,e),. A sobreposição das imagens pode ser visualizada em (b). Adaptado de Omary *et al.*, (2006); Alberts *et al.*, (2008) e www.mie.utoronto.ca/labs/lcdlab/biopic, acessado em 23.02.2011.

1.2.1 FILAMENTOS INTERMEDIÁRIOS

Os filamentos intermediários (FIs) são filamentos longos com um diâmetro em torno de 10 nm, intermediário entre os filamentos de actina (7 nm) e os microtúbulos (25 nm). São polímeros de subunidades fibrosas (Alberts *et al.*, 2008) codificadas por uma das maiores famílias de genes no genoma humano (Hesse *et al.*, 2001). Apresentam um domínio central em α-hélice altamente conservado e regiões amino- e carboxi-terminal variáveis (Figura 3), com diferenças que permitem a classificação dos FI em seis subtipos diferentes. (Fuchs and Weber, 1994; Elder *et al.*, 1999; Herrmann e Aebi, 2000; Inada *et al.*, 2000; Lariviere and Julien, 2004) (Fuchs and Cleveland, 1998; Lariviere and Julien, 2004). A figura 4 ilustra a ocorrência e a classificação dos FIs em humanos.

Figura 3: Representação esquemática da estrutura da subunidade de um FI. Adaptado de Kim et al., 2012.

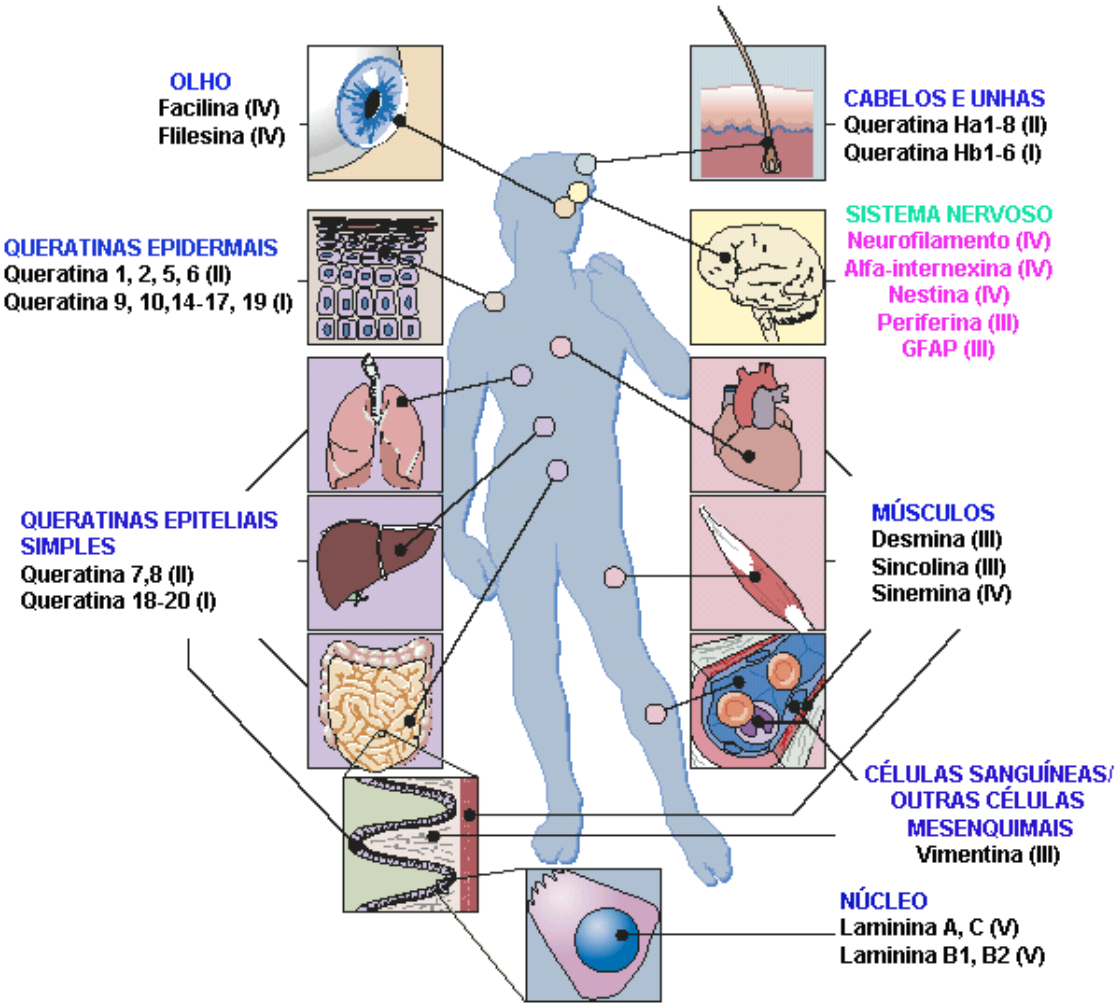

Figura 4: Classificação e ocorrência dos FIs humanos. Os algarismos em romano indicam a família de FI a qual a proteína pertence. Adaptado de Toivola et al., 2005.

Inicialmente os FIs eram considerados estruturas bastante estáticas e rígidas, com funções relacionadas à integridade estrutural de células e tecidos (Chou et al., 1997; Coulombe et al., 2000; Fuchs and Cleveland, 1998; Omary and Ku, 1997). De fato, o papel do FI em conferir resistência mecânica é muito relevante e a consequente perda dessa função pode estar relacionada com doenças envolvendo a fragilidade celular (Fuchs and Cleveland, 1998; Omary *et al.*, 2004). Entretanto, nos últimos anos as

funções atribuídas aos FIs têm ampliado drasticamente, pois os mesmos têm sido relacionados a uma variedade de eventos celulares. Eles desempenham papel ativo no transporte de sinais da periferia celular para o núcleo (Chang e Goldman, 2004; Paramio e Jorcano, 2002), estão envolvidos na motilidade (Eckes *et al.*, 1998; Helfand *et al.*, 2003), adesão e migração celular (Ivaska *et al.*, 2007), participam na definição do posicionamento e forma de organelas (Toivola *et al.*, 2005) e na modificação de vários processos celulares devido a sua habilidade de regular moléculas de sinalização (Pallari e Eriksson, 2006). Outras funções atribuídas aos FIs são a capacidade de agir como proteínas adaptadoras em vias de sinalização, bem como estarem envolvidos no crescimento e regeneração das células (Kim e Coulombe, 2007). Além disso, diversos trabalhos descrevem alterações dos FIs em resposta a injúrias e nos processos de reparo tecidual, câncer e outras doenças (DePianto e Coulombe, 2004; Kuchma et al., 2012).

1.2.1.1 Neurofilamentos

Os neurofilamentos (NFs) são FIs importantes na fisiologia neuronal, sendo o principal componente do citoesqueleto dos neurônios maduros. São formados pela polimerização de três subunidades: os NFs de baixo (NF-L; 68 KDa), médio (NF-M; 150 KDa) e alto peso molecular (NF-H; 200 KDa) (Alberts et al., 2008). A extremidade amino-terminal juntamente com a região em α-hélice da subunidade NF-L interagem lateralmente e longitudinalmente formando a estrutura propriamente dita do NF, (Geisler e Weber, 1981), enquanto que as regiões carboxi-terminais das subunidades NF-M e NF-H são responsáveis pelas projeções laterais, que permitem a interação dos NFs entre si e com os demais constituintes do citoesqueleto (Hisanga e Hirokawa, 1988; Gotow *et al.*, 1992; Kirkpatrick e Brady, 1999). Originalmente se assumia que os NFs

eram compostos apenas pelas subunidades NF-L, NF-M e NF-H, porém estudos recentes indicam que outras proteínas como a α-internexina, no SNC, e a periferina, no SNP, também se associam com os NFs, participando da formação do FI neuronal (Beaulieu *et al.*, 1999b; Yuan *et al.*, 2006).

A principal função atribuída aos NF é a manutenção do calibre axonal e consequentemente o aumento da velocidade de condução do impulso elétrico, processo esse regulado por fosforilação. Além disso, os NFs também contribuem para as propriedades dinâmicas do citoesqueleto axonal durante a diferenciação neuronal e para o crescimento, a regeneração e a orientação dos axônios (Nixon e Shea, 1992). Eles são formados dentro do corpo celular e posteriormente transportados para o axônio, sendo a fosforilação do domínio carboxi-terminal um importante mecanismo regulatório do transporte axonal (Jung *et al.*, 2000).

Acúmulo anormal de NFs é descrito em várias doenças neurodegenerativas, tais como: esclerose lateral amiotrófica, doença de Parkinson, doença de Alzheimer (Al-Chalabi e Miller, 2003; Liu et al.; Liu et al., 2004) e em neuropatias tóxicas (Zhu *et al.*, 1998), sendo considerado, em muitos casos, um marcador dessa disfunção neuronal (Su *et al.* 2012). Ainda não é compreendido como esse acúmulo de NFs contribui para o processo neurodegenerativo nessas doenças, mas sugere-se que o transporte dos NF esteja interrompido nos neurônios afetados (Ackerley *et al.*, 2000; Lariviere and Julien, 2004).

1.2.1.2 Proteína Glial Fibrilar Ácida

A proteína glial fibrilar ácida (GFAP) é uma proteína estrutural de 50 KDa sintetizada nos astrócitos e algumas células de Schwann (Guo-Ross et al., 1999; Kaneko et al., 1995; Kosako et al., 1997). A GFAP é considerada marcador de

astrócitos e é importante na modulação da motilidade e forma celular por fornecer estabilidade estrutural aos astrócitos. Além disso, esse FI é importante para a interação astrócito-neurônio (McCall et al., 1996; Eliasson et al., 1999), participando do sofisticado sistema de comunicação intercelular recíproca que pode regular a liberação de neurotransmissores, a excitabilidade neuronal e a transmissão sináptica (Carmignoto, 2000). A figura 5 mostra processos celulares nos quais a GFAP desempenha um papel importante.

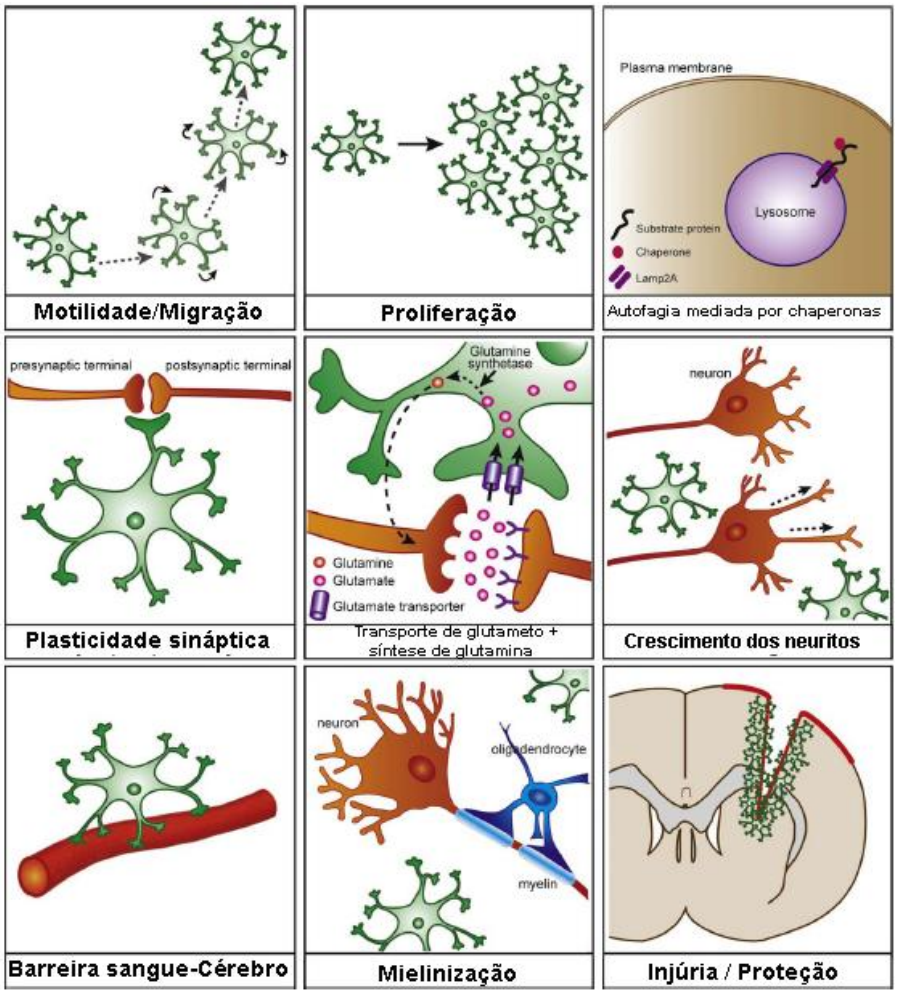

Figura 5: Processos celulares que ocorrem no cérebro nos quais a GFAP desempenha um papel importante. Adaptado de (Middeldorp e Hol 2011).

No SNC, após uma injúria, os astrócitos tornam-se reativos e respondem de uma maneira típica denominada astrogliose, que é caracterizada por uma rápida síntese de GFAP (Eddleston e Mucke, 1993), sendo essa proteína, em muitos casos, um marcador de neurotoxicidade. Mudanças na expressão de GFAP podem alterar a morfologia dos astrócitos, o qual pode afetar indiretamente outros tipos celulares e a estrutura do cérebro (Middeldorp e Hol, 2011). Uma intensa gliose reativa é verificada em doenças como esclerose múltipla (Hallpike et al., 1983), adrenoleucodistrofia (Schaumburg et al., 1975) e doença de Alexander (Eng et al., 1998).

1.2.1.3 Vimentina

Entre as proteínas dos filamentos intermediários, a vimentina é a mais amplamente distribuída, ocorrendo em muitas células de origem mesenquimal. Além disso, é expressa de forma transitória durante o desenvolvimento em muitos tecidos (Alberts et al., 2008). No SNC, é expressa na glia radial, astrócitos imaturos e também na glia de Bergmann no cerebelo. Durante a diferenciação dos astrócitos é substituída progressivamente por GFAP (Menet et al., 2001). Essa proteína, juntamente com a GFAP, participa do processo de gliose reativa após injúria no SNC (Menet et al., 2001; Pekny et al., 1999).

A vimentina desempenha uma função importante na integridade estrutural de células e tecidos (Nieminen et al., 2006), na adesão e migração (Gonzales et al., 2001; Homan et al., 1998; Tsuruta and Jones, 2003; Kreis et al., 2005), na transdução de sinal (Janosch et al., 2000; Ivaska et al., 2005; Perlson et al., 2005; Kumar et al., 2007) e em processos apoptóticos (Yang et al., 2005).

Os FIs sofrem alterações dinâmicas na sua organização citoplasmática durante diferentes estágios do ciclo celular ou em resposta a sinais celulares (Steinert and Roop, 1988; Helfand et al., 2005) sendo a fosforilação um mecanismo central na regulação da organização da rede citoplasmática de FIs (Eriksson e Goldman, 1993).

1.3. FOSFORILAÇÃO DAS PROTEÍNAS DO CITOESQUELETO

A fosforilação proteica é uma modificação pós-traducional importante para as vias de transdução de sinais. Ela afeta processos celulares básicos, que incluem metabolismo, crescimento, divisão e diferenciação celular, motilidade, tráfego de organelas, transporte de membrana, contração muscular, imunidade, memória e aprendizado (Manning et al., 2002a,b).

Essa modificação covalente regula a função das proteínas em resposta a estímulos extracelulares (Nestler e Greengard, 1999). Segundos mensageiros típicos, como AMPc e cálcio, regulam funções neuronais através de alteração no estado de fosforilação de proteínas intracelulares. A fosforilação altera a função da proteína de uma maneira rápida e reversível. O grau de fosforilação de uma proteína alvo reflete um balanço entre as ações contrárias de proteínas quinases e fosfatases, integrando um conjunto de rotas de sinalização celular (Figura 6). Entre os substratos de quinases e fosfatases estão enzimas, receptores de neurotransmissores, canais iônicos e proteínas estruturais (Purves *et al*., 2005).

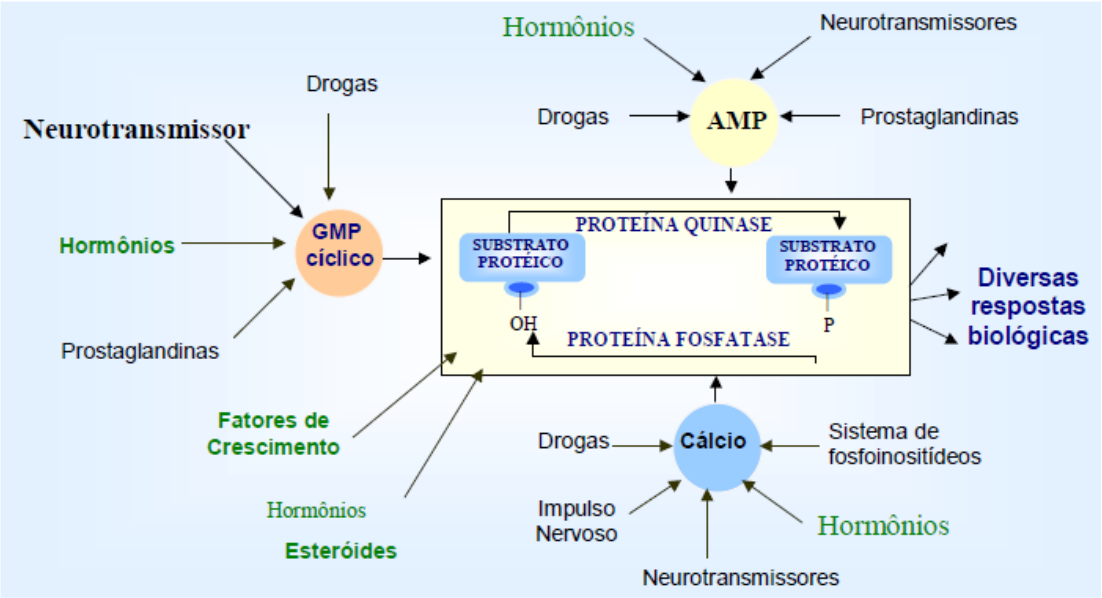

Figura 6: Representação esquemática do sistema de fosforilação de proteínas e alguns dos agentes regulatórios. Adaptado de Nestler e Greengard, 1994.

Os componentes do citoesqueleto estão entre as principais proteínas alvos modificadas em resposta à maioria dos sinais extracelulares que determinam a morfologia neuronal (Sanchez et al., 2000). Nos FIs a fosforilação é o principal mecanismo responsável pela sua modulação, contribuindo na organização e função dos mesmos de maneira célula e tecido-específica (Grant e Pant, 2000; Omary et al., 2006) .

Os FIs são fosforilados na região amino-terminal e carboxi-terminal, como mostrado na figura 7. A fosforilação do domínio amino-terminal está relacionada com a capacidade de associação e desassociação dos FI, sendo controlada por quinases dependentes de segundos mensageiros (Sihag et al. 2007). Já no domínio carboxi-terminal, a fosforilação é realizada por quinases independentes de segundos mensageiros e tem implicações na interação dos FIs com outras estruturas do citoesqueleto (Chou et al., 1997; Grant e Pant, 2000)

Os FIs são substratos de inúmeras serina/treonina quinases, incluindo a proteína quinase C (PKC), a proteína quinase dependente de cálcio e calmodulina (PKCaMII), a proteína quinase dependente de AMPc (PKA), a família das proteínas quinases ativadas por mitógeno (MAPK), a proteína quinase dependente de ciclina 5 (CDK5), entre outras. Estas quinases possuem um papel significativo na regulação da estrutura e associação dos FIs, bem como na interação deles com outras proteínas (Eriksson et al., 2004; Sihag et al., 2007). Além disso, a ação dessas quinases nos FIs é sítio específica, ou seja elas fosforilam um resíduo específico dentro da estrutura proteica (Sihag et al., 2007). Proteínas serina/treonina fosfatases como a proteína fosfatase 1 (PP1), e as proteínas fosfatases 2A (PP2A) e 2B (PP2B ou calcineurina) também desempenham papel importante na regulação do citoesqueleto (Grant e Pant, 2000).

Os NFs são as proteínas mais fosforiladas dos neurônios. O estado de fosforilação dos NFs têm um papel importante no controle da integridade do citoesqueleto, no transporte e no diâmetro axonal (Motil et al., 2006; Sihag et al., 2007; Strack et al., 1997), promove a interação desses FI com as mitocôndrias (Wagner *et al*., 2003), pode modular a função de organelas (Toivola et al., 2005) e protege os NFs da proteólise (Grant e Pant, 2000). Os NFs são altamente fosforilados *in vivo*, porém o grau de fosforilação do NF-M e do NF-H, e especialmente do NF-L, é diferente em cada compartimento neuronal, sendo altamente fosforilados no axônio, mas pouco fosforilado no corpo celular e nos dendritos (Gotow e Tanaka, 1994; Gotow et al., 1994)

A região amino-terminal dos NFs é fosforilada em sítios distintos na NF-L e NF-M. Os maiores sítios de fosforilação dessas subunidades são os resíduo Ser55 na NF-L, fosforilado pela PKA, e Ser 23 na NF-M, fosforilado pela PKC e PKA (Sihag et al., 1990, 1999). Além disso, estudos *in vitro* mostraram que o resíduo Ser57 e Ser51 da

NF-L são substrato da PKCaMII e PKC, respectivamente (Gonda et al., 1990; Hashimoto et al., 2000) (Figura 7).

A fosforilação da região carboxi-terminal das subunidades NF-M e NF-H dos FIs ocorre em uma sequência de repetições de Lisina, Serina e Prolina (KSP *repeats*) (Geisler et al., 1987; Xu et al., 1992; Lee et al., 2002). A fosforilação desses sítios pode ser regulada por cascatas de transdução de sinais disparadas por fatores de crescimento, influxo de cálcio ou neurotoxinas, sendo realizada por quinases direcionadas por prolina, como as quinases ativadas por mitógenos (MAPK) e a quinase dependente de ciclina 5 (CDK5) (Li et al., 1999 a,b; Pierozan et al., 2012) (Figura 7).

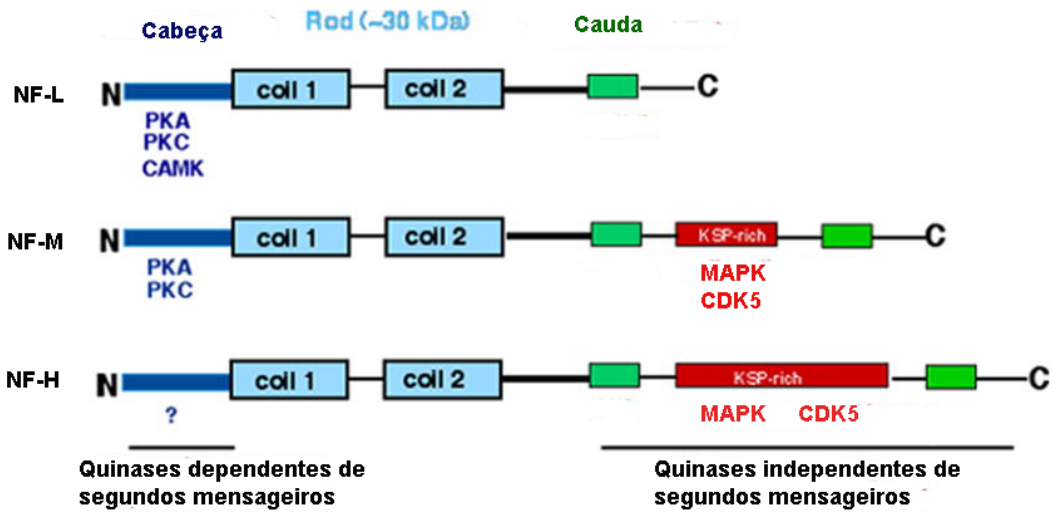

Figura 7: Esquema mostrando a fosforilação das subunidades dos NFs (NF-L, NF-M e NF-H) realizada por várias proteínas quinases nas regiões amino- e carboxi-terminal. Adaptado de Sihag et al., 2007.

Assim como nos NFs, a polimerização da GFAP e da vimentina também é regulada pela fosforilação/desfosforilação do domínio amino-terminal, que contém muitos sítios fosforiláveis (Inagaki *et al*., 1994a; Gohara *et al*., 2001; Takemura *et al*.,

2002). Para a GFAP, 6 diferentes sítios de fosforilação foram identificados: Thr-7, Ser-8, Ser-13, Ser-17 e Ser-34 na região amino-terminal e Ser-389 na região carboxi-terminal (Inagaki et al., 1990; Nakamura et al., 1992; Tsujimura et al., 1994; Sekimata et al., 1996), entretanto pouco se sabe a respeito do papel de cada um deles na associação, organização estrutural e disposição do FI. A fosforilação/desfosforilação da região amino-terminal da GFAP em aminoácidos específicos regula a associação dessa proteína e é importante para a sua distribuição durante o ciclo celular (Ralton et al., 1994, Yasui et al., 1998; Kawajiri et al., 2003). Além disso, sugere-se que a fosforilação da GFAP regula a plasticidade estrutural dos filamentos gliais e eventualmente as funções dos astrócitos e protege a GFAP da degradação (Takemura *et al.*, 2002, Korolainen et al., 2005).

Já a vimentina apresenta vários sítios específicos de fosforilação na região amino-terminal, que estão representados na figura 8. Essa modificação pós traducional nessa proteína parece ter um papel importante na migração celular (Ivaska *et al*., 2005).

Figura 8: Sítios fosforilados pela proteína quinase dependente de AMPc (PKA), proteína quinase C (PKC) e pela proteína quinase dependente de cálcio e calmodulina (PKCaMII) na região amino-terminal da vimentina. Adaptado de Isawa et al., 2006.

1.4. SINALIZAÇÃO CELULAR

A habilidade das células em receber e atuar através de sinais transmitidos a partir da membrana celular é fundamental para a vida de todos os organismos. As várias rotas de sinalização intracelulares ativadas por receptores de superfície diferem em sua complexidade e modo pelo qual ativam sinais, desencadeando assim uma variedade de respostas biológicas. A ligação de moléculas a receptores específicos leva a alterações nos níveis de segundos mensageiros intracelulares, os quais desencadeiam uma série de reações, modificando a atividade de enzimas intermediárias de cascatas de sinalização celular. Este mecanismo é fundamental na propagação e amplificação do sinal iniciado por um ligante extracelular (Cooper et al., 2001; Albert set al., 2008).

1.4.1. CÁLCIO

O cálcio é um importante segundo mensageiro envolvido em várias vias de transdução de sinal. Nas células eucarióticas, a concentração intracelular de cálcio determina o estado fisiológico da célula. Após um estímulo celular, há um aumento da concentração intracelular desse segundo mensageiro a fim de ativar processos dependentes de cálcio, que podem ser comuns a vários tipos celulares como: proliferação, diferenciação, apoptose, ativação de quinases ou fosfatases e transcrição gênica; ou processos específicos para cada tipo celular como a regulação da contração muscular (Berridge et al., 2003). As principais funções do íon cálcio estão representadas na figura 9.

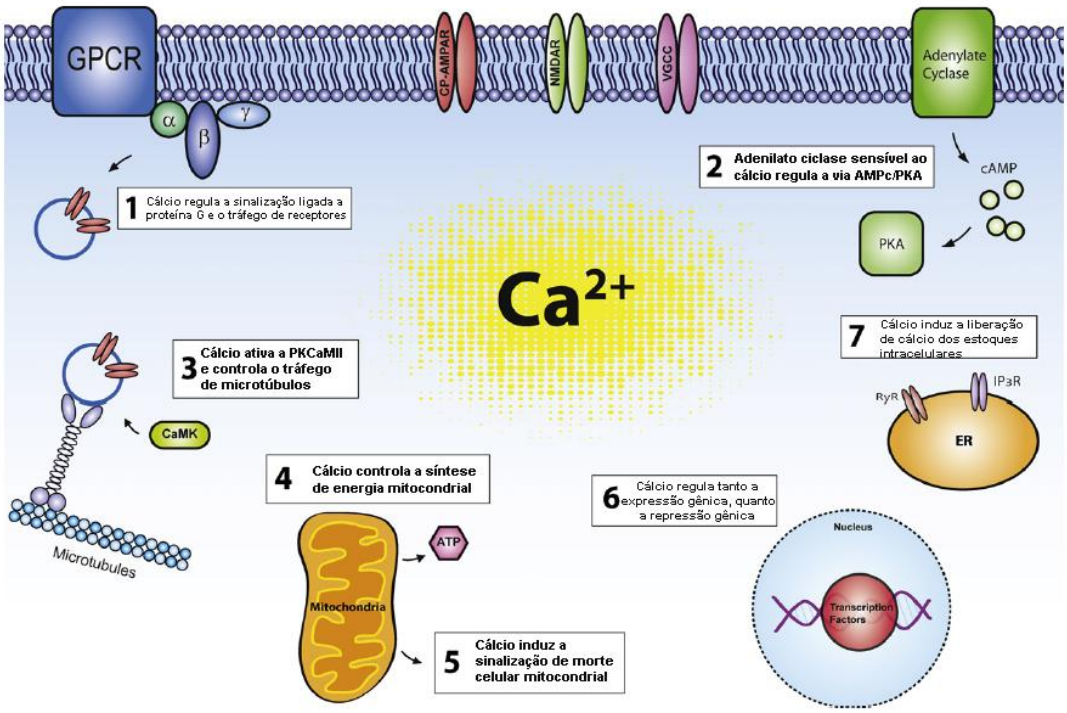

Figura 9: Representação esquemática de diversas funções celulares mediadas pelo cálcio. Adaptada de Seaton et al., 2011a.

Alterações na concentração intracelular de cálcio podem ser decorrentes da ativação de receptores presentes na membrana plasmática ou através da remoção dos estoques intracelulares desse íon. O cálcio pode entrar na célula através dos canais de cálcio dependentes de voltagem (CCVD) ou modulados por ligantes (exemplo, receptor glutamatérgico ionotrópico), assim como através de entrada capacitativa (Burd e Putney, 2006). Após o estímulo dos receptores de membrana, o cálcio pode também ser liberado dos estoques intracelulares presentes principalmente no retículo endoplasmático. Dois importantes receptores que estão envolvidos nesse processo são o receptor inositol-1,4,5-trifosfato (IP3) (Bezprozvanny, 2005; Mikoshiba, 2007) e o receptor rianoidina (Rossi e Sorrentino, 2002; Hamilton, 2005).

Desregulação na homeostase do cálcio pode causar um aumento nos níveis intracelulares desse segundo mensageiro e, consequentemente, morte celular (Siman et al.,1989; Celsi et al., 2009). Quando esse aumento na concentração desse íon está associado à ativação de receptores glutamatérgicos, pode causar excitotoxicidade neuronal (Choi et al., 1987; Tymianski et al., 1993, Pierozan et al.,2012) e eventos mitocondriais apoptóticos (Orrenius et al., 2003). Alteração na homeostase do cálcio está envolvida com várias desordens neurodegenerativas, como doença de Alzheimer, doença de Parkinson e esclerose lateral amiotrófica (Camins et al., 2006; Seaton et al., 2011a,b; Peng et al., 2012).

1.4.2. SISTEMA GLUTAMATÉRGICO

O glutamato é o principal neurotransmissor excitatório do SNC, sendo que 80% a 90% das sinapses do cérebro são glutamatérgicas. Ele é o principal mediador das informações sensoriais, coordenação motora, emoção e cognição, incluindo a formação da memória (Braitenberg e Schüz, 1998; Hassel e Dingledine, 2006). Além disso, o glutamato está envolvido no desenvolvimento de células nervosas, incluindo fenômenos de proliferação, diferenciação, migração e morte celular, assim como no envelhecimento (McDonald e Johnston, 1990; Meldrum, 2000; Segovia et al., 2001). Alterações na homeostase desse neurotransmissor podem desencadear processos tóxicos à célula, fenômeno esse denominado excitotoxicidade glutamatérgica (Olney et al., 1969).

A dinâmica do citoesqueleto também é alterada através de mecanismos glutamatérgicos. Os receptores glutamatérgicos podem controlar o remodelamento da actina e a morfologia das espinhas dendríticas (Schubert et al., 2006; McKinney, 2010),

bem como estão envolvidos com alterações nos FIs (Loureiro et al., 2010; Pierozan et al., 2012).

A diversidade funcional do glutamato como neurotransmissor resulta da existência de uma grande variedade de receptores que coexistem em uma única sinapse. Os receptores glutamatérgicos podem ser classificados de acordo com suas propriedades farmacológicas e funcionais em receptores ionotrópicos (iGluR) e metabotrópicos (mGluR) (Nakanishi, 1992; Seeburg, 1993; Hollmann e Heinemann, 1994).

1.4.2.1. Receptores glutamatérgicos ionotrópicos

Os receptores glutamatérgicos ionotrópicos (iGluRs) são canais iônicos permeáveis ao Na^+, K^+ e Ca^{2+}, que tradicionalmente são divididos em 3 subtipos, os receptores N-methyl-D-aspartate (NMDA), α-amino-3-hydroxy-5-methyl-4-isoxazolepropionate (AMPA) e cainato (KA), com base em especificidades de ligação a agonistas. Entretanto, muitas vezes nenhum agonista ou antagonista distingue claramente os receptores AMPA e KA, portanto eles são muitas vezes denominados apenas como não-NMDA. A afinidade ao glutamato é diferente para os distintos receptores glutamatérgicos (Ozawa et al., 1997; Hassel e Dingledine, 2006).

Os receptores NMDA medeiam a transmissão sináptica lenta, são altamente permeáveis ao Na^+, K^+ e Ca^{2+} (Lipton e Rosemberg, 1994; Ozawa et al., 1998), dependentes de voltagem e possuem glicina como co-agonista (Johson e Ascher, 1992; Hassel e Dingledine, 2006). Já os receptores AMPA e KA estão envolvidos na transmissão excitatória sináptica rápida e estão associados primariamente a canais independentes de voltagem, sendo permeáveis principalmente ao Na^+ e ao K^+ (Cotman et al., 1981, Hassel e Dingledine, 2006).

1.4.2.2. Receptores glutamatérgicos metabotrópicos

Os receptores glutamatérgicos metabotrópicos (mGluRs) pertencem a família dos receptores acoplados as proteínas ligantes dos nucleotídeos guanina (proteína G) e, portanto, promovem a modulação de efetores intracelulares (segundos mensageiros), os quais ativam ou inibem diversos eventos de transdução de sinal (Osawa et al., 1998; Pin e Duvoisin, 1995)

Os mGluR são expressos predominantemente nos tecidos nervosos, onde exibem diferentes padrões de localização subcelular e distribuição regional específica (Baude et al., 1993; Lujan et al., 1996; Lujan et al., 1997; Petralia et al., 1997). Os mGluR do grupo I (mGluR1 e mGluR5) estão principalmente localizados no terminal pós-sináptico e estimulam a fosfolipase C e a liberação de cálcio dos estoques intracelulares. Já os receptores do grupo 2 (mGluR2 e mGluR3) e do grupo 3 (mGluR4, mGluR7 e mGluR8) são preferencialmente encontrados nos axônios terminais e estão relacionados com a inibição da adenilato ciclase (Hassel e Dingledine, 2006).

1.4.3. VIA DAS QUINASES ATIVADAS POR MITÓGENOS

As quinases ativadas por mitógenos (MAPK) são Ser/Thr quinases que convertem os estímulos extracelulares em respostas celulares. As MAPKs estão entre as vias de transdução de sinal mais antigas e foram largamente usadas por toda a evolução em muitos processos fisiológicos (Widmann,et al., 1999). Todas as células eucarióticas possuem múltiplas via de sinalização, sendo a via das MAPK central em várias rotas de transdução de sinal, as quais coordenadamente regulam a expressão gênica, mitose, metabolismo, motilidade, sobrevivência, apoptose e diferenciação celular. (Revisado em Cargnello e Roux, 2011).

A unidade funcional da via das MAPKs é composta de três tipos de quinases, a MAP quinase quinase quinase (MAPKKK), a MAP quinase quinase (MAPKK) e a MAP quinase (MAPK), as quais desencadeiam uma série de fosforilações, que constituem o módulo de ativação dessa via, como está representado na figura 10.

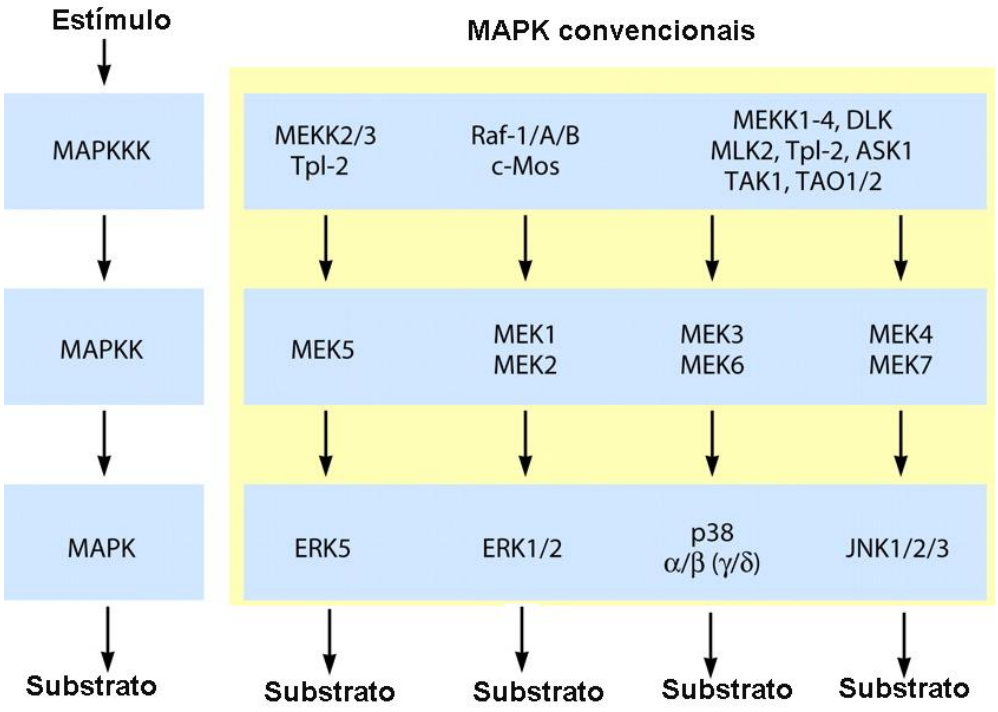

Figura 10: Cascata de sinalização conduzindo a ativação das MAPK. Adaptado de Roux et al., 2004 e Bibbs et al., 2006.

As MAPK convencionais compreendem a quinase regulada por sinal extracellular 1/2 (ERK1/2), a quinase ativada por estresse (c-Jun aminoterminal quinase) (SAP/JNK), a p38MAPK e a ERK5 (Chen et al., 2001; Kyriakis e Avruch., 2001; Pearson et al., 2001). Essas enzimas podem ser ativadas por uma variedade de estímulos diferentes, mas em geral as ERK1 e 2 são preferencialmente ativadas em resposta a fatores de crescimento e ésteres de forbol, enquanto a SAP/JNK e a

p38MAPK respondem ao estresse celular decorrente de fatores como choque osmótico, radiação ionizante, citocinas, neurotoxinas (Pearson et al., 2001; Xu et al., 2011). Vários substratos são alvos dessa família de proteínas, entre eles podemos citar as fosfolipases, os fatores de transcrição e as proteínas do citoesqueleto (Chen et al., 2001, Bibb e Nestler, 2006, Loureiro et al., 2008). Além disso, elas também podem catalisar a fosforilação e ativação de muitas proteínas quinases, o que representa uma atividade enzimática adicional e mais um passo de amplificação na cascata catalítica dessas enzimas (Lewis et al., 1998).

No cérebro, a via das MAPK desempenha um papel importante em processos como crescimento neuronal, diferenciação, sobrevivência, transmissão sináptica, processos inflamatórios e apoptóticos (Bibb e Nestler, 2006) além de aprendizado e memória (Revisado por Peng et al., 2010).

2. OBJETIVO

2.1. OBJETIVO GERAL

O $(PhTe)_2$ é um composto neurotóxico que afeta a funcionalidade de vários sistemas, entre eles o sistema glutamatérgico e a homeostase do cálcio. Além disso, esse organotelureto pode agir sobre enzimas importantes para a fisiologia normal do SNC, inibindo as mesmas. Entretanto, pouco se sabe a respeito do efeito do efeito do $(PhTe)_2$ sobre o citoesqueleto cerebral. Então, considerando que o citoesqueleto é um importante alvo de neurotoxicantes e que existem poucos estudos na literatura relacionando os efeitos neurotóxicos do $(PhTe)_2$ com alterações no citoesqueleto neural, o objetivo geral desse trabalho é investigar os efeitos tóxicos desse organotelureto sobre o citoesqueleto de astrócitos e neurônios, identificando as vias de sinalização envolvidas nas ações desencadeadas pela droga.

Para isso utilizamos 3 modelos de exposição, tentando entender a influência da maneira de contato nos efeitos da droga. O primeiro modelo (modelo 1) é uma injeção subcutânea de $(PhTe)_2$ em ratos jovens, mimetizando o contato direto, ou *in vivo*, com o organotelureto e a influência de todo o organismo em sua ação sobre o citoesqueleto cerebral. O segundo modelo (modelo 2), também considerado um modelo *in vivo*, é o da transmissão vertical, ou seja, mãe-filhote, através do leite materno. O terceiro modelo (modelo 3) tem como objetivo verificar o efeito dessa droga adicionada diretamente sobre a fatia da estrutura cerebral estudada, caracterizando um modelo *in vitro*.

2.2. OBJETIVOS ESPECÍFICOS

2.2.1. Modelo 1

2.2.1.1. Verificar o efeito de uma administração *in vivo* do $(PhTe)_2$ sobre a fosforilação dos FIs neuronais (NF-L, NF-M e NF-H) e gliais (GFAP e vimentina) no estriado e cerebelo de ratos jovens.

2.2.1.2. Determinar a influência do $(PhTe)_2$ no imunoconteúdo, bem como na expressão dos FIs neuronais e gliais do estriado e cerebelo.

2.2.1.3. Estudar o efeito da administração subcutânea de $(PhTe)_2$ em ratos jovens sobre a ativação de importantes quinases (MAPKs, PKA, GSK3β, AKT/PKB) do estriado e cerebelo.

2.2.1.4. Determinar o efeito do $(PhTe)_2$ sobre a viabilidade de astrócitos e neurônios.

2.2.2. Modelo 2

2.2.2.1. Verificar o efeito da administração subcutânea de $(PhTe)_2$ nas ratas mães durante os primeiros 14 dias de lactação sobre a fosforilação da GFAP e subunidades dos NFs (NF-L, NF-M, NF-H) do córtex cerebral, hipocampo, estriado e cerebelo dos filhotes.

2.2.2.2. Estudar o efeito da transmissão vertical do $(PhTe)_2$ sobre o imunoconteúdo dos FIs neuronais e gliais do córtex cerebral, hipocampo, estriado e cerebelo nos filhotes.

2.2.2.3. Determinar o efeito da administração subcutânea de $(PhTe)_2$ nas ratas mães durante períodos iniciais de lactação sobre a atividade das MAPKs e PKA no córtex cerebral, hipocampo, estriado e cerebelo dos filhotes.

2.2.2.4. Verificar o efeito neuroprotetor do disseleneto de difenila sobre os efeitos desencadeados pelo $(PhTe)_2$ nos filhotes.

2.2.3. Modelo 3

2.2.3.1. Realizar um estudo ontogenético dos efeitos do $(PhTe)_2$ sobre a fosforilação *in vitro* dos FIs de córtex cerebral e hipocampo de ratos.

2.2.3.2. Identificar as vias de sinalização envolvidas nesses efeitos, com ênfase especial nas proteínas quinases e fosfatases, bem como mecanismos envolvendo o glutamato e o cálcio.

3. MATERIAIS E MÉTODOS

A seção **Materiais e Métodos** está inserida em cada um dos seis capítulos da parte II dessa tese.

PARTE II

Capítulo 1

IN VIVO TREATMENT WITH DIPHENYL DITELLURIDE INDUCES NEURODEGENERATION IN STRIATUM OF YOUNG RATS: IMPLICATIONS OF MAPK AND AKT PATHWAYS.

Luana Heimfarth[a], Samanta Oliveira Loureiro[a], Márcio Ferreira Dutra[a], Cláudia Andrade[a], Letícia Pettenuzzo[a], Fátima T. Costa Rodrigues Guma[a], Carlos Alberto Saraiva Gonçalves[a], João Batista Teixeira da Rocha[b], and Regina Pessoa-Pureur[a]

Artigo submetido à *Toxicology and Applied Pharmacology*

IN VIVO TREATMENT WITH DIPHENYL DITELLURIDE INDUCES NEURODEGENERATION IN STRIATUM OF YOUNG RATS: IMPLICATIONS OF MAPK AND AKT PATHWAYS.

Luana Heimfarth[a], Samanta Oliveira Loureiro[a], Márcio Ferreira Dutra[a], Cláudia Andrade[a], Letícia Pettenuzzo[a], Fátima T. Costa Rodrigues Guma[a], Carlos Alberto Saraiva Gonçalves[a], João Batista Teixeira da Rocha[b], and Regina Pessoa-Pureur[a]

[a]Departamento de Bioquímica, Instituto de Ciências Básicas da Saúde, UFRGS, Porto Alegre, RS, Brasil

[b]Departamento de Química, Centro de Ciências Naturais e Exatas, Universidade Federal de Santa Maria, RS Brasil

CORRESPONDENCE ADDRESS: Dr. Regina Pessoa-Pureur, Universidade Federal do Rio Grande do Sul, Instituto de Ciências Básicas da Saúde, Departamento de Bioquímica, Rua Ramiro Barcelos 2600 anexo, 90035-003 Porto Alegre - RS, BRASIL, Fax: 5551 3308 5535, Tel: 5551 3308 5565; E-mail: rpureur@ufrgs.br

Abstract

In the present report 15 day-old rats were injected with 0.3 µmol of diphenyl ditelluride $(PhTe)_2$/kg body weight and parameters of neurodegeneration were analyzed in slices from striatum 6 days afterwards. We found hyperphosphorylation of intermediate filament (IF) proteins from astrocyte (glial fibrillary acidic protein -GFAP- and vimentin) and from neuron (low-, medium- and high molecular weight neurofilament subunits: NF-L, NF-M and NF-H, respectively) and increased MAPK (Erk, JNK and p38MAPK) as well as PKA activities. The treatment induced reactive astrogliosis in the striatum, evidenced by increased GFAP and vimentin immunocontent as well as their mRNA overexpression. Also, $(PhTe)_2$ significantly increased the propidium iodide (PI) positive cells in NeuN positive population without altering PI incorporation into GFAP positive cells, indicating that *in vivo* exposure to $(PhTe)_2$ provoked neuronal death. Immunohystochemistry showed a dramatic increase of GFAP staining characteristic of reactive astrogliosis, while decreased NeuN staining showed neuronal loss. Moreover, increased caspase 3 in $(PhTe)_2$ treated striatal slices suggested apoptotic cell death. $(PhTe)_2$ exposure decreased Akt immunoreactivity, however phospho-GSK-3-β (Ser9) was unaltered, suggesting that this kinase is not directly implicated in the neurotoxicity of this compound. Therefore, the present results shed light into the mechanisms of $(PhTe)_2$-induced neurodegeneration in rat striatum, evidencing a critical role for the MAPK and Akt signaling pathways and disruption of cytoskeletal homeostasis, which could be related with apoptotic neuronal death and astrogliosis.

Keywords: diphenyl ditelluride, cytoskeleton, apoptosis, astrogliosis, cell signaling, striatum

Introduction

Tellurium (Te) applications in electronics, optics, batteries and mining industries have expanded during the last few years, leading to an increase in environmental Te contamination, thus renewing biological interest in Te toxicity. The main target sites for Te toxicity are the kidney, nervous system, skin, and the fetus (hydrocephalus) (Taylor, 1996). Nevertheless, several reports support that inorganic and organic tellurium compounds are highly toxic to the CNS of rodents (Maciel, 2000). Organotellurium compounds lead to degradation of the myelin sheath and consequently a transient demyelination of peripheral nerves (Nogueira et al., 2004).

Neurofilaments (NF) are the primary intermediate filaments (IF) in mature neurons. They assemble from three subunit polypeptides of low, medium and high molecular weight, NF-L, NF-M, and NF-H, respectively. This process is finely regulated via phosphorylation of lysine-serine-proline (KSP) repeats in the carboxyl-terminal domain of NF-M and NF-H. The majority of KSP repeats in rat-mouse NF tail domains are phosphorylated by mitogen-activated protein kinases (MAPK) (Veeranna et al., 1998); glycogen synthetase kinase 3 (GSK3) (Guan et al., 1991); p38MAPK (Ackerley et al., 2004;) and c-Jun N-terminus kinase 1 and 3 (JNK1/3) (Brownlees et al., 2000).

Otherwise, phosphorylation sites located on the amino-terminal domains of the three NF subunits are the targets of second messenger-dependent protein kinases, such as cAMP-dependent protein kinase (PKA), Ca^{2+}/calmodulin-dependent protein kinase (PKCaM) and Ca^{2+}/diacylglycerol-dependent protein kinase (PKC) (Sihag and Nixon, 1990). The correct formation of an axonal network of NF is crucial for the

establishment and maintenance of axonal caliber and consequently for the optimization of conduction velocity.

Glial fibrillary acidic protein (GFAP) is the IF of mature astrocytes. GFAP expression is essential for normal white matter architecture and blood-brain barrier integrity, and its absence leads to late-onset CNS dysmyelination (Liedtke et al., 1996).

There is now compelling evidence for the critical role of the cytoskeleton in neurodegeneration (Lee et al 2011). Moreover, aberrant NF phosphorylation is a pathological hallmark of many human neurodegenerative disorders as well as is found after stressor stimuli (Sihag et al., 2007).

While NF abnormalities in neurodegenerative disorders could simply reflect a pathological consequence of neuronal dysfunction, recent studies suggested that disruption of NF homeostasis itself can also produce deleterious effects and therefore could contribute to the neurodegeneration process (for review see Perrot and Eyer, 2009).

Cell death and neuronal loss are the key pathological hallmarks of neurodegeneration in all the neurodegenerative disorders, with apoptosis and necrosis being central to both acute and chronic degenerative processes. In this context, the activation of p38MAPK signaling pathway is involved in the development of the motor neuron degeneration of the spinal cord. In addition, JNKs pathway include important mediators of neurodegeneration beyond NF substrates (Gelderblom et al., 2004).

Also, astrogliosis is a hallmark of diseased CNS tissue (Pekny and Nilsson, 2005). This term refers to progressive changes in gene expression and cellular morphology, often including proliferation. The activation of astrocytes is characterized by changes in their molecular and morphological features. Although reactive

astrogliosis is the normal physiological response essential for damage contention, it can also have detrimental effects on neuronal survival and axon regeneration, particularly in neurodegenerative diseases. It is believed that progressive changes in astrocytes as they become reactive are finely regulated by complex intercellular and intracellular signaling mechanisms. The most commonly used marker of activated astrocytes is their upregulation of GFAP, vimentin, and to some extent nestin, coincident with cellular hypertrophy (Sofroniew and Vinters, 2010).

Previous data from literature have indicated that diphenyl ditelluride $(PhTe)_2$ is extremely neurotoxic to rodents and exposure to low doses of this compound can cause profound neurostructural and neurofunctional deregulation in experimental animals (Stangherlin et al., 2009). Furthermore, $(PhTe)_2$ can also have neurotoxic effects *in vitro*, including citotoxic effect in astrocytes (Roy and Hardej, 2011) and changes in the phosphorylation of IF in slices obtained from different brain structures of young rats (Heimfarth et al., 2011, 2012). Therefore, in an attempt to better understand the toxicity of organotellurium compounds, we studied the effect of $(PhTe)_2$ in the striatum of young rats acutely exposed to the same concentration of the neurotoxicant able to provoke systemic toxicity and to induce hyperphosphorylation of cytoskeletal proteins in cerebral cortex of rats (Heimfarth et al., 2008). Thus, in the present report we describe disruption of the cytoskeletal homeostasis, reactive astrogliosis and apoptotic neuronal death in rat striatum early after $(PhTe)_2$ injection.

Material and methods

Radiochemicals and compounds

[^{32}P]Na_2HPO_4 was purchased from CNEN, São Paulo, Brazil. Benzamidine, leupeptin, antipain, pepstatin, chymostatin, acrylamide and bis-acrylamide, anti-GSK3β, anti-phosphoGSK3β, anti-PKAcα, anti-PKCaMII, anti-active caspase 3, anti-AKT, anti-phosphoAKT, anti-GFAP, anti-vimentin, anti-NF-L, anti-NF-M, anti-NF-H antibodies and propidium iodide were obtained from Sigma (St. Louis, MO, USA). The chemiluminescence ECL kit peroxidase and the conjugated anti- rabbit IgG were obtained from Amersham (Oakville, Ontario, Canada). Anti-ERK, anti-phosphoERK, anti-SAP/JNK, anti-phosphoSAP/JNK, anti-p38, anti-phosphop38 and anti-KSP repeats, were obtained from Cell Signaling Technology (USA). Anti-phosphoSer55NF-L, anti-phosphoSer57NF-L and anti-NeuN antibodies were obtained from Millipore. Anti-rabbit Alexa 488 and anti-mouse Alexa 568 were from Molecular Probes. The organochalcogenide $(PhTe)_2$ was synthesized using the method described by Petragnami (1994). Analysis of the 1H NMR and 13C NMR spectra showed that the compound obtained presented analytical and spectroscopic data in full agreement with their assigned structures. The purity of the compounds were assayed by high ressonance mass spectroscopy (HRMS) and was higher that 99.9%. Diphenyl ditelluride was dissolved in canola oil just before use. Platinum Taq DNA polymerase and SuperScript-II RT pre-amplication system were from Invitrogen. All other chemicals were of analytical grade and were purchased from standard commercial supplier.

Animals

Fifteen day-old male and female Wistar rats were obtained from our breeding stock. Rats were maintained on a 12-h light/12-h dark cycle in a constant temperature (22^o C) colony room. On the day of birth the litter size was culled to seven pups. Litters

smaller than seven pups were not included in the experiments. Water and a 20% (w/w) protein commercial chow were provided *ad libitum*. The experimental protocol followed the "Principles of Laboratory Animal Care" (NIH publication 85-23, revised 1985) and was approved by the Ethics Committee for Animal Research of the Federal University of Rio Grande do Sul.

Drug administration, preparation and labeling of slices

Fifteen day-old Wistar rats were treated with a single subcutaneous (s.c.) injection of $(PhTe)_2$ 0.3 μmol/kg body weight or canola oil (vehicle) (2.8 ml/kg body weight). Six days after treatment the rats were killed by decapitation, the striatum was dissected onto Petri dishes placed on ice and cut into 400 μm thick slices with a McIlwain chopper.

Preincubation

Tissue slices were initially preincubated at 30°C for 20 min in a Krebs-Hepes medium containing 124 mM NaCl, 4mM KCl, 1.2 mM $MgSO_4$, 25 mM Na-HEPES (pH 7.4), 12 mM glucose, 1 mM $CaCl_2$, and the following protease inhibitors: 1 mM benzamidine, 0.1 μM leupeptin, 0.7 μM antipain, 0.7 μM pepstatin and 0.7 μM chymostatin.

In vitro ^{32}P incorporation experiments

After preincubation, the medium was changed and incubation was carried out at 30 ^{o}C with 100 μl of the basic medium containing 80 μCi of [^{32}P] orthophosphate. The labeling reaction was normally allowed to proceed for 30 min at 30 ^{o}C and stopped with 1 ml of cold stop buffer (150 mM NaF, 5 mM, EDTA, 5 mM EGTA, Tris-HCl 50 mM, pH 6.5), and the protease inhibitors described above. Slices were then washed twice with stop buffer to remove excess radioactivity.

Preparation of the high salt-Triton insoluble cytoskeletal fraction from tissue slices

After incubation, preparations of IF-enriched cytoskeletal fractions were obtained from the striatum of rats. After the labeling reaction, slices were homogenized in 400 μl of ice-cold high salt buffer containing 5 mM KH_2PO_4, (pH 7.1), 600 mM KCl, 10 mM $MgCl_2$, 2 mM EGTA, 1 mM EDTA, 1% Triton X-100 and the protease inhibitors described above. The homogenate was centrifuged at 15800 x g for 10 min at 4 °C, in an Eppendorf centrifuge, the supernatant discarded and the pellet homogenized with the same volume of the high salt medium. The resuspended homogenate was centrifuged as described and the supernatant was discarded. The Triton-insoluble IF-enriched pellet, containing NF subunits, Vim and GFAP, was dissolved in 1% SDS and protein concentration was determined.

Polyacrylamide gel electrophoresis (SDS-PAGE)

The cytoskeletal fraction was prepared as described above. Equal protein concentrations were loaded onto 10% polyacrylamide gels and analyzed by SDS-PAGE.

After drying, the gels were exposed to T-MAT films at -70 ^{o}C with intensifying screens and finally the autoradiograph was obtained. Cytoskeletal proteins were quantified by scanning the films with a Hewlett-Packard Scanjet 6100C scanner and determining optical densities with an Optiquant version 02.00 software (Packard Instrument Company). Density values were obtained for the studied proteins.

Preparation of total protein homogenate

Tissues slices were homogenized in 100µl of a lysis solution containing 2 mM EDTA, 50 mM Tris-HCL, pH 6.8, 4% (w/v) SDS. For electrophoresis analysis, samples were dissolved in 25% (v/v) of solution containing 40% glycerol, 5% mercaptoethanol, 50 mM Tris-HCl, pH 6.8 and boiled for 3 min.

Western blot analysis

Protein homogenate (80 µg) was analyzed by SDS-PAGE and transferred to nitrocellulose membranes (Trans-blot SD semi-dry transfer cell, BioRad) for 1 h at 15 V in transfer buffer (48 mM Trizma, 39 mM glycine, 20% methanol and 0.25% SDS). The nitrocellulose membranes were washed for 10 min in Tris-buffered saline (TBS; 0.5 M NaCl, 20 mM Trizma, pH 7.5), followed by 2 h incubation in blocking solution (TBS plus 5% bovine serum albumin and 0.1% Tween 20). After incubation, the blot was washed twice for 5 min with TBS plus 0.05% Tween-20 (T-TBS), and then incubated overnight at 4°C in blocking solution containing the following antibodies: anti-GFAP (clone G-A-5) diluted 1:500, anti-vimentin (Vim 13-12) diluted 1:400, anti-NF-L (clone NR-4) diluted 1:1000, anti- NF-M (clone clone NN-18) diluted 1:400, anti-NF-

H (clone N52) diluted 1:1000, anti-ERK1/2 diluted 1:1000, anti-phosphoERK diluted 1:1000, anti-/JNK diluted 1:1000, anti-phosphoJNK (clone 98F2) diluted 1:1000, anti-p38MAPK (clone A-12) diluted 1:1000, anti-phosphop38MAPK diluted 1:1000, anti-PKAcα diluted 1:1000, anti-PKCaMII diluted 1:500, anti-AKT (clone 2H10) diluted 1:1000, anti-phosphoAKT (clone 244F9) diluted 1:1000, anti-active caspase 3 diluted 1:1000, anti-GSK3β (clone 27C10) diluted 1:1000, anti-phosphoGSK3β, anti-KSP repeats (clone NP1) diluted 1:1000, anti-phoshoNF-LSer55 diluted 1:800, anti-phosphoNF-LSer57 diluted 1:1000 or anti-actin diluted 1:1000. The blot was then washed twice for 5 min with T-TBS and incubated for 2 h in blocking solution containing peroxidase conjugated anti-rabbit IgG diluted 1:2000 or peroxidase conjugated anti-mouse IgG diluted 1:2000. The blot was washed twice again for 5 min with T-TBS and twice for 5 min with TBS. The blot was then developed using a chemiluminescence ECL kit. Immunoblots were quantified by scanning the films with a Helwett-Packard Scanjet 6100C scanner and determining optical densities with an OptiQuant version 02.00 software (Packard Instrument Company). Optical density values were obtained for the studied proteins.

RNA extraction, cDNA synthesis and quantitative PCR

RNA was isolated from striatum using the TRIzol Reagent (Invitrogen). Approximately 2 µg of total RNA were added to each cDNA synthesis reaction using the SuperScript-II RT pre-amplication system. Reactions were performed at 42 ºC for 1 h using the primer T23 V (5` TTT TTT TTT TTT TTT TTT TTTTTV). Quantitative PCR amplification was carried out using specific primer pairs designed with Oligo Calculator version 3.02 (http://www.basic.nwu.edu/biotools/oligocalc.html) and synthesized by IDT (MG, Brazil). The sequences of the primers used are listed in Table 1. Quantitative PCRs were carried out in an Applied-Biosystem StepOne Plus real-time

cycler and done in quadruplicate. Reaction settings were composed of an initial denaturation step of 5 min at 95 ºC, followed by 40 cycles of 10 s at 95 ºC, 10 s at 60 ºC, 10 s at 72 ºC; samples were kept for 1 min at 60 ºC for annealing and then heated from 55 to 99 ºC with a ramp of 0.3 ºC /s to acquire data to produce the denaturing curve of the amplified products. Quantitative PCRs were made in a 20 ul final volume composed of 10 ul of each reverse transcription sample diluted 50–100 times, 2 ul of 10 times PCR buffer, 1.2 ul of 50mM $MgCl_2$, 0.4 ul of 5 mM dNTPs, 0.8 ul of 5 uM primer pairs, 3.55 ul of water, 2.0 ul of SYBRgreen (1:10,000 Molecular Probe), and 0.05 ul of Platinum Taq DNA polymerase (5 U/ ul). All results were analyzed by the 2 -DDCT method (Livak and Schmittgen, 2001). TBP (TATA box binding protein) was used as the internal control gene for all relative expression calculations.

Table 1. Primers used for qPCR (quantitative polymerase chain reaction).

	Forward Primer	Reverse Primer
GFAP	5`CAGAAGCTCCAAGATGAAACCAA	5`TCTCCTCCTCCAGCGACTCAAC
Vim	5´CCCAGATTCAGGAACAGCAT	5´CACCTGTCTCCGGTATTCGT
NF-L	5′CCATGCAGGACACAATCAAC	5′CTGCAAGCCACTGTAAGCAG
NF-M	5′GAGATGTATTACGCAAAGTACG5′	5′CCAGTATGACCTTTATTGAGC
NF-H	5′ACCTATACCCGAATGCCTTCTT	5′AGAAGCACTTGGTTTTATTGCAC
B-actin	5`TATGCCAACACAGTGCTGTCGG	5`TACTCCTGCTTCCTGATCCACAT
TBP	5`CCCCACAACTCTTCCATTCT	5`GCAGGAGTGATAGGGGTCAT

GFAP, glial fibrillary acidic protein; Vim, vimentin; NF-L, low molecular weight neurofilament subunit; NF-M, middle molecular weight neurofilament subunit; NF-H, high molecular weight neurofilament subunit; TBP, TATA box binding protein

Immunofluorescence

Twelve pups (six for group) were anesthetized using ketamine/xylazine (75 and 10 mg/Kg, respectively, i.p.) and were perfused through the left cardiac ventricle with 40 ml of 0,9% saline solution, followed by 40 ml of 4% paraformaldehyde in 0.1 M phosphate buffered saline (PBS), pH 7.4, and the descendent aorta was campled. After the perfusion the brains were removed, post-fixed in the same fixative solution for 4 h at room temperature and cryoprotected by immersing in 15% and after in 30% sucrose solution in PBS at 4°C. The brains were then frozen by immersion in isopentane cooled with CO_2 and stored in a freezer (-80ºC) for later analyses. Serial coronal sections (40 µm) of striatum were obtained using a cryostat at -20ºC (Leica). Some sections were processed for double immunofluorescence for GFAP and NF-L and other sections for immunofluorescence for Neu-N (clone A60). The free-floating sections were preincubated in 2% bovine serum albumin (BSA) diluted in PBS containing 0.3% Triton X-100 (PBS-Triton X-100 0.3%) for 30 min. For double immunofluorescence of GFAP and NF-L, the sections were incubated two overnights at 4°C with rabbit polyclonal anti-GFAP and mouse monoclonal anti-NF-L (clone NR-4), diluted 1:3000 and 1:2000, respectively, in PBS- Triton X-100 0.3%. For Neu-N immunofluorescence, the sections were incubated two overnights at 4°C with mouse polyclonal anti-NeuN diluted 1:1000 in PBS-Triton X-100 0,3%. The negative controls were performed omitting the primary antibodies. After washing several times in PBS, tissue sections were incubated with anti-rabbit Alexa 488 and anti-mouse Alexa 568, both diluted 1:500 in PBS-Triton X-100 0.3% for 1 h at room temperature (for GFAP and NF-L immunofluorescence). Other tissue sections were incubated with anti-mouse Alexa 488, diluted 1:500 in PBS-Triton X-100 0.3% for 1 h at room temperature (for Neu-N immunofluorescence). Afterwards, the sections were washed several times in PBS,

transferred to gelatinized slides, mounted with Fluor Save™ (Merck), covered with coverslips and sealed with nail polish. The images were obtained with an Olympus IX-81 confocal FV-1000 microscope and analyzed with an Olympus Fluoview software.

Flow cytometry analysis

Tissues were dissociated with PBS/Colagenase/DNase, washed once with PBS then suspended in PBS/colagenase containing 10 μg/ml propidium iodide (PI). The integrity of plasma membrane was assessed by determining the ability of cells to exclude PI. The cells were incubated at room temperature in the dark for 30 min, washed with PBS and centrifuged at 3000 rpm for 5 min at 4 °C to remove the free PI. Afterwards, the cell was permeabilized with 0.2% PBS Triton X-100 in for 10 min at room temperature and blocked for 15 min with BSA 5%. After blocking, cells were incubated in blocking solution containing the monoclonal antibodies anti-NeuN (clone A60) diluted 1:100 or anti-GFAP diluted 1:100, for 2 h. The cells were washed twice with PBS and incubated for 1 h in blocking solution containing fluorescein isothiocyanate (FITC)-anti-rabbit IgG diluted 1:200 or Alexa 488-anti-mouse IgG diluted 1:200. The levels of PI incorporation, levels of positive NeuN cells and positive GFAP cells were determined by flow cytometry (FACSCalibur, Becton Dickinson, Franklin Lakes, NJ, USA). FITC or Alexa Fluor 488 and PI dyes were excited at 488 nm using an air-cooled argonlaser. Negative controls (samples with the secondary antibody) were included for setting up the machine voltages. Controls stained with a single dye (Alexa fluor 488 or FITC and propidium iodide) were used to set compensation. The emission of fluorochromes was recorded through specific band-pass fluorescence filters: green (FL-1; 530 nm/30) and red (FL-3; 670 nm long pass).

Fluorescence emissions were collected using logarithmic amplification. In brief, data from 10.000 events (intact cells) were acquired and the mean relative fluorescence intensity was determined after exclusion of debris events from the data set. All flow cytometric acquisitions and analyses were performed using Flow Jo software. Flow cytometry data were analyzed and plotted by density as a dot plot which shows the relative FL1 fluorescence on the x-axis and the relative FL3 fluorescence on the y-axis. The quadrants to determinate the negative and positive area were placed on no stained samples. The number of cells in each quadrant was computed and the proportion of cells stained with PI, GFAP and NeuN were expressed as percentage of PI uptake.

Protein determination

The protein concentration was determined by the method of Lowry et al. (1951) using serum bovine albumin as the standard.

Statistical analysis

Data were analyzed statistically by one-way analysis of variance (ANOVA) followed by the Tukey-Kramer multiple comparison test when the F-test was significant. All analyses were performed using the SPSS software program on an IBM-PC compatible computer.

Results

We have previously described that a single administration of $(PhTe)_2$ (0.3µmol /kg body weight) caused hyperphosphorylation of IF proteins from cortical slices of rats six days after injection (Heimfarth et al., 2008). On the basis on these results, in the present report we attempted to analyze the *in vivo* effects of $(PhTe)_2$ on other cerebral structure. Therefore, slices from striatum of rats injected with 0.3 µmol $(PhTe)_2$/kg body weight were incubated with ^{32}P-orthophosphate and the phosphorylation pattern of astrocyte (GFAP and vimentin) as well as neuron IF proteins (NF-L, NF-M and NF-H) was evaluated 6 days afterwards. As depicted in Figure 1A, we found hyperphosphorylation of all the striatal IF proteins studied. Figure 1B shows a representative experiment.

To examine whether the *in vivo* treatment with $(PhTe)_2$ affected second messenger-independent and -dependent protein kinases we analyzed the involvement of MAPKs, PKA and PKCaMII respectively in the actions of the neurotoxicant. Results showed that the MAPK signaling is activated in striatal slices, as demonstrated by increased immunoreactivity observed for phosphoErk (Figure 2A), phosphop38MAPK (Figure 2B) and phosphoJNK (Figure 2C), determined by Western blot analysis with specific monoclonal antibodies. Figure 2D shows representative blots of total and phospho forms of the kinases studied. The effect $(PhTe)_2$ on PKA and PKCaMII activities are depicted in Figure 3A. Results show an increased striatal PKAcα immunoreactivity detected by Western blot assay, while PKCaMII immunoreactivity was down-regulated in this structure. Representative blot corroborate these findings.

In an attempt to identify the phosphorylating sites targeted by the protein kinases PKCaMII, PKA and MAPK in the striatum, we assayed NF-LSer57 and NF-LSer55 on

NF-L head domain as well as KSP repeats on NF-M/NF-H tail domain, respectively. As depicted in Figure 3B, results obtained with Western blot assay using anti-phosphoSer55 antibody and anti-NFM/NFH KSP repeats showed that the phosphorylation level at these sites, was increased following treatment with $(PhTe)_2$. These findings are consistent with a role for PKA and MAPKs in the hyperphosphorylation of the neuronal IF proteins. On the other hand, $(PhTe)_2$ failed to induce NFLSer57 hyperphosphorylation, corroborating the evidence that PKCaMII is not involved in the action of the neurotoxicant in this cerebral structure. Representative blots are shown and corroborate these findings.

Next, we analyzed the effect of $(PhTe)_2$ on the immunocontent of the IF proteins from total striatal homogenate (Figure 4A) or from protein recovered into the high-salt Triton-insoluble cytoskeletal fraction of tissue slices (Figure 4C) at day 6 after the injection. We found that the immunocontent of both GFAP and vimentin was significantly increased in the striatal homogenate and cytoskeletal fraction. However, the immunocontent of the neuronal IFs (NF-L, NF-M and NF-H) was not altered in response to $(PhTe)_2$ injection. Figures 4B and D refers to representative immunoblot of the cytoskeletal proteins in total homogenate and in the cytoskeletal fraction. Consistent with these results, RT-PCR analysis showed over-expression of GFAP and vimentin mRNA, while expression of NF subunits was not altered (Figure 5), supporting the hypothesis of reactive astrogliosis in this cerebral structure.

For the purpose of assessing cell viability we proceed flow cytometry analysis using PI-exclusion assay to determine the percentage of viable cells. Results showed that $(PhTe)_2$ significantly increased the number of Pi positive cells from 7.5 % in controls to 11.5 % at day 6 after exposure to the neurotoxicant (Figure 6A). However, considering the NeuN positive cells, we found that Pi incorporation significantly

increased from 30 % in controls to 50 % in neurons from injected animals (Figure 6B). Otherwise, PI incorporation into GFAP positive cells was not altered in response to $(PhTe)_2$ injection (Figure 6C). Altogether, these findings indicate that *in vivo* exposure to $(PhTe)_2$ provoked neuronal death in striatum of rats at day 6 after injection. To further attest cell damage and cytoskeletal alterations induced by the *in vivo* exposure to $(PhTe)_2$, we proceeded immunofluorescence analysis of striatal sections. Therefore, the sections were processed for double immunofluorescence for GFAP and NF-L and also for NeuN, and analyzed by confocal microscopy. As depicted in Figure 7A, the confocal analysis for GFAP showed a dramatic increase of GFAP positive cells, and also reactive astrocytes were characterized by increase in the size of the cell body and/or processes, characteristic of reactive astrogliosis. Also, results from confocal microscopy did not show decreased NF-L positive cells in $(PhTe)_2$ treated striatal slices (Figure 7A), corroborating our Western blot analysis indicating that the neurotoxin failed to alter NF-L content. Otherwise, we detected decreased immunofluorescence for NeuN, indicative of neuronal loss (Figure 7B).

Moreover, Western blot analysis with anti-caspase 3 antibody showed that in $(PhTe)_2$ treated striatal slices this key caspase is activated, meaning apoptotic cell death (Figure 8A). In an attempt to determine signaling mechanisms involved in the neuronal death we evaluated the PI3K/Akt signaling pathway. Western blot analysis using anti-Akt antibody showed decreased phosphoAkt immunoreactivity (Figure 8B) in $(PhTe)_2$ treated slices, which is compatible with down-regulated survival mechanisms in the striatum of treated animals (Zhao et al 2006). Also, it was evaluated the GSK-3-β activity, since it is described as a kinase that can be modulated by Akt activity (Zhao et al., 2006). We found that phosphoGSK-3-β (Ser9) was not altered in the striatum of $(PhTe)_2$ injected rats, suggesting that this kinase is not directly implicated in the

neurotoxicity of this compound (Figure 8C). Figure 8D depicts the representative immunological reaction of active caspase 3, Akt and phosphoAkt.

Discussion

We have previously demonstrated that young rats (15 day-old) acutely injected with $(PhTe)_2$ at 0.3 μmol/kg of body weight presented weight loss from day 2 up to day 6 after drug exposure, indicating systemic toxicity at this concentration (Heimfarth et al 2008). In the present study we attempted to further investigate the mechanisms underlying neurotoxicity of $(PhTe)_2$ in acutely injected 15 day-old rats. We have chosen the striatum, since it is well known that, in rodents, neurotoxins produce a number of neurochemical changes in striatal glial and neuronal cells (Pierozan et al., 2012). Therefore, elucidation of the biochemical steps leading to $(PhTe)_2$-induced neurotoxicity provide us new clues to the mechanisms underlying the actions of this neurotoxin in brain.

Hyperphosphorylated IF proteins NF-L, NF-M and NF-H from neurons as well as GFAP and vimentin from astrocytes reflect an altered activity of the phosphorylating system associated with the IF proteins in this cerebral structure. Despite the functional role of NF phosphorylation is to date not completely clear, phosphorylation of amino-terminal domain of NF-L and other IF subunits has been related to their association into filamentous structures (for review see Sihag et al., 2007), while *in vitro* phosphorylation of carboxyl-terminal domains of NF-H and NF-M straightens individual NFs and promotes their alignment into bundles (Leterrier et al., 1996). Otherwise, the *in vivo* phosphorylation of these proteins is associated with an increased interNF spacing (Hsieh et al 1994). As a consequence, NF-H and NF-M carboxyl-terminal side arms

extend and form cross-bridges among NF and other cytoskeletal elements (Gotow et al., 1994).

According with a great deal of evidence, hyperphosphorylation of NF subunits is considered a hallmark of neurodegeneration (for review see Perrot and Eyer, 2009). The present results are consistent with this, since we first observed that the acute administration of $(PhTe)_2$ elicited hyperphosphorylation of GFAP, vimentin and NF subunits, evidencing a response of the cytoskeleton of astrocytes and neurons, to the action of the neurotoxicant. Accordingly, NFLSer55 appeared to be a specific amino-terminal phosphorylation site targeted by $(PhTe)_2$, being PKA the most prominent protein kinase mediating this effect.

It is important to note that PKA (Ser-55), PKC (Ser-51) and PKCaMII (Ser-57) phosphorylation sites are relevant for filament assembly. Furthermore, the phosphate present in Ser55 of NF-L is turned over rapidly following NF-L synthesis in neurons (Sihag and Nixon, 1991), suggesting a possible role in the blockade of NF assembly before their transport into neurites. Like NF-L, PKA-mediated phosphorylation of the head domain of GFAP inhibits filament assembly or induces disassembly (Hisanaga *et al.*, 1990; Hisanaga *et al.*, 1994). Therefore, our results showing NF-LSer55 hyperphosphorylation suggest a key role of $(PhTe)_2$ on IF dynamics preventing filament assembly and disassembling preexisting filaments.

It is known that carboxyl-terminal phosphorylation of NF-H progressively restricts the association of NFs with kinesin, the axonal anterograde motor protein, and stimulates its interaction with dynein, the axonal retrograde motor protein (Motil et al., 2006). This event could represent one of the mechanisms by which carboxyl-terminal phosphorylation would slow NF axonal transport. Consistent with this, MAPK

phosphorylates NF-M and NF-H tail domains at specific carboxyl-terminal located KSP repeats (Veeranna et al., 1998) and alters the association of NF with motor proteins (Yabe et al 2000). It is feasible that extensively phosphorylated KSP repeats on NF-M and NF-H as well as MAPK (Erk, JNK and phospho38MAPK) activation we found in the striatum of $(PhTe)_2$-treated rats could interfere with NF axonal transport and contribute, at least in part, to the neuronal damage provoked by the neurotoxin. Taking into account the present findings, we are tempted to speculate that disruption of cytoskeletal homeostasis in the striatum of injected rats, could be related with the neurodegeneration provoked by the $(PhTe)_2$. This hypothesis is supported by the evidence that p38MAPK and JNK signaling pathways are supposed to act sinergistically upstream of mechanisms leading to apoptotic neuronal death in different models of neurodegeneration (Muscella et al., 2011).

To better understand the molecular mechanisms underlying neuronal loss in acutely $(PhTe)_2$ injected rats, we assayed the caspase 3 activity and we found that this caspase is activated 6 days afterwards. Because activation of caspases, and caspase-3 in particular, appears to be a major factor for neuronal apoptosis execution in brain (Yakovlev and Faden, 2001), the evaluation of upstream modulatory mechanisms is important for understanding the regulation of the apoptotic process elicited by $(PhTe)_2$. In this context, it is important to note that release of cytochrome c from mitochondria plays critical roles in the apoptotic cascade, activating caspase-9 which, in turn, activates executioner caspase-3 and -7 (Slee et al., 1999). Thus, activation of caspase-3 by cytochrome c-mediated caspase-9 activation could explain the neuronal apoptosis in the striatum of $(PhTe)_2$-treated rats. Taking into account that JNK activation is upstream of cytochrome c release from mitochondria and therefore caspase-3 activation, we could establish a causal link between JNK activation and the caspase-3-mediated pro-

apoptotic action of $(PhTe)_2$. However we cannot exclude that caspase 3 be activated by the extrinsic mechanism, independently of cytochrome c release. In a variety of cell types, apoptosis can be regulated by extracellular death factors. These factors are members of the tumor necrosis factor (TNF) family of cytokines (Ashkenazi and Dixit 1998) and caspase-8 appears to play the major role in the initiation of caspase cascade (Boldin et al 1996). However further experiments will be necessary to clarify this point.

Additional evidence of the pro-apoptotic mechanism of action of $(PhTe)_2$ comes from our results showing decreased Akt phosphorylation/activity in striatal slices from injected animals. The PI3K-Akt signaling pathway plays a critical role in mediating survival signals in a wide range of neuronal cell types (Cardone et al., 1998). The identification of a number of substrates for the serine/threonine kinase Akt suggests that it blocks cell death by both impinging on the cytoplasmic cell death machinery and by regulating the expression of genes involved in cell death and survival (Koh et al., 2004). This is in line with Zhou and colleagues (2000) who described that activated Akt may inhibit activation of caspase-9 and -3 by posttranslational modification of a cytosolic factor downstream of cytochrome c and before activation of caspase-9 (Cardone et al., 1998). Therefore, inhibited PI3K-Akt pathway, that was found in $(PhTe)_2$, could be consistent with the apoptotic insult observed in the striatum. Otherwise, GSK3β is a critical downstream element of the PÌ3K/Akt pathway and its activity can be inhibited by Akt-mediated phosphorylation at Ser9 (Srivastava and Pandey, 1998). GSK3β has been implicated in multiple cellular processes and linked with the pathogenesis and neuronal loss in several neurodegenerative diseases (Petit-Paitel, 2010). In his context, Takashima (2006) described that GSK-3β activation through impairment of PI3K/Akt signaling was involved in amyloid-beta (Abeta)-induced neuronal death in rat hippocampal cultures. However, in our experimental model of $(PhTe)_2$-induced

neurodegeneration, Akt inhibition is apparently not implicated in GSK3β (Ser9) hyperphosphorylation, supporting different signaling pathways downstream of different stressor events.

In the CNS, following injury, astrocytes become reactive, a prominent process leading to the formation of the glial scar that inhibits axon regeneration after CNS injury. Upon becoming reactive, astrocytes undergo various molecular and morphological changes including upregulation of their expression of GFAP, vimentin and chondroitin sulfate proteoglycans as well as other molecules that are inhibitory to axon growth (Yu et al., 2012). However, upregulation of IFs is a hallmark of astrogliosis and a well-accepted indicator of structural damage in the CNS (Sofroniew and Vinters, 2010).

Thus, astrocytes could have turned activated in response to neuronal death early after $(PhTe)_2$ injection. In this context, the neuronal loss showed by immunocytochemistry and flow cytometry in the striatum could support the accentuated vacuolization of cellular bodies of rat brain after *in vivo* exposure to $(PhTe)_2$, reported by Maciel et al. (2000).

Consistent with the pro-apoptotic effect of $(PhTe)_2$ on striatal neurons, we found a prominent increase of GFAP and vimentin expression apparent at 6 days post injection, which suggest that, at least at this time, cells were reactive astrocytes. Astrogliosis is the normal physiological response essential for damage contention. However, it can also have detrimental effects on neuronal survival and axon regeneration, particularly in neurodegenerative insults. It is believed that progressive changes in astrocytes as they become reactive are finely regulated by complex intercellular and intracellular signaling mechanisms. Reports describing whether the

MAPK pathways are upregulated in astrocytes *in vivo* are mixed. Nonetheless, increased phosphorylation level of Erk and/or p38MAPK takes part in the response of astrocytes to insults (Ito et al., 2009). Although the evident complexity involving the participation of these signaling mechanisms in reactive astrogliosis, different components of MAPK signaling are activated under distinct pathological conditions and in different cell types, which may indicate a common mechanism. Thus, the activation of MAPKs detected in the striatum of acutely treated rats could be associated with the program of astrogliosis detected in our experimental condition.

Conclusion

The present results shed light into the mechanisms of $(PhTe)_2$-induced neurodegeneration in rat striatum, evidencing a critical role for the MAPK and Akt signaling pathways causing disruption of cytoskeletal homeostasis, which could be related with apoptotic neuronal death and astrogliosis presented here.

Conflict of interest statement

The authors declare that there are no conflicts of interest.

Ackowledgements

This work was supported by Conselho Nacional de Desenvolvimento Científico e Tecnológico (CNPq), Fundação de Amparo à Pesquisa do Estado do Rio Grande do Sul (FAPERGS), PRONEX and Propesq-UFRGS. The authors thank to Electron

Microscopy Center of the Federal University of Rio Grande do Sul for the microscopy analyzes. The authors also thank Mr. Henrique Biehl for technical assistance.

References

Ackerley, S., Grierson, A.J., Banner, S., Perkinton, M.S., Brownlees, J., Byers, H.L., Ward, M., Thornhill, P., Hussain, K., Waby, J. S., Anderton, B.H., Cooper, J.D., Dingwall, C., Leigh, P.N., Shaw, C.E., Miller, C.C., 2004. p38alpha stress-activated protein kinase phosphorylates neurofilaments and is associated with neurofilament pathology in amyotrophic lateral sclerosis. Mol. Cell. Neurosci. 26, 354–364.

Ashkenazi, A., Dixit V.M., 1998. Death receptors: signaling and modulation. Science 281, 1305–1308.

Boldin, M.P., Goncharov, T.M., Goltsev, Y.V., Wallach, D., 1996. Involvement of MACH, a novel MORT1/FADD-interacting protease, in Fas/APO-1- and TNF receptor-induced cell death. Cell 85, 803–815.

Brownlees, J., Yates, A., Bajaj, N.P., Davis, D., Anderton, B.H., Leigh, P.N., Shaw, C. E., Miller, C.C., 2000. Phosphorylation of neurofilament heavy chain side-arms by stress activated protein kinase-1b/Jun N-terminal kinase-3. J. Cell Sci. 113(Pt 3), 401–407.

Cardone, M.H., Roy, N., Stennicke, H R., Salvesen, G.S., Franke, T.F., Stanbridge, E., Frisch, S., Reed, J.C., 1998. Regulation of cell death protease caspase-9 by phosphorylation. Sci. 282, 1318–1321.

Eng, L.F., Ghirnikar, R.S., Lee, Y.L., 2000. Glial fibrillary acidic protein: GFAP-thirty-one years (1969–2000). Neurochem. Res. 25, 1439-1451.

Gelderblom, M., Eminel, S., Herdegen, T., Waetzig, V., 2004. c-Jun N-terminal kinases (JNKs) and the cytoskeleton—functions beyond neurodegeneration. Int. J. Devl Neurosci. 22, 559–564.

Gotow, T., Tanaka, T., Nakamura, Y., Takeda, M., 1994. Dephosphorylation of the largest neurofilament subunit protein influences the structure of crossbridges in reassembled neurofilaments. J. Cell Sci. 107, 1949–1957.

Guan, R.J., Khatra, B.S., Cohlberg, J.A., 1991. Phosphorylation of bovine neurofilament proteins by protein kinase FA (glycogen synthase kinase 3). J. Biol. Chem. 266, 8262–8267.

Heimfarth, L., Loureiro, S.O., Zamoner, A., Pelaez, P. L., Nogueira, C.W., Rocha, J. B., Pessoa-Pureur, R., 2008. Effects of in vivo treatment with diphenyl ditelluride on the phosphorylation of cytoskeletal proteins in cerebral cortex and hippocampus of rats. Neurotoxicol. 29, 40-47.

Heimfarth, L., Loureiro, S.O., Reis, K.P., de Lima, B.O., Zamboni, F., Gandolfi, T., Narvaes, R., da Rocha, J.B., Pessoa-Pureur, R., 2011. Cross-talk among intracellular signaling pathways mediates the diphenyl ditelluride actions on the hippocampal cytoskeleton of young rats. Chem. Res. Toxicol. 24, 1754-1764.

Heimfarth, L., Loureiro, S.O., Reis, K.P., de Lima, B.O., Zamboni, F., Lacerda, S., Soska, A.K., Wild, L., da Rocha, J.B., Pessoa-Pureur, R., 2012. Diphenyl ditelluride induces hypophosphorylation of intermediate filaments through modulation of DARPP-32-dependent pathways in cerebral cortex of young rats. Arch. Toxicol. 86, 217-230.

Hisanaga, S., Matsuoka, Y., Nishizawa, K., Saito, T., Inagaki, M., Hirokawa, N., 1994. Phosphorylation of native and reassembled neurofilaments composed of NF-L, NF-M, and NF-H by the catalytic subunit of cAMP-dependent protein kinase. Mol. Biol. Cell 5(2), 161-172.

Hsieh, S.T., Kidd, G.J., Crawforg, T.O., Xu, Z., Lin, W.M., Trapp, B.D., Cleveland, D. W., Griffin, J.W., 1994. Regional modulation of neurofilament organization by myelination in normal axons. J. Neurosci. 14, 6392–6401.

Koh, S.H., Park Y., Song, C.W., Kim, J.G., Kim, K., Kim, J., Kim, M.H., Lee, S.R., Kim, D.W., Yu, H.J., Chang, D.I., Hwang, S.J., Kim, S.H., 2004. The effect of PARP inhibitor on ischaemic cell death, its related inflammation and survival signals. Eur. J. Neurosci. 20(6), 1461–1472.

Lee, S.B., Bagley, J.A., Lee, H.Y., Jan, L.Y., Jan, Y.N., 2011. Pathogenic polyglutamine proteins cause dendrite defects associated with specific actin cytoskeletal alterations in Drosophila. Proc. Natl. Acad. Sci. USA. 108, 16795-16800.

Leterrier, J.F., Kas, J., Hartwig, J., Vegners, R., Janmey, P.A., 1996. Mechanical effects of neurofilament cross-bridges. Modulation by phosphorylation, lipids, and interactions with F-actin. J. Biol. Chem. 271, 15687–15694.

Liedtke, W., Edelmann, W., Bieri, P.L., Chiu, F.C., Cowan, N.J., Kucherlapati, R., Raine, C.S., 1996. GFAP is necessary for the integrity of CNS white matter architecture and long-term maintenance of myelination. Neuron. 17, 607-615.

Livak, K.J. Schmittgen, T.D., 2001. Analysis of relative gene expression data using real-time quantitative PCR and the 2(-Delta Delta C(T). Method. Methods 25, 402– 408.

Lowry, O.H., Rosebrough, N.J., Farr, A.L., Randall, R. J., 1951. Protein measurement with the Folin phenol reagent. J. Biol. Chem. 193, 265–275.

Maciel, E.N., Bolzan, R.C., Braga, A.L. and Rocha, J.BT., 2000. Diphenyl diselenide and diphenyl ditelluride differentially affect delta-aminolevulinate dehydratase from liver, kidney, and brain of mice. J. Biochem. Mol. Toxicol. 14, 310-319.

Motil, J., Chan, W.K., Dubey, M., Chaudhury, P., Pimenta, A., Chylinski, T.M., Ortiz, D.T., Shea, T. B., 2006. Dynein mediates retrograde neurofilament transport within axons and anterograde delivery of NFs from perikarya into axons: regulation by multiple phosphorylation events. Cell Motil. Cytoskeleton 63, 266-286.

Muscella, A., Calabriso, N., Vetrugno, C., Fanizzi, F.P., De Pascali, S.A., Marsigliante, S., 2011. The signalling axis mediating neuronal apoptosis in response to [Pt(O,O'-acac)(γ-acac)(DMS)]. Biochem. Pharmacol. 81, 1271-1285.

Nogueira, C.W., Zeni, G., Rocha, J.B.T., 2004. Organoselenium and organotellurium compounds: Toxicol. and pharmacol. Chem. Rev. 104, 6255–6285.

Pekny, M., Nilsson, M., 2005. Astrocyte activation and reactive gliosis. Glia 50, 427–434.

Perrot, R., Eyer, J., 2009. Neuronal intermediate filaments and neurodegenerative disorders. Brain. Res. Bull. 80, 282-295.

Petit-Paitel, A., 2010. GSK-3beta: a central kinase for neurodegenerative diseases? Med. Sci (Paris). 26(5), 516-21.

Petragnani, N., 1994. Preparation of the principal classes of organic tellurium compounds. In: Tellurium in Organic Synthesis. Academic Press, London, pp. 9–88.

Pierozan, P., Zamoner, A., Soska, Â.K., de Lima, B.O., Reis, K.P., Zamboni, F., Wajner, M., Pessoa-Pureur, R., 2012. Signaling mechanisms downstream of quinolinic acid targeting the cytoskeleton of rat striatal neurons and astrocytes. Experiment. Neurol. 233, 391-399.

Roy, S., Hardej, D., 2011. Tellurium tetrachloride and diphenyl ditelluride cause cytotoxicity in rat hippocampal astrocytes. Food Chem. Toxicol. 49, 2564-2574.

Sihag, R.K., Nixon, R.A., 1991. Identification of Ser-55 as a major protein kinase A phosphorylation site on the 70-kDa subunit of neurofilaments. Early turnover during axonal transport. J. Biol. Chem. 266(28), 18861-18867.

Sihag, R.K., Nixon, R.A., 1990. Phosphorylation of the aminoterminal head domain of the middle molecular mass 145-kDa subunit of neurofilaments. Evidence for regulation by second messenger-dependent protein kinases. J. Biol. Chem. 265, 4166–4171.

Sihag, R.K., Inagaki, M., Yamaguchi, T., Shea, T. B., Pant, H. C., 2007. Role of phosphorylation on the structural dynamics and function of types III and IV intermediate filaments. Exp. Cell Res. 313, 2098–2109.

Slee E.A., Harte M.T., Kluck R.M., Wolf B.B., Casiano C.A., Newmeyer D.D., Wang H.G., Reed J.C., Nicholson D.W., Alnemri E.S., Green D.R., Martin S.J., 1999. Ordering the cytochrome c-initiated caspase cascade: hierarchical activation of caspases- 2, -3, -6, -7, -8, and -10 in a caspase-9- dependent manner. J. Cell Biol. 144, 281–292.

Sofroniew, M.V., Vinters, H.V., 2010. Astrocytes: biology and pathology. Acta Neuropathol. 119, 7–35.

Srivastava, A.K., Pandey, S.K., 1998. Potential mechanism(s) involved in the regulation of glycogen synthesis by insulin. Mol. Cell. Biochim. 182, 135-141.

Stangherlin, E.C., Rocha, J.B. and Nogueira, C.W., 2009. Diphenyl ditelluride impairs short-term memory and alters neurochemical parameters in young rats. Pharmacol. Biochem. Behav. 91, 430-435.

Takashima A., 2006. GSK-3 is essential in the pathogenesis of Alzheimer's disease. J Alzheimers Dis. 9(3 Suppl), 309-17.

Taylor A., 1996. Biochemistry of tellurium. Biol. Trace Elem. Res. 55, 231-239.

Veeranna, Amin N.D., Ahn N.G., Jaffe H., Winters C.A., Grant P., Pant H.C., 1998. Mitogen-activated protein kinases (Erk1, 2) phosphorylate Lys–Ser–Pro (KSP) repeats in neurofilament proteins NF-H and NF-M. J. Neurosci. 18, 4008–4021.

Yabe, J.T., Chan, W., Shea, T.B., 2000. Phospho-dependent association of neurofilament proteins with kinesin in situ. Cell Motil. Cytoskeleton. 45, 249–265.

Yakovlev, A.G. and Faden, A.I., 2001. Caspase-Dependent Apoptotic Pathways in CNS Injury. Mol. Neurobiol. 24, 131–144.

Yu, P., Wang, H., Katagiri, Y., Geller, H.M., 2012. An in vitro model of reactive astrogliosis and its effect on neuronal growth. Methods Mol. Biol. 814, 327-340.

Zhao, H., Sapolsky, R.M. and Steinberg, G.K., 2006. Phosphoinositide-3-kinase/akt survival signal pathways are implicated in neuronal survival after stroke. Mol. Neurobiol. 34, 249-270.

Zhou, H., L,i X.M., Meinkoth, J., Pittman, R.N., 2000. Akt regulates cell survival and apoptosis at a postmitochondrial level. J. Cell Biol. 151, 483–494.

Legends to the Figures

Figure 1: Effect of $(PhTe)_2$ on the *in vitro* phosphorylation of IF proteins (A). Slices of striatum were incubated in the presence of ^{32}P orthophosphate, the cytoskeletal fraction was extracted and the radioactivity incorporated into IF subunits was measured. NF-H, high molecular weight NF subunit; NF-M, middle molecular weight NF subunit; NF-L, low molecular weight NF subunit; Vim, vimentin and GFAP, glial fibrillary acidic protein. Representative stained gel and autoradiograph of the proteins studied are shown (B). Data are reported as mean ± S.E.M. of 8–10 animals and expressed as percent of control. Statistically significant differences from canola oil-treated rats, as determined by one-way ANOVA followed by Tukey-Kramer test are indicated: *$P < 0.05$.

Figure 2: Effect of $(PhTe)_2$ on MAPK pathways ERK1/2 (A), JNK (B) and p38MAPK (C) Representative Western blots of the proteins studied are shown (D). Data are reported as mean ± S.E.M. of 8–10 animals and expressed as percent of control. Statistically significant differences from canola oil-treated rats, as determined by one-way ANOVA followed by Tukey-Kramer test are indicated: *$P < 0.05$.

Figure 3: Effect of $(PhTe)_2$ on total immunocontent of PKAcα and PKCaMII (A) and on the immunocontent of phosphoNF-H KSP reapeats, phosphoNF-LSer55 and phosphoNF-LSer57 (B). Representative Western blots of the proteins studied are

shown. β-actin was used as loading control. Data are reported as means ± S.E.M. of 8–10 animals and expressed as percent of control. Statistically significant differences from canola oil-treated rats, as determined by one-way ANOVA followed by Tukey-Kramer test are indicated: *P < 0.05.

Figure 4: Effect of $(PhTe)_2$ on IF protein immunoreactivity in the tissue homogenate and in the cytoskeletal fraction. Immunocontent of IF proteins in the homogenate (A); in the cytoskeletal fraction (C). Representative Western blots of the proteins studied are shown (B,D). β-actin was used as loading control . Data are reported as means ± S.E.M. of 8–10 animals and expressed as percent of control. Statistically significant differences from canola oil-treated rats, as determined by one-way ANOVA followed by Tukey-Kramer test are indicated: *P < 0.05. NF-H, high molecular weight NF subunit; NF-M, middle molecular weight NF subunit; NF-L, low molecular weight NF subunit; Vim, vimentin and GFAP, glial fibrillary acidic protein.

Figure 5: Quantitative real-time PCR analysis in striatum of animals treated with $(PhTe)_2$. The expression of IF subunits was analyzed by real-time PCR six days after treatment. Data represent mean ± S.E.M. of 8–10 animals in each group. Statistically significant differences from controls determined by one-way ANOVA followed by Tukey-Kramer test are indicated: *P < 0.05. NF-H, high molecular weight neurofilament NF subunit; NF-M, middle molecular weight NF subunit; NF-L, low molecular weight NF subunit, Vim, vimentin and GFAP, glial fibrillary acidic protein.

Figure 6: Quantitative propidium iodide (PI) positive cells (A), neurons (B) and astrocytes (C) in $(PhTe)_2$ injected rats. Total PI positive cells (A), NeuN-PI positive cells (B) and GFAP-PI positive cells (C) were measured by flow cytometry analysis. (D,E) representative flow cytometry data. Data are reported as means ± S.E.M. of 8–10 animals and expressed as percent of control. Statistically significant differences from canola oil-treated rats, as determined by one-way ANOVA followed by Tukey-Kramer test are indicated: *P < 0.05.

Figure 7: Immunohistochemistry for GFAP, NF-L, NeuN and merged. The panels obtained by confocal microscopy show increased GFAP, unaltered NF-L and decreased NeuN staining, meaning astrogliosis and decreased neuronal integrity in the striatum of $(PhTe)_2$ injected rats. Merged panels show colocalization of astrocytes and neurons. Representative images of 6 animals. Bar scale = 30μm (magnification: 40x); 50μm (magnification:20x).

Figure 8: Effect of $(PhTe)_2$ on caspase (A), AKT/PKB (B) and GSK3β (C) pathways in the striatum of rats. Total immunocontent of active caspase 3 (A); total and phosphoAKT (B); and total and phosphoGSK3β (C). Representative Western blots of the proteins studied are shown (D). β-actin was used as loading control. Data are reported as means ± S.E.M. of 8–10 animals and expressed as percent of control. Statistically significant differences from canola oil-treated rats, as determined by one-way ANOVA followed by Tukey-Kramer test are indicated: *P < 0.05.

Figure 1:

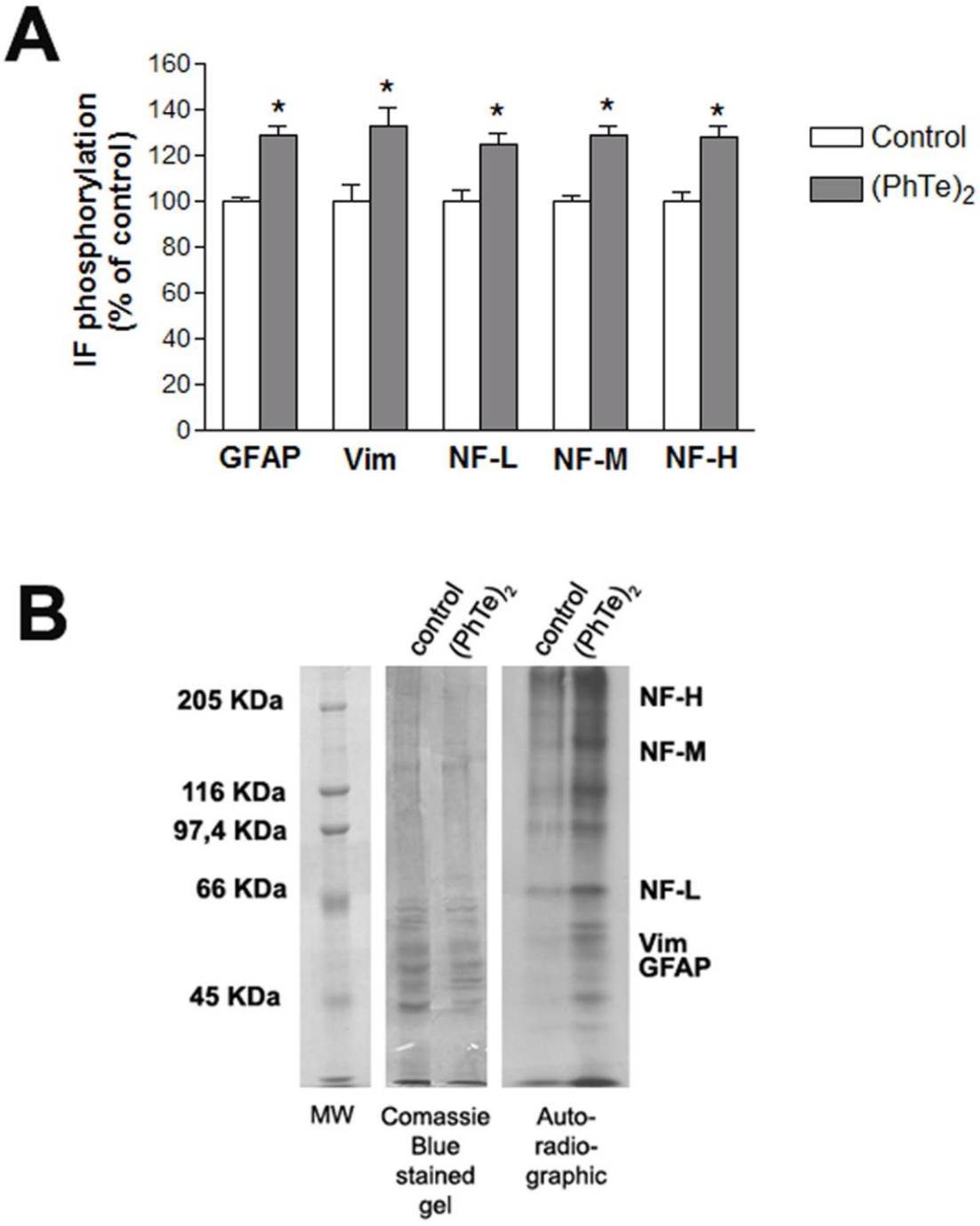
A
IF phosphorylation (% of control)
160
140
120
100
80
60
40
20
0
*
GFAP
Vim
NF-L
NF-M
NF-H
Control
(PhTe)2
B
control
(PhTe)2
control
(PhTe)2
205 KDa
116 KDa
97,4 KDa
66 KDa
45 KDa
NF-H
NF-M
NF-L
Vim
GFAP
MW
Comassie Blue stained gel
Auto-radio-graphic

Figure 2:

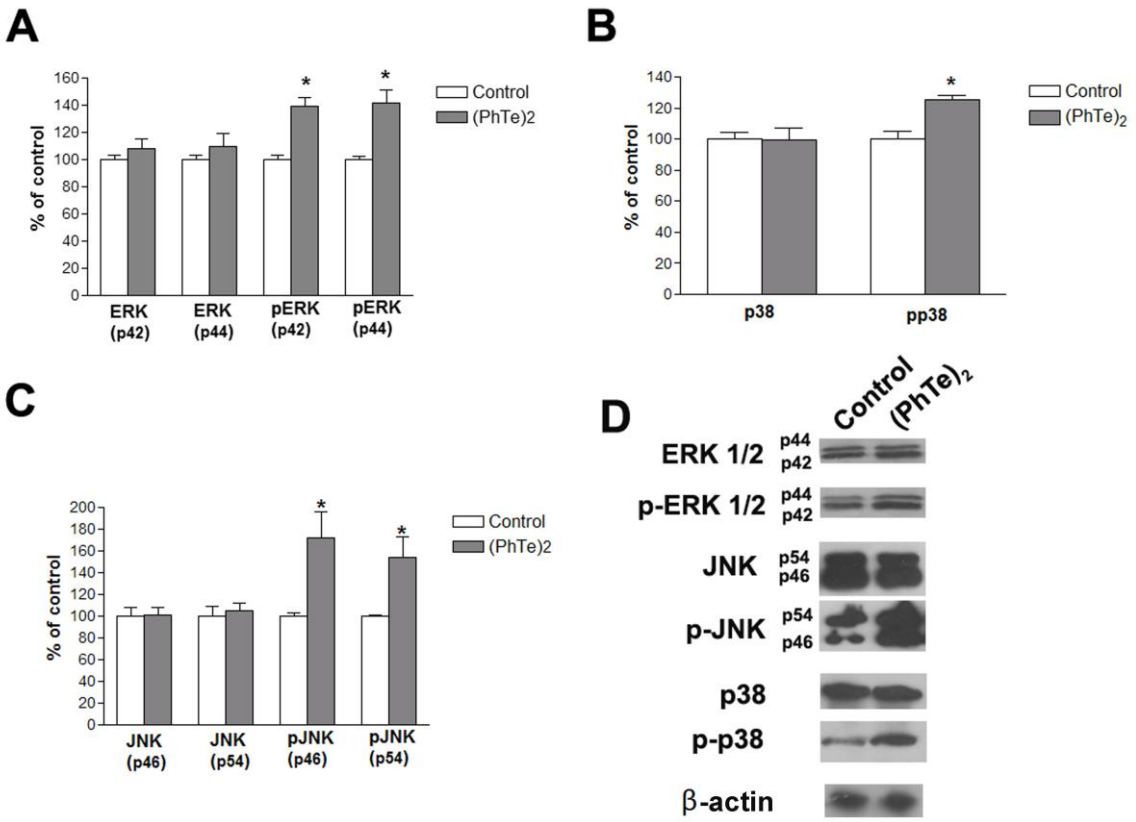
A
% of control
Control
(PhTe)2
ERK (p42)
ERK (p44)
pERK (p42)
pERK (p44)
B
% of control
Control
(PhTe)2
p38
pp38
C
% of control
Control
(PhTe)2
JNK (p46)
JNK (p54)
pJNK (p46)
pJNK (p54)
D
Control
(PhTe)2
ERK 1/2
p44
p42
p-ERK 1/2
p44
p42
JNK
p54
p46
p-JNK
p54
p46
p38
p-p38
β-actin

Figure 3:

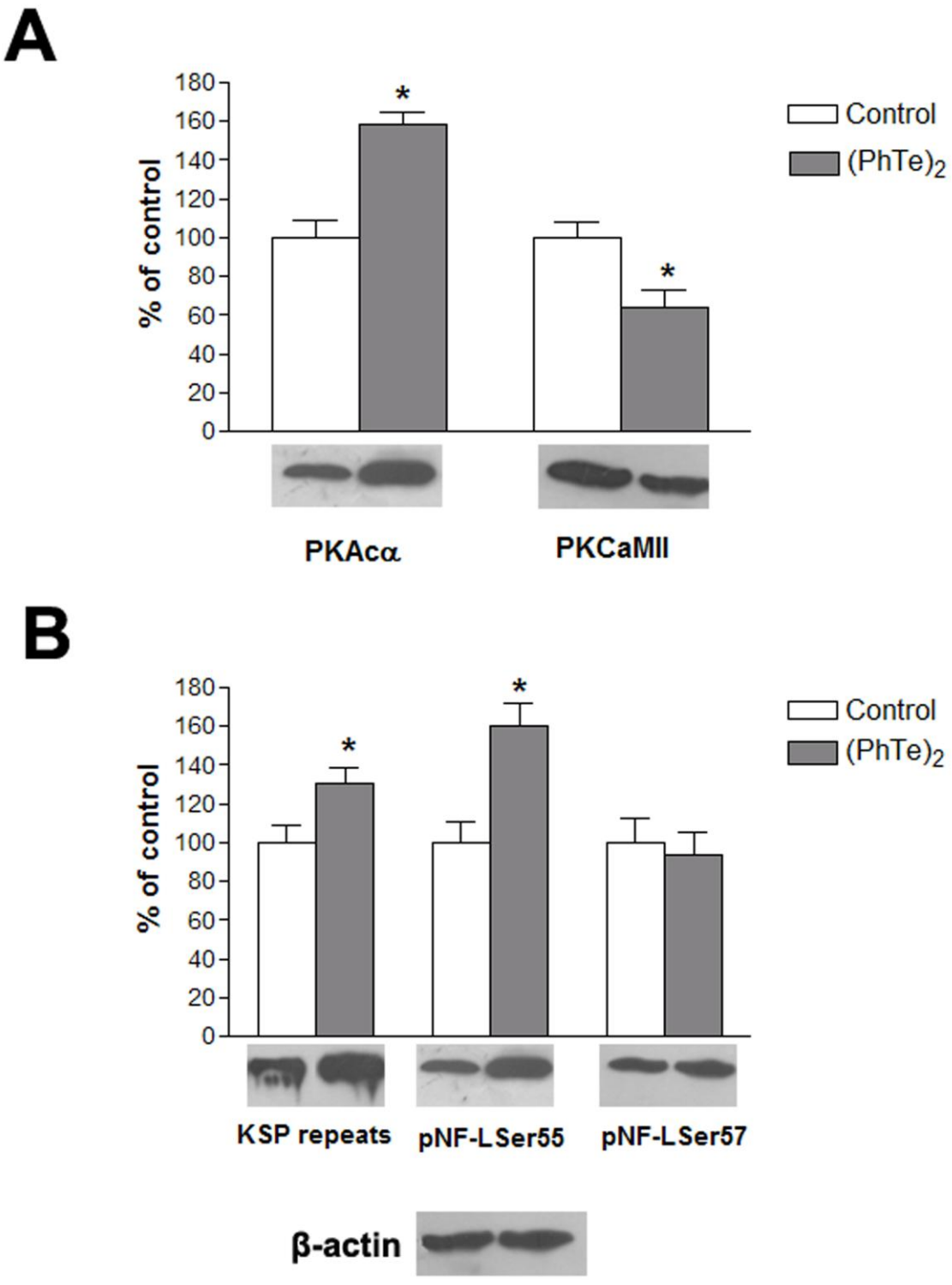
A
180
160
140
120
100
80
60
40
20
0
% of control
*
*
Control
(PhTe)2
PKAcα
PKCaMII
B
180
160
140
120
100
80
60
40
20
0
% of control
*
*
Control
(PhTe)2
KSP repeats
pNF-LSer55
pNF-LSer57
β-actin

Figure 4:

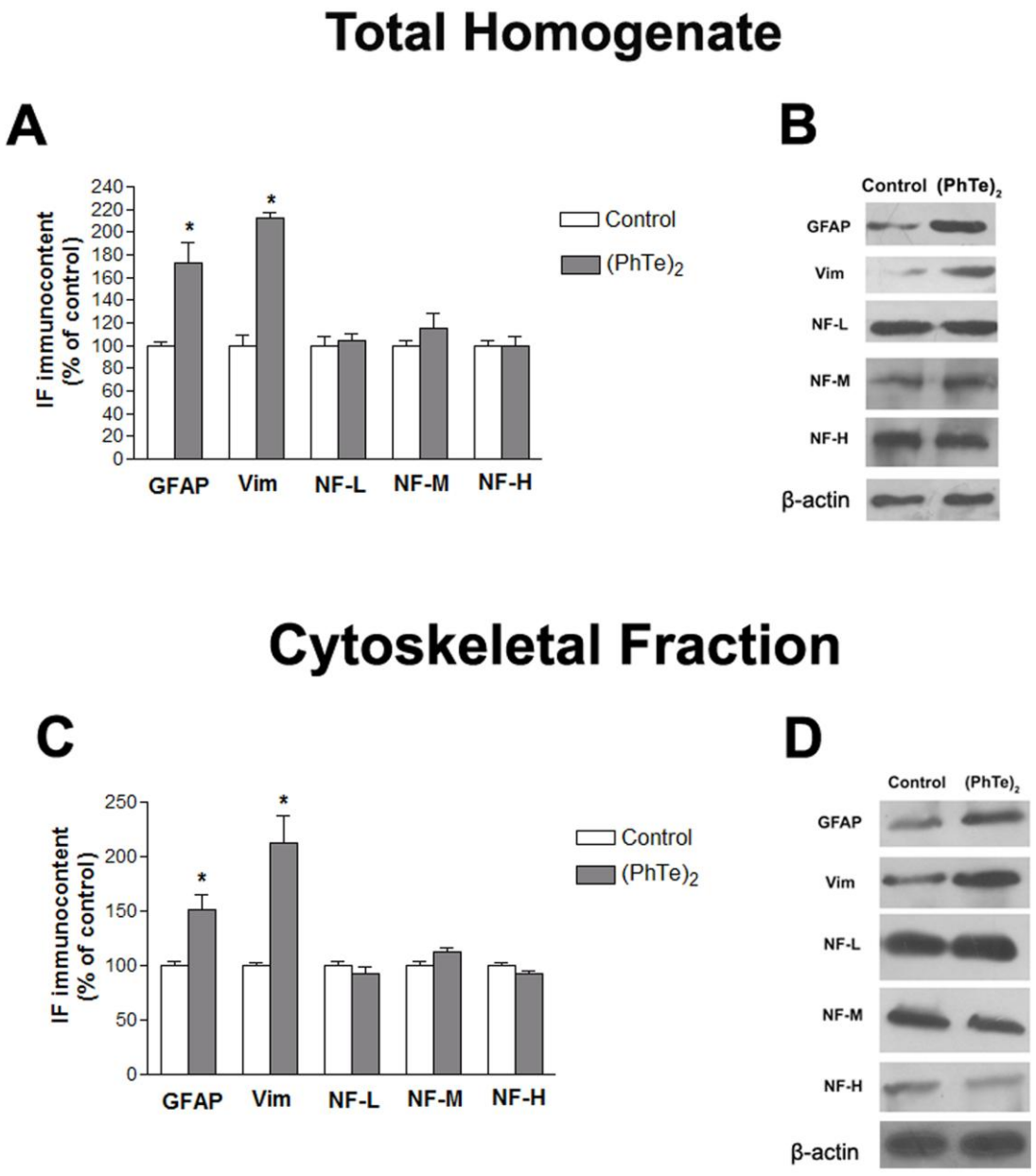
Total Homogenate
A
IF immunocontent (% of control)
240
220
200
180
160
140
120
100
80
60
40
20
0
GFAP
Vim
NF-L
NF-M
NF-H
Control
(PhTe)2
B
Control
(PhTe)2
GFAP
Vim
NF-L
NF-M
NF-H
β-actin
Cytoskeletal Fraction
C
IF immunocontent (% of control)
250
200
150
100
50
0
GFAP
Vim
NF-L
NF-M
NF-H
Control
(PhTe)2
D
Control
(PhTe)2
GFAP
Vim
NF-L
NF-M
NF-H
β-actin

Figure 5:

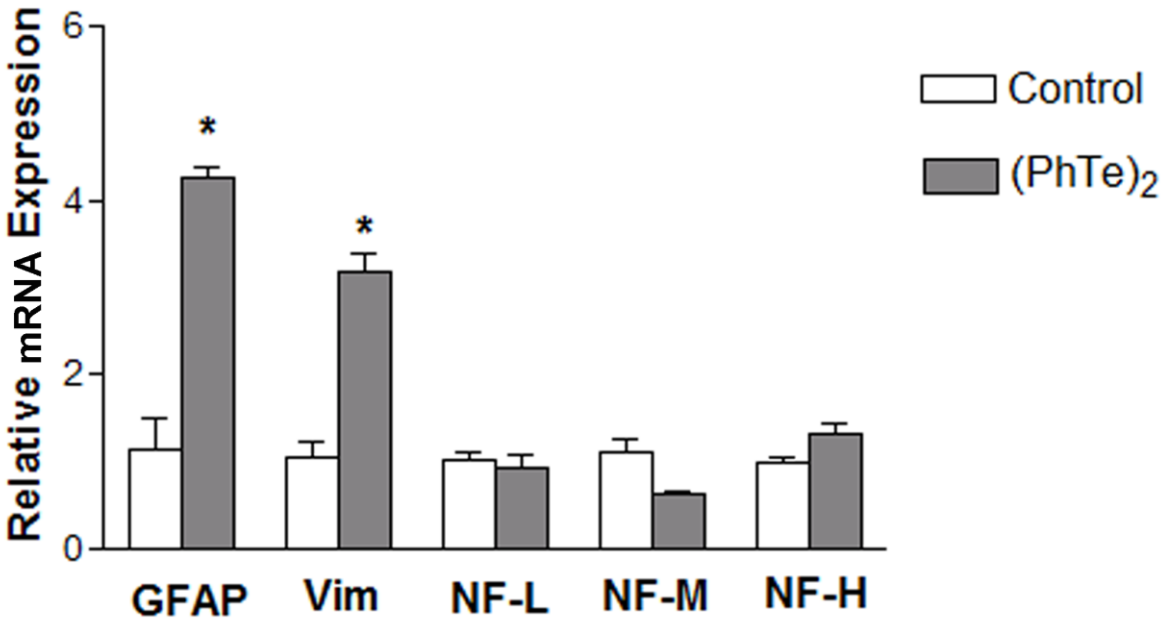
Relative mRNA Expression
6
4
2
0
*
*
GFAP
Vim
NF-L
NF-M
NF-H
Control
(PhTe)2

Figure 6:

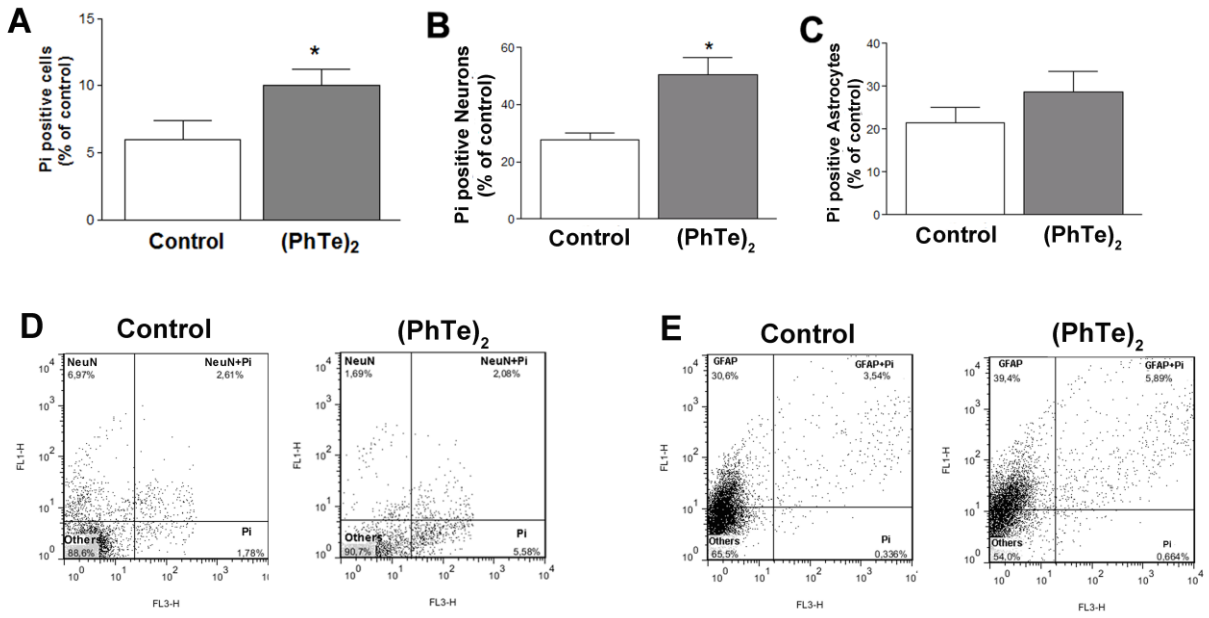
A
Pi positive cells (% of control)
15
10
5
0
*
Control
(PhTe)2
B
Pi positive Neurons (% of control)
60
40
20
0
*
Control
(PhTe)2
C
Pi positive Astrocytes (% of control)
40
30
20
10
0
Control
(PhTe)2
D
Control
(PhTe)2
NeuN
6,97%
NeuN+Pi
2,61%
Others
88,6%
Pi
1,78%
NeuN
1,69%
NeuN+Pi
2,08%
Others
90,7%
Pi
5,58%
FL1-H
FL3-H
E
Control
(PhTe)2
GFAP
30,6%
GFAP+Pi
3,54%
Others
65,5%
Pi
0,336%
GFAP
39,4%
GFAP+Pi
5,89%
Others
54,0%
Pi
0,664%
FL1-H
FL3-H

Figure 7:

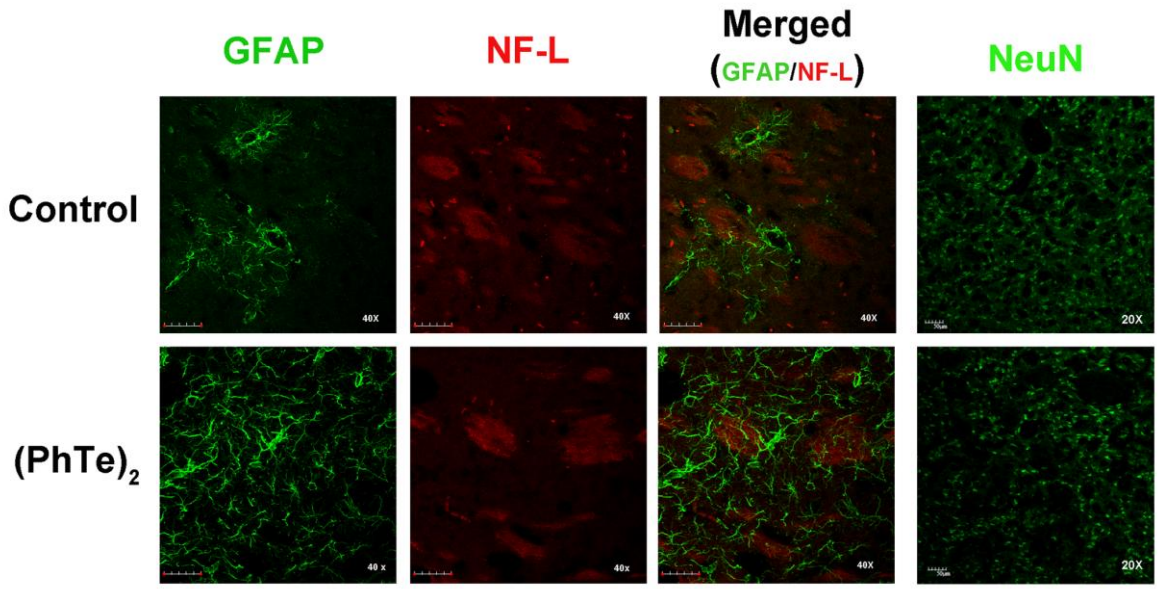
GFAP
NF-L
Merged
(GFAP/NF-L)
NeuN
Control
(PhTe)2
40X
40X
40X
20X
40 x
40x
40X
20X

Figure 8:

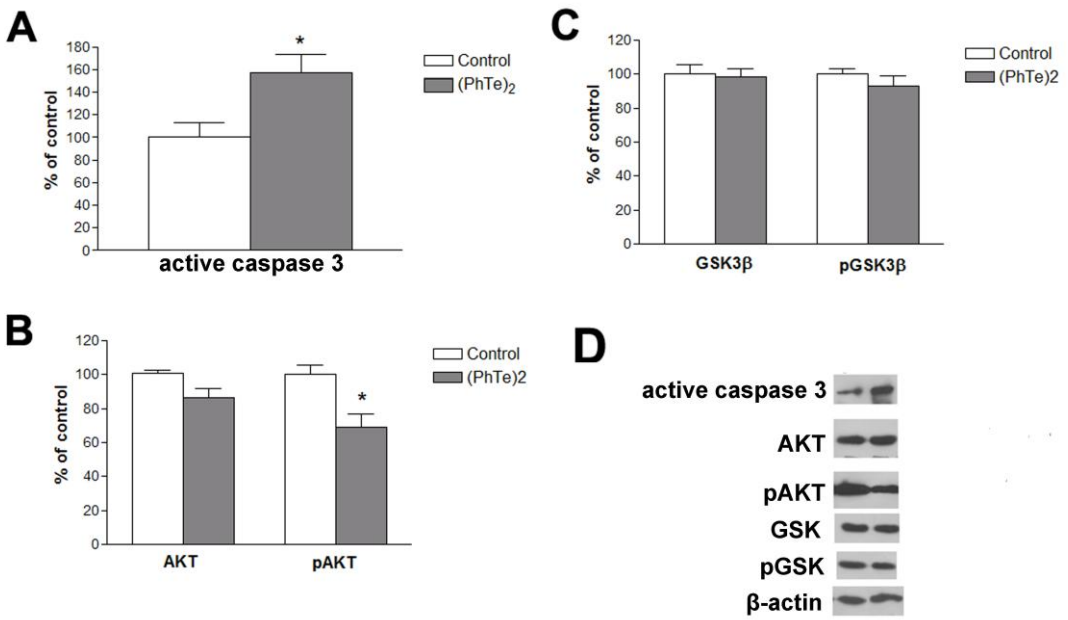
A
% of control
Control
(PhTe)2
active caspase 3
B
% of control
Control
(PhTe)2
AKT
pAKT
C
% of control
Control
(PhTe)2
GSK3β
pGSK3β
D
active caspase 3
AKT
pAKT
GSK
pGSK
β-actin

Capítulo 2

DISRUPTED CYTOSKELETAL HOMEOSTASIS, ASTROGLIOSIS AND APOPTOTIC CELL DEATH IN THE CEREBELLUM OF YOUNG RATS INJECTED WITH DIPHENYL DITELLURIDE

Luana Heimfarth‡, Samanta Oliveira Loureiro‡, Márcio Ferreira Dutra‡, Letícia Pettenuzzo‡, Cláudia Andrade‡, Bárbara Ortiz de Lima‡, Carolina Fernandez Gonçalves‡, Fátima Therezinha Costa Rodrigues Guma‡, Carlos Alberto Saraiva Gonçalves‡, João Batista Teixeira da Rocha§, and Regina Pessoa-Pureur‡

Artigo submetido à revista *Chemical Research in Toxicology*

DISRUPTED CYTOSKELETAL HOMEOSTASIS, ASTROGLIOSIS AND APOPTOTIC CELL DEATH IN THE CEREBELLUM OF YOUNG RATS INJECTED WITH DIPHENYL DITELLURIDE

Luana Heimfarth‡, Samanta Oliveira Loureiro‡, Márcio Ferreira Dutra‡, Letícia Pettenuzzo‡, Cláudia Andrade‡, Bárbara Ortiz de Lima‡, Carolina Fernandez Gonçalves‡, Fátima Therezinha Costa Rodrigues Guma‡, Carlos Alberto Saraiva Gonçalves‡, João Batista Teixeira da Rocha§, and Regina Pessoa-Pureur‡

‡Departamento de Bioquímica, Instituto de Ciências Básicas da Saúde, UFRGS, Porto Alegre, RS, Brasil

§Departamento de Química, Centro de Ciências Naturais e Exatas, Universidade Federal de Santa Maria, RS Brasil

CORRESPONDENCE ADDRESS: Dr. Regina Pessoa-Pureur, Universidade Federal do Rio Grande do Sul, Instituto de Ciências Básicas da Saúde, Departamento de Bioquímica, Rua Ramiro Barcelos 2600 anexo, 90035-003 Porto Alegre - RS, BRASIL, Fax: 5551 3308 5535, Tel: 5551 3308 5565; E-mail: rpureur@ufrgs.br

RUNNING TITLE: Diphenyl ditelluride causes cerebellar damage in young rats

KEYWORDS: cerebellum, diphenyl ditelluride, astrogliosis, cytoskeleton, neurodegeneration

Abstract

In the present report 15 day-old rats were injected with 0.3 μmol of diphenyl ditelluride $(PhTe)_2$/kg body weight and parameters of neurodegeneration were analyzed in slices from cerebellum 3 and 6 days afterwards. The earlier responses (3 days after injection) included hyperphosphorylation of intermediate filament (IF) proteins from astrocyte (glial fibrillary acidic protein -GFAP- and vimentin) and neuron (low-, medium- and high molecular weight neurofilament subunits: NF-L, NF-M and NF-H). Increased mitogen-activated protein kinase (MAPK) (Erk and p38MAPK) and cAMP-dependent prrotein kinase (PKA) activities were also observed. Also, reactive astrogliosis takes part of the early responses, evidenced by upregulation of GFAP in Western blot, PCR and immunofluorescence analysis. Six days after $(PhTe)_2$ injection we found persistent astrogliosis and increased propidium iodide (PI) positive cells in NeuN positive population evidenced by flux cytometry and reduced immunofluorescence for NeuN, indicating that *in vivo* exposure to $(PhTe)_2$ progressed to neuronal death. Moreover, activated caspase 3 suggested apoptotic neuronal death. Neurodegeneration was related with decreased [3H]glutamate uptake and decreased Akt immunoreactivity, however phospho-GSK-3-β (Ser9) was not altered in $(PhTe)_2$ injected rat. Therefore, the present results show that the earlier cerebellar responses to $(PhTe)_2$ included disruption of cytoskeletal homeostasis, which could be related with MAPK and PKA activation and reactive astrogliosis. Akt inhibition observed at this time could also play a role in the neuronal death evidenced afterwards. The later events

of the neurodegenerative process were characterized by persistent astrogliosis and activation of apoptotic neuronal death through caspase 3 mediated mechanisms, which could be related with glutamate excitotoxicity. The progression of these responses are therefore likely to be critical for the outcome of the neurodegeneration provoked by $(PhTe)_2$ in rat cerebellum.

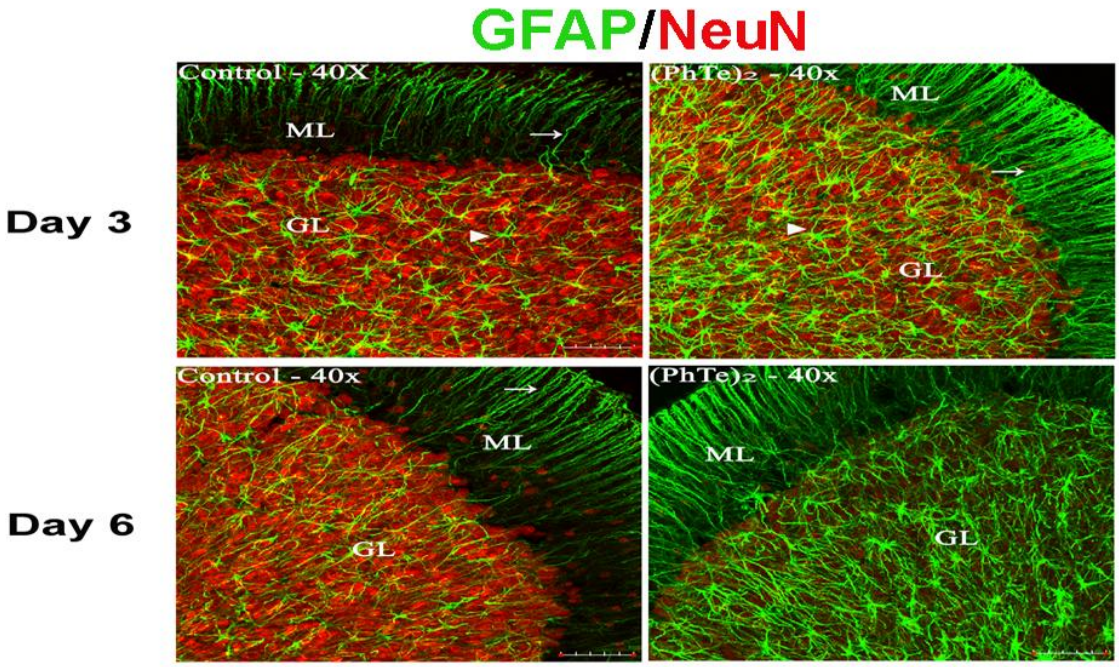

Introduction

The cerebellar functions include the control of attention and other cognitive functions, emotions and mood, and social behavior, which were all thought to represent cortical functions[1]. The cerebellum is considered particularly vulnerable in the newborn human as well as in the developing animal because of its very rapid growth at that time[2]. The concept of a particular vulnerability of the cerebellum during its phase of rapid growth is documented in experimental models of undernutrition, glucocorticoid

exposure, and X-irradiation[3,4,5]. Also, the importance of cerebellar physiology has been confirmed by the frequency of neuropsychiatric disorders in individuals with cerebellar abnormalities[1] .

Cell death and neuronal loss are the key pathological hallmarks of neurodegeneration in all the neurodegenerative disorders, with apoptosis and necrosis being central to both acute and chronic degenerative processes. In this context, the activation of p38MAPK signaling pathway is involved in the development of the motor neuron degeneration of the spinal cord. In addition, Paulino and colleagues[6] described that neurotoxicity in neural cells, may be mediated by the sustained activation of ERK pathway.

Also, astrogliosis is a hallmark of diseased CNS tissue[7]. This term refers to progressive changes in gene expression and cellular morphology, often including proliferation. The activation of astrocytes is characterized by changes in their molecular and morphological features. Although reactive astrogliosis is the normal physiological response essential for damage contention, it can also have detrimental effects on neuronal survival and axon regeneration, particularly in neurodegenerative diseases. It is believed that progressive changes in astrocytes as they become reactive are finely regulated by complex intercellular and intracellular signaling mechanisms. The most commonly used marker of activated astrocytes is the upregulation of the cytoskeletal proteins glial fibrillary acidic protein (GFAP), vimentin, and to some extent nestin, coincident with cellular hypertrophy[8].

Molecular mechanisms of neurotoxicity include oxidative/nitrosative stress, neuroinflammatory mechanisms and N-methyl-D-aspartate (NMDA) glutamate receptor-mediated excitotoxicity[9]. In this context, extracellular concentrations of

glutamate are maintained at relatively low levels to ensure an appropriate signal-to-noise ratio and to prevent excessive activation of glutamate receptors that can result in cell death. The latter phenomenon is known as excitotoxicity and has been associated with a wide range of acute and chronic neurodegenerative disorders, as well as disorders that result in the loss of non-neural cells such as oligodendroglia in multiple sclerosis[10].

Neurodegeneration has already been related with disruption of the cytoskeletal homeostasis of neural cells[11]. Neurofilaments (NF) are the most abundant cytoskeletal components of large myelinated axons from adult central and peripheral nervous system. They are constituted of the association of three NF subunits of low, medium and high molecular weight (NF-L, MF-M and NF-H). The assembly, axonal transport and functions of NF are responsible for the normal physiology of the nervous system. Conversely, misregulation of the cytoskeletal homeostasis might be responsible for the toxicity leading to pathological situations and to neuronal death. Following their synthesis and assembly in the cell body, NFs are transported along the axon. This process is finely regulated via phosphorylation of the carboxyl-terminal part of the two high-molecular-weight subunits of NF. The correct formation of an axonal network of NF is crucial for the establishment and maintenance of axonal caliber and consequently for the optimisation of conduction velocity and the frequent disruption of the NF network is observed in several neuropathologies[12].

Although the tellurium (Te) element rarely occurs in the free state in nature, metallic Te is known to be present in plant material, particularly in members of the Allium family, such as garlic[13]. A number of studies have shown that trace amounts of Te are present in body fluids, such as blood and urine[14,15]. Neurotoxicity of tellurium has been reported in the literature. In this context, inorganic tellurium treatment was found to cause significant impairment in retention of the spatial learning task[16]. But to

date, no telluroproteins have been identified in animal cells. Nowadays, two cases of toxicity in young children from ingestion of metal-oxidizing solutions that contained substantial concentrations of Te were reported in the literature[17]. Clinical features of acute Te toxicity include a metallic taste, nausea, blackened oral mucosa and skin and garlic odor of the breath[18,19].

Previous data from literature indicated that the organic compound of tellurium, diphenyl ditelluride $(PhTe)_2$ is extremely neurotoxic to rodents and exposure to low doses of this compound can cause profound neurostructural and neurofunctional deregulation in experimental animals[20]. Furthermore, $(PhTe)_2$ can also have neurotoxic effects *in vitro*, including cytotoxic effect in astrocytes[21] and changes in the phosphorylation of intermediate filaments (IF) in slices obtained from different brain structures of young rats[22,23]. In addition, Nogueira and colleagues[24] described decreased ^{3}[H]glutamate uptake after acute *in vivo* exposure to $(PhTe)_2$ in rat synaptic membranes. Corroborating these findings, Moretto and colleagues[25] found that neurotoxicity caused by $(PhTe)_2$ in slices of cerebral cortex could be related with the inhibition of ^{3}[H]glutamate uptake. Therefore, in an attempt to better understand the toxicity of organotellurium compounds, we studied the effect of $(PhTe)_2$ in the cerebellum of young rats acutely exposed to the same concentration of the neurotoxicant able to provoke systemic toxicity and to induce hyperphosphorylation of cytoskeletal proteins in cerebral cortex of rats[26]. In the present report we describe the progressive disruption of the cytoskeletal homeostasis, reactive astrogliosis and apoptotic neuronal death in the cerebellum of young rats 3 and 6 days after $(PhTe)_2$ injection. Also, we aimed to investigate some mechanisms related with the neurodegeneration elicited by the neurotoxicant.

Experimental Procedures

Radiochemical and compounds

[^{32}P]Na_2HPO_4 was purchased from CNEN, São Paulo, Brazil. l-[^{3}H]glutamate (52 Ci/mmol) was purchased from PerkinElmer Life and Analytical Sciences (Boston, MA, USA. Benzamidine, leupeptin, antipain, pepstatin, chymostatin, acrylamide and bis-acrylamide, anti-GSK3β, anti-phosphoGSK3β, anti-PKAcα, anti-PKCaMII, anti-active caspase 3, anti-AKT, anti-phosphoAKT, anti-GFAP (St. Louis, MO, USA; DAKO), anti-vimentin, anti-NF-L, anti-NF-M, anti-NF-H antibodies and propidium iodide were obtained from Sigma (St. Louis, MO, USA). The chemiluminescence ECL kit peroxidase and the conjugated anti-rabbit IgG were obtained from Amersham (Oakville, Ontario, Canada). Anti-ERK, anti-phosphoERK, anti-SAP/JNK, anti-phosphoSAP/JNK, anti-p38MAPK, anti-phosphop38MAPK and anti-KSP repeats, were obtained from Cell Signaling Technology (USA). Anti-phosphoSer55NF-L, anti-phosphoSer57NF-L and anti-NeuN antibodies were obtained from Millipore. Anti-rabbit Alexa 488 and anti-mouse Alexa 568 were from Molecular Probes. Fluor Save™ was from Merck. The organochalcogenide $(PhTe)_2$ was synthesized using the method described by Petragnami[27]. Analysis of the 1H NMR and 13C NMR spectra showed that the compound obtained presented analytical and spectroscopic data in full agreement with their assigned structures. The purity of the compounds were assayed by high ressonance mass spectroscopy (HRMS) and was higher that 99.9%. Diphenyl ditelluride was dissolved in dimethylsulfoxide (DMSO) just before use. The final concentration of DMSO was adjusted to 0.1%. Solvent controls attested that at this concentration DMSO did not interfere with the phosphorylation measurement. Platinum Taq DNA

polymerase and SuperScript-II RT pre-amplfication system were from Invitrogen. All other chemicals were of analytical grade and were purchased from standard commercial supplier.

Animals

Fifteen day-old Wistar rats were obtained from our breeding stock. Rats were maintained on a 12-h light/12-h dark cycle in a constant temperature (22^{o} C) colony room. On the day of birth the litter size was culled to seven pups. Litters smaller than seven pups were not included in the experiments. Water and a 20% (w/w) protein commercial chow were provided *ad libitum*. The experimental protocol followed the "Principles of Laboratory Animal Care" (NIH publication 85-23, revised 1985) and was approved by the Ethics Committee for Animal Research of the Federal University of Rio Grande do Sul.

Drug administration, preparation and labeling of slices

Fifteen day-old Wistar rats were treated with a single subcutaneous (s.c.) injection of $(PhTe)_2$ 0.3 μmol/kg body weight or canola oil (vehicle) (2.8 ml/kg body weight). Three or six days after treatment the rats were killed by decapitation, the cerebellum was dissected onto Petri dishes placed on ice and cut into 400 μm thick slices with a McIlwain chopper.

Preincubation

Tissue slices were initially preincubated at 30°C for 20 min in a Krebs-Hepes medium containing 124 mM NaCl, 4mM KCl, 1.2 mM $MgSO_4$, 25 mM Na-HEPES (pH 7.4), 12 mM glucose, 1 mM $CaCl_2$, and the following protease inhibitors: 1 mM benzamidine, 0.1 μM leupeptin, 0.7 μM antipain, 0.7 μM pepstatin and 0.7 μM chymostatin.

In vitro ^{32}P-sodium ortophosphate incorporation experiments

After preincubation, the medium was changed and incubation was carried out at 30 °C with 100 μl of the basic medium containing 80 μCi of [^{32}P] orthophosphate. The labeling reaction was normally allowed to proceed for 30 min at 30 °C and stopped with 1 ml of cold stop buffer (150 mM NaF, 5 mM, EDTA, 5 mM EGTA, l50 mM Tris-HCl, pH 6.5), and the protease inhibitors described above. Slices were then washed twice with stop buffer to remove excess radioactivity.

Preparation of the high salt-Triton insoluble cytoskeletal fraction from tissue slices

After incubation, preparations of IF-enriched cytoskeletal fractions were obtained from cerebellum of rats as described by Funchal and colleagues[28]. Briefly, after the labeling reaction, slices were homogenized in 400 μl of ice-cold high salt buffer containing 5 mM KH_2PO_4, (pH 7.1), 600 mM KCl, 10 mM $MgCl_2$, 2 mM EGTA, 1 mM EDTA, 1% Triton X-100 and the protease inhibitors described above. The homogenate was centrifuged at 15800 x g for 10 min at 4 °C, in an Eppendorf centrifuge, the supernatant was discarded and the pellet was homogenized with the same volume of the high salt medium. The resuspended homogenate was centrifuged as

described and the supernatant was discarded. The Triton-insoluble IF-enriched pellet, containing NF subunits, vimentin and GFAP, was dissolved in 1% SDS and protein concentration was determined.

Polyacrylamide gel electrophoresis (SDS-PAGE)

The cytoskeletal fraction was prepared as described above. Equal protein concentrations were loaded onto 10 % polyacrylamide gels and analyzed by SDS-PAGE[29]. After drying, the gels were exposed to T-MAT films at -70 ^{o}C with intensifying screens and finally the autoradiograph was obtained. Cytoskeletal proteins were quantified by scanning the films with a Hewlett-Packard Scanjet 6100C scanner and determining optical densities with an Optiquant version 02.00 software (Packard Instrument Company). Density values were obtained for the studied proteins.

Preparation of total protein homogenate

Tissue slices were homogenized in 100µl of a lysis solution containing 2 mM EDTA, 50 mM Tris-HCL, pH 6.8, 4% (w/v) SDS. For electrophoresis analysis, samples were dissolved in 25% (v/v) of solution containing 40% glycerol, 5% mercaptoethanol, 50 mM Tris-HCl, pH 6.8 and boiled for 3 min.

Western blot analysis

Protein homogenate (80 µg) or cytoskeletal fraction (60 µg) was analyzed by SDS-PAGE and transferred to nitrocellulose membranes (Trans-blot SD semi-dry

transfer cell, BioRad) for 1 h at 15 V in transfer buffer (48 mM Trizma, 39 mM glycine, 20% methanol and 0.25% SDS). The nitrocellulose membranes were washed for 10 min in Tris-buffered saline (TBS; 0.5 M NaCl, 20 mM Trizma, pH 7.5), followed by 2 h incubation in blocking solution (TBS plus 5% bovine serum albumin and 0,1% Tween 20). After incubation, the blot was washed twice for 5 min with TBS plus 0.05% Tween-20 (T-TBS), and then incubated overnight at 4°C in blocking solution containing the following antibodies: anti-GFAP (clone G-A-5) diluted 1:500; anti-vimentin (Vim 13-12) diluted 1:400; anti-NF-L (clone NR-4) diluted 1:1000; anti- NF-M (clone clone NN-18) diluted 1:400; anti-NF-H (clone N52) diluted 1:1000; anti-ERK1/2 diluted 1:1000; anti-phosphoERK diluted 1:1000; anti-SAP/JNK diluted 1:1000; anti-phosphoSAP/JNK (clone 98F2) diluted 1:1000; anti-p38MAPK (clone A-12) diluted 1:1000; anti-phosphop38MAPK diluted 1:1000; anti-PKAcα diluted 1:1000; anti-AKT (clone 2H10) diluted 1:1000, anti-phosphoAKT (clone 244F9) diluted 1:1000, anti-active caspase 3 diluted 1:1000; anti-GSK3β (clone 27C10) diluted 1:1000; anti-phosphoGSK3β diluted 1:1000; anti-KSP repeats (clone NP1) diluted 1:1000; anti-phoshoNF-LSer55 diluted 1:800, and anti-actin diluted 1:1000. The blot was then washed twice for 5 min with T-TBS and incubated for 2 h in blocking solution containing peroxidase conjugated anti-rabbit IgG diluted 1:2000 or peroxidase conjugated anti-mouse IgG diluted 1:2000. The blot was washed twice again for 5 min with T-TBS and twice for 5 min with TBS. The blots were then developed using a chemiluminescence ECL kit. Immunoblots were quantified by scanning the films with a Helwett-Packard Scanjet 6100C scanner and optical densities were determined with an OptiQuant version 02.00 software (Packard Instrument Company). Optical density values were obtained for the studied proteins.

RNA extraction, cDNA synthesis and quantitative PCR

RNA was isolated from cerebellum using the TRIzol Reagent (Invitrogen). Approximately 2 µg of total RNA were added to each cDNA synthesis reaction using the SuperScript-II RT pre-amplification system. Reactions were performed at 42 ºC for 1 h using the primer T23 V (5` TTT TTTTTTTTTTTTTT TTTTTV). Quantitative PCR amplification was carried out using specific primer pairs designed with Oligo Calculator version 3.02 (http://www.basic.nwu.edu/biotools/oligocalc.html) and synthesized by IDT (MG, Brazil). The sequences of the primers used are listed in Table 1. Quantitative PCRs were carried out in an Applied-Biosystem Step One Plus real-time cycler and done in quadruplicate. Reaction settings were composed of an initial denaturation step of 5 min at 95 ºC, followed by 40 cycles of 10 s at 95 ºC, 10 s at 60 ºC, 10 s at 72 ºC; samples were kept for 1 min at 60 ºC for annealing and then heated from 55 to 99 ºC with a ramp of0.3 ºC /s to acquire data to produce the denaturing curve of the amplified products. Quantitative PCRs were made in a 20 µl final volume composed of 10 µl of each reverse transcription sample diluted 50–100 times, 2 µl of 10 times PCR buffer, 1.2 µl of 50 mM $MgCl_2$, 0.4 µl of 5 mM dNTPs, 0.8 µl of 5 µM primer pairs, 3.55 µl of water, 2.0 µl of SYBR green (1:10,000 Molecular Probe), and 0.05 µl of Platinum Taq DNA polymerase (5 U/ ul). All results were analyzed by the 2 - DDCT method (Livak and Schmittgen, 2001). TBP (TATA box binding protein) was used as the internal control gene for all relative expression calculations[30].

Table 1. Primers used for qPCR (quantitative polymerase chain reaction).

Forward Primer	Reverse Primer

GFAP	5`CAGAAGCTCCAAGATGAAACCAA	5`TCTCCTCCTCCAGCGACTCAAC
Vim	5´CCCAGATTCAGGAACAGCAT	5´CACCTGTCTCCGGTATTCGT
NF-L	5′CCATGCAGGACACAATCAAC	5′CTGCAAGCCACTGTAAGCAG
NF-M	5′GAGATGTATTACGCAAAGTACG5′	5′CCAGTATGACCTTTATTGAGC
NF-H	5′ACCTATACCCGAATGCCTTCTT	5′AGAAGCACTTGGTTTTATTGCAC
B-actin	5`TATGCCAACACAGTGCTGTCGG	5`TACTCCTGCTTCCTGATCCACAT
TBP	5`CCCCACAACTCTTCCATTCT	5`GCAGGAGTGATAGGGGTCAT

GFAP, glial fibrillary acidic protein; Vim, vimentin; NF-L, low molecular weight neurofilament subunit; NF-M, middle molecular weight neurofilament subunit; NF-H, high molecular weight neurofilament subunit; TBP, TATA box binding protein

Immunofluorescence

Twelve pups (six for group) were anesthetized using ketamine/xylazine (75 and 10 mg/Kg, respectively, i.p.) and were perfused through the left cardiac ventricle with 40 ml of 0,9% saline solution, followed by 40 ml of 4% paraformaldehyde in 0.1 M phosphate buffered saline (PBS), pH 7.4, and the descendent aorta was campled. After the perfusion the brains were removed, post-fixed in the same fixative solution for 4 h at room temperature and cryoprotected by immersing in 15% and after in 30% sucrose solution in PBS at 4°C. The brains were then frozen by immersion in isopentane cooled with CO_2 and stored in a freezer (-80 ºC) for later analyses. Serial coronal sections (40 µm) of cerebellum were obtained using a cryostat at -20 ºC (Leica). The free-floating sections were incubated two overnights with rabbit polyclonal anti-GFAP and mouse anti-NeuN (clone A60), diluted 1:3000 and 1:1000, respectively, in PBS containing 0.3% Triton X-100 (PBS-Triton X-100 0.3%) and 2% bovine serum albumin (BSA 2%). The negative controls were performed omitting the primary antibodies. After

washing several times in PBS, tissue sections were incubated with anti-rabbit Alexa 488 and anti-mouse Alexa 568, both diluted 1:500 in PBS-Triton X-100 0.3% and BSA 2% for 1 h at room temperature. Afterwards, the sections were washed several times in PBS, transferred to gelatinized slides, mounted with Fluor Save™, covered with coverslips and sealed with nail polish. The images were obtained with an Olympus IX-81 confocal FV-1000 microscope and analyzed with an Olympus Fluoview software.

Flow cytometry analysis

Tissues were dissociated with PBS/colagenase/DNase, washed once with PBS then suspended in PBS/colagenase containing 10 μg/ml propidium iodide (PI). The integrity of plasma membrane was assessed by determining the ability of cells to exclude PI. The cells were incubated at room temperature for 30 min in the dark, washed with PBS and centrifuged at 3000 rpm for 5 min at 4 °C to remove the free PI. Afterwards, the cell was permeabilized with 0.2% PBS Triton X-100 in for 10 min at room temperature and blocked for 15 min with BSA 5%. After blocking, cells were incubated in blocking solution containing the monoclonal antibodies anti-NeuN (clone A60) diluted 1:100 or anti-GFAP diluted 1:100, for 2 h. The cells were washed twice with PBS and incubated for 1 h in blocking solution containing FITC-anti-rabbit IgG diluted 1:200 or Alexa 488-anti-mouse IgG diluted 1:200. The levels of PI incorporation, levels of positive NeuN cells and positive GFAP cells were determined by flow cytometry (FACSCalibur, Becton Dickinson, Franklin Lakes, NJ, USA). FITC or Alexa Fluor 488 and PI dyes were excited at 488 nm using an air-cooled argonlaser. Negative controls (samples with the secondary antibody) were included for setting up the machine voltages. Controls stained with a single dye (Alexafluor 488 or FITC and

propidium iodide) were used to set compensation. The emission of fluorochromes was recorded through specific band-pass fluorescence filters: green (FL-1; 530 nm/30) and red (FL-3; 670 nm long pass). Fluorescence emissions were collected using logarithmic amplification. In brief, data from 10.000 events (intact cells) were acquired and the mean relative fluorescence intensity was determined after exclusion of debris events from the data set. All flow cytometric acquisitions and analyses were performed using Flow Jo software. Flow cytometry data were analyzed and plotted by density as a dot plot which shows the relative FL1 fluorescence on the x-axis and the relative FL3 fluorescence on the y-axis. The quadrants to determinate the negative and positive area were placed on no stained samples. The number of cells in each quadrant was computed and the proportion of cells stained with PI, GFAP and NeuN were expressed as percentage of PI uptake and percentage of astrocytes or neurons.

Glutamate Uptake

The animals were decapitated, and the brain was immediately removed and submerged in Hank's balanced salt solution (HBSS) containing 137 mM NaCl, 0.63 mM $Na_2HPO_4 \cdot 7H_2O$, 4.17 mM $NaHCO_3$, 5.36 mM KCl, 0.44 mM KH_2PO_4, 1.26 mM $CaCl_2 \cdot 2H_2O$, 0.41 mM $MgSO_4 \cdot 7H_2O$, 0.49 mM $MgCl_2 \cdot 6H_2O$, and 1.11 mM glucose, adjusted to pH 7.2. Cerebellum was dissected, and cortical slices (400 µm) were obtained using a McIlwain chopper. The slices were washed with HBSS, and the sections were finally separated with the help of a magnifying glass. Glutamate uptake was performed according to Frizzo and colleagues[31]. Briefly, slices were preincubated at 35°C for 15 min. Incubation was carried out at 35 °C by adding 12.2 MBq/L L^3[H]glutamate and 100 µM unlabeled glutamate in HBSS to the incubation system.

The reaction was stopped after 7 min by five ice-cold washes with 0.5 ml HBSS, immediately followed by addition of 0.5 M NaOH, which was kept overnight. Sodium independent uptake (nonspecific uptake) was determined by using *N*-methyl-D-glucamine instead of sodium chloride. Sodium dependent uptake was calculated as the difference between the uptake measured in a medium containing sodium and the uptake measured in a similar medium in the absence of sodium. Radioactivity incorporated was determined with a Wallac scintillation spectrometer. Protein concentration was measured. All experiments were performed in triplicate, and the mean was used for the statistical calculations.

Protein determination

The protein concentration was determined by the method of Lowry and colleagues[32] using serum bovine albumin as the standard.

Statistical analysis

Data were analyzed statistically by one-way analysis of variance (ANOVA) followed by the Tukey-Kramer multiple comparison test when the F-test was significant. All analyses were performed using the SPSS software program on an IBM-PC compatible computer.

Results

We have previously described that a single administration of $(PhTe)_2$ (0.3µmol /kg body weight) caused hyperphosphorylation of IF proteins from cortical[26] slices of young rats six days after injection. On the basis on these results, in the present report we attempted to analyze the *in vivo* effects of $(PhTe)_2$ on the cerebellum. Therefore, slices from cerebellum of rats injected with 0.3 µmol $(PhTe)_2$/kg body weight were incubated with ^{32}P-orthophosphate and the phosphorylation pattern of astrocyte (GFAP and vimentin) as well as neuron IF proteins (NF-L, NF-M and NF-H) were evaluated 3 and 6 days afterwards. As depicted in Figure 1A, we found hyperphosphorylation of all the cerebellar IF proteins studied 3 days after injection, however phosphorylation levels returned to control levels 6 days afterwards (Figure 1B). Figure 1C shows a representative phosphorylation experiment.

Next, we examined the involvement of MAPKs and PKA respectively in the actions of the neurotoxicant by Western blot analysis with specific monoclonal antibodies. Results showed that the MAPK signaling was activated in cerebellar slices 3 days after injection (Figure 2 A,C and E) returning to control levels 6 days afterwards (Figure 2 B,D and F). PhosphoErk (Figure 2A) and phosphop38MAPK (Figure 2 E) were also activated by $(PhTe)_2$ 3 days after injection. However, phosphoJNK (Figure 2 C,D), was not activated until 6 days after injection. Figure 2G shows representative blots of total and phospho forms of the kinases studied. The effect of $(PhTe)_2$ on PKA activity showed an increased cerebellar PKAcα immunoreactivity by Western blot assay only 3 days after injection (Figure 3A), returning to control levels at day 6 (Figure 3B). This is compatible with a transient activation of this protein kinase early after the insult. Representative blots are shown.

In an attempt to identify the phosphorylating sites targeted by the protein kinases PKA and MAPK in the cerebellum, we assayed NF-LSer55 on NF-L head domain as well as KSP repeats on NF-M/NF-H tail domain, respectively. As depicted in Figure 4, results obtained with Western blot assay using anti-phosphoSer55 antibody and anti-NFM/NFH KSP repeats showed that the phosphorylation level at these sites, was increased 3 days after treatment with $(PhTe)_2$. These findings are consistent with a role for PKA and MAPKs in the hyperphosphorylation of the neuronal IF proteins 3 days after injection. Representative blots are shown.

Next, we analyzed the effect of $(PhTe)_2$ on the immunocontent of the IF proteins from total homogenate from cerebellum or from the proteins recovered into the high-salt Triton-insoluble cytoskeletal fraction of tissue slices 3 and 6 days after the injection. We found that the immunocontent of GFAP was significantly increased in the cerebellar homogenate and in the cytoskeletal fraction 3 days after injection (Figure 5A and B). This effect persisted until 6 days after the insult, since at this time both GFAP and vimentin immunocontent remained significantly increased (Figure 5C and D). Conversely, the immunocontent of the neuronal IFs (NF-L, NF-M and NF-H) was not altered in response to $(PhTe)_2$ injection until day 6 (Figure 5 A,B,C and D). Representative immunoblots of the cytoskeletal proteins in total homogenate and in the cytoskeletal fraction are shown. Consistent with the persistent increase of GFAP and vimentin levels, RT-PCR analysis showed over-expression of GFAP and vimentin mRNA at day 6 after injection, while expression of NF subunits was not altered (Figure 6), supporting increased astrocyte proliferation compatible with reactive astrogliosis in this cerebral structure at this time.

For the purpose of assessing cell viability we carried out flow cytometry analysis using PI-exclusion assay to determine the percentage of viable cells. Results showed

that $(PhTe)_2$ was not able to alter the number of PI positive cells 3 days after injection, however 80% increased Pi positive cells were found at day 6 after exposure to the neurotoxicant (Figure 7A). Considering the NeuN positive cells, we found 100% increased Pi incorporation compared with control neurons 6 days after injection, while at day 3 after injection this number was not significantly different from controls (Figure 7B). Similarly, PI incorporation into GFAP positive cells increased 60% in response to $(PhTe)_2$ injection only at day 6 (Figure 7C). The number of neuronal cells was evaluated by the specific staining with NeuN. Results showed 50% decreased NeuN positive cells in the cerebellum 6 days after $(PhTe)_2$ injection (Figure 7D). Otherwise, GFAP positive cells were 50% increased at day 3, maintaining 30% increase 6 days afterwards (Figure 7E). Altogether, these findings indicate that *in vivo* exposure to $(PhTe)_2$ provoked neuronal death in the cerebellum of rats at day 6 after injection. However, RT-PCR analysis showed over-expression of GFAP and vimentin mRNA. Otherwise, the expression of NF subunits was not altered (Figure 6), supporting the hypothesis of reactive astrogliosis in this cerebral structure.

To further characterize the tissue damage after the *in vivo* exposure to $(PhTe)_2$, we carried out immunofluorescence analysis of cerebellar sections. Therefore, the tissue sections were processed for double immunofluorescence for GFAP and Neu-N, and analyzed by confocal microscopy. As depicted in Figure 8A, the confocal analysis showed a dramatic astrogliosis in the gray and white matters at day 3 after injection. In the molecular layer (ML) it was observed an enhanced expression of the glial processes (radial or Bergmann fibers) and in the granular layer (GL) a clear increase in GFAP expression of protoplasmatic astrocytes was evidenced, in which reactive astrocytes were characterized by increase in the size of the cell body and/or processes. Also, results showed no difference in NeuN immunofluorescence in the cerebellum of $(PhTe)_2$

injected rats compared with control ones (Figure 8A) at this time. Otherwise, at day 6 after injection we observed persistent astrogliosis and an accentuated decrease in NeuN staining in GM and ML layers (Figure 8B).

Western blot analysis with anti-caspase 3 antibody showed that in $(PhTe)_2$ treated cerebellar slices this key caspase is activated only 6 days after injection, suggesting apoptotic cell death (Figure 9A and B). In an attempt to determine signaling mechanisms involved in the neuronal death we evaluated the PI3K/Akt signaling pathway. Western blot analysis using anti-Akt antibody showed decreased phosphoAkt immunoreactivity (Figure 9 C and D) in $(PhTe)_2$ treated slices 3 and 6 days after injection, which is compatible with down-regulated survival mechanisms in the cerebellum of treated animals[33]. Also, it was evaluated the GSK-3-β activity, since it is described as a kinase that can be modulated by Akt activity[33]. We found that phosphoGSK-3-β (Ser9) was not altered in the cerebellum of $(PhTe)_2$ injected rats 3 or 6 days after treatment, suggesting that this kinase is not directly implicated in the neurotoxicity of this compound (Figure 9E and F). The representative immunological reactions are shown.

Since it has been previously described that *in vitro* treatment with $(PhTe)_2$ inhibited ^{3}[H]glutamate uptake in synaptosomes of 14 day old rats[34], we investigated the possibility that the neurodegeneration we are evidencing could be related with glutamate-mediated mechanisms. Results showed that 3 and 6 days after $(PhTe)_2$ injection ^{3}[H]glutamate uptake was decreased (Figure 10), suggesting that glutamate excitotoxicity could be involved in the neurodegeneration provoked by the neurotoxicant in the cerebellum of the young rats.

Discussion

We have previously demonstrated that young rats (15 day-old) acutely injected with 0.3 μmol $(PhTe)_2$ /kg of body weight presented weight loss from day 2 up to day 6 after drug exposure, indicating systemic toxicity at this concentration[26]. In the present study we attempted to further investigate the mechanisms underlying neurotoxicity of $(PhTe)_2$ in acutely injected 15 day-old rats. In our experimental approach we have chosen the cerebellum, going along with the progression of the damage 3 and 6 days after injection, since in these young rats this developmental period corresponds to intense cerebellar maturation. Cerebellar neurons are generated in two germinative neuroepithelia in two waves of proliferation and migration processes. During the embryonic period the first neurons to be generated are the deep nuclear neurons and all the Purkinje cells that migrate immediately after to the cerebellar plate. During postnatal life, the second wave of proliferation occurs in the external granular layer (EGL), the secondary germinal zone giving rise to the granular cells which migrate radially inward to their final destination in the internal granular layer (IGL). The proliferation of granular cells is regulated by Purkinje cells (PC). In the rat, although the extension of the lateral domain of the dendritic tree of the PC is achieved at postnatal day 15, its final extension, that is, adult size, is reached at postnatal day 30[2]. Therefore, elucidation of the biochemical steps leading to $(PhTe)_2$-induced neurotoxicity in this developmental period provide us new clues to the mechanisms underlying the actions of this neurotoxin in the cerebellum.

There is now compelling evidence for the critical role of the cytoskeleton in neurodegeneration[35]. Aberrant NF phosphorylation is a pathological hallmark of many human neurodegenerative disorders as well as is found after stressor stimuli[11,36] reflecting an altered activity of the phosphorylating system associated with the IF

proteins. Despite the functional role of NF phosphorylation is to date not completely clear, phosphorylation of amino-terminal domain of NF-L and other IF subunits has been related with their association into filamentous structures (for review see[36]), while *in vitro* phosphorylation of carboxyl-terminal domains of NF-H and NF-M straightens individual NFs and promotes their alignment into bundles[37]. Otherwise, the *in vivo* phosphorylation of these proteins is associated with an increased interNF spacing[38]. As a consequence, NF-H and NF-M carboxyl-terminal side arms extend and form cross-bridges among NF and other cytoskeletal elements[39]. The present results are consistent with a role for the cytoskeleton in the neural injury, since we observed that the acute administration of $(PhTe)_2$ elicited hyperphosphorylation of GFAP, vimentin and NF subunits 3 days after injection, returning to control values 6 days afterwards, evidencing an early and transient response to the action of the neurotoxicant. Accordingly, NFLSer55 appeared to be a specific amino-terminal phosphorylation site targeted by $(PhTe)_2$, being PKA the most prominent protein kinase mediating this effect. It is important to note that PKA (Ser-55) phosphorylation sites are relevant for filament assembly. Furthermore, the phosphate present in Ser55 of NF-L is turned over rapidly following NF-L synthesis in neurons[40] suggesting a possible role in the blockade of NF assembly before their transport into neurites. Like NF-L, PKA-mediated phosphorylation of the head domain of GFAP inhibits filament assembly or induces disassembly[41]. Therefore, our results showing NF-LSer55 hyperphosphorylation suggest a key role for $(PhTe)_2$ on IF dynamics preventing filament assembly and disassembling preexisting filaments.

It is known that carboxyl-terminal phosphorylation of NF-H progressively restricts the association of NFs with kinesin, the axonal anterograde motor protein, and stimulates its interaction with dynein, the axonal retrograde motor protein[42]. This event

could represent one of the mechanisms by which carboxyl-terminal phosphorylation would slow NF axonal transport. Consistent with this, MAPK phosphorylates NF-M and NF-H tail domains at specific carboxyl-terminal located KSP repeats[43] and alters the association of NF with motor proteins[44]. It is feasible that extensively phosphorylated KSP repeats on NF-M and NF-H as well as MAPK (Erk, and phospho38MAPK) activation we found in the cerebellum of $(PhTe)_2$-treated rats at day 3 after injection could interfere with NF axonal transport and contribute, at least in part, to the neuronal damage provoked by the neurotoxin.

Taking into account the present findings, we are tempted to speculate that disruption of cytoskeletal homeostasis in the cerebellum of injected rats was mediated by the transient MAPK activation and preceded the neurodegeneration provoked by the $(PhTe)_2$. Interestingly, in our experimental model JNK apparently was not implicated in the response to the neurotoxicant, although p38MAPK and JNK signaling pathways are supposed to act sinergistically upstream of mechanisms leading to apoptotic neuronal death in different models of neurodegeneration[45].

To better understand the progression of the molecular mechanisms underlying neuronal loss in acutely $(PhTe)_2$ injected rats, we assayed the caspase 3 activity and we found that this caspase is activated only at day 6, consistent with data from flux cytometry and immunohistochemistry, showing neuronal death at this time. Because activation of caspases, and caspase-3 in particular, appears to be a major factor for neuronal apoptosis execution in brain[46], the evaluation of upstream modulatory mechanisms is important for understanding the regulation of the apoptotic process elicited by $(PhTe)_2$. In this context, it is important to note that release of cytochrome c from mitochondria plays critical roles in the apoptotic cascade, activating caspase-9 which, in turn, activates executioner caspase-3 and -7[47]. Thus, activation of caspase-3

by cytochrome c-mediated caspase-9 activation could explain the neuronal apoptosis in the cerebellum of $(PhTe)_2$-treated rats. However we cannot exclude that caspase 3 be activated by extrinsic mechanisms, independently of cytochrome c release.

Additional evidence of the pro-apoptotic mechanism of action of $(PhTe)_2$ comes from our results showing decreased Akt phosphorylation/activity in cerebellar slices until 6 days after injection. The PI3K-Akt signaling pathway plays a critical role in mediating survival signals in a wide range of neuronal cell types[48]. The identification of a number of substrates for the serine/threonine kinase Akt suggests that it blocks cell death by both impinging on the cytoplasmic cell death machinery and by regulating the expression of genes involved in cell death and survival[49]. This is in line with Zhou and colleagues[50] who described that activated Akt may inhibit activation of caspase-9 and -3 by posttranslational modification of a cytosolic factor downstream of cytochrome c and before activation of caspase-9[48]. Therefore, inhibited PI3K-Akt pathway that was found in $(PhTe)_2$ could be consistent with the apoptotic insult observed in the cerebellum. Otherwise, GSK3β is a critical downstream element of the PÌ3K/Akt pathway and its activity can be inhibited by Akt-mediated phosphorylation at Ser9[51]. However, in our experimental model of $(PhTe)_2$-induced neurodegeneration, Akt inhibition is apparently not implicated in GSK3β (Ser9) hyperphosphorylation, supporting different signaling pathways downstream of different stressor events.

On the other hand, we verified the role of glutamate uptake since cerebellar granule cells are targets to the glutamate excitotoxicity[52] and we found that $(PhTe)_2$ inhibited ^{3}[H]glutamate uptake at day 6 after injection. It is known that excessive activation ionotropic and metabotropic glutamate receptors leads to excitotoxicity, especially in brain regions that are developmentally and regionally vulnerable to this kind of injury, therefore it is feasible to propose that the neurodegeneration we found at

day 6 after the insult could be related with excitotoxic mechanisms. Although the relevance of glutamate-mediated excitotoxicity, the molecular mechanisms underlying excitotoxicity-induced neurodegeneration remain poorly understood. However, overstimulation of the ionotropic NMDA receptor results in enhanced calcium influx and death of the cells. Mitochondria play a central role in directing cell death signaling generated at the NMDA receptors. The influx of cytoplasmic calcium resulting from excitotoxicity leads to the accumulation of calcium in the mitochondria[53]. In this context, mitochondrial dysfunction and reactive oxygen species (ROS) production[54,55, 56] have been largely related with glutamate excitotoxicity in different brain regions. Also, disruption of microtubule-based retrograde cargo transport through dynein and dynactin complexes are among the molecular mechanisms proposed to mediate glutamate-induced neuronal death. Taking into account that glutamate excitotoxicity is upstream of cytochrome c release from mitochondria and therefore caspase-3 activation, we could establish a causal link between inhibited ^{3}[H]glutamate uptake and the caspase-3-mediated pro-apoptotic action of $(PhTe)_2$.

In the CNS, following injury, astrocytes become reactive, a prominent process leading to the formation of the glial scar that inhibits axon regeneration after CNS injury. Upon becoming reactive, astrocytes undergo various molecular and morphological changes including upregulation of their expression of GFAP, vimentin and chondroitin sulfate proteoglycans as well as other molecules that are inhibitory to axon growth[57]. Upregulation of IFs is a hallmark of astrogliosis and a well-accepted indicator of structural damage in the CNS[8]. Upon $(PhTe)_2$ exposure, the GFAP levels increased at day 3, remaining upregulated until day 6. At this time vimentin was also upregulated and mRNA overexpression of these proteins was confirmed by quantitative PCR. It is interesting to note that mRNA overexpression was much more relevant than

GFAP levels present in the astrocytes at day 6. This could be ascribed to increased GFAP degradation in astrocytes from $(PhTe)_2$ damaged cerebellum. Moreover, it is important to note that increased PI positive astrocytes were found concomitantly with overexpressing GFAP positive cells in the flow cytometry data. The meaning of these findings are not well understood, however they could reflect different signaling pathways elicited by $(PhTe)_2$ in distinct astrocyte populations, while a cell population respond with an intense cell proliferation another could be simultaneously going to death at day 6 after the insult.

Consistent with the pro-apoptotic effect of $(PhTe)_2$ on cerebellar neurons at day 6 after the insult, we found a prominent increase of GFAP and vimentin expression earlier, at day 3, which suggests astrogliosis preceding neuronal death. Astrogliosis is the normal physiological response essential for damage contention. However, it can also have detrimental effects on neuronal survival and axon regeneration, particularly in neurodegenerative insults. It is believed that progressive changes in astrocytes as they become reactive are finely regulated by complex intercellular and intracellular signaling mechanisms. Reports describing whether the MAPK pathways are upregulated in astrocytes *in vivo* are mixed. Nonetheless, increased phosphorylation level of Erk and/or p38MAPK takes part in the response of astrocytes to insults[58]. Although the evident complexity involving the participation of these signaling mechanisms in reactive astrogliosis, different components of MAPK signaling are activated under distinct pathological conditions and in different cell types, which may indicate a common mechanism. Thus, the early activation of MAPKs detected in the cerebellum of acutely treated rats could be associated with the program of astrogliosis detected in our experimental condition.

The present results shed light into the mechanisms of $(PhTe)_2$-induced neurodegeneration in the cerebellum of young rats. We could hypothesize that the cerebellar neurodegeneration following $(PhTe)_2$ exposure includes disruption of cytoskeletal homeostasis that could be related with MAPK and PKA activation and reactive astrogliosis. Akt inhibition observed at this time could also play a role in the neuronal death evidenced afterwards. The following events of the neurodegenerative process are characterized by persistent astrogliosis and activation of apoptotic neuronal death probably through caspase 3 mediated mechanisms, which in turn, could be related with glutamate excitotoxicity. The progression of these responses are therefore likely to be critical for the outcome of the neurodegeneration provoked by $(PhTe)_2$ in rat cerebellum.

Conflict of interest: The authors declare no competing financial interest

Ackowledgements

This work was supported by Conselho Nacional de Desenvolvimento Científico e Tecnológico (CNPq), Fundação de Amparo à Pesquisa do Estado do Rio Grande do Sul (FAPERGS), PRONEX and Propesq-UFRGS. The authors thank to Electron Microscopy Center of the Federal University of Rio Grandedo Sul for the microscopy analyzes. The authors also thank Mr. Henrique Biehl for technical assistance.

References

1-Villanueva, R. (2012) The cerebellum and neuropsychiatric disorders. *Psychiatry Res.* 10.1016/j.psychres.2012.02.023 20 published online March 2012

2-Biran, V., Verney, C. and Ferriero, D.M. (2012) Perinatal Cerebellar Injury in Human and Animal Models. *Neurol. Res. Int.* doi:10.1155/2012/858929

3-Dobbing, J., Hopewell, J. W., Lynch A, and Sands J. (1970) Vulnerability of developing brain: I. Some lasting effects of X irradiation. *Exp. Neurol. 28,* 442–449.

4-Dobbing, J. and Sands, J. (1973) Quantitative growth and developmentof human brain. *Arch. Dis. Childhood 48,* 757–767.

5-Dobbing, J. (1974) The later growth of the brain and its vulnerability. *Pediatrics 53,* 2–6.

6-Paulino, A.D., Ubhi, K., Rockenstein, E., Adame, A., Crews, L., Letendre, S., Ellis, R., Everall, I.P., Grant, I., and Masliah, E. (2011) Neurotoxic effects of the HCV core protein are mediated by sustained activation of ERK via TLR2 signaling. *J. Neurovirol. 17,* 327-30.

7-Pekny, M., and Nilsson, M. (2005) Astrocyte activation and reactive gliosis. *Glia 50,* 427–434.

8-Sofroniew, M.V., and Vinters, H.V. (2010). Astrocytes: biology and pathology. *Acta Neuropathol. 119,* 7–35.

9-Butterworth, R.F. (2010) Metal toxicity, liver disease and neurodegeneration. *Neurotox Res. 18,*100-105.

10-Sheldon, A.L., and Robinson, M.B. (2007) The role of glutamate transporters in neurodegenerative diseases and potential opportunities for intervention. *Neurochem. Int. 51*, 333-355.

11-Perrot, R., and Eyer, J. (2009) Neuronal intermediate filaments and neurodegenerative disorders.Brain. *Res. Bull. 80*, 282-295.

12-Perrot, R., Berges, R., Bocque,t A., and Eyer, J. (2008) Review of the multiple aspects of neurofilament functions, and their possible contribution to neurodegeneration. *Mol. Neurobiol. 38*, 327-365.

13-Larner, A.J. (1995) How does garlic exert its hypocholesterolaemic action? The tellurium hypothesis. *Med. Hypotheses 44*, 295–297.

14-Newman, R.A., Osborn, S., and Siddik, Z.H. (1989) Determination of tellurium in biological fluids bymeans of electrothermal vapourization-inductively coupled to plasma mass spectrometry (ETV-ICP-MS). *Clin. Chim. Acta 179*, 191–196.

15-Siddik, Z.H., and Newman RA. (1988) Use of platinum as a modifer in the sensitive detection of tellurium in biological samples. *Anal. Biochem. 172*, 190–196.

16-Widy-Tyszkiewicz, E., Piechal, A., Gajkowska, B., and Smialek, M. (2002) Tellurium-induced cognitive deficits in rats are related to neuropathological changes in the central nervous system. *Toxicol. Lett. 131*, 203–214.

17-Yarema, M. C., and Curry, S. C. (2005) Acute tellurium toxicity from ingestion of metal-oxidizing solutions. *Pediatrics 116*, e319–321.

18-Muller, R., Zschiesche, W., Steffen, H., and Schaller, K. (1989) Tellurium-intoxication. *Klin Wochenschr 67*, 1152–1155.

19-Taylor, A. (1996) Biochemistry of tellurium. *Biol. Trace Elem. Res. 55*, 231–239.

20-Stangherlin, E.C., Rocha, J.B. and Nogueira, C.W. (2009) Diphenyl ditelluride impairs short-term memory and alters neurochemical parameters in young rats. *Pharmacol.Biochem.Behav. 91*, 430-435.

21-Roy, S., and Hardej, D. (2011) Tellurium tetrachloride and diphenyl ditelluride cause cytotoxicity in rat hippocampal astrocytes. *Food Chem. Toxicol. 49*, 2564-2574.

22-Heimfarth, L., Loureiro, S.O., Reis, K.P., de Lima, B.O., Zamboni, F., Gandolfi, T., Narvaes, R., da Rocha, J.B. and Pessoa-Pureur, R. (20110 Cross-talk among intracellular signaling pathways mediates the diphenyl ditelluride actions on the hippocampal cytoskeleton of young rats. *Chem. Res. Toxicol. 24*, 1754-1764.

23-Heimfarth, L., Loureiro, S.O., Reis, K.P., de Lima, B.O., Zamboni, F., Lacerda, S., Soska, A.K., Wild, L., da Rocha, J.B. and Pessoa-Pureur, R. (2012) Diphenyl ditelluride induces hypophosphorylation of intermediate filaments through modulation of DARPP-32-dependent pathways in cerebral cortex of young rats. *Arch. Toxicol. 86*, 217-230.

24-Nogueira, C.W., Rotta, L.N., Perry, M.L., Souza, D.O., and Rocha, J.B.T. (2001) Diphenyl diselenide and diphenyl ditelluride affect the rat glutamatergic system in vitro and in vivo. *Brain Re. 906*, 157-163.

25-Moretto, M.B., Thomazi, A.P., Godinho, G., Roessler, T.M., Nogueira, C.W., Souza, D.O., Wofchuk, S.T. and Rocha, J.B.T. (2007) Ebselen and diorganylchalcogenides decrease in vitro glutamate uptake by rat brain slices: prevention by DTT and GSH. *Toxicol. in Vitro 21*, 639-45.

26-Heimfarth, L., Loureiro, S.O., Zamoner, A., Pelaez, P. L., Nogueira, C.W., Rocha, J. B., and Pessoa-Pureur, R. (2008) Effects of in vivo treatment with diphenyl ditelluride on the phosphorylation of cytoskeletal proteins in cerebral cortex and hippocampus of rats. *Neurotoxicol. 29,* 40-47.

27-Petragnani, N. (1994). Preparation of the principal classes of organic tellurium compounds. In: Tellurium in Organic Synthesis. *Academic Press*, London, pp. 9–88.

28-Funchal, C., de Almeida, L.M., Oliveira Loureiro, S., Vivian, L., de Lima Pelaez, P., Dall Bello Pessutto, F., Rosa, A.M., Wajner, M., and Pessoa-Pureur, R. (2003) In vitro phosphorylation of cytoskeletal proteins from cerebral cortex of rats. *Brain Res. Prot. 11*, 111–118.

29-Laemmli, U.K. (1970) Cleavage of structural proteins during the assembly of the head of bacteriophage T4. *Nature 227,* 680-685.

30-Andrade, C.M., Roesch, G.C., Wink, M.R..Guimaraes. E.L, Souza, L.F., Jardim, F.R., Guaragna, R.M.,.Bernard, E.A,. Margis, R., Borojevic, R., Battastini, A.M., and Guma F.C. (2008) Activity and expression of ecto-5′-nucleotidase/CD73 are increased during

31-Frizzo, M. E. S., Lara, D. R., Prokopiuk, A. S., Vargas, C. R., Salbego, C. G., Wajner, M., and Souza, D. O. (2002) Guanosineenhances glutamate uptake in brain cortical slices at normal and excitotoxic conditions. *Cell. Mol. Neurobiol. 22,* 353–363.phenotype conversion of a hepatic stellate cell line. *Life Sci. 82*, 21–29.

32-Lowry, O.H., Rosebrough, N.J., Farr, A.L., and Randall, R.J. (1951) Protein measurement with the Folin phenol reagent. *J. Biol. Chem. 193*, 265–275.

33-Zhao, H., Sapolsky, R.M., and Steinberg, G.K. (2006) Phosphoinositide-3-kinase/akt survival signal pathways are implicated in neuronal survival after stroke. *Mol. Neurobiol. 34*, 249-270.

34-Souza, A.C., Stangherlin, E.C., Ardais, A.P., and Nogueira, C.W. (2010) Diphenyl diselenide and diphenyl ditelluride: neurotoxic effect in brain of young rats, in vitro. *Mol. Cell. Biochem. 340*, 179-185.

35-Lee, S.B., Bagley, J.A., Lee, H.Y., Jan, L.Y., and Jan, Y.N. (2011). Pathogenic polyglutamine proteins cause dendrite defects associated with specific actin cytoskeletal alterations in Drosophila. *Proc. Natl. Acad. Sci. USA. 108*, 16795-16800.

36-Sihag, R.K., Inagaki, M., Yamaguchi, T., Shea, T. B., and Pant, H. C. (2007) Role of phosphorylation on the structural dynamics and function of types III and IV intermediate filaments. *Exp. Cell Res. 313*, 2098–2109.

37-Leterrier, J.F., Kas, J., Hartwig, J., Vegners, R., Janmey, and P.A. (1996). Mechanical effects of neurofilament cross-bridges. Modulation by phosphorylation, lipids, and interactions with F-actin. *J. Biol. Chem. 271*, 15687–15694.

38-Hsieh, S.T., Kidd, G.J., Crawforg, T.O., Xu, Z., Lin, W.M., Trapp, B.D., Cleveland, D. W. and Griffin, J.W. (1994) Regional modulation of neurofilament organization by myelination in normal axons. *J. Neurosci. 14*, 6392–6401.

39-Gotow, T., Tanaka, T., Nakamura, Y., and Takeda, M. (1994) Dephosphorylation of the largest neurofilament subunit protein influences the structure of crossbridges in reassembled neurofilaments. *J. Cell Sci. 107*, 1949–1957.

40-Sihag, R.K., and Nixon, R.A. (1991) Identification of Ser-55 as a major protein kinase A phosphorylation site on the 70-kDa subunit of neurofilaments. Early turnover during axonal transport. *J. Biol. Chem. 266*, 18861-18867.

41-Hisanaga, S., Matsuoka, Y., Nishizawa, K., Saito, T., Inagaki, M. and Hirokawa, N. (1994) Phosphorylation of native and reassembled neurofilaments composed of NF-L, NF-M, and NF-H by the catalytic subunit of cAMP-dependent protein kinase. *Mol. Biol. Cell 5*, 161-172.

42-Motil, J., Chan, W.K., Dubey, M., Chaudhury, P., Pimenta, A., Chylinski, T.M., Ortiz, D.T., and Shea, T. B. (2006) Dynein mediates retrograde neurofilament transport within axons and anterograde delivery of NFs from perikarya into axons: regulation by multiple phosphorylation events. *Cell Motil. Cytoskeleton 63*, 266-286.

43-Veeranna, Amin N.D., Ahn N.G., Jaffe H., Winters C.A., Grant P. and Pant H.C. (1998). Mitogen-activated protein kinases (Erk1, 2) phosphorylate Lys–Ser–Pro (KSP) repeats in neurofilament proteins NF-H and NF-M. *J. Neurosci. 18*, 4008–4021.

44-Yabe, J.T., Chan, W., and Shea, T.B. (2000) Phospho-dependent association of neurofilament proteins with kinesin in situ. *Cell Motil.Cytoskeleton 45*, 249–265.

45-Muscella, A., Calabriso, N., Vetrugno, C., Fanizzi, F.P., De Pascali, S.A.,and Marsigliante, S. (2011) The signalling axis mediating neuronal apoptosis in response to [Pt(O,O'-acac)(γ-acac)(DMS)]. *Biochem. Pharmacol. 81*, 1271-1285.

46-Yakovlev, A.G. and Faden, A.I. (2001) Caspase-Dependent Apoptotic Pathways in CNS Injury. *Mol. Neurobiol. 24*, 131–144.

47-Slee, E.A., Harte, M.T., Kluck, R.M., Wolf, B.B., Casiano, C.A., Newmeyer, D.D., Wang, H.G., Reed, J.C., Nicholson, D.W., Alnemri, E.S., Green, D.R., and Martin, S.J.

(1999) Ordering the cytochrome c-initiated caspase cascade: hierarchical activation of caspases- 2, -3, -6, -7, -8, and -10 in a caspase-9- dependent manner. *J. Cell Biol. 144*, 281–292.

48-Cardone, M.H., Roy, N., Stennicke, H R., Salvesen, G.S., Franke, T.F., Stanbridge, E., Frisch, S., and Reed, J.C. (1998) Regulation of cell death protease caspase-9 by phosphorylation. *Science 282*, 1318–1321.

49-Koh, S.H., Park Y., Song, C.W., Kim, J.G., Kim, K., Kim, J., Kim, M.H., Lee, S.R., Kim, D.W., Yu, H.J., Chang, D.I., Hwang, S.J., and Kim, S.H. (2004) The effect of PARP inhibitor on ischaemic cell death, its related inflammation and survival signals. *Eur. J. Neurosci. 20*, 1461–1472.

50-Zhou, H., L,i X.M., Meinkoth, J., and Pittman, R.N. (2000) Akt regulates cell survival and apoptosis at a postmitochondrial level. *J. Cell Biol. 151*, 483–494.

51-Srivastava, A.K., and Pandey, S.K. (1998). Potential mechanism(s) involved in the regulation of glycogen synthesis by insulin. *Mol. Cell. Biochim. 182*, 135-141.

52-Smith, A.J., Tauskela, J.S., Stone, T.W., and Smith, R.A. (2009) Preconditioning with 4-aminopyridine protects cerebellar granule neurons against excitotoxicity. *Brain Res. 1294*, 165-175.

53-Jahani-Asl, A., Pilon-Larose, K., Xu, W., MacLaurin, J.G., Park, D.S., McBride, H.M., and Slack, R.S. (2011) The mitochondrial inner membrane GTPase, optic atrophy 1 (Opa1), restores mitochondrial morphology and promotes neuronal survival following excitotoxicity. *J. Biol Chem. 286*, 4772-4782.

54-Yang, E.J., Min, J.S., Ku, H.Y., Choi, H.S., Park, M.K., Kim, M.K., Song, K.S., Lee, D.S. (2012) Isoliquiritigenin isolated from Glycyrrhiza uralensis protects neuronal cells

against glutamate-induced mitochondrial dysfunction. *Biochem. Biophys. Re. Commun. 421*, 658-664.

55-Liu, W., Xu, Z., Deng, Y., Xu, B., Yang, H., Wei, Y., and Feng, S. (2012) Excitotoxicity and oxidative damages induced by methylmercury in rat cerebral cortex and the protective effects of tea polyphenols. *Environ. Toxicol.* doi: 10.1002/tox.21755 published online Jan 5 2012.

56-Nguyen, D., Alavi, M.V., Kim, K.Y., Kang, T., Scott, R.T., Noh, Y.H,, Lindsey, J.D., and Wissinger, B., Ellisman, M.H. Weinreb RN, Perkins GA, Ju WK. (2011) A new vicious cycle involving glutamate excitotoxicity, oxidative stress and mitochondrial dynamics. *Cell Death Dis.* doi: 10.1038/cddis.2011.117 published online Dec 8 2011.

57-Yu, P., Wang, H., Katagiri, Y., and Geller, H.M. (2012). An in vitro model of reactive astrogliosis and its effect on neuronal growth. *Methods Mol. Biol. 814*, 327-340.

58-Ito, M., Natsume, A., Takeuchi, H., Shimato, S., Ohno, M., Wakabayashi, T., and Yoshida, J. (2009) Type I interferon inhibits astrocytic gliosis and promotes functional recovery after spinal cord injury by deactivation of the MEK/ERK pathway. *J. Neurotrauma. 26*, 41-53.

Legends to the Figures

Figure 1: Effect of a single subcutaneous injection of $(PhTe)_2$ on the *in vitro* phosphorylation of IF proteins in cerebellum of rats 3 (A) or 6 (B) days after the injection. NF-H, high molecular weight neurofilament, NF-M, middle molecular weight

neurofilament subunit; NF-L, low molecular weight neurofilament subunit; Vim, vimentin and GFAP, glial fibrillary acidic protein. Representative stained gels and autoradiographs of the proteins studied are shown (C). Data are reported as means ± S.E.M. of 8–10 animals and expressed as percent of control. Statistically significant differences from canola oil-treated rats, as determined by oneway ANOVA followed by Tukey-Kramer test are indicated: *P < 0.05.

Figure 2: Effect of $(PhTe)_2$ on MAPK pathways by Western blot analysis. ERK1/2 (A,B), JNK (C,D) and p38 MAPK (E,F) 3 (A, C, E) or 6 (B, D, F) days after the injection. Representative Western blots of the proteins studied are shown (G). Western blot of β-actin was used as loading control. Data are reported as means ± S.E.M. of 8–10 animals and expressed as percent of control. Statistically significant differences from canola oil-treated rats, as determined by oneway ANOVA followed by Tukey-Kramer test are indicated: *P < 0.05.

Figure 3: Effect of $(PhTe)_2$ on PKAc-α levels by Western blot analysis 3 (A) or 6 (B) days after the injection. Representative Western blots of the proteins studied are shown. Western blot of β-actin was used as loading control. Data are reported as means ± S.E.M. of 8–10 animals and expressed as percent of control. Statistically significant differences from canola oil-treated rats, as determined by oneway ANOVA followed by Tukey-Kramer test are indicated: *P < 0.05.

Figure 4: Effect of $(PhTe)_2$ on the phosphoNF-H/NF-M KSP repeats and phosphoNF-L ser55 3 days after the injection. Representative Western blot of the proteins studied are shown. Western blot of β-actin was used as loading control. Data are reported as means ± S.E.M. of 8–10 animals and expressed as percent of control. Statistically significant differences from canola oil-treated rats, as determined by oneway ANOVA followed by Tukey-Kramer test are indicated: *P < 0.05.

Figure 5: Effect of $(PhTe)_2$ on IF protein immunoreactivity in the tissue homogenate (A,C) and in the cytoskeletal fraction (B, D) from cerebellum 3 (A,B) or 6 (C,D) days after treatment. Representative Western blots of the proteins studied are shown. Western blot of β-actin was used as loading control. Data are reported as means ± S.E.M. of 8–10 animals and expressed as percent of control. Statistically significant differences from canola oil-treated rats, as determined by oneway ANOVA followed by Tukey-Kramer test are indicated: *P < 0.05. NF-H, high molecular weight neurofilament subunit; NF-M, middle molecular weight neurofilament subunit; NF-L, low molecular weight neurofilament subunit; Vim, vimentin and GFAP, glial fibrillary acidic protein.

Figure 6: Quantitative real-time PCR analysis of GFAP, vimentin, NF-L, NF-M and NF-H at day 6 after $(PhTe)_2$ injection . Data represent mean ± S.E.M. of 8–10 animals in each group. Statistically significant differences from canola oil-treated rats, as determined by oneway ANOVA followed by Tukey-Kramer test are indicated: *P < 0.05.NF-H, high molecular weight neurofilament subunit; NF-M, middle molecular weight neurofilament subunit; NF-L, low molecular weight neurofilament subunit, Vim, vimentin and GFAP, glial fibrillary acidic protein.

Figure 7: Flow cytometry analysis 3 and 6 days after $(PhTe)_2$ injection. Propidium iodide (PI) positive cells (A), PI positive neurons (B), PI positive astrocytes (C), NeuN positive cells (D), GFAP positive cells (E). Data are reported as means ± S.E.M. of 8–10 animals and expressed as percent of control. Statistically significant differences from canola oil-treated rats, as determined by oneway ANOVA followed by Tukey-Kramer test are indicated: *P < 0.05.

Figure 8: Immunohystochemistry for GFAP, NF-L, NeuN and merged at days 3 and 6 after $(PhTe)_2$ injection. The panels obtained by confocal microscopy show increased GFAP and unaltered NeuN staining, meaning astrogliosis and absence of neuronal death at day 3 after injection in (A). Panel (B) shows increased GFAP staining and decreased NeuN, indicating persistent astrogliosis and neuronal death at day 6 after $(PhTe)_2$ injection. Merged panels show colocalization of astrocytes and neurons. Representative images of 6 animals. ML = molecular layer; GL = granular layer. Bar scale = 30μm (magnification: 40 x); 50 μm (magnification: 20 x).

Figure 9: Effect of $(PhTe)_2$on caspase (A, B), AKT/PKB (C, D) and GSK3β (E, F) activities 3 (A, C, E) and 6 (B, D, F) days after the injection. Representative Western blots of the proteins studied are shown. β-actin was used as loading control. Data are reported as means ± S.E.M. of 8–10 animals and expressed as percent of control. Statistically significant differences from canola oil-treated rats, as determined by oneway ANOVA followed by Tukey-Kramer test are indicated: *P < 0.05.

Figure 10: Effect of $(PhTe)_2$ on glutamate uptake in cerebellar slices 3 and 6 days after injection. Data are reported as means ± S.E.M. of 6 animals and expressed as percent of control. Statistically significant differences from canola oil-treated rats, as determined by oneway ANOVA followed by Tukey-Kramer test are indicated: *$P < 0.05$.

Figure 1:

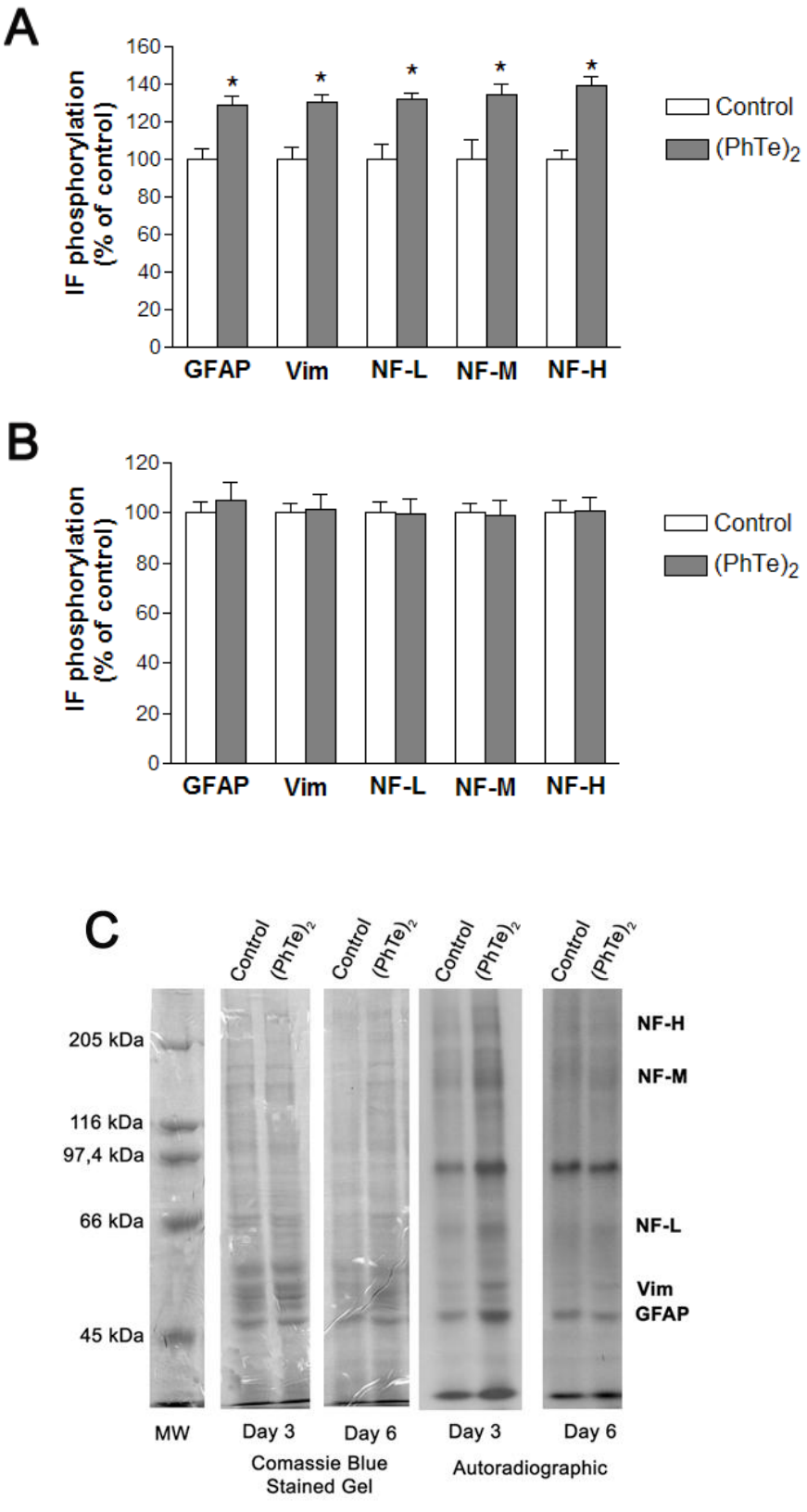
A
IF phosphorylation (% of control)
160
140
120
100
80
60
40
20
0
GFAP
Vim
NF-L
NF-M
NF-H
Control
(PhTe)2
B
IF phosphorylation (% of control)
120
100
80
60
40
20
0
GFAP
Vim
NF-L
NF-M
NF-H
Control
(PhTe)2
C
Control
(PhTe)2
Control
(PhTe)2
Control
(PhTe)2
Control
(PhTe)2
205 kDa
116 kDa
97,4 kDa
66 kDa
45 kDa
NF-H
NF-M
NF-L
Vim
GFAP
MW
Day 3
Day 6
Day 3
Day 6
Comassie Blue Stained Gel
Autoradiographic

Figure 2:

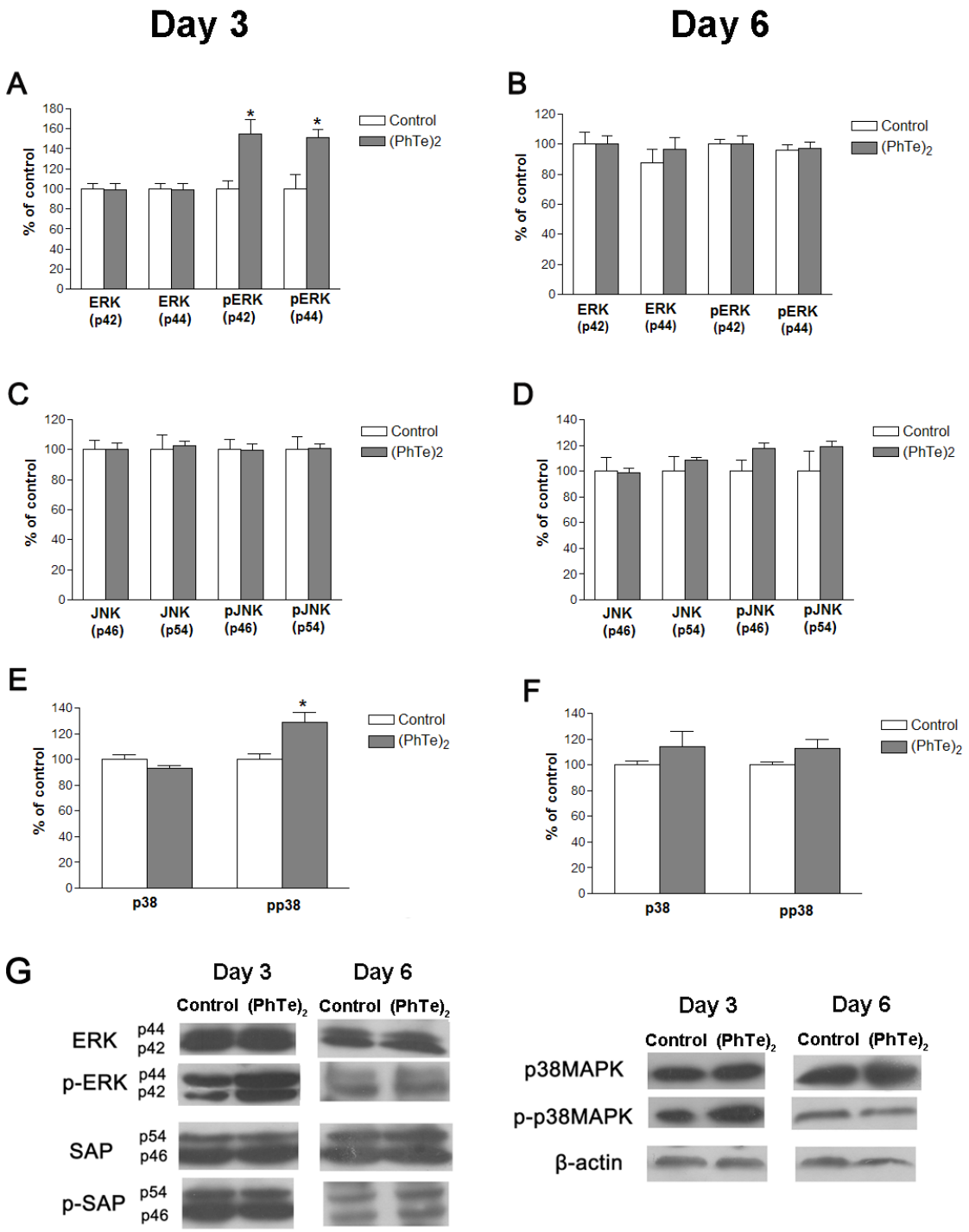
Day 3
Day 6
A
B
C
D
E
F
G
% of control
Control
(PhTe)2
ERK (p42)
ERK (p44)
pERK (p42)
pERK (p44)
JNK (p46)
JNK (p54)
pJNK (p46)
pJNK (p54)
p38
pp38
Control (PhTe)2
ERK
p-ERK
SAP
p-SAP
p44
p42
p54
p46
p38MAPK
p-p38MAPK
β-actin

Figure 3:

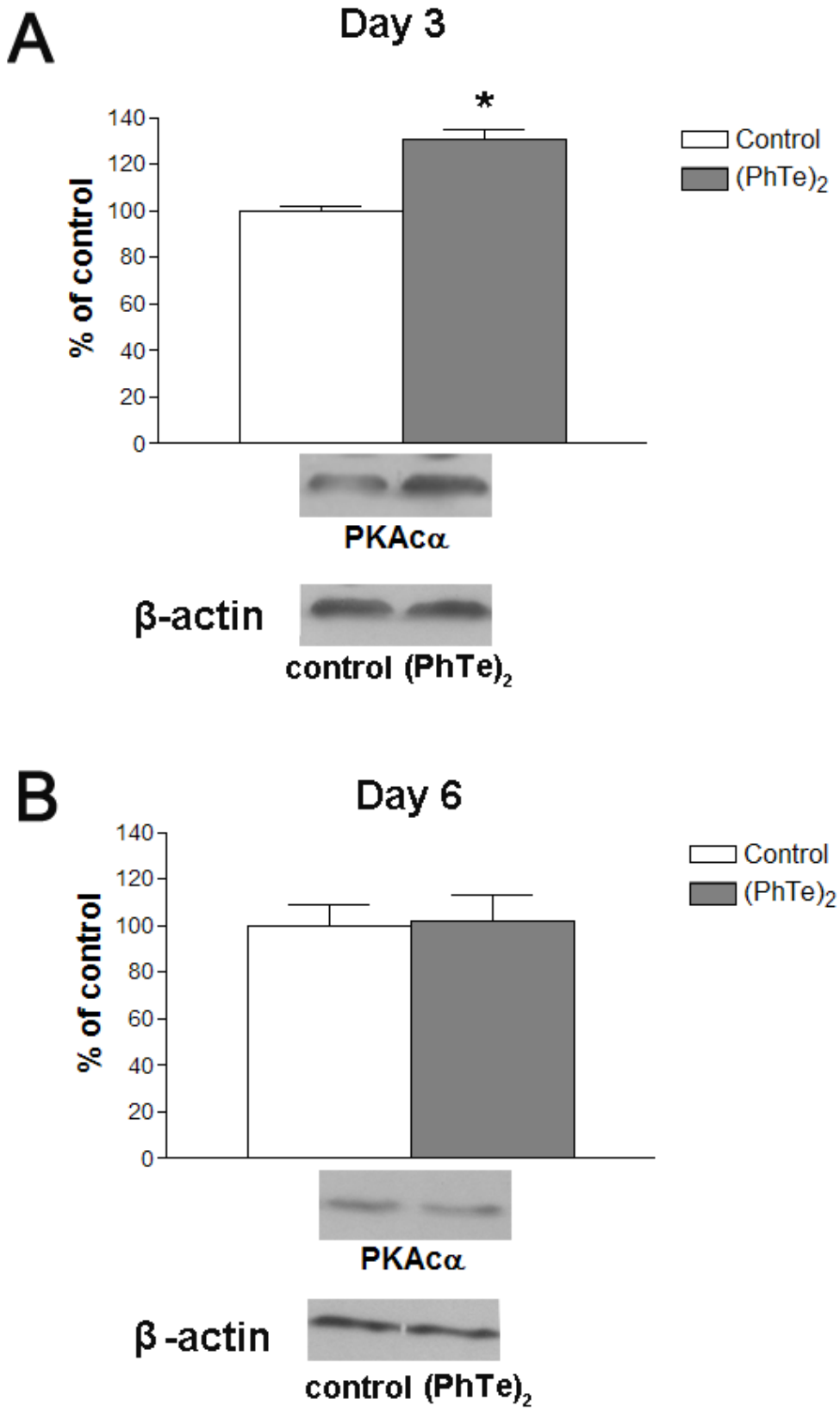
A
Day 3
*
140
120
100
80
60
40
20
0
% of control
Control
(PhTe)2
PKAcα
β-actin
control (PhTe)2
B
Day 6
140
120
100
80
60
40
20
0
% of control
Control
(PhTe)2
PKAcα
β-actin
control (PhTe)2

Figure 4:

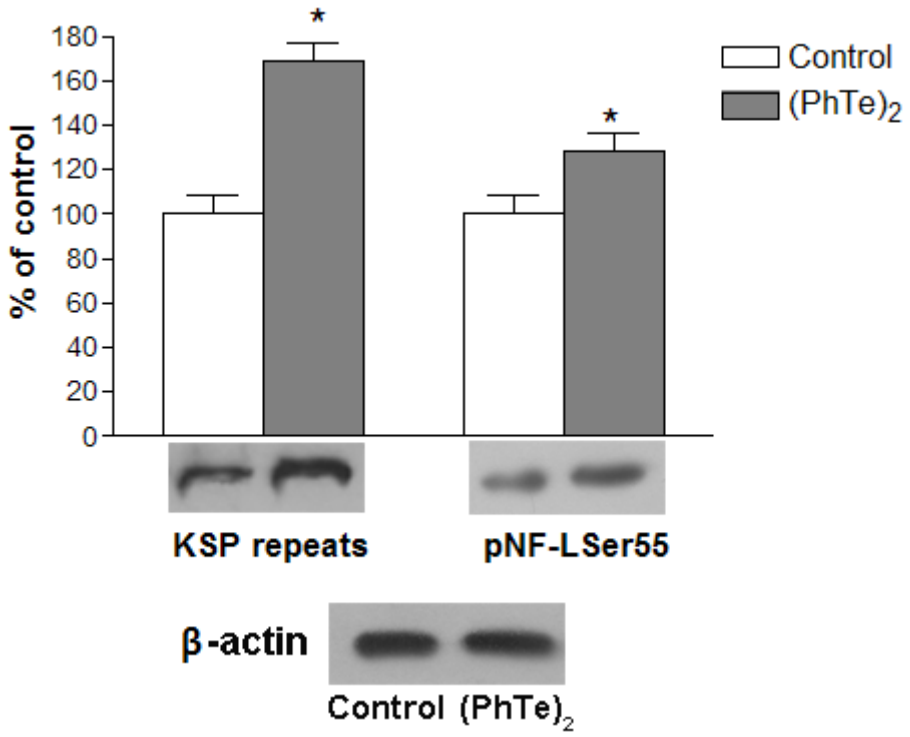
180
160
140
120
100
80
60
40
20
0
% of control
*
*
Control
(PhTe)2
KSP repeats
pNF-LSer55
β-actin
Control (PhTe)2

Figure 5:

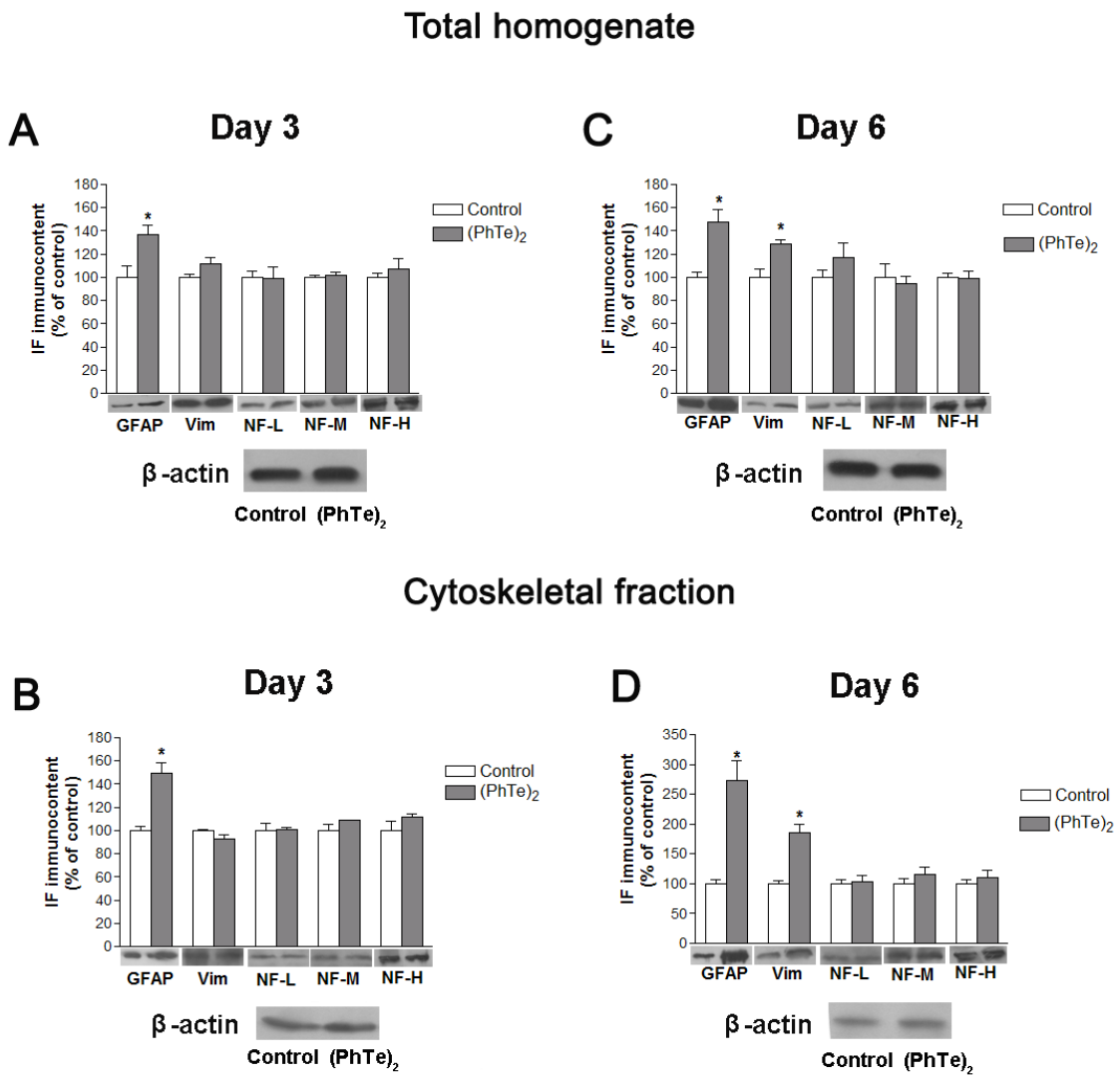
Total homogenate
A
Day 3
C
Day 6
IF immunocontent (% of control)
Control
(PhTe)2
GFAP
Vim
NF-L
NF-M
NF-H
β-actin
Control (PhTe)2
Cytoskeletal fraction
B
Day 3
D
Day 6

Figure 6:

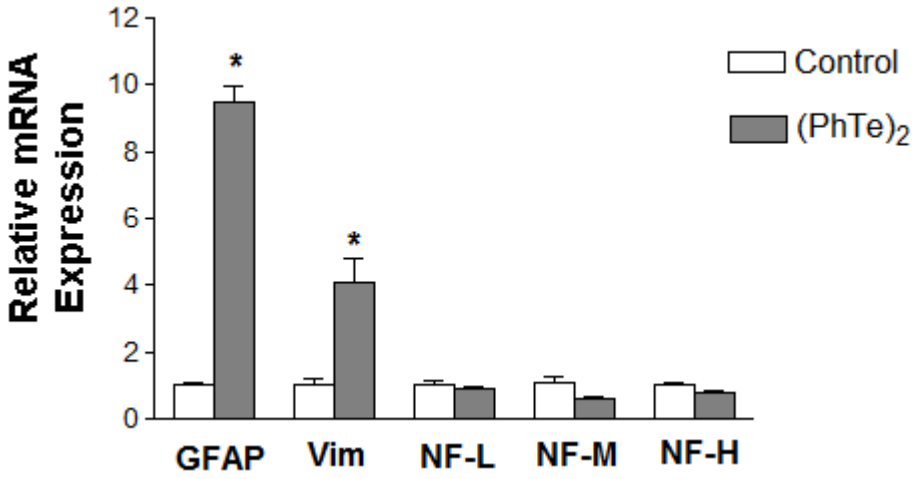
Relative mRNA Expression
12
10
8
6
4
2
0
*
*
Control
(PhTe)2
GFAP
Vim
NF-L
NF-M
NF-H

Figure 7:

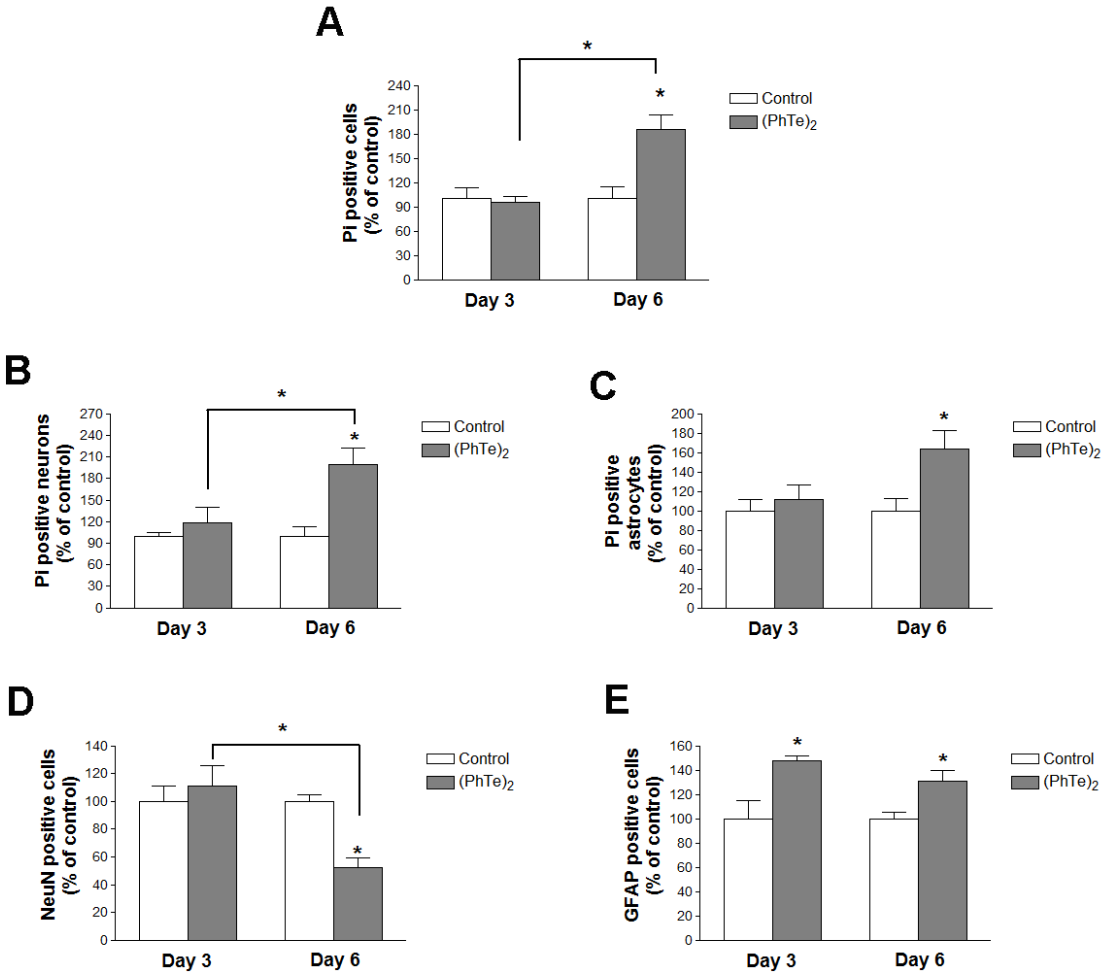
A
PI positive cells (% of control)
Control
(PhTe)2
Day 3
Day 6
B
PI positive neurons (% of control)
C
PI positive astrocytes (% of control)
D
NeuN positive cells (% of control)
E
GFAP positive cells (% of control)

Figure 8:

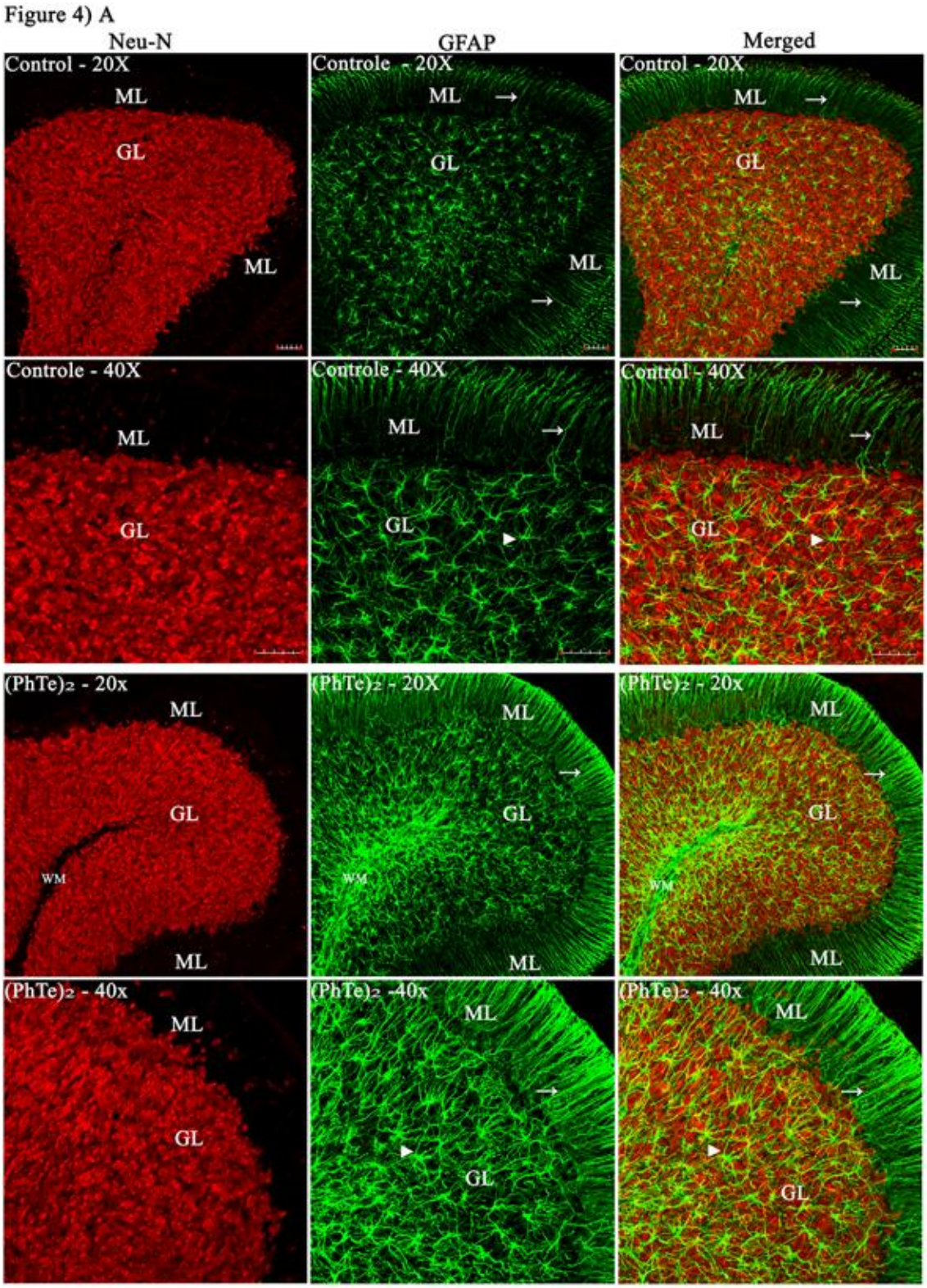
Figure 4) A
Neu-N
GFAP
Merged
Control - 20X
Controle - 20X
Control - 20X
Controle - 40X
Controle - 40X
Control - 40X
(PhTe)2 - 20x
(PhTe)2 - 20X
(PhTe)2 - 20x
(PhTe)2 - 40x
(PhTe)2 -40x
(PhTe)2 - 40x
ML
GL
WM

Figure 4) B

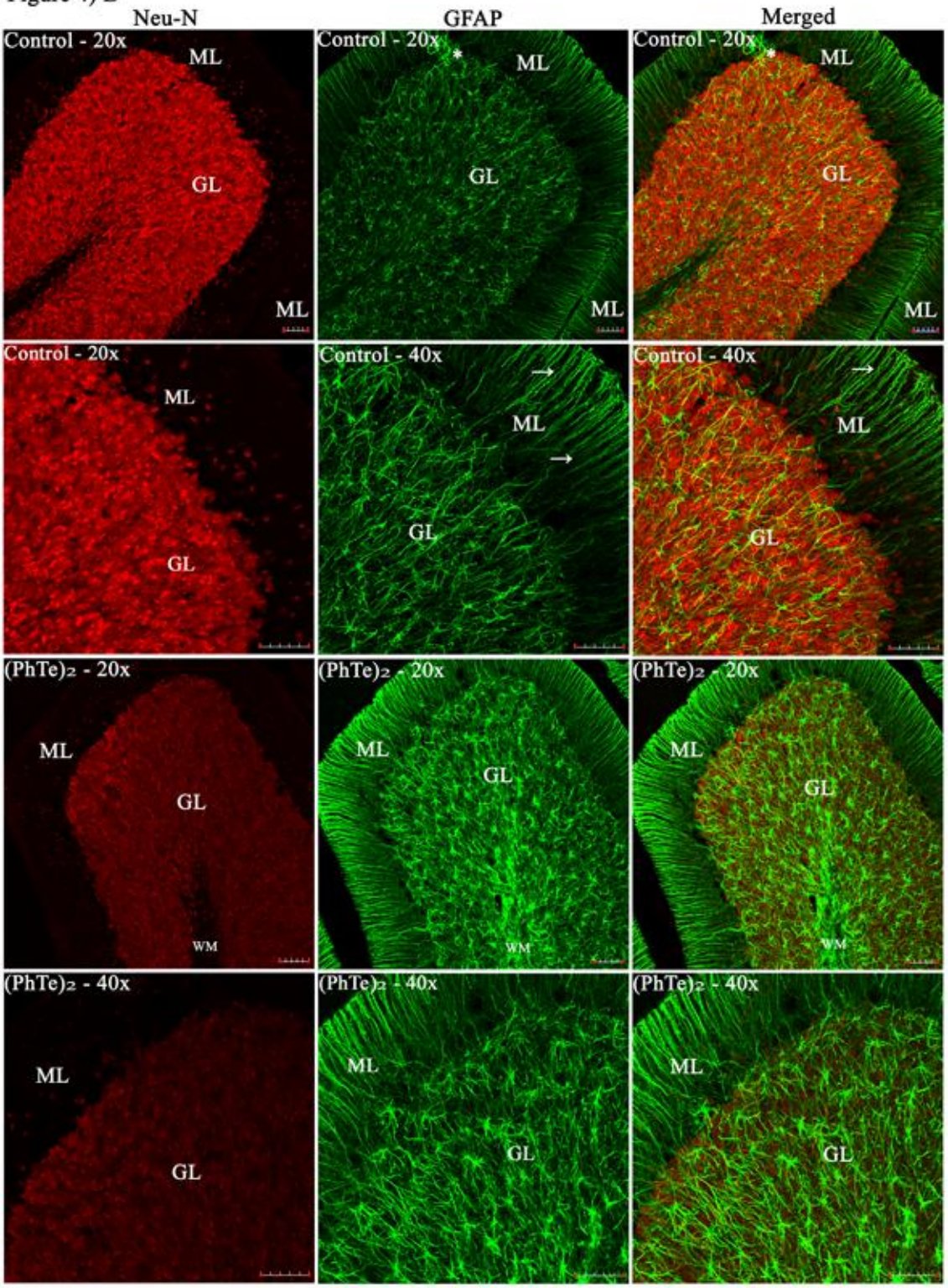
Neu-N
GFAP
Merged
Control - 20x
ML
GL
Control - 40x
(PhTe)2 - 20x
(PhTe)2 - 40x
WM

Figure 9:

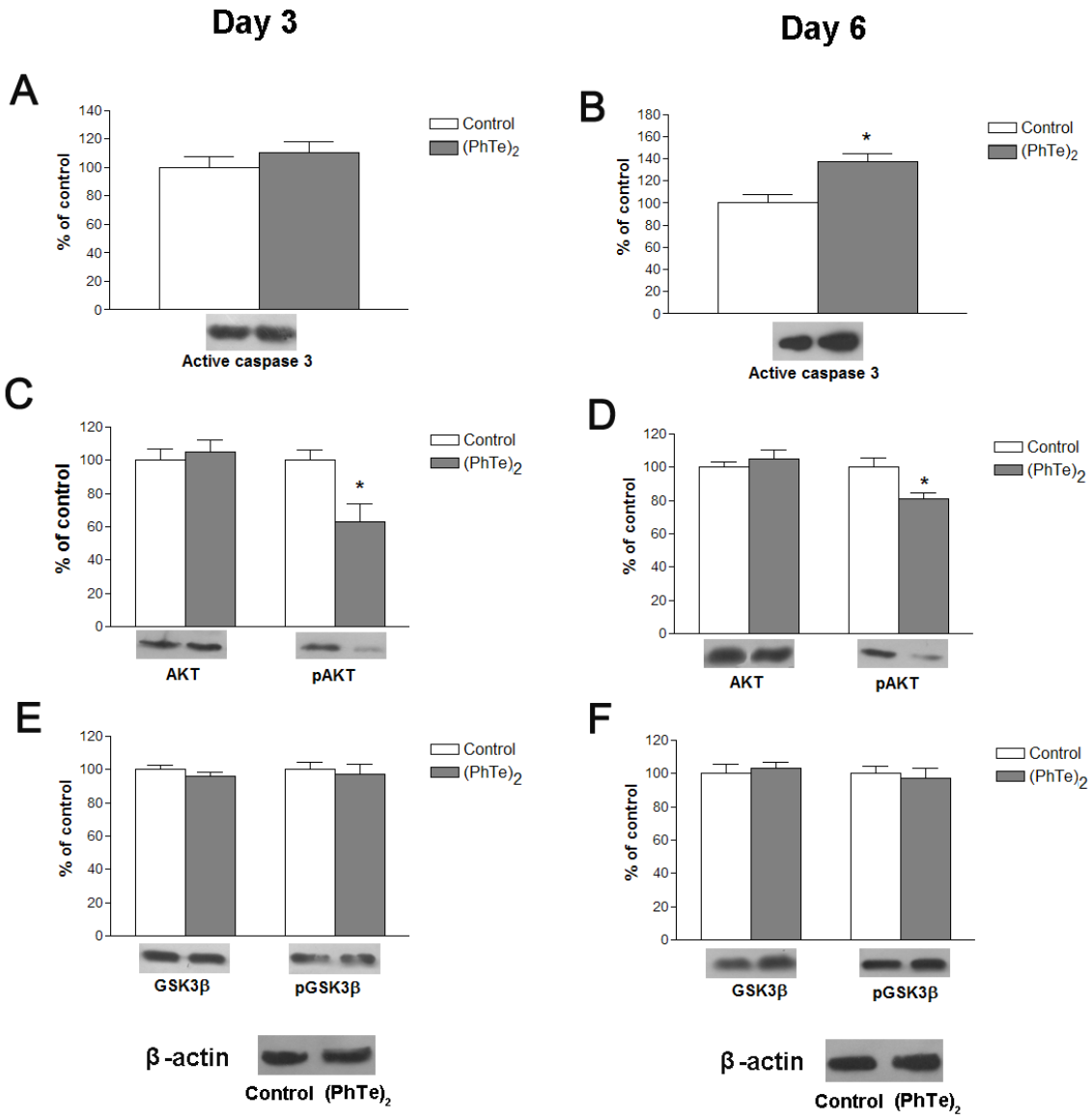
Day 3
Day 6
A
B
C
D
E
F
% of control
Control
(PhTe)2
Active caspase 3
AKT
pAKT
GSK3β
pGSK3β
β-actin
Control (PhTe)2
*

Figure 10:

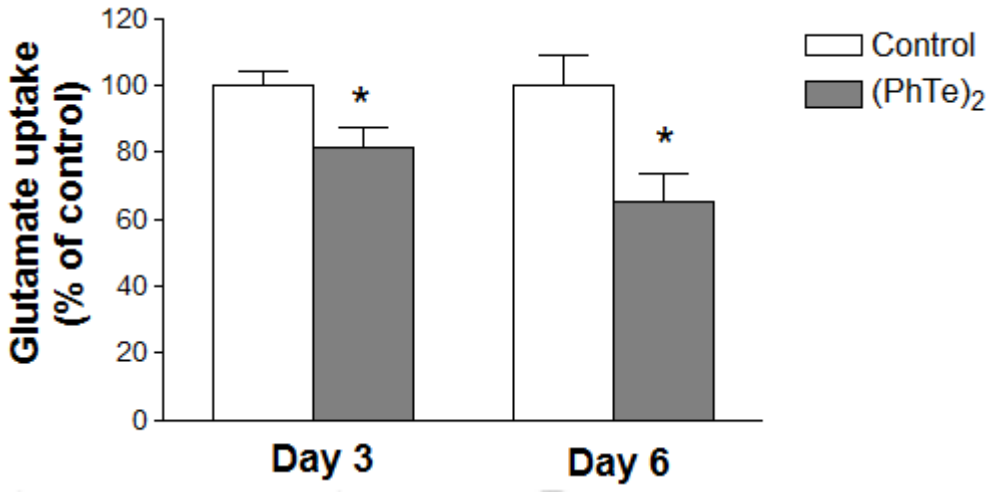
Glutamate uptake
(% of control)
120
100
80
60
40
20
0
*
*
Day 3
Day 6
Control
(PhTe)2

Capítulo 3

EXPOSURE OF YOUNG RATS TO DIPHENYL DITELLURIDE DURING LACTATION AFFECTS THE HOMEOSTASIS OF THE CYTOSKELETON IN NEURAL CELLS FROM STRIATUM AND CEREBELLUM

Luana Heimfarth[a], Karina Pires Reis[a], Samanta Oliveira Loureiro[a], Bárbara Ortiz de Lima[a], João Batista Teixeira da Rocha[b] and Regina Pessoa-Pureur[a]

Artigo aceito para ser publicado na revista *Neurotoxicology*

EXPOSURE OF YOUNG RATS TO DIPHENYL DITELLURIDE DURING LACTATION AFFECTS THE HOMEOSTASIS OF THE CYTOSKELETON IN NEURAL CELLS FROM STRIATUM AND CEREBELLUM

Luana Heimfarth[a], Karina Pires Reis[a], Samanta Oliveira Loureiro[a], Bárbara Ortiz de Lima[a], João Batista Teixeira da Rocha[b] and Regina Pessoa-Pureur[a]

[a]Departamento de Bioquímica, Instituto de Ciências Básicas da Saúde, UFRGS, Porto Alegre, RS, Brasil

[b]Departamento de Química, Centro de Ciências Naturais e Exatas, Universidade Federal de Santa Maria, RS Brasil

CORRESPONDING AUTHOR: Dr. Regina Pessoa-Pureur, Universidade Federal do Rio Grande do Sul, Instituto de Ciências Básicas da Saúde, Departamento de Bioquímica, Rua Ramiro Barcelos 2600 anexo, 90035-003 Porto Alegre - RS, BRASIL, Fax: 5551 3308 5535, Tel: 5551 3308 5565; E-mail: rpureur@ufrgs.br

Running title: Diphenyl ditelluride affects the cytoskeleton of lactating pups

Abstract

In the present report we examined the effect of maternal exposure to diphenyl ditelluride $(PhTe)_2$ (0.01 mg/kg body weight) during the first 14 days of lactational period on the activity of some protein kinases targeting the cytoskeleton of striatum and cerebellum of their offspring. We analyzed the phosphorylating system associated with glial fibrillary acidic protein (GFAP), and neurofilament of low, medium and high molecular weight (NF-L, NF-M and NF-H, respectively) of pups on PND 15, 21, 30 and 45. We found that $(PhTe)_2$ induced hyperphosphorylation of all the proteins studied on PND 15 and 21, recovering control values on PND 30 and 45. The immunocontent of GFAP, NF-L, NF-M and NF-H in the cerebellum of 15 day-old pups was increased. Western blot assays showed activation/phosphorylation of Erk1/2 on PND 21 and activation/phosphorylation of JNK on PND 15. Otherwise, p38MAPK was not activated in the striatum of $(PhTe)_2$ exposed pups. On the other hand, the cerebellum of pups exposed to $(PhTe)_2$ presented activated/phosphorylated Erk1/2 on PND 15 and 21 as well as activated/phosphorylated p38MAPK on PND 21, while JNK was not activated. Western blot assays showed that both in the striatum and in the cerebellum of $(PhTe)_2$ exposed pups, the immunocontent of the catalytic subunit of PKA (PKAcα) was increased on PND 15. Western blot showed that the phosphorylation level of NF-L Ser55 and NF-M/NF-H KSP repeats was increased in the striatum and cerebellum of both 15 and 21 day-old pups exposed to $(PhTe)_2$. Diphenyl diselenide $(PhSe)_2$, the selenium analog of $(PhTe)_2$, prevented $(PhTe)_2$-induced hyperphosphorylation of striatal intermediate filament (IF) proteins but it failed to prevent the action of $(PhTe)_2$ in cerebellum. Western blot assay showed that the $(PhSe)_2$ prevented activation/phosphorylation of Erk1/2, JNK and PKAcα but did not prevent the stimulatory effect of $(PhTe)_2$ on p38MAPK in cerebellum at PND 21. In conclusion,

this study demonstrated that dam exposure to low doses of $(PhTe)_2$ can alter cellular signaling targeting the cytoskeleton of striatum and cerebellum in the offspring in a spatiotemporal manner, which can be related to the neurotoxic effects of $(PhTe)_2$.

Keywords: Diphenyl ditelluride, lactation, cytoskeleton, cell signaling, striatum, cerebellum

1. Introduction

The neuronal cytoskeleton comprises a protein network formed mainly by microtubules (MT) and neurofilaments (NF), the intermediate filaments (IFs) of neurons. Neurofilaments are composed of three different polypeptides whose approximate molecular masses are 200, 160, and 68 kDa, and are commonly referred to as heavy (NF-H), medium (NF-M) and light (NF-L) neurofilament subunits (Ackerley et al., 2000). The assembly of the three NF subunits forms a typical NF, in which NF-L is known to polymerize on its own, whilst NF-M and NFH form lateral side-arms (Petzold, 2005). Glial fibrillary acidic protein (GFAP) is the IF of mature astrocytes (Eng et al., 2000) and vimentin (Vim) is the IF of cells of mesenchymal origin (Alberts et al., 2008).

The IF proteins are important phosphoproteins whose phosphorylation is a dynamic process mediated by the action of several protein kinases and phosphatases. The phosphorylation level of IFs provides the cells a mechanism to reorganize the filaments contributing to the maintenance of their homeostasis (Chang and Goldman, 2004). In particular, physiological levels of phosphorylation of NFs promote their integration into a cytoskeleton lattice, controlling the axonal caliber and stabilizing the axon. Therefore the physiological phosphorylation of IF proteins plays a major role on the cellular dynamics and this is dependent on the activation of several signaling pathways involved in phosphorylating specific sites on IF subunits in response to intra and extracellular signals (Sihag et al., 2007).

The major sites of phosphorylation of NF-L and NF-M subunits were identified as Ser-55, which is phosphorylated by protein kinase A (PKA); Ser-57, which is phosphorylated by Ca^{2+}/calmodulin-dependent protein kinase II (PKCaMII); Ser-51, by

protein kinase C (PKC), (Gill et al., 1990; Heins et al., 1993); and Ser-23, by PKA and protein kinase C (PKC), respectively (Daile et al., 1975; Kemp et al., 1975). On the other hand, most of the phosphorylation sites on NF-M and NF-H are located on multiple lysine-serine-proline (KSP) repeat motifs abundant in the carboxyl-terminal tail domain of these NF subunits (Geisler et al., 1987; Lee et al., 1988; Xu et al., 1992). It is now evident that proline-directed kinases, such as cyclin-dependent kinase 5 (Cdk5) and mitogen-dependent protein kinase (MAPK) are the main kinases that phosphorylate Ser residues on the KSP repeats (Jaffe et al., 1998; Sun et al., 1996; Veeranna et al., 1998).

Phosphorylation of the amino-terminal head domain sites on GFAP and NF proteins plays a key role in the assembly/disassembly of IF subunits into 10 nm filaments and influences the phosphorylation of sites on the carboxyl-terminal tail domain (Sihag *et al.*, 2007). Otherwise, the C-terminal regions of NF-H and NF-M protrude laterally from the filament backbone when phosphorylated (Sihag et al. 2007) and a considerable body of evidence supports the notion that phosphorylation of C-terminal side arms, in particular those of NF-H, regulates NF axonal transport (Shea and Chan, 2008).

The importance of types III and IV IFs, including GFAP and NF subunits, on cellular function is evident from the fact that perturbation of their function accounts for several genetically determined protein misfolding/aggregation diseases (Arbustini et al., 2006; Green et al., 2005). In this scenario, studies showing increased axonal accumulation of NFs in transgenic mice or in mice expressing mutant NF subunit have shown that aberrant organization or assembly of NFs is sufficient to cause disease arising from selective dysfunction and degeneration of neurons (Beaulieu et al., 1999a; Julien et al., 1995). In fact, perikaryal accumulation/aggregation of aberrantly

phosphorylated neurofilaments is a pathological feature of several human neurodegenerative diseases, such as Alzheimer's disease, motor neuron diseases and Parkinson's disease (Grant and Pant, 2000; Lariviere and Julien, 2004; Nixon, 1993; Sasaki et al., 2006).

Although the tellurium (Te) element rarely occurs in the free state in nature, metallic Te is known to be present in plant material, particularly in members of the Allium family, such as garlic (Larner, 1995). A number of studies have shown that trace amounts of Te are present in body fluids, such as blood and urine (Newman et al. 1989; Siddik and Newman, 1988). Neurotoxicity of tellurium has been reported in the literature. In this context, inorganic tellurium treatment was found to cause significant impairment in retention of the spatial learning task (Widy-Tyszkiewicz et al. 2002). But to date, no telluroproteins have been identified in animal cells. Nowadays, two cases of toxicity in young children from ingestion of metal-oxidizing solutions that contained substantial concentrations of Te were reported in the literature (Yarema and Curry, 2005). Clinical features of acute Te toxicity include a metallic taste, nausea, blackened oral mucosa and skin and garlic odor of the breath (Muller et al.,1989; Taylor, 1996).

Our laboratory have obtained persuasive evidence indicating that diphenyl ditelluride $(PhTe)_2$ is a neurotoxic compound for rats, disrupting the homeostasis of the cytoskeleton. In this context, cytoskeletal proteins from different brain regions of rats constitute important molecular targets of $(PhTe)_2$ both *in vivo* and *in vitro*. We reported that $(PhTe)_2$ induced *in vitro* hyperphosphorylation of GFAP, vimentin and NF subunits in hippocampus of PND 21 rats. This action showed a significant cross-talk among signaling pathways elicited by $(PhTe)_2$, connecting glutamate metabotropic cascade with activation of Ca^{2+} channels (Heimfarth et al. 2011). Nonetheless, $(PhTe)_2$ induced hypophosphorylation of GFAP and NF subunits only in cerebral cortex (not in

hippocampus) of 9- and 15-day-old animals through Ca^{2+}-mediated mechanisms (Heimfarth et al. 2012).

In contrast to $(PhTe)_{2,}$ diphenyl diselenide $(PhSe)_2$ exhibits neuroprotective and anti-inflammatory activities in different *in vivo* and *in vitro* models, including against the toxicity of $(PhTe)_{2.}$ (Moretto et al. 2005; Funchal et al. 2006; Nogueira and Rocha, 2011). Accordingly, data from our laboratory showed that $(PhSe)_2$ prevented the *in vitro* effects of $(PhTe)_2$ on the phosphorylating levels of IF proteins in slices of cerebral cortex of 17 day old rats (Funchal et al. 2006, Moretto et al. 2005). Most importantly, the *in vivo* hyperphosphorylation of cortical IF proteins, induced by a subcutaneous injection of $(PheTe)_2$, was totally reversed by a single injection of $(PheSe)_2$ 24h after $(PheTe)_2$ administration (Heimfarth et al. 2008).

Taking into account the importance of $(PhTe)_2$ as an intermediate in organic synthesis, the increasing evidence of its neurotoxicity, the high lipophilicity and the increasing possibility of occupational exposure to this compound, the present study evaluated the toxicity of $(PhTe)_2$ transmitted via maternal milk on the homeostasis of the cytoskeleton of pups during lactation as well as the ability of $(PhSe)_2$ in preventing these effects induced by low levels of exposure to $(PhTe)_2$.The purpose of these experiments was to define lactation as an important via of intoxication with Te and the susceptibility of specific brain structures to $(PhTe)_2$ during a period of intense brain development. In fact, during lactation intense biochemical and morphological changes make brain more susceptible to disruption by neurotoxic agents.

Considering the lipophylicity of this compound, we can suppose that it is excreted in milk like other hydrophobic toxicants, for instance, polychlorinated biphenyls (Nar et al 2012).Data about the metabolism of $(PhTe)_2$ are also not available

in the literature. However, the transformation of part of $(PhTe)_2$ to inorganic Te(IV), which is extremely reactive and could bind to milk proteins, cannot be ruled out. In fact, the determination of tellurium speciation in mothers and pups will be highly needed and, consequently, analytical methodologies must be developed to allow such type of toxicological studies.

We have chosen to study the effects of $(PhTe)_2$ in the cerebellum since the development of this brain structure is mainly postnatal and the vulnerability during this phase of rapid growth has been largely described (Dobbing et al.1970; Dobbing and Sands 1973;Dobbing, Pediatrics 53: 2–6, 1974). Similarly, important developmental events are described in the striatum during the first postnatal weeks (Chesselet et al 2007; Navarro et al 1993). Therefore, considering striatum and cerebellum, elucidation of the biochemical steps leading to $(PhTe)_2$-induced neurotoxicity in this developmental period provide us new clues to the mechanisms underlying the actions of this neurotoxin in these two brain structures**.** Therefore, in the present report we describe the effects of dam exposure to $(PhTe)_2$ and/or $(PhSe)_2$ on the cellular signaling targeting the cytoskeleton of striatum and cerebellum in their offspring.

2. Material and Methods

2.1.Radiochemical and compounds

[^{32}P]Na_2HPO_4 was purchased from CNEN, São Paulo, Brazil. Benzamidine, leupeptin, antipain, pepstatin, chymostatin, acrylamide and bis-acrylamide and anti-PKAcα, anti-GFAP (G3893), anti-NF-L (N5264), anti NF-M (N2787) and anti-NF-H (N0142) antibodies were obtained from Sigma (St. Louis, MO, USA). The chemiluminescence ECL kit peroxidase and the conjugated anti rabbit IgG (A0545) were obtained from

Amersham (Oakville, Ontario, Canada). Anti-ERK (#9102), anti-pERK (#3371), anti-anti-SAP/JNK (#4671S), anti-pSAP/JNK (#4671), anti-actin (#4967), anti PKA (#4782), anti-KSP repeat (#MAB1592) antibodies were obtained from Cell Signaling Technology (USA) and anti-pSer55NF-L (sc12965-R) p38MAPK (sc7972), anti-phospho p38MAPK (sc17852R), were obtained from Santa Cruz Biotechnology Inc.. The organochalcogenides $(PhSe)_2$ and $(PhTe)_2$ were synthesized using the method described by Paulmier (1986) and Petragnami (1994), respectively. Analysis of the 1H NMR and ^{13}C NMR spectra showed that the compound obtained presented analytical and spectroscopic data in full agreement with their assigned structures. The purity of the compounds were assayed by high resonance mass spectroscopy (HRMS) and was higher that 99.9%. $(PhTe)_2$ was dissolved in dimethylsulfoxide (DMSO) just before use. The final concentration of DMSO was adjusted to 0.1%. Solvent controls attested that at this concentration DMSO did not interfere with the phosphorylation measurement. All other chemicals were of analytical grade and were purchased from standard commercial supplier.

2.2.Animals

Adult female Wistar rats (200–250 g) and their offspring were obtained from our breeding stock. Rats were maintained on a 12-h light/12-h dark cycle in a constant temperature (22^o C) colony room. On the day of birth the litter size was culled to seven-eigth pups. Litters smaller than seven pups were not included in the experiments. Water and a 20% (w/w) protein commercial chow were provided *ad libitum*. The experimental protocol followed the "Principles of Laboratory Animal Care" (NIH publication 85-23, revised 1985) and was approved by the Ethics Committee for Animal Research of the Federal University of Rio Grande do Sul.

2.3.Exposure to diphenyl ditelluride

Animal exposure to $(PhTe)_2$ was carried out as described by Stangherlin et al. (2006). Briefly, sexually naive female rats were mated with males previously tested as fertile (three females and one male in each cage). The onset of pregnancy was confirmed by the presence of sperm in vaginal smears (day 0 of pregnancy) and pregnant dams were immediately housed in individual cages. At birth, the dams received $(PhTe)_2$ (0.01 mg/kg, experimental group) or canola oil (1 ml/kg, control group) via subcutaneous (s.c.) injection once daily during the first 14 days of lactational period (sub-chronic exposure). At birth, all litters were culled to seven-eight pups. On PND 15, 21, 30 or 45 the animals from an entire litter were killed by decapitation without anesthesia, the brain was removed and cerebral structures—striatum and cerebellum—were separated. In the experiments with 30 or 45 day old animals, pups from entire litters were weaned on PND 21 and placed on *ad libitum* standard rat chow diets until sacrifice. In the experiments designed to study prevention of $(PhTe)_2$ effects, animals were treated with a subcutaneous injection of $(PhSe)_2$ (1 mg/Kg body weight) 30 minutes before each $(PhTe)_2$ administration. Rats were sacrificed on PND 21.

2.4.Preparation and labeling of slices

Rats were killed by decapitation, striatum and cerebellum were dissected onto Petri dishes placed on ice and cut into 400 μm thick slices with a McIlwain chopper.

2.5. Preincubation

Tissue slices were initially preincubated at 30 °C for 20 min in a Krebs-Hepes medium containing 124 mM NaCl, 4 mM KCl, 1.2 mM $MgSO_4$, 25 mM Na-HEPES (pH 7.4), 12

mM glucose, 1 mM $CaCl_2$, and the following protease inhibitors: 1 mM benzamidine, 0.1 μM leupeptin, 0.7 μM antipain, 0.7 μM pepstatin and 0.7 μM chymostatin.

2.6.*In vitro* ^{32}P incorporation experiments

After preincubation, the medium was changed and incubation was carried out at 30 °C with 100 μl of the basic medium containing 80 μCi of [^{32}P] orthophosphate. The labeling reaction was normally allowed to proceed for 30 min at 30 °C and stopped with 1 ml of cold stop buffer (150 mM NaF, 5 mM, EDTA, 5 mM EGTA, Tris–HCl 50 mM, pH 6.5), and the protease inhibitors described above. Slices were then washed twice with stop buffer to remove excess radioactivity.

2.7.Preparation of the high salt-Triton insoluble cytoskeletal fraction from tissue slices

After treatment, IF-enriched cytoskeletal fractions were obtained from striatum and cerebellum of 15, 21, 30 or 45-day-old rats as described by Funchal et al. (2003). Briefly, after the labelling reaction, slices were homogenized in 400 μl of ice-cold high salt buffer containing 5 mM KH_2PO_4 (pH 7.1), 600 mM KCl, 10 mM $MgCl_2$, 2 mM EGTA, 1 mM EDTA, 1% Triton X-100 and the protease inhibitors described above. The homogenate was centrifuged at 14000 x g for 10 min at 4°C, in Eppendorf centrifuge, the supernatant was discarded and the pellet homogenized with the same volume of the high salt medium. The suspended pellet was centrifuged as described and the supernatant was discarded. The final Triton-insoluble IF-enriched pellet, containing NF subunits, Vim and GFAP, was dissolved in 1% SDS and protein concentration was determined (Lowry et al. 1951).

2.8. Polyacrylamide gel electrophoresis (SDS-PAGE)

The cytoskeletal fraction was prepared as described above. Equal protein concentrations were loaded onto 10% polyacrylamide gels and analyzed by SDS-PAGE according to the discontinuous system of Laemmli (1970). After drying, the gels were exposed to X-ray films (Kodak T-Mat) at -70^{o}C with intensifying screens and finally the autoradiograph was obtained. Cytoskeletal proteins were quantified by scanning the films with a Hewlett-Packard Scanjet 6100C scanner and determining optical densities with an Optiquant version 02.00 software (Packard Instrument Company). Density values were obtained for the studied proteins.

2.9. Preparation of total protein homogenate

Tissue slices were homogenized in 100 µl of a lysis solution containing 2 mM EDTA, 50 mM Tris–HCl, pH 6.8, 4% (w/v) SDS. For electrophoresis analysis, samples were dissolved in 25% (v/v) of solution containing 40% glycerol, 5% mercaptoethanol, 50 mM Tris–HCl, pH 6.8 and boiled for 3 min.

2.10. Western blot assay

Cytoskeletal fractions (50 µg) or homogenate (80 µg) were separated by SDS-PAGE and transferred to nitrocellulose membranes (Trans-blot SD semi-dry transfer cell, BioRad) for 1 h at 15 V in transfer buffer (48 mM Trizma, 39 mM glycine, 20% methanol and 0.25% SDS). The nitrocellulose membranes were washed for 10 min in Tris-buffered saline (TBS; 0.5 M NaCl, 20 mM Trizma, pH 7.5), followed by 2 h incubation in blocking solution (TBS plus 5% defatted dried milk). After incubation, the blot was washed twice for 5 min with TBS plus 0.05% Tween-20 (T-TBS), and then incubated overnight at 4 °C in blocking solution containing the following monoclonal

antibodies: anti-NF-H (clone N52), diluted 1:1000, anti-NF-150 (clone NN-18) diluted 1:500, anti-NF-68 (clone NR-4) diluted 1:1000, anti-GFAP (clone G-A-5) diluted 1:400, anti-ERK diluted 1:1000, anti-pERK diluted 1:1000, anti-SAP/JNK (clone 98F2) diluted 1:1000, anti pSAP/JNK, diluted 1:1000, anti p38MAPK (A-12) diluted 1:1000, anti-phospho p38, diluted 1:1000, anti-PKAcα, diluted 1:1000, anti-KSP repeats diluted 1:1000 or anti-pSer55NF-L diluted 1:800. The blot was then washed twice for 5 min with T-TBS and incubated for 2 h in blocking solution containing peroxidase conjugated anti-rabbit IgG diluted 1:2000 or peroxidase conjugated anti-mouse IgG diluted 1:2000. The blot was washed twice again for 5 min with T-TBS and twice for 5 min with TBS. The blot was then developed using a chemiluminescence ECL kit. Immunoblots were quantified by scanning the films as described above. Optical density values were obtained for the studied proteins.

2.11. Protein determination

The protein concentration was determined by the method of Lowry et al. (1951) using serum bovine albumin as the standard.

2.12. Statistical analysis

Data were statistically analyzed by one-way analysis of variance (ANOVA) followed by the Tukey-Kramer multiple comparison test when the F-test was significant. All analyses were performed using the SPSS software program on an IBM-PC compatible computer.

3. Results

In the present report we attempted to analyze the *in vivo* effects of $(PhTe)_2$ (0.01 mg/kg of body weight) administered to dams during lactation on the homeostasis of the

cytoskeleton of their pups. We therefore analyzed the phosphorylating system associated with the IF proteins of striatum and cerebellum of pups on PND 15, 21, 30 and 45. To access the systemic toxicity of the neurotoxin, the body weight of dams and their offspring were initially recorded during the experimental period. Results showed that $(PhTe)_2$ did not reduce body weight of dams during the first 14 days of lactation period, when compared with non-exposed control dams (Figure 1A). Also, the body weight of offspring from $(PhTe)_2$-injected dams was not altered until PND 45 when compared with control pups (Figure 1B).

Slices from striatum and cerebellum of pups were incubated with ^{32}P-orthophosphate and the phosphorylation pattern of astrocyte (GFAP) as well as neuron (NF-L, NF-M and NF-H) IF proteins recovered in the cytoskeletal fraction was evaluated during development. As depicted in Figure 2, we found that $(PhTe)_2$ induced hyperphosphorylation of all the IF proteins studied in the striatum (Figure 2 A, B, C and D) and cerebellum (Figure 2 F, G, H and I) at PND 15 and 21, recovering control values at PND 30 and 45. Protein levels evaluated by Western blot assay showed increased immunocontent of the GFAP, NF-L, NF-M and NF-H in the cerebellum of 15 day-old pups (Figure 3B), while in the striatum $(PhTe)_2$ failed to alter the immunocontent of the proteins studied (Figure 3A).

Next, we investigated the potential participation of the second messenger-independent protein kinases, which phosphorylate sites located on the carboxyl-terminal tail domain and second messenger-dependent protein kinases, described to target residues on the amino-terminal head domains of the IF subunits (Grant and Pant, 2000) in the $(PhTe)_2$-induced hyperphosphorylation of the IF proteins from striatum and cerebellum of pups.

Western blot assays using specific antibodies against total and phosphorylated forms of MAPKs in the striatum showed activation/phosphorylation of Erk1/2 on PND 21 (Figure 4A) and activation/phosphorylation of JNK on PND 15 (Figure 4B). Otherwise, p38MAPK was not activated in the striatum of $(PhTe)_2$ exposed pups (Figure 4C). On the other hand, the cerebellum of pups exposed to $(PhTe)_2$ presented activated/phosphorylated Erk1/2 at PND 15 and 21 (Figure 4D) as well as activated/phosphorylated p38MAPK on PND 21 (Figure 4F), while JNK was not activated (Figure 4 E). In addition, Western blot assays showed that either in the striatum or in the cerebellum of $(PhTe)_2$ exposed pups, the immunocontent of the catalytic subunit of PKA (PKAcα) was increased on PND 15 and 21 (Figure 5 A and B).

In an attempt to identify the phosphorylating sites targeted by the protein kinases PKA and MAPK, we assayed NF-LSer55, the main phosphorylating site targeted by PKA on NF-L, as well as KSP repeats, targeted by MAPKs (Heimfarth et al. 2011) on NF-M/NF-H, respectively. Western blot assay using anti-phosphoSer55 antibody and anti-NF-M/NF-H KSP repeats showed that the phosphorylation level of NF-M/NF-H KSP repeats and NF-LSer55 was increased in striatum (Figure 6A and B) and cerebellum (Figure 6 C and D) of both 15 and 21 day-old pups exposed to $(PhTe)_2$. These findings are in line with the evidence that activated MAPKs and PKA target phosphorylating sites on IFs in the cerebral structures of lactating rats whose dams were injected with $(PhTe)_2$.

To access the ability of $(PhSe)_2$ to prevent the action of $(PhTe)_2$ on the phosphorylating system associated with the cytoskeleton, dams were injected with the organic selenium (1 mg/Kg body weight) 30 minutes before each $(PhTe)_2$ administration. Interestingly, we found that $(PhSe)_2$ prevented hyperphosphorylation of

striatal IF proteins from astrocytes and neurons, but it failed to prevent the action of $(PhTe)_2$ in the cerebellum, as demonstrated in 21 day old pups (Figure 7 A and B).

Next, we intended to identify some protein kinases involved in the ability of $(PhSe)_2$ to prevent the action of $(PhTe)_2$ on the cytoskeletal proteins. Therefore, we evaluated the effects of that compound on MAPKs and PKAcα activities. Western blot assays using specific antibodies against total and phosphorylated forms of Erk1/2 showed that the Se compound prevented activation of this protein kinase either in striatum or in cerebellum of 21 day-old pups (Figure 8 A and B). Similarly, Western blot assay using anti-PKAcα antibody showed that in the presence of $(PhSe)_2$ the level of the active form of the enzyme was not different from control levels in both striatum and cerebellum of PND 21 pups (Figure 9 A and B). Interestingly, we found that $(PhSe)_2$ failed to prevent the stimulatory effect of $(PhTe)_2$ on p38MAPK in cerebellum (Figure 10).

4. Discussion

The suckling period in the rat represents a period of intense development of brain, particularly of neural components that will modulate synaptogenesis. Consequently, neurotoxicants that disrupt neural development during this critical period can cause permanent changes in brain biochemistry and behavior (Rice and Barone, 2000). In this context, the lactation in rats corresponds to a period of brain development ranging from the last gestational period to the onset of puberty in humans (Haut et al. 2004). Although extrapolation of conclusions from animal data to humans must be done with caution, the use of experimental animals of various developmental ages give us important clues about the evolution of neurotoxicant-induced brain damage and its possible consequences in humans. Therefore in the present study we used an

experimental model of lactational intoxication with $(PhTe)_2$ to determine potential changes in IF phosphorylation in rat brain. We demonstrate that exposure to $(PhTe)_2$, via maternal milk lead to altered homeostasis of the cytoskeleton of striatum and cerebellum of PND 15 and 21 pups. In our experimental conditions we used a low dose of $(PhTe)_2$ (0.01 mg/kg of body weight) which did not provoke any significant specific overt sign of maternal intoxication, such as reduction of body weight, tremor, garlic odor and loss of hair. Also, pups presented a normal development and gain of body weight. However, despite the absence of an apparent systemic toxicity, we found altered protein kinase activities and disruption of the homeostasis of the cytoskeleton in neural cells of both striatum and cerebellum of these pups.

Although we cannot exclude the involvement of a systemic toxicity of $(PhTe)_2$ on the observed IF hyperphosphorylation in lactating pups, our previous data showing hyperphosphorylation induced by *in vitro* treatment with $(PhTe)_2$ (Heimfarth, 2011, 2012) strongly suggest that the effect of the neurotoxicant is mainly related to an action on signaling mechanisms upstream of the enzymatic activities targeting the cytoskeleton, rather than an indirect effect in organs other than the brain.

The neurotoxic effect of this compound was evidenced by hyperphosphorylation of IF proteins associated with the IF enriched cytoskeletal fraction of glial cells (mainly astrocytes) and neurons from the two brain structures studied on PND 15 and 21 pups. The treatment with $(PhTe)_2$ provoked activation of PKA and MAPKs such as Erk1/2, JNK and p38MAPK, targeting neuronal cytoskeletal proteins both on NF-LSer55 and on KSP repeats. Activation of the protein kinases is a spatiotemporally regulated event providing an interesting insight on the differential susceptibility of the protein kinases associated with the IF cytoskeleton of striatum and cerebellum at different

developmental stages, in response to the injury induced by this neurotoxicant via maternal milk.

It is important to note that IF hyperphosphorylation was observed on PND 15 and 21, restoring control values afterwards. It is difficult to evaluate the molecular mechanisms leading to the disruption of cytoskeletal homeostasis until PND 21, however they could be related with the maturation program of these brain structures. In fact, during the suckling period, the brain of rats undergoes intensive morphological and biochemical modifications (Ben-Ari and Holmes, 2006). In this context, Tepper et al. (1998) showed that the postnatal third week is an intense period of morphological and electrophysiological changes in the striatum. Therefore, it is feasible that the most prominent susceptibility of striatum until the third postnatal week be related to the developmental events characteristic of this period. Moreover, in the cerebellum, the susceptibility to $(PhTe)_2$ could be related to the postnatal appearance of granule cells (Fonnum and Lock, 2000).

In the cerebellum of 15 day-old pups, the IF hyperphosphorylation was accompanied by an increased immunocontent of the astrocyte and neuron IF proteins. This is in line with previously reported data showing increased immunocontent of IF proteins in cerebral cortex of 15 day-old rats injected with $(PhTe)_2$ (0.3 mmol/kg body weight) (Heimfarth et al. 2008).

The IF organization in eukaryotic cells depends on the phosphorylation level of its constituent proteins which are controlled by the activity of the cytoskeletal-associated phosphorylating/dephosphorylating system (Sihag et al. 2007). In this context, aberrant phosphorylation/dephosphorylation of cytoskeletal proteins in response to different stressors could be a consequence of changes in the activity of IF-

associated kinases or phosphatases and may have serious consequences for cellular function and structure (Loureiro et al. 2010, 2011;Pierozan et al. 2012). This evidence is supported by the present results, showing the action of $(PhTe)_2$ on the protein kinase activities which, in turn, disrupt the homeostasis of the cytoskeleton and this could be on the basis of the neurotoxicity of this compound. Aberrant phosphorylation of cytoskeletal proteins is thought to be related to neuronal damage and formation of aggregates of cytoskeletal elements in different cell compartments, which can be considered a common characteristic of some neurodegenerative diseases (Petzold, 2005). It is known that carboxyl-terminal phosphorylation of NF-H progressively restricts association of NF with kinesin, the axonal anterograde motor protein, and stimulates its interaction with dynein, the axonal retrograde motor protein (Motil et al. 2006). This event could represent one of the mechanisms by which carboxyl-terminal phosphorylation would slow NF axonal transport. Consistent with this, MAPK phosphorylates NF-M and NF-H tail domains (Chan et al. 2004, Li et al. 1999, Veeranna et al 1998) and alters the association of neurofilaments with motor proteins (Yabe et al. 2000). Therefore, extensively phosphorylated NF-M and NF-H as well as MAPK activation could interfere with NF axonal transport and explain, at least in part, the consequent neural dysfunction associated with this intoxication. In astrocytes, the action of $(PhTe)_2$ induced hyperphosphorylation of GFAP, by PKA. It is of note that this protein kinase is implicated in the phosphorylation of sites in the head domain of GFAP, as well as NF-L in neurons (Pierozan et al. 2012). Phosphorylation of the head domain of these IF subunits is known to be important for filament assembly. Therefore, abnormal phosphorylation of the head domain sites of these IF proteins could lead to nonphysiological disassembly of IFs contributing to disruption of cell homeostasis (Gill et al., 1990; Heins et al., 1993).

Also, misregulation of the phosphorylating level of the cytoskeletal proteins in intoxicated pups could be related with the behavioral deficits reported in $(PhTe)_2$ injected rats (Widy-Tyszkiewicz et al. 2002). It is always expected that the deleterious effects of tellurium are preferentially expressed during development, since the intense plasticity underlying the developmental events (Xie et al 2006, Tolias et al. 2011) are dependent on efficient remodeling of the cytoskeleton which, in turn, is dependent on the physiological phosphorylation of the cytoskeletal proteins. Improper developmental plasticity likely impedes information processing in the brain.

It is important to emphasize that the effect of $(PhTe)_2$ was not mimicked by its analogous selenium compound $(PhSe)_2$, since diselenide *per se* was unable to cause alterations in the phosphorylation level of the IF proteins. Nonetheless, exposure to $(PhTe)_2$ plus $(PhSe)_2$ via maternal milk prevented activation of Erk1/2 and PKA in the striatum on PND 21 pups, but failed to prevent activation of p38MAPK in the cerebellum at the same developmental stage. Considering that p38MAPK was phosphorylated/activated only in the cerebellum of PND 21, we are tempted to speculate that these findings support the inability of $(PhSe)_2$ to prevent hyperphosphorylation of the IF proteins of this cerebral structure.

Supporting the relevance of maternal milk as via of exposure for the $(PhTe)_2$ toxicity, Stangherlin and colleagues (2009a) reported the effect of $(PhTe)_2$ (0.03mg/kg of body weight) exposure to mothers on the cerebral oxidative status in hippocampus and striatum of their offspring. Also, the same concentration of $(PhTe)_2$ administered to dams caused cognitive impairment in pups intoxicated via maternal milk (Stangherlin et al. 2009b). Otherwise, higher doses of $(PhTe)_2$ (0.12 mg/kg of body weight) administered to dams provoked reduction of body weight gain of dams and teratogenic effects in fetuses (Stangherlin et al. 2005).

The neuroprotective effect of $(PhSe)_2$ against the neurotoxic effects of $(PhTe)_2$ can be related in part to the antioxidant and anti-inflammatory properties of the selenium compound (Nogueira and Rocha, 2011). Furthermore, $(PhSe)_2$ could also change the distribution of tellurium in the dam and pups. We could also propose that prevention of the toxic effects of $(PhTe)_2$ could be related to the fact that $(PhSe)_2$ is less reactive than $(PhTe)_2$, and consequently could interact with target proteins without interfering with the protein function.

Also, it is important to note that our group previously reported that young rats injected with $(PhTe)_2$ (0.3 µmol/kg body weight) presented hyperphosphorylation of NF subunits, GFAP and vimentin in cerebral cortex as well as GFAP and vimentin in hippocampus, reinforcing that one of the actions of the neurotoxicant *in vivo* is focused on the signaling mechanisms upstream of the homeostasis of the cytoskeleton of neural cells. Interestingly, these effects were totally reversed by a single subcutaneous injection of $(PhSe)_2$ (5 µmol/kg body weight) (Heimfarth et al. 2008). Therefore, the present data together with evidence in the literature are in line with Stangerlin et al. (2006) who proposed that it seems plausible to assume that tellurium become bioavailable to suckling rats after exposure of their mothers to $(PhTe)_2$.

5. Conclusions

In conclusion, $(PhTe)_2$ injected to dams markedly activated MAPKs and PKA taking part of the phosphorylating system associated with the cytoskeleton in striatum and cerebellum of their offspring, reinforcing the relevance of maternal milk as transmission via for this neurotoxicant. This effect was spatiotemporally regulated, and apparently in lactating pups, the posttraductional mechanisms regulating the cytoskeleton from

striatum and cerebellum in younger pups is more susceptible to the action of the neurotoxicant than in older ones. In fact, suckling rats can be considered extremely susceptible to $(PhTe)_2$-induced neurotoxicity, since the dose of $(PhTe)_2$ given to dams was extremely low. As corollary, the offspring of $(PhTe)_2$-treated dams is expected to be exposed to telluride levels much lower than that given to their mothers. Regarding to the ability of selenium compounds to protect against the tellurium toxicity toward the phosphorylating system associated with the cytoskeletal proteins, the present findings show a promising route to be exploited for a possible treatment of organic tellurium poisoning.

Taking into account the relevance of the signaling mechanisms targeting the cytoskeleton during early postnatal brain development (Guardiola-Diaz et al. 2012; Riederer, 1992), we presume that misregulation of the homeostasis of the cytoskeleton we evidenced can probably contribute to the deleterious action of $(PhTe)_2$ on the developing and adult brain, a fact that might explain at least in part the neurotoxicity of this compound, however these consequences need further investigation.

Although the exposure of pregnant humans to $(PhTe)_2$ is unlike, the extensive use of this compound in organic synthesis and, particularly, its high lipophilicity can determine it deposition in adipose tissue for a long time. Consequently, an occasional exposure to $(PhTe)_2$ in a period before pregnancy could lead to exposure to this compound during pregnancy and/or lactation, depending on the it mobilization from adipose tissue. The results presented here clearly indicate that manipulation and use of $(PhTe)_2$ must be done with caution in order to avoid contamination. This is more important to women in the reproductive period particularly in view of the neurotoxicity of very low doses of $(PhTe)_2$.

6. Conflict of interest statement

The authors declare no conflicts of interest.

7. Ackowledgements

This work was supported by Conselho Nacional de Desenvolvimento Científico e Tecnológico (CNPq), Fundação de Amparo à Pesquisa do Estado do Rio Grande do Sul (FAPERGS), PRONEX and Propesq-UFRGS.

8. References

Ackerley S, Grierson AJ, Brownlees J, Thornhiel P, Anderton BH, Leight PN, et al. Glutamate slow axonal transport of neurofilaments in transfected neurons. J Cell Biol 2000;150:165–75.

Alberts B, Johnson A, Lewis J, Raff M, Roberts K, Walter P. The cytoskeleton. In: Alberts B, Johnson A, Lewis J, Raff M, Roberts K, Walter P, editors. Molecular biology of the cell. New York: Garland Science; 2008. p. 965–1025.

Arbustini E, Pasotti M, Pilotto A, Pellegrini C, Grasso M, Previtali S, Repetto A, Bellini O, Azan G, Scaffino M, Campana C, Piccolo G, Vigano M, Tavazzi L. Desmin accumulation restrictive cardiomyopathy and atrioventricular block associated with desmin gene defects. Eur J Heart Fail 2006;8:477-83.

Ben-Ari Y, Holmes G. Effects of seizures on developmental processes in the immature brain. http://neurology.thelancet.com 2006;5:1055-63.

Beaulieu JM, Nguyen MD, Julien JP. Late onset of motor neurons in mice overexpressing wild-type peripherin. J Cell Biol 1999;147:531-44.

Chan, W.K.-C.; Dickerson, A.; Otriz, D.; Pimenta, A.; Moran, C.; Malik, K.; Motil, J.; Snyder, S.; Pant, H.C.; Shea, T.B. Mitogen activated protein kinase regulates neurofilament axonal transport. *J. Cell Sci.,* **2004**, *117*, 4629–4642.

Chang L, Goldman RD. Intermediate filaments mediate cytoskeletal crosstalk. Nature Rev/Mol Cell Biol 2004;5:601-13.

Chesselet MF, Plotkin JL, Wu N, Levine MS. Development of striatal fast-spiking GABAergic interneurons. Prog Brain Res. 2007;160:261-72.

Daile P, Carnegie PR, Young JD. Synthetic substrate for cyclic AMP-dependent protein kinase. Nature 1975; 257:416–8.

Dobbing J, Hopewell JW, Lynch A Sands J. Vulnerability of developing brain.I. Some lasting effects of X-irradiation. Exp. Neurol. 28: 442-449, 1970

Dobbing J, Sands J. Quantitative growth and development of human brain. Arch Dis Child. 48:757-67, 1973

Dobbing J The later growth of the brain and its vulnerability. Pediatrics. 53:2-6, 1974.

Eng LF, Ghirnikar RS, Lee YL. Glial fibrillary acidic protein: GFAP-thirty-one years (1969–2000). Neurochem Res 2000;25:1439–51.

Fonnum F, Lock EA. Cerebellum as a target for toxic substances. Toxicol Lett 2000; 112–113:9–16.

Funchal C, de Almeida LM, Oliveira Loureiro S, Vivian L, de Lima Pelaez P, Dall Bello Pessutto F, Rosa AM, Wajner M, Pessoa-Pureur R. In vitro phosphorylation of cytoskeletal proteins from cerebral cortex of rats. Brain Res Prot 2003; 11:111–8.

Funchal C, Moretto MB, Vivian L, Zeni G, Rocha JB, Pessoa-Pureur R. Diphenyl ditelluride- and methylmercury-induced hyperphosphorilation of the high molecular weight neurofilament subunit is prevented by organoselenium compounds in cerebral cortex of young rats. Toxicology. 2006 May 1;222(1-2):143-53. Epub 2006 Mar 6.

Geisler N, Vandekerckhove J, Weber K. Location and sequence characterization of the major phosphorylation sites of the high molecular mass neurofilament proteins M and H. FEBS Lett 1987;221:403–7.

Gill SR, Wong PC, Monteiro MJ, Cleveland DW. Assembly properties of dominant and recessive mutations in the small mouse neurofilament (NF-L) subunit. J Cell Biol 1990;111 (5 Pt 1):2005–19.

Grant P, Pant HC. Neurofilament protein synthesis and phosphorylation. J Neurocytol 2000; 29: 843-72.

Green SL, Westendorf JM, Jaffe H, Pant HC, Cork LC, Ostrander EA, Vignaux F, Ferrell JE Jr. Allelic variants of the canine heavy neurofilament (NFH) subunit and extensive phosphorylation in dogs with motor neuron disease. J Comp Pathol 2005; 132:33-50.

Guardiola-Diaz HM, Ishii A, Bansal R. Erk1/2 MAPK and mTOR signaling sequentially regulates progression through distinct stages of oligodendrocyte differentiation. Glia doi: 10.1002/glia.22281, 2011.

Heimfarth L, Loureiro SO, Zamoner A, Pelaez P de L, Nogueira CW, Rocha JB, Pessoa-Pureur R. Effects of in vivo treatment with diphenyl ditelluride on the phosphorylation of cytoskeletal proteins in cerebral cortex and hippocampus of rats. Neurotoxicology 2008;29:40-7.

Heimfarth L, Loureiro SO, Reis KP, de Lima BO, Zamboni F, Gandolfi T, Narvaes R, da Rocha JB, Pessoa-Pureur R. Cross-talk among intracellular signaling pathways mediates the diphenyl ditelluride actions on the hippocampal cytoskeleton of young rats. Chem Res Toxicol 2011;24:1754-64.

Heimfarth L, Loureiro SO, Reis KP, de Lima BO, Zamboni F, Lacerda S, Soska AK, Wild L, da Rocha JB, Pessoa-Pureur R. Diphenyl ditelluride induces hypophosphorylation of intermediate filaments through modulation of DARPP-32-dependent pathways in cerebral cortex of young rats. Arch Toxicol 2012;86:217-30.

Heins S, Wong PC, Muller S, Goldie K, Cleveland DW, Aebi U. The rod domain of NF-L determines neurofilament architecture, whereas the end domains specify filament assembly and network formation. J Cell Biol 1993;123 (6 Pt 1):1517–33.

Haut SH, Velisková J, Moshé SL. Susceptibility of immature and adult brains to seizure effects. Lancet Neurol 2004;3:608-17.

Jaffe H, Veeranna, Shetty KT, Pant HC. Characterization of the phosphorylation sites of human high molecular weight neurofilament protein by electrospray ionization tandem mass spectrometry and database searching. Biochemistry 1998;37,3931–40.

Julien JP, Cote F, Collard JF. Mice overexpressing the human neurofilament heavy gene as a model of ALS. Neurobiol Aging 1995;16:487-90; discussion 490-82.

Kemp BE, Bylund DB, Huang TS, Krebs EG. Substrate specificity of the cyclic AMP-dependent protein kinase. Proc Natl Acad Sci U S A. 1975;72,3448–52.

Laemmli UK. Cleavage of structural proteins during the assembly of the head of bacteriophage T4. Nature 1970;227:680-85.

Lariviere RC, Julien JP. Functions of intermediate filaments in neuronal development and disease. J Neurobiol 2004;58:131-48.

Larner AJ. How does garlic exert its hypocholesterolaemic action? The tellurium

hypothesis. Med Hypotheses 1995;44:295–7.

Lee, VM, Otvos Jr, L, Carden MJ, Hollosi M, Dietzschold B, Lazzarini RA. Identification of the major multiphosphorylation site in mammalian neurofilaments. Proc Natl Acad Sci U S A 1988;85,1998–2002.

Li, B.S.; Veeranna, Gu. J;; Grant, P.; Pant, H.C. Activation of mitogen-activated protein kinases (Erk1 and Erk2) cascade results in phosphorylation of NF-M tail domains in transfected NIH 3T3 cells. *Eur. J. Biochem.*, **1999**, *262*, 211–217.

Loureiro SA, Heimfarth L, de Lima Pelaez P, Arcce Lacerda B, Fedatto Vidal L, Soska A, Gomes dos Santos N, Andrade C, Tagliari B, Scherer EBS, Guma FTCR, Wyse ATS Pessoa-Pureur R. Hyperhomocysteinemia selectively alters expression and stoichiometry of intermediate filament and induces glutamate- and calcium-mediated mechanisms in rat brain during development. Int J Dev Neurosci 2010;28:21-30.

Loureiro SO, Heimfarth L, Reis K, Wild L, Andrade C, Guma FTCR, Gonçalves CA, Pessoa-Pureur R. Acute ethanol exposure disrupts actin cytoskeleton and generates reactive oxygen species in C6 cells. Toxicol in vitro 2011;25:28-36.

Lowry OH, Rosebrough NJ, Farr AL, Randall RJ. Protein measurement with the Folin phenol reagent. J Biol Chem 1951;193:265-75.

Moretto MB, Funchal C, Zeni G, Rocha JBT, Pessoa-Pureur R. Organoselenium compounds prevent hyperphosphorylation of cytoskeletal proteins induced by the

neurotoxic agent diphenyl ditelluride in cerebral cortex of young rats. Toxicology 2005;210:213–22.

Motil, J.; Chan, W.K.; Dubey, M.; Chaudhury, P.; Pimenta, A.; Chylinski, T.M.; Ortiz, D.T.; Shea, T.B. Dynein mediates retrograde neurofilament transport within axons and anterograde delivery of NFs from perikarya into axons: regulation by multiple phosphorylation events. *Cell Motil. Cytoskeleton*, **2006,** *63*, 266-286.

Muller R, Zschiesche W, Steffen H, Schaller K. Tellurium-intoxication. Klin Wochenschr 1989;67:1152–5.

Nar AA, Diesel B, Desor F, Feidt C, Bouayed J, Kiemer AK, Soulimani R. Neurodevelopmental and behavioral toxicity of lactational exposure to the sum of six indicator non-dioxin-like-polychlorinated biphenyls (∑6 NDL-PCBs) in offspring mice. Toxicology. 2012 [Epub ahead of print]

Nogueira CW, Rocha JB. Toxicology and pharmacology of selenium: emphasis on synthetic organoselenium compounds. Arch Toxicol. 85:1313-1359, 2011

Pérez-Navarro E, Alberch J, Marsal J. Postnatal development of functional dopamine, opioid and tachykinin receptors that regulate acetylcholine release from rat neostriatal slices. Effect of 6-hydroxydopamine lesion. Int J Dev Neurosci. 11:701-708,1993.

Newman RA, Osborn S, Siddik ZH. Determination of tellurium in biological fluids by

means of electrothermal vapourization-inductively coupled to plasma mass spectrometry (ETV-ICP-MS). Clin Chim Acta 1989;179:191–6.

Nixon RA. The regulation of neurofilament protein dynamics by phosphorylation: clues to neurofibrillary pathobiology. Brain Pathol 1993;3:29-38.

Nogueira CW, Quinhones EB, Jung EA, Zeni G, Rocha JB Anti-inflammatory and antinociceptive activity of diphenyl diselenide. Inflamm Res. 2003 Feb;52(2):56-63.

Paulmier C. Selenium reagents and intermediates in organic synthesis, Pergamon Press, New York 1986; p. 463.

Pierozan P, Zamoner A, Soska ÂK, de Lima BO, Reis KP, Zamboni F, Wajner M, Pessoa-Pureur R. Signaling mechanisms downstream of quinolinic acid targeting the cytoskeleton of rat striatal neurons and astrocytes. Exp Neurol 2012; 233:391-9.

Petragnami N. Preparation of the principal classes of organic tellurium compounds, A.R. Katritzky, O. Meth-Cohn, C.W. Rees, Editors, Tellurium in Organic Synthesis, London: Academic Press 1994; pp. 9–88.

Petzold A. Neurofilament phosphoforms: surrogate markers for axonal injury, degeneration and loss. J Neurol Sci 2005;233:83–198.

Rice D, Barone S Jr. Critical periods of vulnerability for the developing nervous system: evidence from humans and animal models. Environ Health Perspect 2000; 108:511–33.

Riederer BM. Differential phosphorylation of some proteins of the neuronal ytoskeleton during brain development. Histochem J 1992; 24:783-90.

Sasaki T, Gotow T, Shiozaki M, Sakaue F, Saito T, Julien JP, Uchiyama Y, Hisanaga S. Aggregate formation and phosphorylation of neurofilament-L Pro22 Charcot-Marie-Tooth disease mutants. Hum Mol Genet 2006;15:943-52.

Siddik ZH, Newman RA. Use of platinum as a modifer in the sensitive detection of tellurium in biological samples. Anal Biochem 1988;172:190–6.

Shea TB, Yabe JT, Ortiz D, Pimenta A, Loomis P, Goldman RD Amin N, Pant HC. 2004. CDK5 regulates axonal transport and phosphorylation of neurofilaments in cultured neurons. J. Cell Sci 117: 933-941.

Shea TB, Chan WK. Regulation of neurofilament dynamics by phosphorylation. Eur J Neurosci 2008;27,1893–1901.

Sihag RK, Inagaki M, Yamaguchi T, Shea TB, Pant HC. Role of phosphorylation on the structural dynamics and function of types III and IV intermediate filaments. Exp Cell Res 2007;313:2098-2109.

Stangherlin EC, Favero AM, Zeni G et al. Exposure of mothers to diphenyl ditelluride during the suckling period changes behavioral tendencies in their offpring. Brain Res Bull 2006; 69:311–17.

Stangherlin E C, Ardais AP, Rocha J B T, Nogueira C W. Exposure to diphenyl ditelluride, via maternal milk, causes oxidative stress in cerebral cortex, hippocampus and striatum of young rats. Arch Toxicol 2009a; 83:485–91.

Stangherlin EC, Rocha JBT, Nogueira CW. Diphenyl ditelluride impairs short-term memory and alters neurochemical parameters in young rats. Pharmacol Biochem Behav 2009b; 91:430–5.

Stangherlin EC, Favero AM, Zeni G, Rocha JBT, Nogueira CW. Teratogenic vulnerability of Wistar rats to diphenyl ditelluride. Toxicology 2005; 207: 231–9.

Sun D, Leung CL, Liem RK. Phosphorylation of the high molecular weight neurofilament protein (NF-H) by Cdk5 and p35. J Biol Chem 1996;271, 14245–51.

Taylor A. Biochemistry of tellurium. Biol Trace Elem Res. 1996;55:231-9.

Tepper JM, Sharpe NA, Koós TZ, Trent F. Postnatal development of the rat neostriatum: electrophysiological, lightand electron-microscopic studies. Dev Neurosci 1998; 20:125– 45.

Tolias KF, Duman JG, Um K Control of synapse development and plasticity by Rho GTPase regulatory proteins. Prog Neurobiol. 2011 Jul;94(2):133-48. doi: 10.1016/j.pneurobio.2011.04.011. Epub 2011 Apr 22.

Veeranna, Amin ND, Ahn NG, Jaffe H, Winters CA, Grant P, Pant HC. Mitogen-activated protein kinases (Erk1,2) phosphorylate Lys-Ser-Pro (KSP) repeats in neurofilament proteins NF-H and NF-M. J Neurosci 1998;18: 4008–21.

Xie Z, Samuels BA, Tsai LH. Cyclin-dependent kinase 5 permits efficient cytoskeletal remodeling--a hypothesis on neuronal migration. Cereb Cortex. 2006 Jul;16 Suppl 1:i64-8.

Xu ZS, Liu WS, Willard MB. Identification of six phosphorylation sites in the COOH-terminal tail region of the rat neurofilament protein M. J Biol Chem 1992;267: 4467–71.

Yabe, J.T.; Chan, W.; Shea, T.B. Phospho-dependent association of neurofilament proteins with kinesin in situ. *Cell Motil. Cytoskeleton*, **2000**, *45*, 249–265.

Yarema MC, Curry SC. Acute tellurium toxicity from ingestion of metal-oxidizing solutions. Pediatrics 2005;116:319–21.

Widy-Tyszkiewicz E, Piechal A, Gajkowska B, Smiałek M. Tellurium-induced cognitive deficits in rats are related to neuropathological changes in the central nervous system. Toxicol Lett. 2002;131:203-14.

9. Legends to the figures

Figure 1: Effects of $(PhTe)_2$ administered to dams during lactation period on the gain of weight of the dams (A) and on the body weight of their pups (B). Body weight was obtained daily after $(PhTe)_2$ administration. Data are reported as means ± S.E.M. of 8-16 animals and expressed in grams. 1=control; 2= $(PhTe)_2$

Figure 2: Effects of $(PhTe)_2$ administered to dams during lactation period on the *in vitro* phosphorylation of IF proteins in striatum (A, B,C, D and E) and cerebellum (F, G, H, I and J) of their pups. At birth, dams received $(PhTe)_2$ (0.01 mg/kg, experimental group) or canola oil (1 ml/kg, control group) via subcutaneous injection once daily during the first 14 days of lactational period. On PND 15, 21, 30 or 45 the animals were killed by decapitation without anesthesia, the brain was removed, striatum and cerebellum were isolated and the *in vitro* phosphorylation of IF proteins in the striatum (A, B,C, D and E) and cerebellum (F, G, H, I and J) of the pups were determined. NF-H, high molecular weight neurofilament; NF-M, middle molecular weight neurofilament subunit; NF-L, low molecular weight neurofilament subunit and GFAP, glial fibrillary acidic protein. Representative stained gel and autoradiographs of the proteins studied are shown (E, striatum; J, cerebellum). Data are reported as means ± S.E.M. of 10-12 animals and expressed as percent of control. Statistically significant differences from canola oil-treated rats, as determined by one-way ANOVA followed by Tukey-Kramer test are indicated: *$P < 0.05$.

Figure 3: Effect of $(PhTe)_2$ administered to dams during lactation on the immunoreactivity of IFs in the cytoskeletal fraction from striatum (A) and cerebellum (B) of pups on PND 15 and 21. The IF immunocontent was measured by Western blot

assay, as described in section 2.10, using specific antibodies. Representative blots are shown (C). β-actin was used as loading control. Data are reported as means ± S.E.M. of 10-12 animals and expressed as percent of control. Statistically significant differences from canola oil-treated rats, as determined by one-way ANOVA followed by Tukey-Kramer test are indicated: *P < 0.05. NF-H, High molecular weight neurofilament subunit; NF-M, middle molecular weight neurofilament subunit; NF-L, low molecular weight neurofilament subunitand GFAP, glial fibrillary acidic protein.

Figure 4: Effect of $(PhTe)_2$ administered to dams during lactation on MAPK pathways of their pups on PND 15 and 21. Western blot assay of total and phosphorylated forms of ERK1/2 (A, D), JNK (B, E) and p38MAPK (C, F) of striatum (A, B, C) and cerebellum (D, E, F) were carried out as described in section 2.10. Representative blots are shown (G). β-actin was used as loading control. Data are reported as means ± S.E.M. of 10-12 animals and expressed as percent of control. Statistically significant differences from canola oil-treated rats, as determined by one-way ANOVA followed by Tukey-Kramer test are indicated: *P < 0.05.

Figure 5: Effect of $(PhTe)_2$ administered to dams during lactation on PKAc-α immunoreactivity in the striatum (A) and cerebellum (B) of their pups on PND 15 and 21. Western blot assay of PKAc-α was carried out as described in the section 2.10. Representative blots are shown. β-actin was used as loading control. Data are reported as means ± S.E.M. of 10-12 animals and expressed as percent of control. Statistically significant differences from canola oil-treated rats, as determined by one-way ANOVA followed by Tukey-Kramer test are indicated: *P < 0.05.

Figure 6: Effect of $(PhTe)_2$ administered to dams during lactation on the immunocontent of phosphoNF-H KSP repeats (A,C) and phosphoNF-L Ser55 (B,D) of striatum (A,B) and cerebellum (C,D) of their pups on PND 15 and 21. Western blot assays were carried out as described in section 2.10. Representative blots are shown (D). Data are reported as means ± S.E.M. of 10-12 animals and expressed as percent of control. Statistically significant differences from canola oil-treated rats, as determined by one-way ANOVA followed by Tukey-Kramer test are indicated: *P < 0.05.

Figure 7: Prevention of the effect of $(PhTe)_2$ on the phosphorylation of IF proteins by $(PhSe)_2$ on PND 21 pups. Striatum (A); cerebellum (B). Dams received $(PhSe)_2$ (1 mg/Kg body weight) 30 minutes before each $(PhTe)_2$ or canola oil administration once daily during the first 14 days of lactation, as described in section 2.3. NF-H, high molecular weight neurofilament; NF-M, middle molecular weight neurofilament subunit; NF-L, low molecular weight neurofilament subunit and GFAP, glial fibrillary acidic protein. Data are reported as means ± S.E.M. of 10-12 animals and expressed as percent of control. Statistically significant differences from canola oil-treated rats, as determined by one-way ANOVA followed by Tukey-Kramer test are indicated: *P < 0.05.

Figure 8: Prevention of the effect of $(PhTe)_2$ on ERK1/2 MAPK by $(PhSe)_2$ on PND 21 pups. Dams received $(PhSe)_2$ (1 mg/Kg body weight) 30 minutes before each $(PhTe)_2$ or canola oil administration once daily during the first 14 days of lactation, as described in section 2.3. The immunocontent of ERK 1/2 and phospho-ERK 1/2 were determined by Western blot assay in striatum (A) and cerebellum (B) of their pups. Representative blots are shown. Data are reported as means ± S.E.M. of 10-12 animals and expressed

as percent of control. Statistically significant differences from canola oil-treated rats, as determined by one-way ANOVA followed by Tukey-Kramer test are indicated: *P < 0.05.

Figure 9: Prevention of the effect of $(PhTe)_2$ on PKA activation by $PhSe)_2$ on PND 21 pups. Striatum (A); cerebellum (B). Dams received $(PhSe)_2$ (1 mg/Kg body weight) 30 minutes before each $(PhTe)_2$ or canola oil administration once daily during the first 14 days of lactation, as described in section 2.3. The immunocontent of PKAcα was determined by Western blot assay. Representative blots are shown. β-actin was used as loading control. Data are reported as means ± S.E.M. of 10-12 animals and expressed as percent of control. Statistically significant differences from canola oil-treated rats, as determined by one-way ANOVA followed by Tukey-Kramer test are indicated: *P < 0.05.

Figure 10: Prevention of the effect of $(PhTe)_2$ on p38MAPK activation from cerebellum of 21 day-old pups by $(PhSe)_2$. Dams received $(PhSe)_2$ (1 mg/Kg body weight) 30 minutes before each $(PhTe)_2$ or canola oil administration once daily during the first 14 days of lactation, as described in section 2.3. The immunocontent of p38MAPK and phospho-p38MAPK was determined by Western blot assay. Representative blots are shown. Data are reported as means ± S.E.M. of 10-12 animals and expressed as percent of control. Statistically significant differences from canola oil-treated rats, as determined by one-way ANOVA followed by Tukey-Kramer test are indicated: *P < 0.05.

Figure 1:

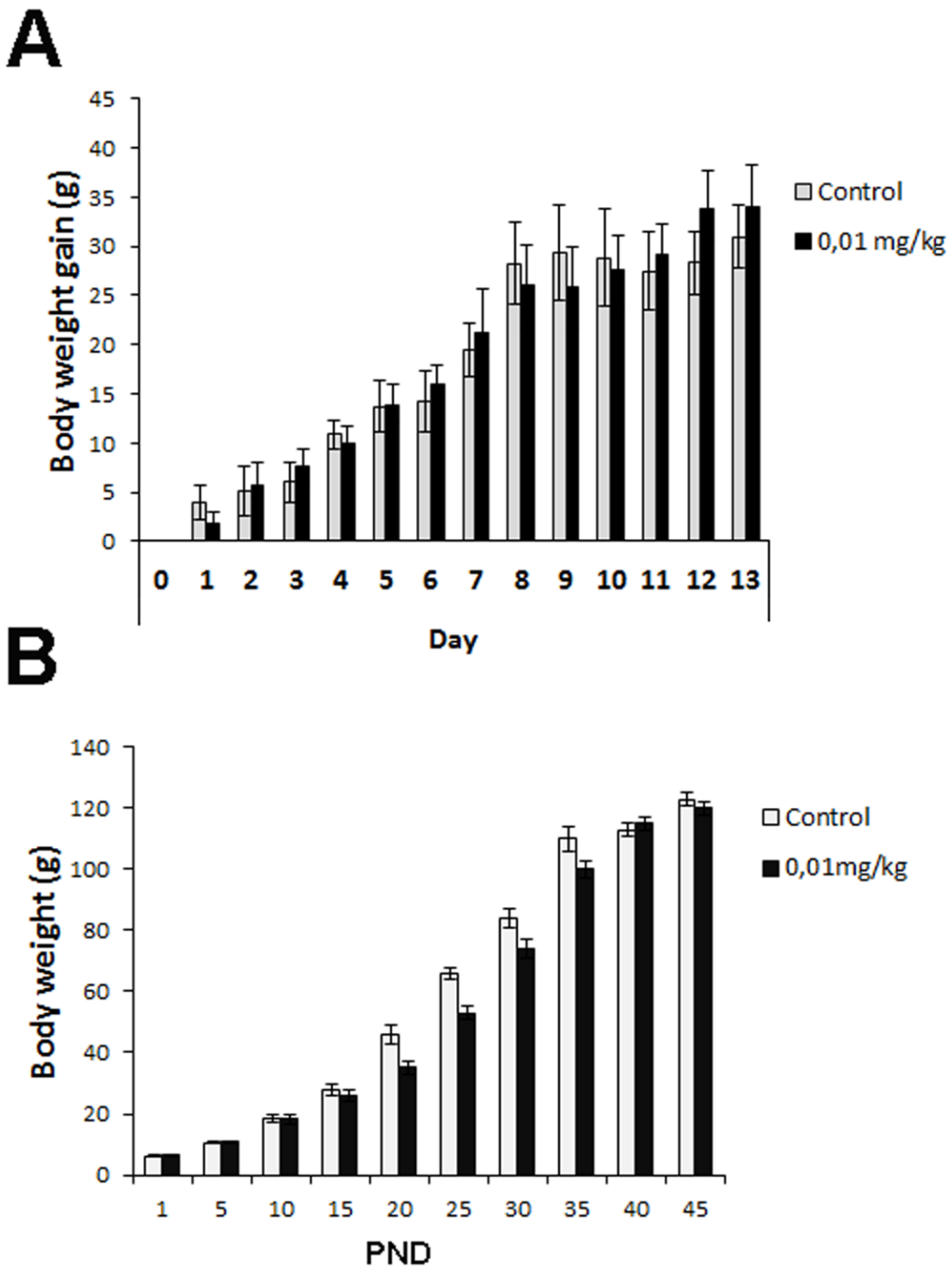
A
Body weight gain (g)
45
40
35
30
25
20
15
10
5
0
0 1 2 3 4 5 6 7 8 9 10 11 12 13
Day
Control
0,01 mg/kg
B
Body weight (g)
140
120
100
80
60
40
20
0
1 5 10 15 20 25 30 35 40 45
PND
Control
0,01mg/kg

Figure 2:

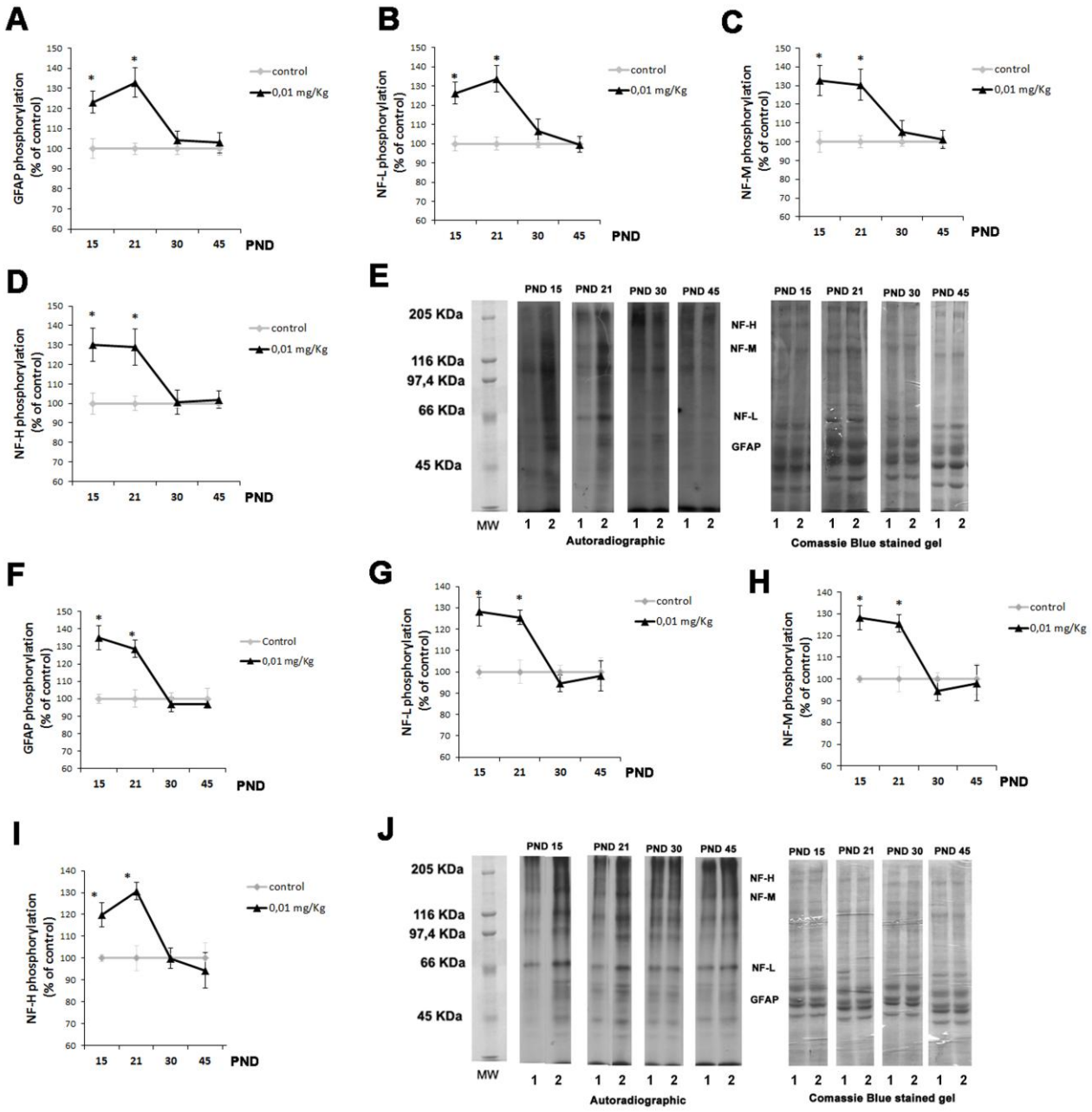
A
GFAP phosphorylation (% of control)
control
0,01 mg/Kg
PND
B
NF-L phosphorylation (% of control)
C
NF-M phosphorylation (% of control)
D
NF-H phosphorylation (% of control)
E
PND 15
PND 21
PND 30
PND 45
205 KDa
116 KDa
97,4 KDa
66 KDa
45 KDa
MW
Autoradiographic
NF-H
NF-M
NF-L
GFAP
Comassie Blue stained gel
F
Control
G
H
I
J

Figure 3:

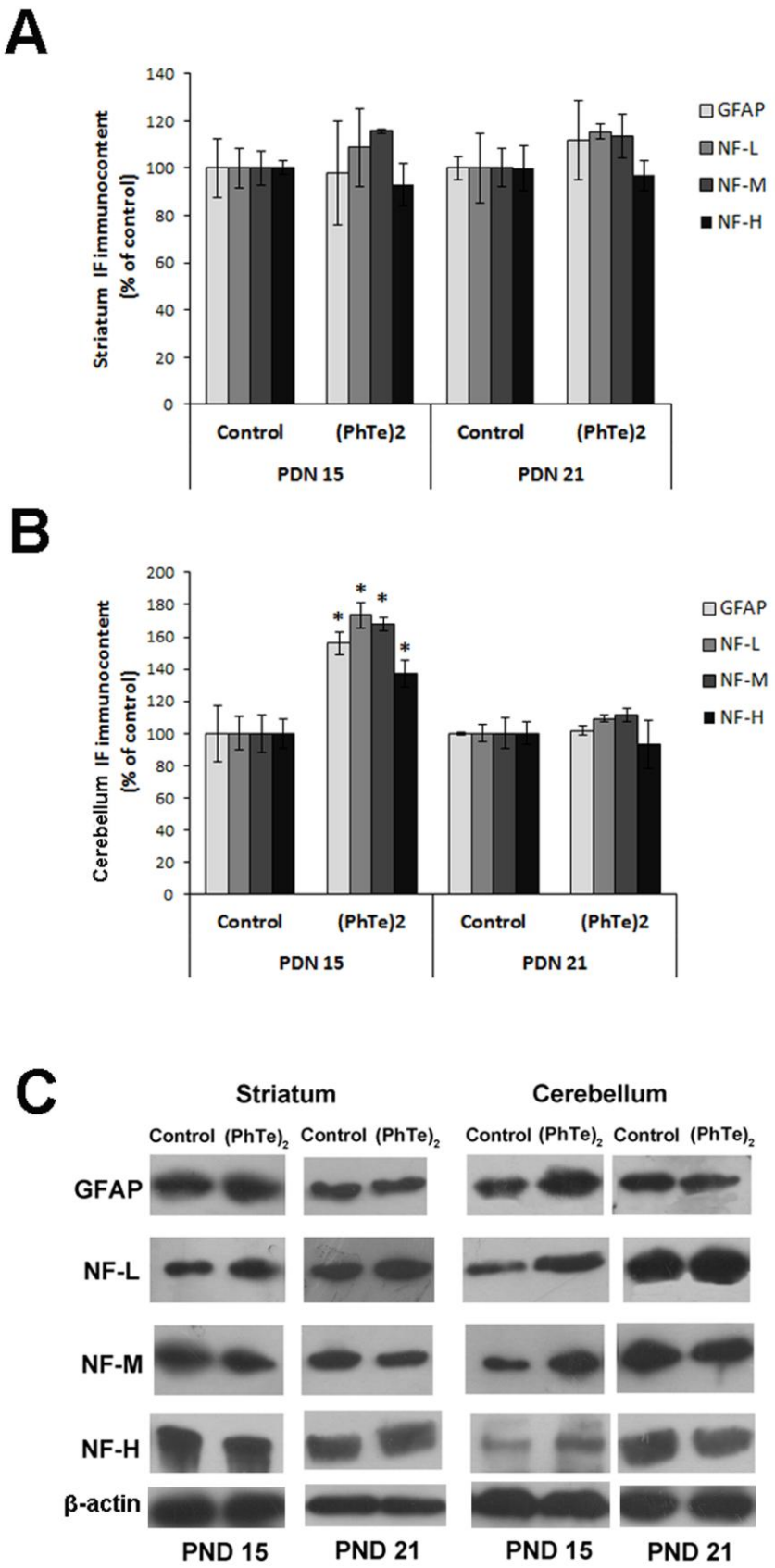
A
Striatum IF immunocontent (% of control)
140
120
100
80
60
40
20
0
GFAP
NF-L
NF-M
NF-H
Control
(PhTe)2
Control
(PhTe)2
PDN 15
PDN 21
B
Cerebellum IF immunocontent (% of control)
200
180
160
140
120
100
80
60
40
20
0
*
*
*
*
GFAP
NF-L
NF-M
NF-H
Control
(PhTe)2
Control
(PhTe)2
PDN 15
PDN 21
C
Striatum
Cerebellum
Control (PhTe)2 Control (PhTe)2
Control (PhTe)2 Control (PhTe)2
GFAP
NF-L
NF-M
NF-H
β-actin
PND 15
PND 21
PND 15
PND 21

Figure 4:

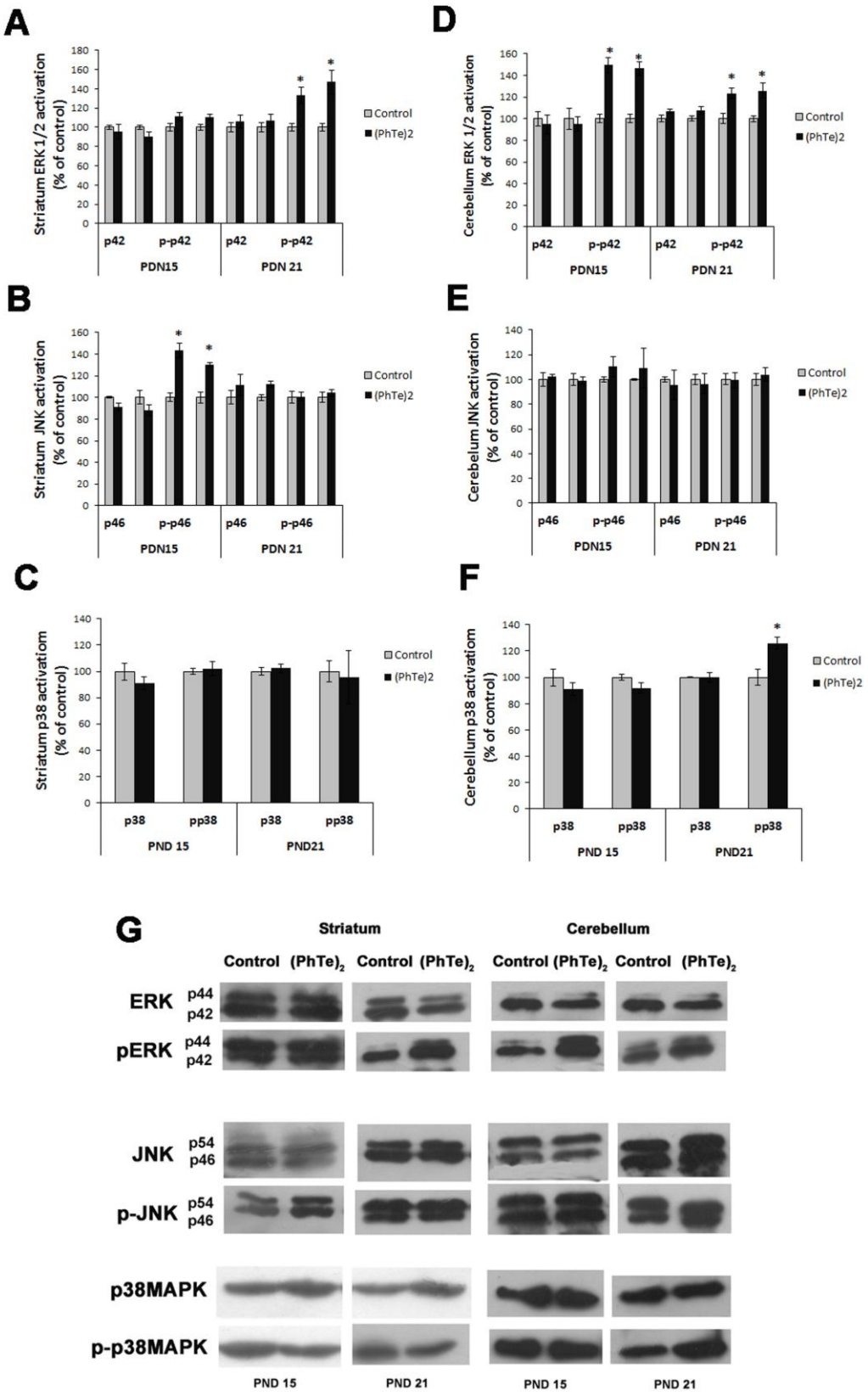
A
Striatum ERK1/2 activation (% of control)
Control
(PhTe)2
p42
p-p42
PDN15
PDN 21
D
Cerebellum ERK 1/2 activation (% of control)
B
Striatum JNK activation (% of control)
p46
p-p46
E
Cerebellum JNK activation (% of control)
C
Striatum p38 activatiom (% of control)
p38
pp38
PND 15
PND21
F
Cerebellum p38 activatiom (% of control)
G
Striatum
Cerebellum
Control
(PhTe)2
ERK
p44
p42
pERK
JNK
p54
p46
p-JNK
p38MAPK
p-p38MAPK
PND 15
PND 21

Figure 5:

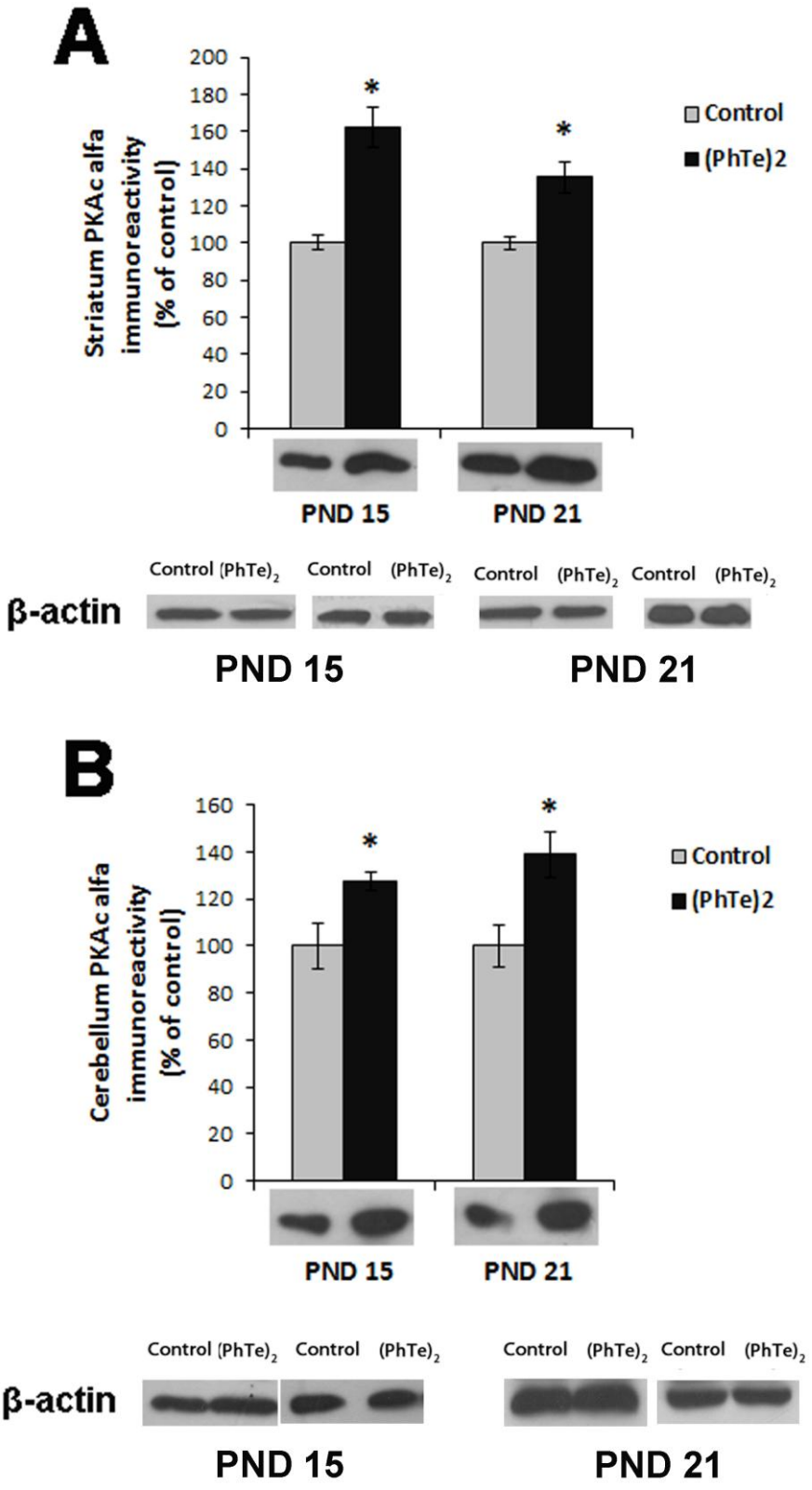
A
Striatum PKAc alfa immunoreactivity (% of control)
200
180
160
140
120
100
80
60
40
20
0
*
*
Control
(PhTe)2
PND 15
PND 21
Control (PhTe)2 Control (PhTe)2 Control (PhTe)2 Control (PhTe)2
β-actin
PND 15
PND 21
B
Cerebellum PKAc alfa immunoreactivity (% of control)
160
140
120
100
80
60
40
20
0
*
*
Control
(PhTe)2
PND 15
PND 21
Control (PhTe)2 Control (PhTe)2 Control (PhTe)2 Control (PhTe)2
β-actin
PND 15
PND 21

Figure 6:

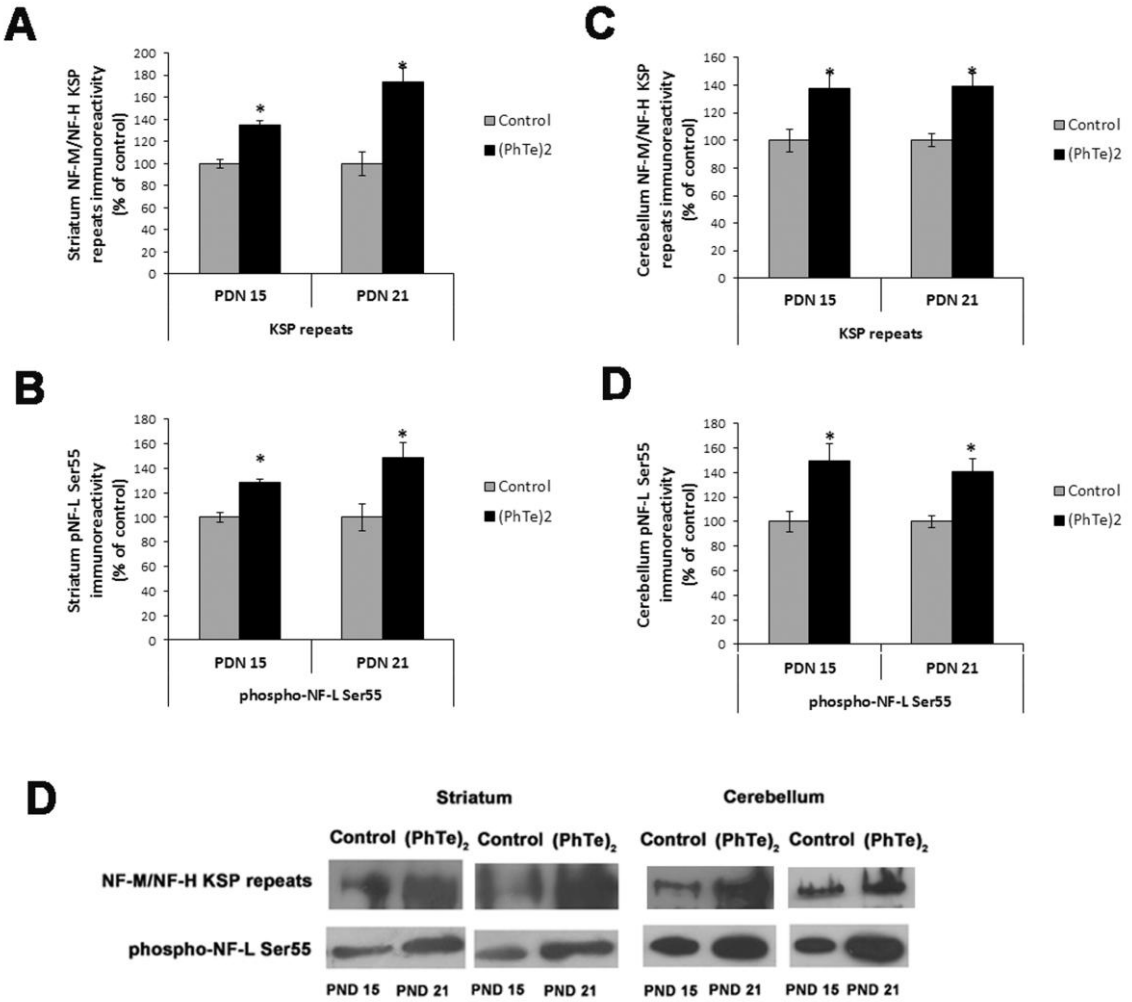
A
Striatum NF-M/NF-H KSP repeats immunoreactivity (% of control)
Control
(PhTe)2
PDN 15
PDN 21
KSP repeats
C
Cerebellum NF-M/NF-H KSP repeats immunoreactivity (% of control)
Control
(PhTe)2
PDN 15
PDN 21
KSP repeats
B
Striatum pNF-L Ser55 immunoreactivity (% of control)
Control
(PhTe)2
PDN 15
PDN 21
phospho-NF-L Ser55
D
Cerebellum pNF-L Ser55 immunoreactivity (% of control)
Control
(PhTe)2
PDN 15
PDN 21
phospho-NF-L Ser55

D
Striatum
Cerebellum
Control (PhTe)2 Control (PhTe)2
Control (PhTe)2 Control (PhTe)2
NF-M/NF-H KSP repeats
phospho-NF-L Ser55
PND 15 PND 21 PND 15 PND 21
PND 15 PND 21 PND 15 PND 21

Figure 7:

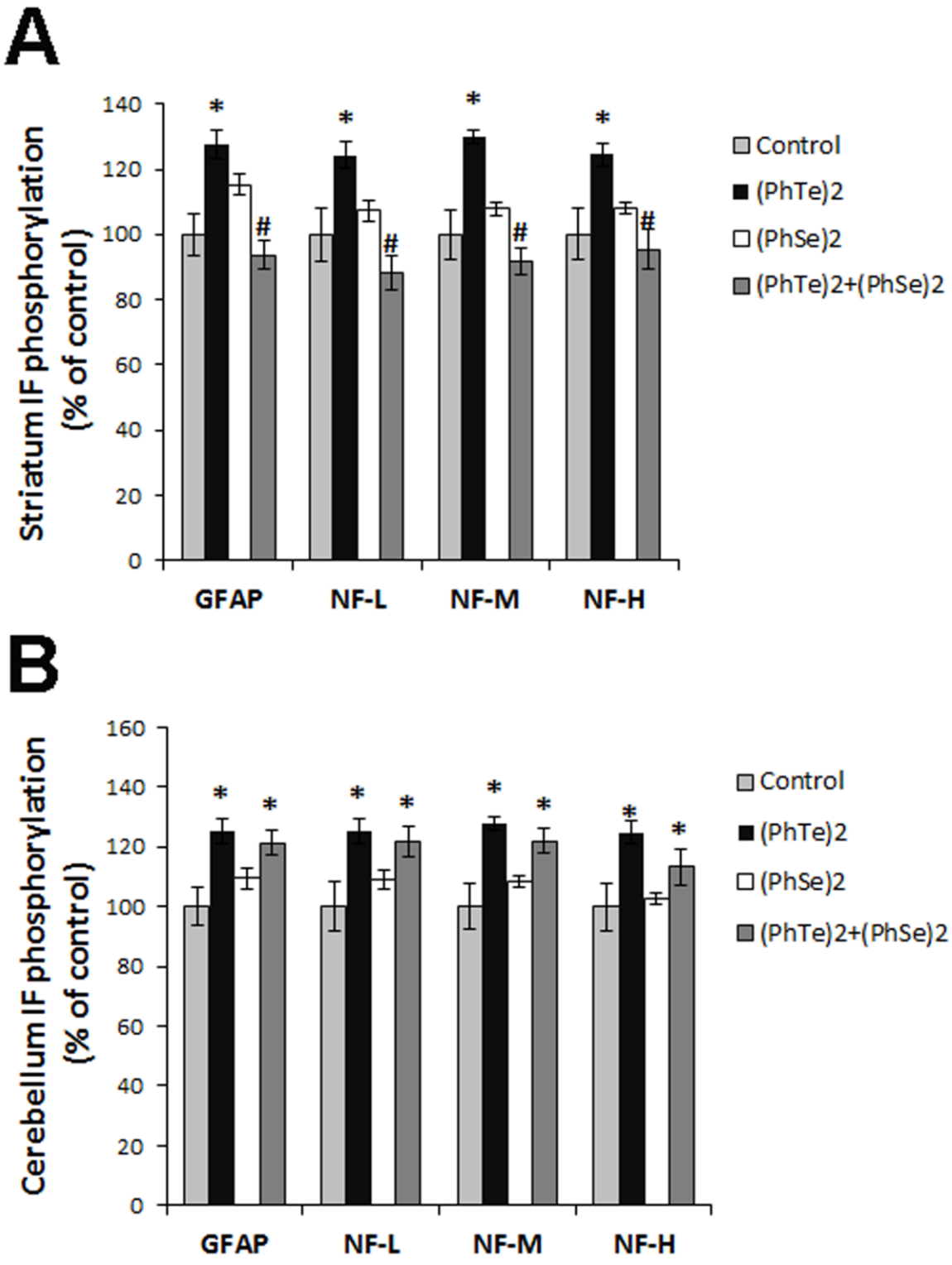
A
Striatum IF phosphorylation (% of control)
140
120
100
80
60
40
20
0
GFAP
NF-L
NF-M
NF-H
Control
(PhTe)2
(PhSe)2
(PhTe)2+(PhSe)2
B
Cerebellum IF phosphorylation (% of control)
160
140
120
100
80
60
40
20
0
GFAP
NF-L
NF-M
NF-H
Control
(PhTe)2
(PhSe)2
(PhTe)2+(PhSe)2

Figure 8:

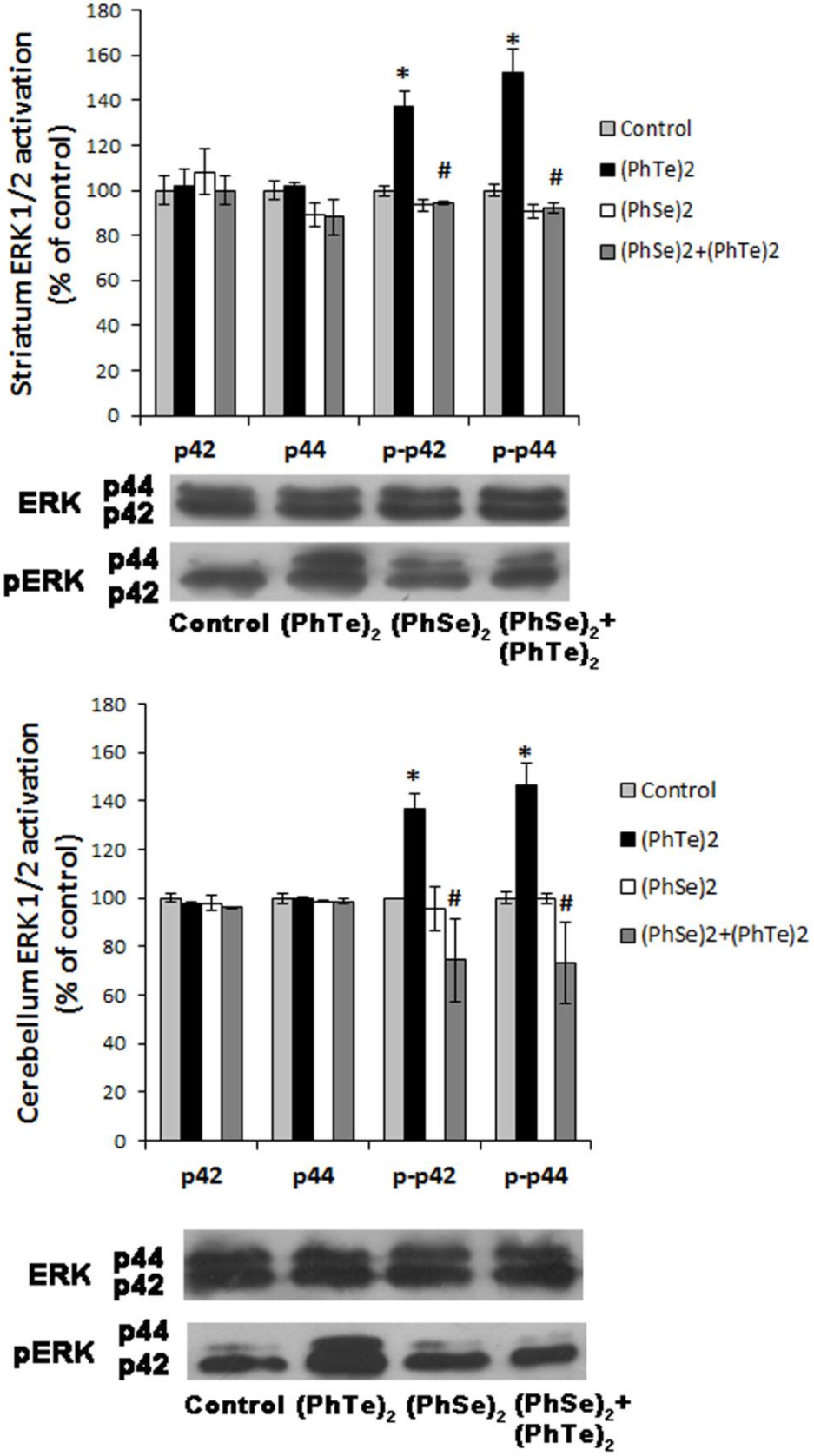
Striatum ERK 1/2 activation (% of control)
180
160
140
120
100
80
60
40
20
0
*
*
#
#
Control
(PhTe)2
(PhSe)2
(PhSe)2+(PhTe)2
p42
p44
p-p42
p-p44
ERK
p44
p42
pERK
p44
p42
Control
(PhTe)2
(PhSe)2
(PhSe)2+
(PhTe)2
Cerebellum ERK 1/2 activation (% of control)
180
160
140
120
100
80
60
40
20
0
*
*
#
#
Control
(PhTe)2
(PhSe)2
(PhSe)2+(PhTe)2
p42
p44
p-p42
p-p44
ERK
p44
p42
pERK
p44
p42
Control
(PhTe)2
(PhSe)2
(PhSe)2+
(PhTe)2

Figure 9:

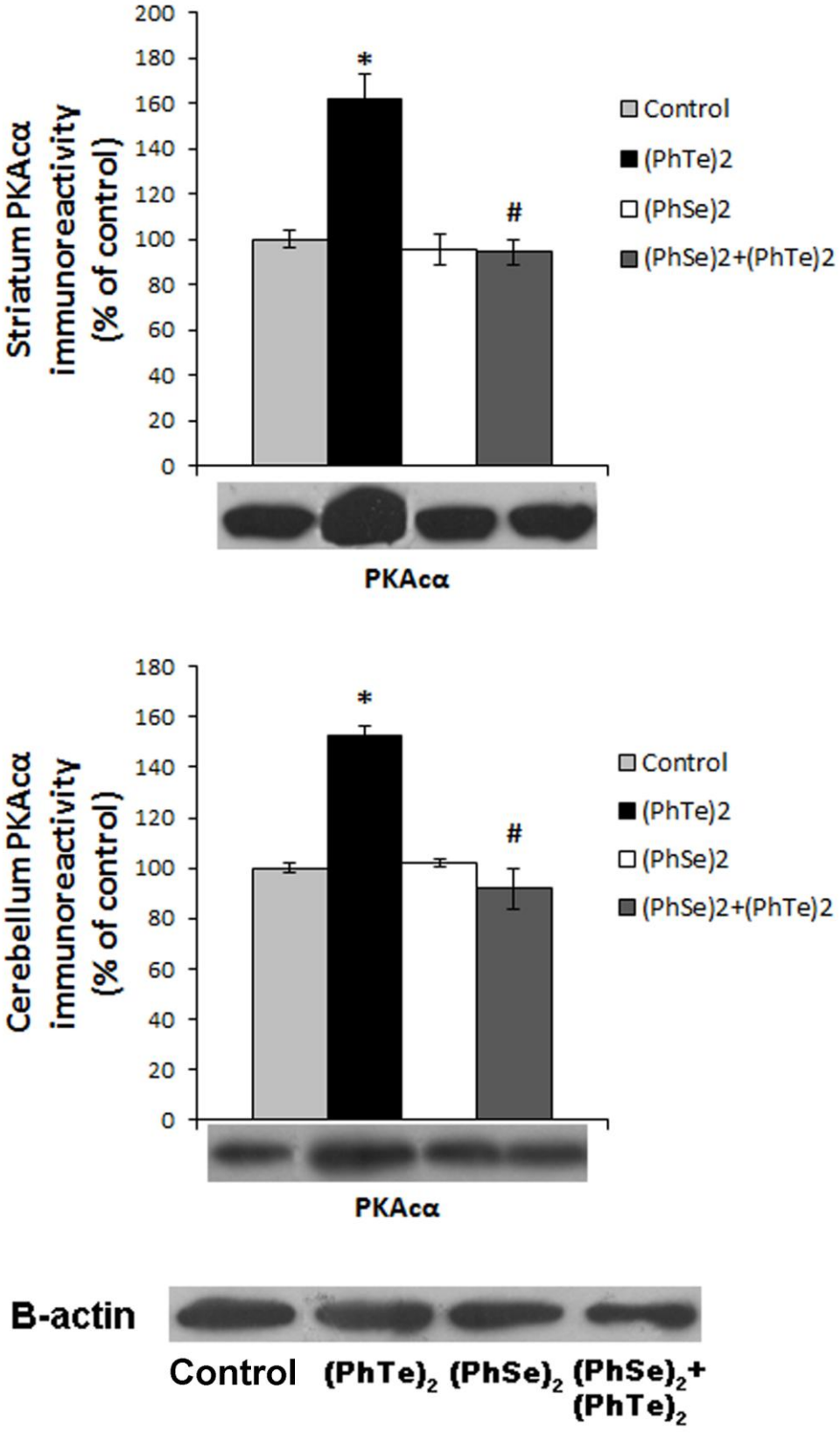
Striatum PKAcα immunoreactivity (% of control)
200
180
160
140
120
100
80
60
40
20
0
*
#
Control
(PhTe)2
(PhSe)2
(PhSe)2+(PhTe)2
PKAcα
Cerebellum PKAcα immunoreactivity (% of control)
180
160
140
120
100
80
60
40
20
0
*
#
Control
(PhTe)2
(PhSe)2
(PhSe)2+(PhTe)2
PKAcα
B-actin
Control
(PhTe)2
(PhSe)2
(PhSe)2+ (PhTe)2

Figure 10:

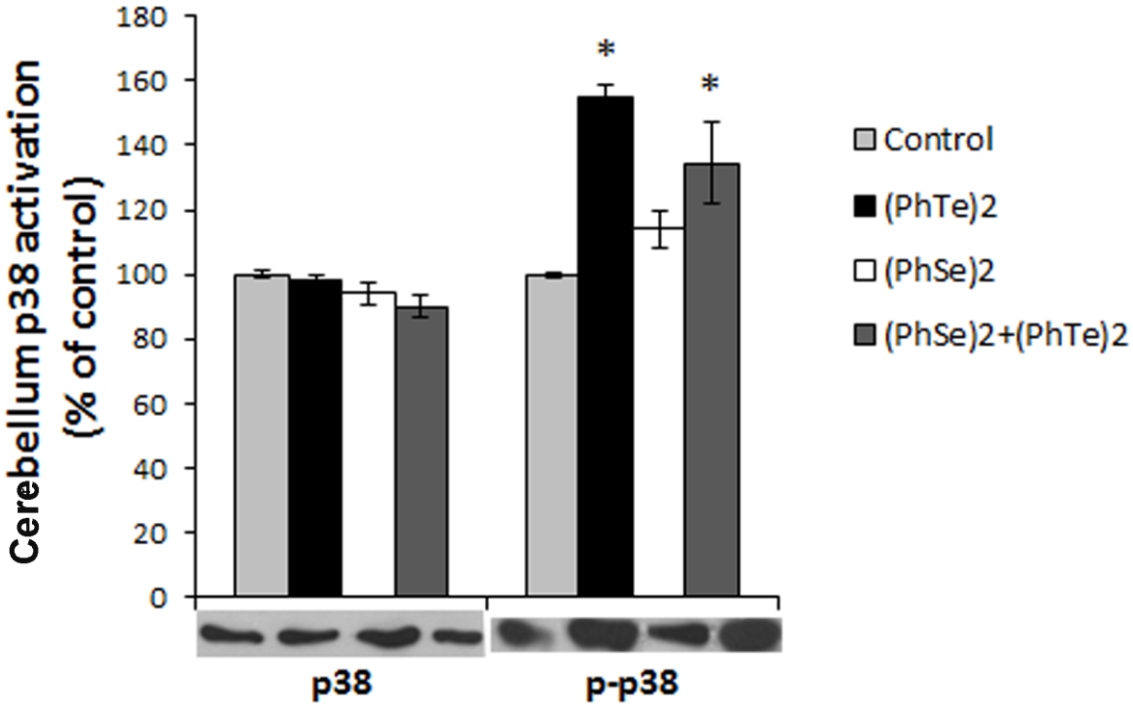
Cerebellum p38 activation
(% of control)
180
160
140
120
100
80
60
40
20
0
*
*
Control
(PhTe)2
(PhSe)2
(PhSe)2+(PhTe)2
p38
p-p38

Capítulo 3

RESULTADOS ADICIONAIS

EFEITO DA TRANSMISSÃO VERTICAL DO DITELURETO DO DIFENILA SOBRE O CITOESQUELETO, MAPK E PKA DO CÓRTEX CEREBRAL E HIPOCAMPO DE RATOS JOVENS

EFEITO DA TRANSMISSÃO VERTICAL DO DITELURETO DO DIFENILA SOBRE O CITOESQUELETO, MAPK E PKA DO CÓRTEX CEREBRAL E HIPOCAMPO DE RATOS JOVENS

1. RESUMO

No presente trabalho analisamos a influência da exposição das mães ao ditelureto de difenila [$(PhTe)_2$] (0,01 mg/kg de peso corporal) s.c. durante os primeiros 14 dias de lactação sobre a homeostase do citoesqueleto e a atividade de importantes quinases cerebrais (via das MAPK e PKA) do córtex cerebral e hipocampo dos filhotes. Nós verificamos o efeito desse contato sobre a fosforilação dos filamentos intermediários (FIs) neurais (neurofilamento de baixo (NF-L), médio (NF-M) e alto (NF-H) peso molecular) e gliais (proteina glial fibrilar ácida-GFAP) nos filhotes quando esses tinham 15, 21, 30 ou 45 dias de vida. Os resultados mostraram que o $(PhTe)_2$ administrado nas mães durante o período de lactação não altera a fosforilação dos FI no córtex cerebral, entretanto, no hipocampo ocorre uma hiperfosforilação da GFAP em animais de 15 dias e hipofosforilação do NF-L, NF-M, NF-H e GFAP em animais de 30 dias. Além disso, os resultados mostraram que no córtex cerebral ocorre uma diminuição da forma ativa das enzimas SAP/JNK, p38MAPK, pertencentes à via das quinases ativadas por mitógenos (MAPK), além da forma cataliticamente ativa da quinase dependente de AMP cíclico (PKA). No hipocampo há uma diminuição da ativação da ERK 1/2 (também pertencente à via das MAPK) e um aumento da PKA. Em conclusão, esse estudo mostra que a transmissão pelo leite materno pode ser uma importante via de intoxicação com $(PhTe)_2$, alterando importantes vias de sinalização como a via das MAPK e PKA, bem como a homeostase do citoesqueleto em córtex

cerebral e hipocampo dos filhotes, características essas que podem estar associadas a neurotoxicidade desse organotelureto.

2. INTRODUÇÃO

As células devem ter a capacidade de organizar-se no espaço, reorganizar seus componentes internos, interagir mecanicamente com o meio ambiente, mover-se de um lugar a outro e apresentar uma correta morfologia, modificando sua forma quando necessário. Todas essas funções estruturais e mecânicas apresentam-se altamente desenvolvidas em células eucarióticas e são dependentes de um extraordinário sistema de filamentos denominado citoesqueleto (Alberts et al., 2008). A notável rede do citoesqueleto é composta por três tipos de filamentos protéicos – filamentos de actina (microfilamentos) (MF), microtúbulos (MT) e filamentos intermediários (FIs) – cada um deles possuindo propriedades bioquímicas e biofísicas únicas (Carraway, 2000; Helfand et al., 2004; Alberts et al., 2008).

Os FIs conferem à célula resistência ao estresse mecânico e não mecânico e a consequente perda dessa função pode estar relacionada com doenças envolvendo fragilidade celular (Fuchs and Cleveland, 1998; Omary et al., 2004). Além disso, estudos mais recentes têm demonstrado que os FIs influenciam também no crescimento e morte celular através da interação dinâmica com proteínas não estruturais (Coulombe e Wong, 2004). A proteína glial fibrilar ácida (GFAP) é o FI característico dos astrócitos e os neurofilamentos (NFs) são os FIs específicos dos neurônios. Os NFs são

formados por subunidades de alto (NF-H), médio (NF-M) e baixo (NF-L) peso molecular (Albert et al., 2010).

É bem estabelecido que o acúmulo de NFs é um marco para várias doenças neurodegenerativas, como a esclerose lateral amiotrófica, a doença de Alzheimer, a doença de Parkinson, a doença de Charcot-Marie-Tooth e a neuropatia axonal gigante (Hirano et al., 1984; Watson et al., 1994; Schmidt et al., 1996; Schmidt et al., 1997; Bomont et al., 2000; Shepherd et al., 2002). Além disso, um dos mais dramáticos fenótipos de doenças provocadas por mutações nos FIs está relacionado à GFAP, sendo um exemplo disso a doença de Alexander, uma desordem fatal do SNC, evidenciada por devastadores distúrbios no desenvolvimento normal do cérebro e do crânio (Li et al., 2002).

Com relação aos FIs, uma modificação pós traducional de grande importância para a regulação de seu comportamento dinâmico é a fosforilação das subunidades formadoras desses filamentos. A alteração da fosforilação dos FIs regula o equilíbrio de polimerização e despolimerização dessas proteínas, levando muitas vezes à reorganização do citoesqueleto e consequente alteração morfológica e disfunção celular. Além disso, a alteração da atividade do sistema fosforilante associado ao citoesqueleto é um mecanismo muito importante para a transmissão de sinais intra e extracelulares que levam a uma resposta celular apropriada. (Carraway, 2000; Alberts et al., 2008). Os FIs são substratos de numerosas proteínas quinases, incluindo a proteína quinase dependente de AMPc (PKA), proteína quinase dependente de cálcio e calmodulina (PKCaM), proteína quinase dependente de cálcio (PKC) e via das quinases ativadas por mitógenos (MAPK), que podem alterar drasticamente a estrutura desses filamentos (Inagaki et al., 1987; Eriksson et al, 2004; Chang e Goldmann, 2004; Sihag et al., 2007; Zamoner et al., 2008; Pierozan e al., 2011).

Uma vez que o transporte, polimerização e disposição das subunidades dos NFs, FIs dos neurônios, são moduladas por eventos de fosforilação e desfosforilação em diferentes microambientes da célula, é fácil perceber como anormalidades nesses eventos metabólicos podem afetar as funções dos NFs, causando direta ou indiretamente consequências patológicas (Nixon e Sihag, 1991; Fabrizi et al., 2004; Lariviere et al., 2004). É importante considerar, portanto, que alterações na fosforilação das proteínas do citoesqueleto estão relacionadas com inúmeras doenças neurodegenerativas (Veeranna et al., 2004), entre elas podemos citar a doença de Alzheimer (Gong et al., 2003). Além disso, estudos do nosso grupo já demonstraram que tanto os NFs, quanto a GFAP e a vimentina (FIs de astrócitos) são alvos de metabólitos acumulados em determinadas doenças, bem como de neurotoxinas (Funchal et al., 2005, Loureiro et al., 2008; Pierozan et al., 2012). Alterações nas proteínas do citoesqueleto, portanto, são descritas em várias situações patológicas e podem estar relacionadas, pelo menos em parte, com a neurotoxicidade de uma determinada substância (Moretto et al., 2005, Heimfarth et al. 2008; Loureiro et al., 2008; Pierozan et al., 2011).

O telúrio é um elemento relativamente raro e pertence ao grupo dos calcogênios, assim como o enxofre e o selênio, mas ao contrário do selênio não apresenta nenhuma função fisiológica descrita até o momento (Taylor, 1996). Compostos de telúrio são usados ou produzidos em vários processos industriais como, na produção de aço, no refino eletrolítico de metais pesados, na manufatura de semicondutores, na indústria de componentes eletrônicos, síntese de fármacos e explosivos, na vulcanização de borracha, em lubrificantes sólidos, na petroquímica, entre outros (Clayton and Clayton, 1981; Taylor, 1996). Além disso, há relatos na literatura mostrando casos de intoxicação acidental de crianças a essa substância (Yarema e Curry, 2005). O uso industrial desse composto químico, bem como o contato acidental, provoca riscos ocupacionais e

ambientais para a saúde humana, porém a bioquímica e o significado biológico da exposição a essa substância são pouco compreendidos (Meotti et al, 2003). Tanto as formas orgânicas quanto as inorgânicas do telúrio são tóxicas para o SNC de roedores (Maciel et al, 2000; Nogueira et al., 2001; Widy-Tysziewicz et al., 2002, Souza et al., 2010), entretanto o grau de toxicidade desse elemento está associada ao composto específico, ou seja, depende da forma química em que ele se encontra, inorgânica ou orgânica (Ba et al., 2010).

O ditelureto de difenila [$(PhTe)_2$] é um composto orgânico do telúrio. Os dados sobre a possível toxicidade de compostos orgânicos de telúrio são controversos. Há estudos, entretanto, mostrando que essas substâncias podem modificar a funcionalidade do sistema glutamatérgico *in vivo* e *in vitro* (Nogueira *et al*., 2001; Souza et al., 2010) e são capazes de inibir enzimas, como a escaleno monooxigenase, alterando a biossíntese do colesterol e provocando desmielinização do sistema nervoso periférico (Wagner-Recio et al., 1991; Laden e Porter, 2001). Está bem descrito que a exposição ao $(PhTe)_2$, via leite materno, é capaz de provocar alterações comportamentais (Stangherlin et al., 2006), neuroquímicas (Stangherlin et al., 2009a) e aumentar o estresse oxidativo (Stangherlin et al., 2009b) na prole. Além disso, uma única injeção subcutânea desse composto em ratas prenhas foi teratogênica para os fetos e tóxica para as mães (Stangherlin et al., 2005).

Além disso, nosso laboratório tem demonstrado que o $(PhTe)_2$ é um composto neurotóxico para os ratos por alterar a homeostase do citoesqueleto. Estudos *in vivo* revelaram que esse organocalcogênio causa hiperfosforilação dos FI no córtex cerebral e hipocampo quando administrado subcutaneamente em ratos jovens (Heimfarth et al., 2008). Estudos *in vitro* mostraram que ele afeta o sistema fosforilante associado ao citoesqueleto de maneira dependente do desenvolvimento e da estrutura cerebral, ou

seja, aumenta a fosforilação dos NFs, GFAP e vimentina no hipocampo de animais de 21 dias e diminui a incorporação de ^{32}P nessas proteínas no córtex cerebral de animais de 9 e 15 dias (Heimfarth et al., 2011; 2012). Estudos de nosso grupo mostraram também (Heimfarth et al. 2011; 2012) o envolvimento da via das MAPK, bem como da PKA nos efeitos desencadeados por essa droga neurotóxica. Entretanto, existem poucos relatos demostrando os efeitos desse composto quando transmitidos via leite materno, sobre o citoesqueleto cerebral.

Os roedores possuem, no período pós-natal, um considerável desenvolvimento do cérebro, caracterizado por uma intensa síntese de proteínas (Gottlieb et al., 1977). De fato, a maturação ocorre por diversas semanas após o nascimento, durante as quais o cérebro é extremamente sensível a agentes químicos ou ambientais que podem induzir o aparecimento de alterações no desenvolvimento pós-natal dos animais jovens. Visto que a barreira hematoencefálica não é bem formada nesse período, drogas presentes no leite materno podem alcançar o sistema nervoso central da prole, interferindo no seu desenvolvimento (Favero et al., 2006).

Levando em consideração que o $(PhTe)_2$ é um composto neurotóxico, que alterações do citoesqueleto são marcadores de neurodegeneração e que, em especial, alterações na atividade do sistema fosforilante associado ao citoesqueleto estão relacionadas à disfunção neural, este capítulo apresenta dados adicionais sobre os efeitos do $(PhTe)_2$ administrado subcutaneamente nas ratas mães durante o período inicial de lactação (P0-P13) sobre a fosforilação das subunidades dos FIs neuronais (NF-L, NF-M e NF-H) e gliais (GFAP) no córtex cerebral e hipocampo da prole. Além disso, analisamos também a influência da administração de $(PhTe)_2$ nas mães durante o período de lactação na atividade das MAPKs e PKA dos filhotes no período de amamentação.

3. MATERIAIS E MÉTODOS

3.1. Substâncias radioativas e reagentes

Ortofosfato de sódio radioativo ($^{[32]}$ P-Na_2P0_4) foi adquirido do CNEN, São Paulo, Brasil. Ortofosfato de sódio radioativo ($^{[32]}$ P-Na_2P0_4) foi adquirido do CNEN, São Paulo, Brasil. Benzamidina, leupeptina, antipaína, pepstatin, chimostatina, acrilamida e bisacrilamida e os anticorpos anti-PKAcα, anti-GFAP, anti-NF-L, anti NF-M e anti-NF-H foram obtidos da Sigma (St. Louis, MO, USA). O kit de quimioluminescência ECL e os anticorpos secundários acoplados a peroxidase foram obtidos da Amersham (Oakville, Ontario, Canada). Os anticorpos anti-ERK, anti-pERK, anti-p38, anti-phospho p38, anti-SAP, anti-pSAP foram obtidos da empresa Cell Signaling Technology (USA). O $(PhTe)_2$ foi sintetizado de acordo com o método de Petragnami (1994). Análise através de técnicas espectrofotométricas ^{1}H NMR e ^{13}C NMR mostraram que o composto obtido apresenta características analíticas e espectroscópicas adequadas. A pureza do composto foi determinada como maior que 99% através da técnica de espectroscopia de ressonância acoplada a massas (HRMS). Todos os outros produtos utilizados tinham grau analítico e foram obtidos de fornecedores comerciais padrões.

3.2. Animais

Utilizamos ratos da linhagem *Wistar* obtidos do Departamento de Bioquímica, Instituto de Ciências Básicas da Saúde, Universidade Federal do Rio Grande do Sul, Porto Alegre, Brasil. Todos os animais incluídos nos experimentos provinham de ninhadas de 8 filhotes que foram mantidas em condições de temperatura constante

(22ºC) e em um ciclo artificial de iluminação 12 horas claro/12 horas escuro, com alimentos e água *at libitum*. O protocolo experimental seguiu o "Principles of Laboratory Animal Care" (NIH publicação 85-23, revisado 1985) e foi aprovado pela Comissão de Ética em Pesquisa Animal da Universidade Federal do Rio Grande do Sul.

3.3. Exposição ao $(PhTe)_2$

A exposição ao $(PhTe)_2$ foi realizado de acordo com Stangherlin et al. (2006). Descrevendo, ratas virgens foram mantidas com machos previamente testados como férteis por 3 a 5 dias (3 fêmeas e um macho por caixa). O primeiro dia (E0) de gravidez foi confirmada pela presença de esperma no esfregaço vaginal e as ratas grávidas foram imediatamente separadas e colocadas em caixas individuais. No dia do nascimento dos filhotes (P0), as mães começaram a receber por via subcutânea uma injeção de $(PhTe)_2$ (0,01mg/Kg de peso corporal, grupo teste) ou óleo de canola (1 mg/Kg de peso corporal, grupo controle). A administração do $(PhTe)_2$ ou óleo de canola foi feita durante os 14 primeiros dias do período de lactação (P0-P13) (exposição subcrônica). No dia do nascimento as ninhadas foram padronizadas em 8 animais. Quando estes filhotes completaram 15, 21, 30 ou 45 dias, os animais foram mortos por decapitação e o córtex cerebral e o hipocampo foram dessecados. Nos experimentos em que se usou animais de 30 ou 45 dias, no 21º dia pós-natal os filhotes foram retirados da mãe e colocados em outras caixas, separados de acordo com o sexo. Esses animais receberam água e ração padrão *ad libitum*.

3.4. Preparação das fatias de tecido

Ratos de 15, 21, 30 ou 45 dias de idade foram decapitados e, rapidamente, o cérebro retirado. O córtex cerebral e o hipocampo foram dissecados sobre placa de Petri colocada em gelo. As estruturas foram fatiadas em fatias de 400µm de espessura com Mcllwain Chopper. Dependendo da idade do animal foram selecionadas de 1 a 5 fatias que foram inicialmente pré-incubadas em solução de Krebs-Hepes conforme descrito abaixo.

3.5. Pré-incubação

Fatias de tecidos foram inicialmente pré-incubadas a 30°C por 20 min em meio Krebs-Hepes contendo NaCl 124 mM, KCl 4 mM, $MgSO_4$ 1.2 mM, Na-HEPES 25 mM (pH 7,4), glicose 12 mM e $CaCl_2$ 1 mM, juntamente com os seguintes inibidores de proteases: benzamidina 1mM, leupeptina 0.1 µM, antipaína 0.7 µM, pepstatina 0.7 µM e quimostatina 0.7 µM.

3.6. Incubação in vitro e incorporação de $^{[32]}$P-Na_2P0_4

Após a pré-incubação, o meio foi removido e a incubação foi realizada a 30°C com 100 µl do meio básico, contendo 80 µCi $^{[32]}$ P-Na_2P0_4, como descrito por Funchal et al. (Funchal *et al.*, 2003). A reação de fosforilação ocorreu por 30 min a 30°C e foi parada com 1 ml de um tampão fluoreto de sódio a 4°C (NaF 150 mM, EDTA 5 mM, EGTA 5 mM, Tris-HCl 50 mM, pH 6.5) e os inibidores de proteases acima descritos. As fatias foram então lavadas duas vezes com o mesmo tampão para remover o excesso de radioatividade.

3.7. Preparação da fração citoesquelética enriquecida em filamentos intermediários

Após o tratamento, a fração citoesquelética enriquecida em filamentos intermediários foi obtida a partir do córtex cerebral e do hipocampo. Resumidamente, após a reação de marcação com fosfato radioativo, as fatias foram homogeneizadas em 400 µl de um tampão de alta força iônica (4°C), contendo KH_2PO_4 5 mM (pH 7.1), KCl 600 mM, $MgCl_2$ 10 mM, EGTA 2 mM, EDTA 1 mM, Triton X-100 1% e os inibidores de proteases acima descritos. O homogeneizado foi centrifugado a 14.000 rpm por 10 min a 4°C em centrífuga para microtubo, o sobrenadante foi descartado e o sedimento homogeneizado com o mesmo volume do tampào de alta força iônica. O homogeneizado foi suspenso e centrifugado conforme descrito e o sobrenadante foi descartado. O sedimento enriquecido em filamentos intermediários insolúveis em Triton X-100, contendo subunidades de NFs (NF-L, NF-M e NF-H), vimentina e GFAP foi dissolvido em SDS 1% e a de proteína foi determinada como descrito abaixo.

3.8. Homogeneizado total do tecido

Fatias de córtex cerebral ou hipocampo foram homogeneizadas em 100 µl de uma solução de lise contendo EDTA 2 mM, Tris-HCl 50 mM, pH 6.8, (v\v) SDS 4%. Para a análise por eletroforese em gel de poliacrilamida (SDS-PAGE), as amostras foram diluídas em 25% (V/V) de uma solução contendo 40% glicerol, 5% mercaptoetanol, 50 mM Tris–HCl, pH 6.8 e aquecidas por 3 minutos.

3.9.Dosagem de proteínas

A quantidade de proteína foi determinada pelo método de Lowry (Lowry et al., 1951) usando albumina bovina como padrão.

3.10. Eletroforese em gel de poliacrilamida (SDS-PAGE)

A fração citoesquelética de tecido foi preparada conforme descrito acima. Para a análise em eletroforese, as amostras foram dissolvidas em 25% (v\v) de uma solução contendo glicerol 40%, mercaptoetanol 5%, Tris-HCl 50 mM, pH 6.8 e fervidas por 3 min. As concentrações de proteína foram igualmente aplicadas em gel de poliacrilamida 7,5 % e analisadas por SDS-PAGE de acordo com o sistema descontínuo de Laemmli (Laemmli, 1970). Em experimentos *in vitro* de incorporação do ^{32}P-ortofosfato, os géis contendo a fração citoesquelética enriquecida em FIs foram expostos a filmes de raio-X (T-Mat G\RA) a -70°C, com intensificadores de radioatividade (*screen)* e, finalmente, a autoradiografia foi obtida e quantificada por digitalização dos filmes com um *scanner* HP Scanjet 6100C Hewlett-Packard e a densidade óptica determinada com uma versão de software Optiquant 02.00 (Packard Instrument Company). Valores de densidade óptica foram obtidos para a faixa correspondente a cada proteína. A quantidade de amostra aplicada e a qualidade da migração na placa de eletroforese foram controladas por coloração com Brilliant Blue R. Todas as bandas medidas estavam dentro da faixa linear de sensibilidade do filme.

3.11. Análise do imunoconteúdos das proteínas pela técnica de *Western blot*

O homogeneizado total de proteínas (80 μg) ou a fração citoesquelética (50 μg), preparada como descrito anteriormente, foram analisados através da técnica de SDS-

PAGE e transferidas para uma membrana de nitrocelulose (Trans-blot SD semi-dry transfer cell, BioRad) por 1 hora a 15 V, utilizando para isso o tampão de transferência contendo 48 mM Trizma, 39 mM glicina, 20% metanol e 0.25% SDS. Posteriormente as membranas de nitrocelulose foram lavadas por 10 minutos com tampão TBS (0,.5 M NaCl, 20 mM Tris, pH 7.5), seguido de 2 horas de incubação com solução de bloqueio contendo TBS adicionado de 5% de albumina bovina sérica e 0,1% Tween 20. Após o bloqueio, as membranas de nitrocelulose foram lavadas 2 vezes por 5 minutos com TBS contendo 0,05% Tween-20 (T-TBS), e então incubadas durante a noite a 4°C com os seguintes anticorpos diluídos em tampão de bloqueio: anti-GFAP (clone G-A-5) diluído 1:500, anti-vimentina (Vim 13-12) diluída 1:400, anti-NF-L (clone NR-4) diluída 1:1000, anti- NF-M (clone clone NN-18) diluída 1:400, anti-NF-H (clone N52) diluída 1:1000, anti-ERK1/2 diluída 1:1000, anti-fosfoERK diluída 1:1000, anti-SAP/JNK diluída 1:1000, anti-fosfoSAP/JNK (clone 98F2) diluída 1:1000, anti-p38MAPK (clone A-12) diluída 1:1000, anti-fosfo38MAPK diluída 1:1000, anti-PKAcα diluída 1:1000 e anti-actina diluída 1:1000. As membranas de nitrocelulose foram então lavadas 4 vezes por 5 minutos com T-TBS e incubadas por 2 horas com os anticorpos secundários conjugados com peroxidase diluídos em solução de bloqueio (anti-IgG de camundongo diluído 1:2000 e anti- IgG de coelho diluído 1:2000). Posteriormente, as membranas de nitrocelulose foram lavadas 2 vezes com T-TBS e 2 vezes com TBS por 5 minutos. O *blot*, então, foi revelado usando o *kit* de quimioluminescência ECL. O imunoconteúdo das proteínas foi quantificado através da técnica de densitometria óptica, usando para isso o programa OptiQuant, software versão 02.00 (Packard Instrument Company). Como controle da quantidade de proteínas foi utilizada a β-actina.

3.12. Viabilidade celular em fatias de tecido

A viabilidade celular foi determinada através do método de MTT (brometo de 3-(4,5-dimetiltiazol-2-il)-2,5-difenil-tetrazólio), que se baseia na capacidade que as células viáveis possuem de clivar o anel tetrazólico presente no MTT pela ação de enzimas desidrogenases presentes na mitocôndria ativa, formando cristais de formazan de cor azul que se acumulam em compartimentos endossomais e/ou lisossomais, sendo depois transportados para fora das células por exocitose (Mosmann, 1983; Liu *et al.*, 1997). Fatias de tecido de córtex cerebral ou hipocampo foram incubadas com MTT (0,5 mg\mL) em meio Krebs-Hepes, pH 7.4 por 30 min a 37°C. Posteriormente, o meio foi removido e o formazan precipitado foi solubilizado com dimetilsulfóxido (DMSO) sob agitação durante 10 min. As células viáveis foram quantificadas por espectrofotometria no comprimento de onda de 550 nm.

4. RESULTADOS

Inicialmente avaliamos a influência da administração crônica do $(PhTe)_2$ (0,01 mg/kg de peso corporal) sobre o ganho de peso corporal das mães durante o período inicial de lactação (do nascimento ao 13° dia). Os resultados mostraram que não houve diferença significativa no ganho de peso corporal das mães expostas ao $(PhTe)_2$ quando comparadas com os animais controles, nos quais apenas óleo de canola foi injetado (Figura 1A). Ao analisarmos o efeito da exposição materna ao $(PhTe)_2$, sobre o de peso corporal da prole durante os 45 dias subsequentes ao nascimento, verificamos que também não ocorreu alteração desse parâmetro nos filhotes (Figura 1B).

Posteriormente, determinamos se a administração subcutânea de $(PhTe)_2$ nas ratas durante o período de lactação afetava a viabilidade celular do córtex cerebral e do

hipocampo dos filhotes quando esses tinham 15, 21, 30 ou 45 dias, através da técnica de MTT. Os resultados mostraram que esse tipo de exposição ao neurotoxicante não alterou a viabilidade celular do córtex cerebral (Figura 2A) e do hipocampo (Figura 2B) em nenhuma das idades estudadas, quando comparado com os animais controles que receberam apenas óleo de canola.

Visto que o composto orgânico do telúrio, alvo de nosso estudo, é descrito como neurotóxico e que trabalhos anteriores demostraram que ele é capaz de alterar parâmetros do citoequeleto cerebral (Heimfarth et al., 2008), determinamos, no presente estudo, se o $(PhTe)_2$ cronicamente administrado às mães durante o período inicial de lactação afeta o citoesqueleto do córtex cerebral e do hipocampo dos filhotes durante o desenvolvimento. Para isso, fatias de córtex cerebral ou hipocampo foram incubadas com ^{32}P-ortofosfato e a fosforilação das subunidades do NFs (NF-L, NF-M, NF-H), bem como da GFAP foi determinada na fração citoesquelética dos filhotes aos 15, 21, 30 ou 45 dias de idade. Os resultados mostraram que o $(PhTe)_2$ não alterou a fosforilação dos filamentos intermediários gliais e neuronais em nenhuma das idades estudadas no córtex cerebral (Figura 3 A, B, C e D). Já, no hipocampo esse organotelureto induziu a uma hiperfosforilação da GFAP em animais de 15 dias e uma hipofosforilação dos FI estudados nos animais de 30 dias sem alterar a incorporação do ortofosfato radioativo nos dias 21 e 45. (Figura 4 A, B, C e D).

Analisando o imunoconteúdo das proteínas GFAP, NF-L, NF-M, NF-H pela técnica de *Western blot*, verificou-se que ocorreu um aumento do imunoconteúdo de todas as proteínas estudadas no hipocampo no nos filhotes de 21 dias (Figura 5B), bem como diminuição da GFAP no hipocampo aos 15 dias (Figura 5B). No córtex cerebral há um aumento do imunoconteúdo da GFAP em animais de 15 dias, não ocorrendo alteração do imunoconteúdo dos NFs em nenhuma das idades estudadas (Figura 5 A).

Visto que relatos da literatura mostram que neurotoxinas agem sobre as MAPK (Rigon et al., 2008; Yin et al., 2011; Xu et al., 2011), bem como sobre a PKA (Naseer et al., 2010; Kumar et al., 2012) e que estudos de nosso grupo mostraram que essas vias são alvos do $(PhTe)_2$ (Heimfarth et al., 2011; 2012), verificamos a influência da administração subcutânea do composto orgânico do telúrio nas mães durante o período de lactação sobre a atividade dessas importantes enzimas nos filhotes. Os resultados obtidos em córtex cerebral mostraram que o $(PhTe)_2$ causou diminuição da forma fosforilada e ativa das enzimas SAP/JNK, em animais de 21 dias, e p38MAPK, em animais de 15 dias de idade (Figura 6 B, C), não alterando a atividade da ERK 1/2 (Figura 6A). Além disso, ocorreu no córtex cerebral uma diminuição da forma cataliticamente ativa da PKA tanto em animais de 15 como de 21 dias (Figura 6 D). No hipocampo, os resultados mostraram uma diminuição da forma ativa, ou seja, fosforilada, da ERK 1/2 em animais de 15 dias (Figura 7 A) e um aumento da PKA cataliticamente ativa em animais de 15 e 21 dias (Figura 7 D). Esse tipo de exposição não afetou a atividade da SAP/JNK, nem da p38MAPK no hipocampo dos filhotes (Figura 7 B, C).

5. DISCUSSÃO

O telúrio é um elemento traço usado como componente industrial de muitas ligas e na indústria eletrônica. Ele é uma substância tóxica, a qual pode produzir além de sintomas neurotóxicos como diminuição do aprendizado e da memória espacial (Walbran and Robins 1978; Widy-Tyszkiewicz et al 2002), teratogênese (Stangherlin et al 2006), danos renais, hepáticos (Meotti et al., 2003; Borges et al., 2007) e pulmonares (Piton et al., 2011). Quando transmitido via leite materno, essa substância provoca

mudanças neurocomportamentais e danos cognitivos na prole (Stangherlin et al., 2006b; 2009), bem como alteração no estado redox das células (Stangherlin et al., 2009).

As consequências da exposição a uma toxina durante o período de lactação é extremamente relevante para a função do cérebro no ponto de vista de saúde humana. O contato com neurotoxinas durante esse estágio da vida pode causar problemas no funcionamento, bem como no desenvolvimento cerebral (Rigon et al., 2008; Sulkowski et al., 2011). Portanto, o objetivo do presente trabalho foi estudar alguns aspectos da neurotoxicidade do $(PhTe)_2$ transmitida pelo leite materno. Para tanto, verificamos a influência da administração subcutânea de $(PhTe)_2$ em ratas durante a lactação sobre a homeostase do sistema fosforilante associados aos FI e a atividade de importantes vias de sinalização no córtex cerebral e hipocampo dos filhotes.

Os resultados mostram que na concentração utilizada o $(PhTe)_2$ (0,01 mg/kg de peso corporal) administrado nas mães nos primeiros 14 dias de lactação não provocou nenhum sinal específico de intoxicação nos filhotes ou nas mães, como redução do peso corporal, odor de alho ou tremor, sintomas esses característicos de uma intoxicação por telúrio (Yarema e Curry, 2005; Heimfarth et al., 2008). Estes resultados estão de acordo com outros relatos da literatura que também não descrevem alteração no peso corporal das mães, nem dos filhotes nesse modelo de exposição ao $(PhTe)_2$ (Stangherlin et al, 2009 a, b).

Esse trabalho também demonstrou que uma administração subcutânea de $(PhTe)_2$ nas mães não causou dano mitocondrial nas células do córtex cerebral ou hipocampo dos filhotes em nenhuma das idades estudadas (15, 21, 30 ou 45 dias). O insulto celular foi determinado através do método do MTT, o qual, através da marcação das mitocôndrias viáveis, nos permite ter uma medida da viabilidade celular. Entretanto,

o $(PhTe)_2$ alterou a atividade de quinases pertencentes a importantes vias de sinalização celular, bem como a homeostase do citoesqueleto do córtex cerebral e do hipocampo de ratos jovens. Isto sugere que a toxicidade encontrada na prole, aparentemente não está relacionada com a alteração da viabilidade celular.

A exposição ao organotelureto via leite materno não afetou a fosforilação das proteínas do citoesqueleto neuronal do córtex cerebral da prole. Entretanto, houve um aumento no imunoconteúdo da GFAP no córtex cerebral dos animais de 15 dias de idade, provavelmente alterando a homeostase do citoesqueleto em astrócitos corticais. Estes resultados diferem de trabalhos prévios de nosso grupo, onde o tratamento *in vivo* com $(PhTe)_2$ causou alteração no estado de fosforilação dos FIs gliais e neuronais em córtex cerebral de ratos jovens (Heimfarth et al., 2008). Ainda, a incubação de fatias de córtex cerebral de ratos jovens com $(PhTe)_2$ também alterou a atividade do sistema fosforilante associado ao citoesqueleto *in vitro* (Moretto et al., 2005). Analisando o conjunto desses dados, podemos propor que embora o córtex cerebral seja suscetível aos níveis tóxicos de $(PhTe)_2$ *in vivo* e também à exposição *in vitro*, este tecido é menos suscetível aos efeitos tóxicos do $(PhTe)_2$ ou de eventuais metabólitos que possam ser secretados através do leite materno. Por outro lado, os presentes resultados estão e acordo com Stangerling et al. (2009), demostrando que a injeção desse organutelureto em ratas durante a lactação causou alteração no estado redox, principalmente no estriado e hipocampo dos filhotes, sendo o córtex cerebral a estrutura menos afetada.

No hipocampo, o $(PhTe)_2$ causou hiperfosforilação da GFAP em ratos de 15 dias e hipofosforilação dos FI neuronais e gliais nos ratos de 30 dias. Nos animais de 21 dias tivemos um aumento no imunoconteúdo de todos os FIs estudados, o que pode nos levar a pensar que provavelmente a atividade do sistema fosforilante já esteja diminuída no 21º dia pós-natal. Isso está de acordo com nossos trabalhos anteriores que mostram que

em animais de 21 dias há alteração nos níveis das proteínas do citoesqueleto de hipocampo (Heimfarth et al., 2008, 2011). Esse efeito sobre as proteínas do citoesqueleto é dependente do desenvolvimento, uma vez que as alterações descritas nos FIs neuronais ocorreram apenas quando os animais têm 21 e 30 dias, não ocorrendo alteração nos filhotes de 15 ou 45 dias.

Analisando o nível de fosforilação da GFAP em astrócitos hipocampais dos filhotes durante a lactação, verificamos que ocorreu alteração no seu estado de fosforilação ao longo do desenvolvimento, ou seja, houve hiperfosforilação em ratos de 15 dias e hipofosforilação em animais de 30 dias. Estudos realizados em ratos jovens já demonstraram que a toxicidade induzida por esse organotelureto é dependente da idade do animal e consequentemente do estágio de desenvolvimento do cérebro (Souza et al., 2010). É descrito que esse neurotoxicante induz mudanças na homeostase do glutamato e danos cognitivos de uma maneira dependente da idade do animal (Souza et al., 2010). Portanto, podemos propor que o efeito desencadeado por esse organotelureto sobre o FI glial é dependente do estágio de maturação hipocampo. Isso pode estar relacionado com a plasticidade sináptica durante o desenvolvimento, quando as sinapses formadas geram conexões que existem apenas transitoriamente, sendo eliminadas posteriormente (Squire et al., 2008). Essa plasticidade pode influenciar na resposta de diferentes estruturas cerebrais ao contato com uma mesma substância tóxica, gerando janelas de suscetibilidade relacionadas ao programa de maturação das diferentes regiões cerebrais. Sabe-se que as várias regiões do cérebro se desenvolvem em tempos diferentes e apresentam diferentes janelas de vulnerabilidade a neurotoxinas (Rice e Barone, 2000). Além disso, a maturação do cérebro dos roedores ocorre por diversas semanas após o nascimento, período esse em que o cérebro é extremamente sensível a toxinas que

podem induzir alterações nas diferentes estruturas cerebrais (Favero el al., 2006, Sulkowski et al., 2011).

A alteração de fosforilação dos FI neuronais e gliais pode modificar a capacidade de polimerização/despolimerização desses filamentos (Inagaki *et al*., 1987), e tem implicações na interação com outras estruturas do citoesqueleto (Chou *et al*., 1996). Além disso, uma modificação no estado fosforilante dos NFs pode alterar o transporte e o calibre axonal (Sihag et al., 1991; 2007). Portanto, mudanças na homeostase do citoesqueleto podem estar relacionadas, pelo menos em parte, com a neurotoxicidade do $(PhTe)_{2.}$ No entanto mais experimentos serão necessários para compreender os mecanismos de ação dessa droga neurotóxica sobre o citoesqueleto cerebral.

Analisando os resultados até o presente momento podemos concluir que os efeitos desencadeados pela administração de $(PhTe)_2$ nas mães sobre o citoesqueleto dos filhotes são tempo e estrutura dependentes, ou seja, o desenvolvimento do animal, bem como as características individuais de cada estrutura são fundamentais para a ação desse composto.

Nos ratos, a última semana pré-natal e as primeiras três semanas pós-natal são o período de maior vulnerabilidade dos neurotransmissores aos metais pesados (Antonio et al., 1999), portanto, uma intoxicação nesse período pode levar também à ativação ou inibição de várias vias de sinalização celular (Ledig et al., 1988; Othman et al., 2002). Sabe-se que o $(PhTe)_2$ é um composto neurotóxicos que provoca alterações em várias proteínas e enzimas (Borges et al., 2005, Lugokenski et al., 2011), portanto, nesse trabalho estudamos também o efeito da administração subcutânea de $(PhTe)_2$ durante o período de lactação sobre a atividade de duas importantes vias de sinalização, a via das

MAPK e da PKA, já previamente descritas como alvos desse organotelureto (Heimfarth et al., 2011; 2012).

A via das MAPK regula vários processos biológicos como proliferação, diferenciação, sobrevivência, morte e transformação celular (McCubrey e Lahair, 2006; Torii et al. 2006; Dhillon et al., 2007) além de processos patológicos, como processos inflamatórios (Beyaert et al, 1996), doenças neurodegenerativas (Kim e Choi, 2010) e distúrbios do desenvolvimento (Tidyman e Rauen, 2009). Já, a ativação da PKA está relacionada com um vasto número de processos biológicos, entre eles metabolismo (Krebs et al., 1979), crescimento, divisão e diferenciação celular (Liu, 1982; Lara et al 2003). Além disso, essa enzima está envolvida em mecanismos de neurotoxicidade induzida por metais (Saijoh et al., 1993).

Nossos resultados mostraram que no córtex cerebral o $(PhTe)_2$ administrado nas mães durante a lactação causou uma diminuição da forma fosforilada, da p38MAPK e da SAP/JNK nos filhotes de 15 e 21 dias, respectivamente. Além disso, houve uma diminuição da forma cataliticamente ativa da PKA em ambas as idades. Esses resultados reforçam a transmissão via leite materno como uma importante via de intoxicação para os filhotes. A inibição da via das MAPK pode ser um mecanismo de proteção, pois é bem descrito que a ativação da p38MAPK e da SAP/JNK está envolvida com mecanismos de morte celular (Rockwell et al. 2004). Entretanto mais estudos serão necessários para comprovar essa hipótese. Os resultados da PKA estão de acordo com outros achados de nosso grupo que descrevem a diminuição da atividade desta enzima no córtex cerebral de ratos jovens (Heimfarth et al., 2012), reforçando que esta enzima é um importante alvo do organotelureto nessa estrutura cerebral e está de acordo com a literatura, a qual descreve a PKA como um importante alvo de neurotoxinas, (Saijoh et al., 1993; Kuo, 2008)

Analisando os resultados do hipocampo verificamos que essa estrutura apresenta uma suscetibilidade diferente do córtex cerebral. O $(PhTe)_2$ inibe a ERK1/2 nos animais de 15 dias, sem alterar a atividade da SAP/JNK e da p38/MAPK. Estudos recentes têm associado a ERK1/2 com desenvolvimento do aprendizado e da memória (Revisado por Peng et al., 2010). É bem descrito na literatura que o hipocampo é a estrutura cerebral relacionada com essas duas funções (Bear et al., 2008) e Stangherlin et al. (2009) demonstrou que a o $(PhTe)_2$ administrado nas mães durante os primeiros dias de lactação causou comprometimento cognitivo nos filhotes. Portanto, podemos propor que essa inibição da ERK 1/2 no hipocampo possa estar relacionada com os danos cognitivos à prole.

Diferentemente da via das MAPK, o $(PhTe)_2$ transmitido via leite materno causou um aumento da forma cataliticamente ativa da PKA no hipocampo. A PKA tem papel importante na liberação de neurotransmissores, dessensibilização de receptores, plasticidade sináptica e transcrição gênica (Borrelli et al 1992; Nestler and Greengard 1994; Riccio et al 1999). Portanto, a alteração na atividade dessa enzima pode estar relacionada com as alterações comportamentais (Stangherlin et al., 2006) e/ou neuroquímicas (Stangherlin et al., 2009a) dos filhotes descritas para esse composto quando administrado nas mães durante o período de lactação.

Um dos principais alvos das MAPK e da PKA é o citoesqueleto das células neurais (Loureiro et al., 2008; Zamoner et al., 2008), porém nesse trabalho verificamos que houve uma alteração na atividade dessas enzimas sem ocorrer modificação na fosforilação das subunidades dos NFs nos filhotes de 15 e 21 dias. Portanto, provavelmente, pelo menos durante o período de lactação, os FIs não estão sendo alvos dessas importantes enzimas cerebrais. Esta evidência remete à complexidade dos

mecanismos de sinalização celular, onde uma infinidade de fatores como tipo, intensidade e duração do sinal determinam a resposta celular.

Considerando o conjunto dos presentes resultados, podemos concluir que uma administração subcutânea de $(PhTe)_2$ nas mães durante os primeiros 14 dias de lactação causa alteração na homeostase do sistema fosforilante associado ao citoesqueleto no hipocampo dos filhotes com diferentes janelas de suscetibilidades, sem alterar esse parâmetro no córtex cerebral nos filhotes Os resultados também mostram que a toxicidade via leite materno altera vias de sinalização, via da PKA e das MAPK, nestas estruturas cerebrais, entretanto essas alterações não estão diretamente relacionadas à homeostase do sistema fosforilante associados aos FIs das células neurais nestas estruturas.

Levando em consideração a importância do citoesqueleto cerebral, bem como da PKA e das MAPK para a fisiologia cerebral, nós propomos que estas alterações fazem parte da toxicidade do $(PhTe)_2$ ou de seus metabólitos em filhotes intoxicados pelo leite materno. Entretanto, mais estudos serão necessários para clarear a importância desta via de transmissão para a neurotoxicidade da prole.

Figura 1

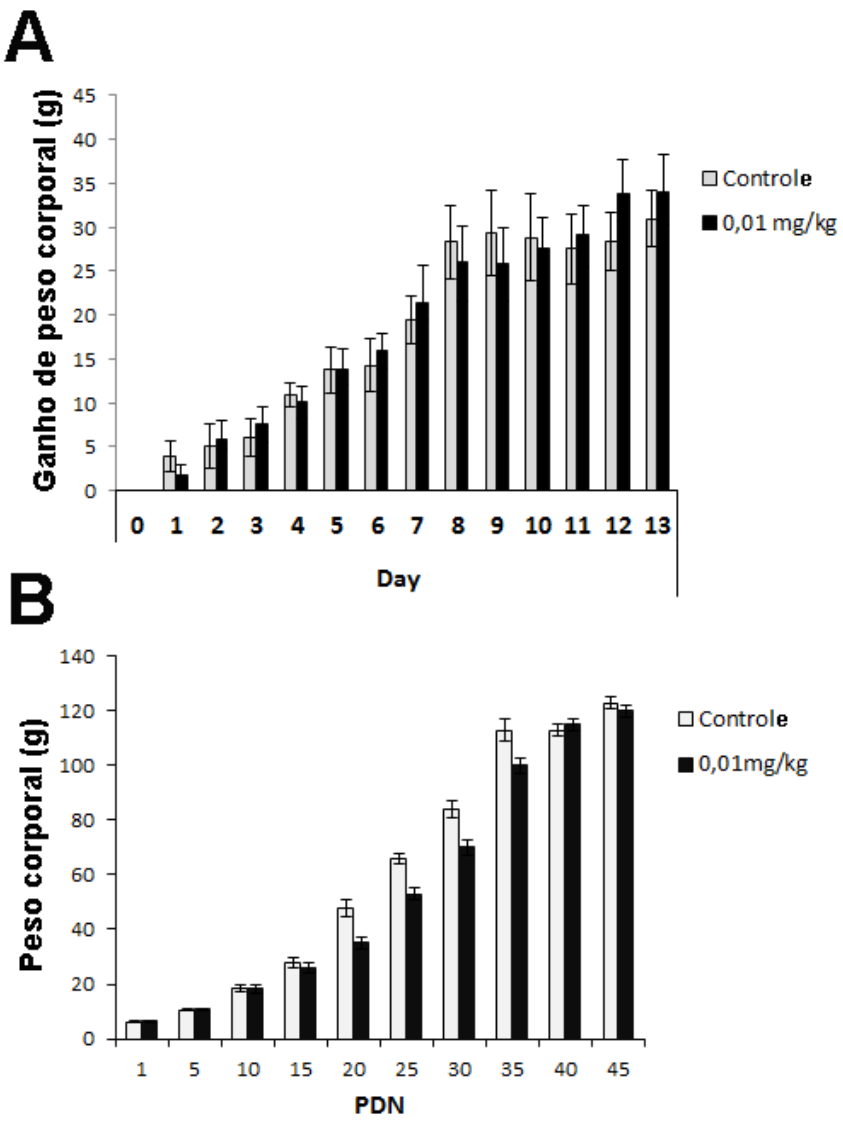

Figura 1: Efeito do $(PhTe)_2$ (0,01 mg/kg de peso corporal) administrado nas mães durante o período de lactação sobre o ganho de peso corporal das mães (A) e sobre o peso corporal dos filhotes (B). O peso corporal foi obtido diariamente após a administração do $(PhTe)_2$. Dados são reportados como média ± EPM de 8-16 animais e expressos em grama.

Figura 2

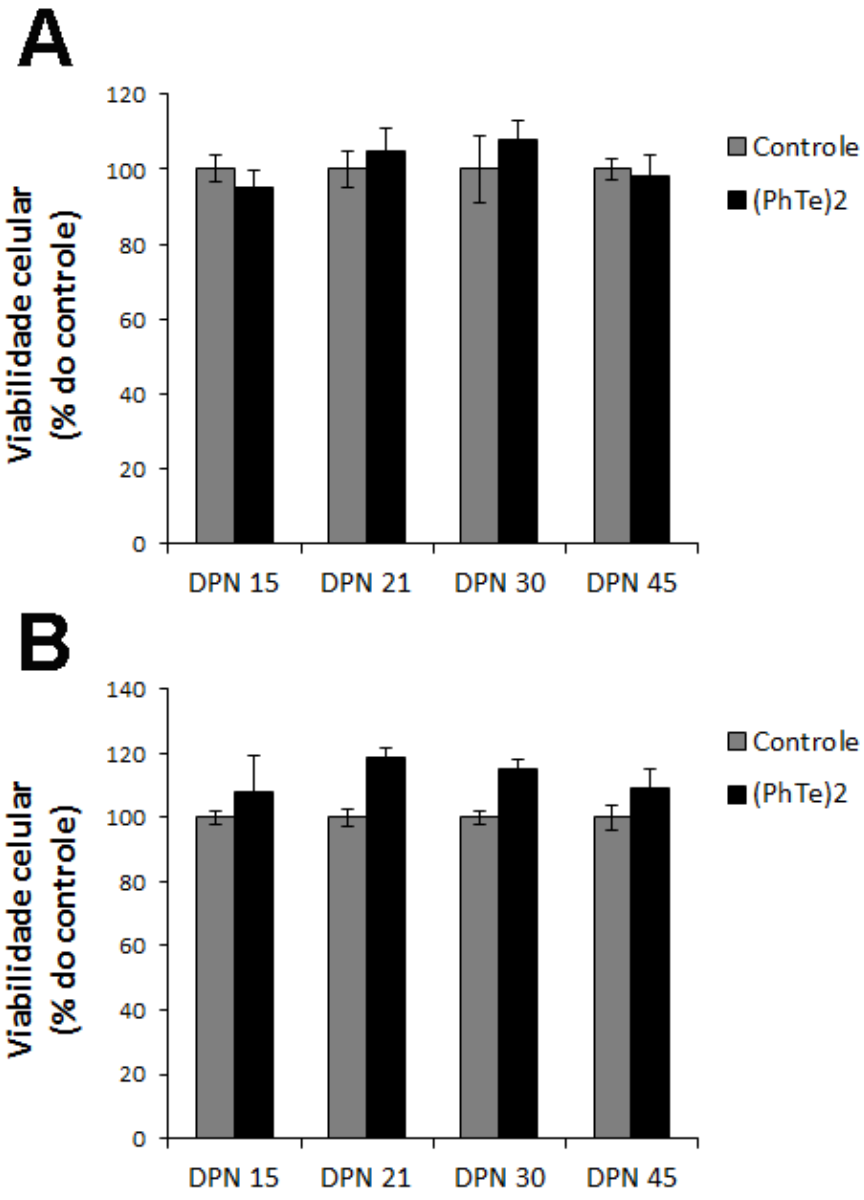

Figura 2: Efeito da administração subcutânea de $(PhTe)_2$ (0,01 mg/kg de peso corporal) nas mães durante o período de lactação sobre a viabilidade celular de fatias de córtex cerebral (A) e hipocampo (B) dos filhotes quando estes tinham 15, 21 30 ou 45 dias. Dados são descritos como média ± E.P.M. de 10-12 animais e expressos como % do controle.

Figura 3

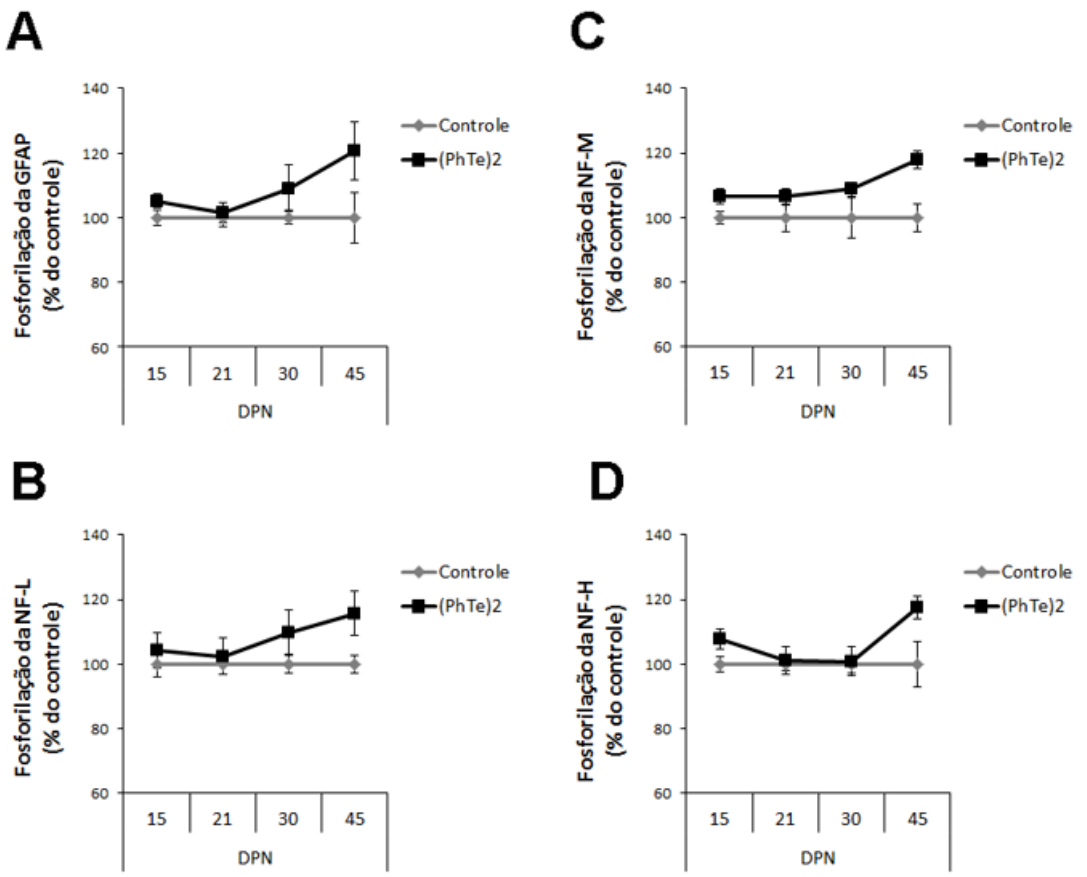

Figura 3: Efeito da administração subcutânea de (PhTe)2 (0,01 mg/kg de peso corporal) nas mães durante o período de lactação sobre a fosforilação *in vitro* dos FI do córtex cerebral de seus filhotes. A fosforilação foi medida nos dias pós-natal (DPN) 15, 21, 30 e 45. NF-H, neurofilamento de alto peso molecular; NF-M, neurofilamento de médio peso molecular; NF-L, neurofilamento de baixo peso molecular; GFAP, proteína glial fibrilar ácida. Dados são descritos como média ± E.P.M de 10-12 animais e expressos como % do controle.

Figura 4

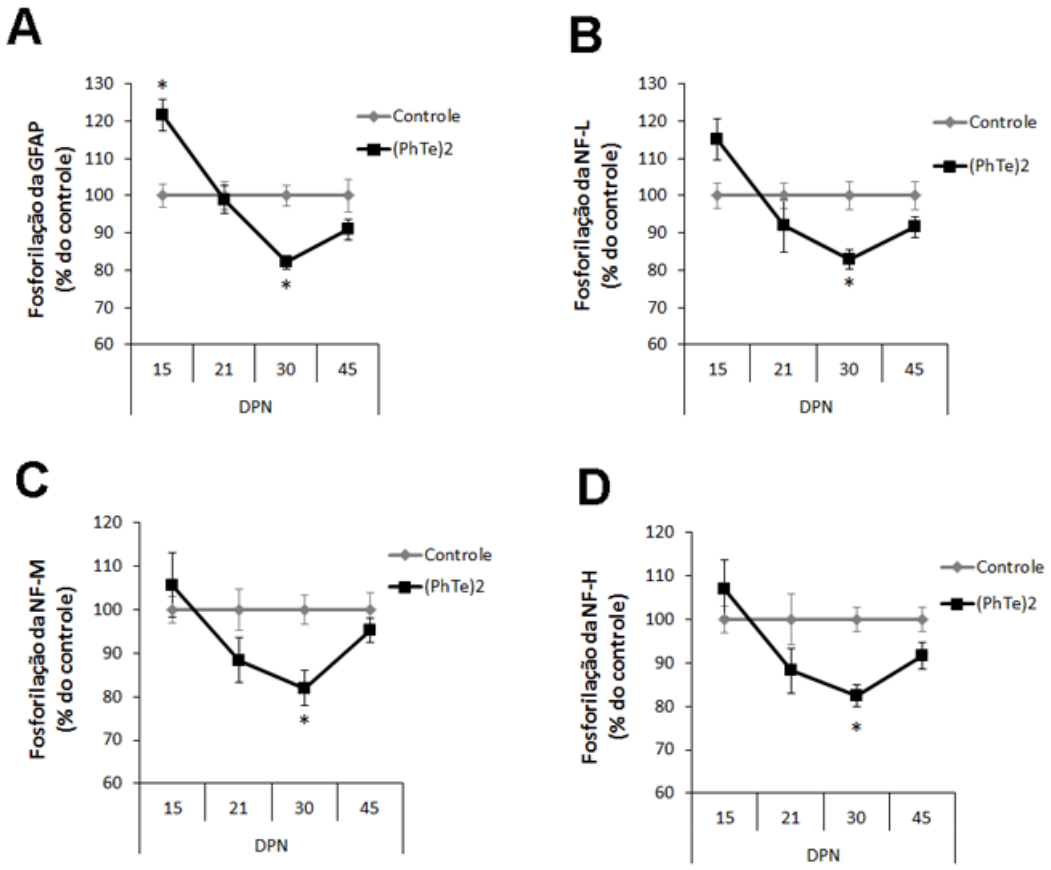

Figura 4: Efeito da administração subcutânea de (PhTe)2 (0,01 mg/kg de peso corporal) nas mães durante o período de lactação sobre a fosforilação *in vitro* dos FI do hipocampo de seus filhotes. A fosforilação foi medida nos dias pós-natal (DPN) 15, 21, 30 e 45. NF-H, neurofilamento de alto peso molecular; NF-M, neurofilamento de médio peso molecular; NF-L, neurofilamento de baixo peso molecular; GFAP, proteína glial fibrilar ácida. Dados são descritos como média ± E.P.M de 10-12 animais e expressos como % do controle. Diferenças estatisticamente significativas comparadas com os animais controle, que receberam óleo de canola, foram determinadas por ANOVA de uma via, seguida pelo pós-teste Tukey-Kramer e são indicadas por: $p<0,05$.

Figura 5

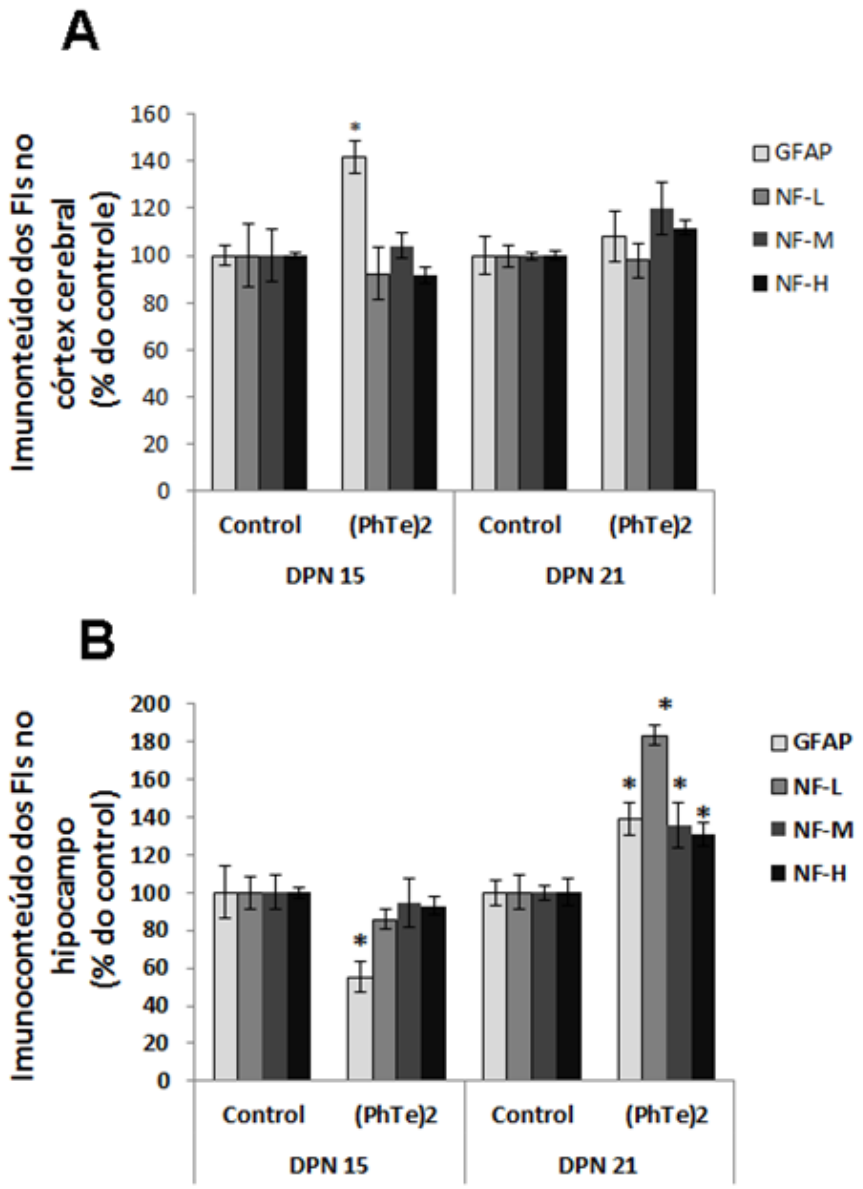

Figura 5: Efeito da administração subcutânea de (PhTe)2 (0,01 mg/kg de peso corporal) nas mães durante o período de lactação sobre o imunonteúdo dos FI neuronais (NF-L, NF-M e NF-H) e gliais (GFAP) de fatias de córtex cerebral (A) e hipocampo (B) dos filhotes quando estes tinham 15, 21 30 ou 45 dias. Dados são descritos como média ± E.P.M de 10-12 animais e expressos como % do controle.

Figura 6

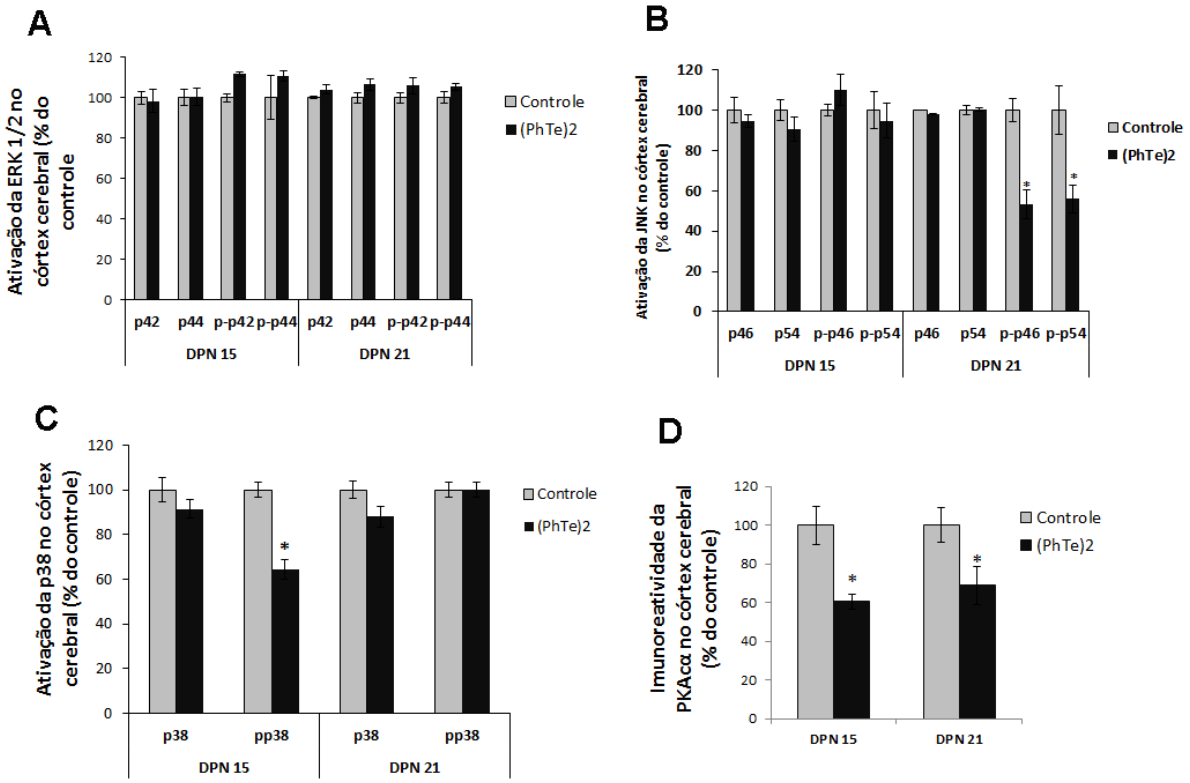

Figura 6: Efeito da administração subcutânea de (PhTe)2 (0,01 mg/kg de peso corporal) nas mães durante o período de lactação sobre a ativação da ERK 1/2 (A), SAP/JNK (B), p38MAPK (C) e PKAcα (D) do córtex cerebral dos filhotes nos dias pós-natal 15 e 21. Dados são descritos como média ± E.P.M de 10-12 animais e expressos como % do controle. Diferenças estatisticamente significativas comparadas com os animais controle, que receberam óleo de canola, foram determinadas por ANOVA de uma via, seguida pelo pós-teste Tukey-Kramer e são indicadas por: $p<0,05$.

Figura 7:

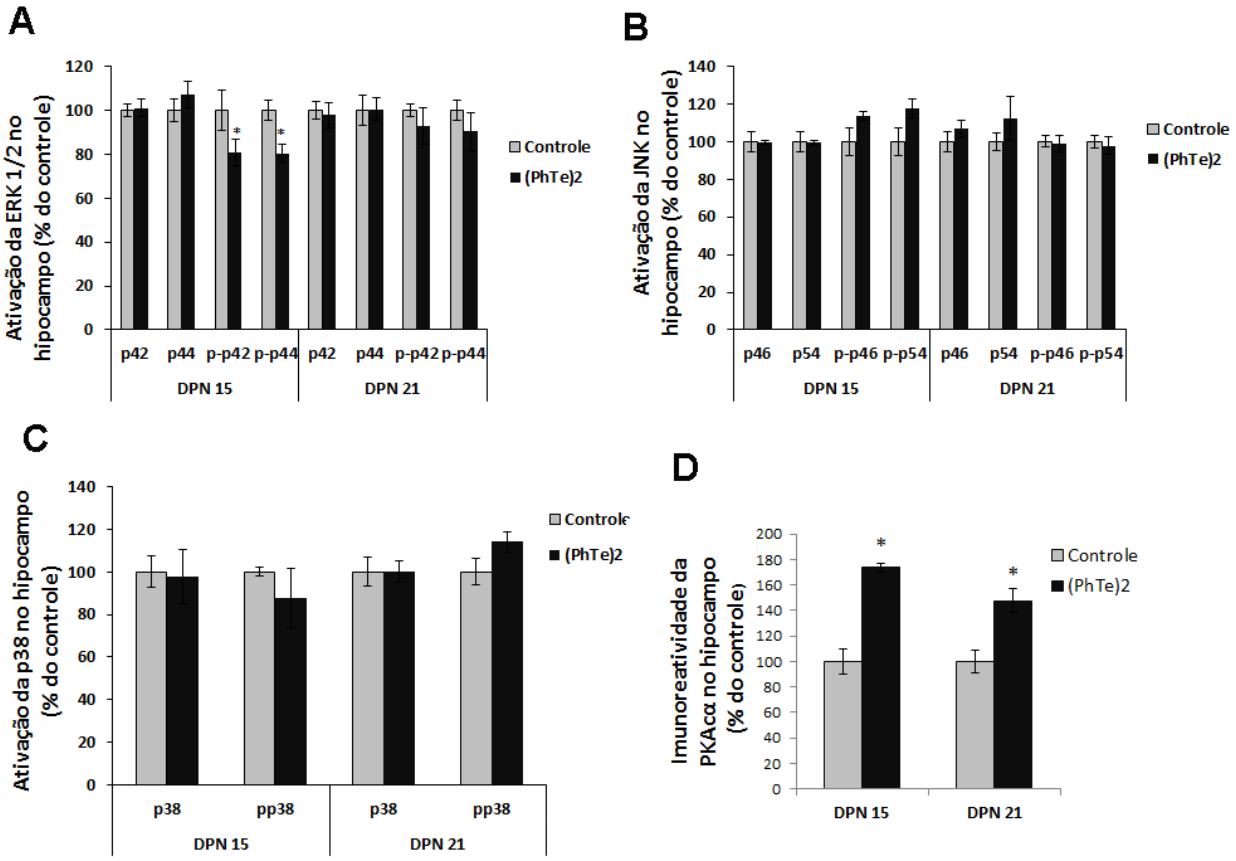

Figura 7: Efeito da administração subcutânea de (PhTe)2 (0,01 mg/kg de peso corporal) nas mães durante o período de lactação sobre a ativação da ERK 1/2 (A), SAP/JNK (B), p38MAPK (C) E PKAcα (D) do hipocampo dos filhotes nos dias pós-natal 15 e 21. Dados são descritos como média ± E.P.M de 10-12 animais e expressos como % do controle. Diferenças estatisticamente significativas comparadas com os animais controle, que receberam óleo de canola, foram determinadas por ANOVA de uma via, seguida pelo pós-teste Tukey-Kramer e são indicadas por: $p<0,05$.

6. REFERÊNCIAS BIBLIOGRÁFICAS

Alberts B., Johnson A., Lewis J., Raff M., Roberts K. & Walter P. O Citoesqueleto. In: Alberts B., Johnson A., Lewis J., Raff M, Roberts K, Walter P. (Eds) *Biologia Molecular da Célula.* 6. ed. New York: Garland Science, 2008, 907-982

Ba, L.A., Döring M., Jamier V., Jacob C. Tellurium: an element with great biological potency and potential. *Org Biomol Chem*. Oct 7;8(19):4203-16, 2010.

Bear, M.F., Connors, B.W., Paradiso, M.A. Neurociências. Desvendando o Sistema Nervoso. 3 ed. Porto Alegre: Artmed. Mecanismo Moleculares de Aprendizado e memória, 761. 2008.

Bomont, P., Cavalier, L., Blondeau, F., Ben Hamida, C., Belal, S., Tazir, M., Demir, E., Topaloglu, H., Korinthenberg, R., Tuysuz, B., Landrieu, P., Hentati, F., Koenig, M. The gene encoding gigaxonin, a new member of the cytoskeletal BTB/kelch repeat family, is mutated in giant axonal neuropathy. *Na.t Genet.* 26, 370-374, 2000.

Borges V.C., Rocha J.B., Nogueira C.W. Effect of diphenyl diselenide, diphenyl ditelluride and ebselen on cerebral Na(+), K(+)-ATPase activity in rats. *Toxicol.* 2005 Nov 15;215(3):191-7, 2005.

Borges V.C., Rocha J.B., Savegnago L., Nogueira C.W. Repeated administration of diphenyl ditelluride induces hematological disorders in rats. Food Chem Toxicol. 45(8):1453-8, 2007.

Borrelli E., Montmayeur J.P., Foulkes N.S., Sassone-Corsi P. Signal transduction and gene control: The cAMP pathway. *Crit Rev Oncog*, 3:321–38, 1992.

Carraway, C.A.C.,. The cytoskeleton in the transduction of signal and regulation of cellular function. In: Carraway, K.L., Carraway, C.A.C. (Ed.), Cytoskeleton: signalling and cellular regulation. Oxford University Press, New York, 2000, pp. 1-7.

Chang, L., Goldman, R.D. Intermediate filaments mediate cytoskeletal crosstalk. *Nat. Rev. Mol. Cell Biol*. 5, 601-613, 2004.

Clayton, G.D., Clayton, F.E. Patty`s Industrial Hygiene and Toxicology. Wiley, Chichester, 1981.

Coulombe P.A., Wong P. Cytoplasmic intermediate filaments revealed as dynamic and multipurpose scaffolds. *Nat. Cell Biol*., 6: 699-706, 2004.

Dhillon A.S., Hagan S., Rath O., Kolch W. MAP kinase signalling pathways in cancer. *Oncogene. 26*(22):3279-90, 2007.

Eriksson J.E., He T., Trejo-Skalli A.V., Härmälä-Braskén A.S., Hellman J., Chou Y.H., Goldman R.D. Specific in vivo phosphorylation sites determine the assembly dynamics of vimentin intermediate filaments. *J Cell Sci*. Feb 29;117(Pt 6):919-32, 2004.

Fabrizi G.M., Cavallaro T., Angiari C., Bertolasi L., Cabrini I., Ferrarini M., Rizzuto N. Giant axon and neurofilament accumulation in Charcot-Marie-Tooth disease type 2E. *Neurol.* 27;62(8):1429-31, 2004.

Favero, A. M., Weis, S. N., Zeni, G., Rocha J. B., Nogueira, C. W. Diphenyl diselenide changes behavior in female pups. *Neurotoxicol Teratol*. 28, 607–616, 2006.

Fuchs, E., Cleveland, D.W. A structural scaffolding of intermediate filaments in health and disease. *Science* 279, 514-519, 1998.

Funchal C., Zamoner A., Dos Santos A.Q., Moretto M.B., Rocha J.B., Wajner M., Pessoa-Pureur R.. Evidence that intracellular Ca2+ mediates the effect of alpha-ketoisocaproic acid on the phosphorylating system of cytoskeletal proteins from cerebral cortex of immature rats. *J. Neurol. Sci*. 15, 238(1-2):75-82, 2005.

Gong C.X., Wang J.Z., Iqbal K., Grundke-Iqbal I. Inhibition of protein phosphatase 2A induces phosphorylation and accumulation of neurofilaments in metabolically active rat brain. *Neurosci Lett*. 10, 340(2):107-10. 2003.

Gottlieb, A., Keydar, I., Epstein, H.T. Rodent brain growth stages: an analytical review. *Biol. Neonate*. 32, 166–176, 1977.

Heimfarth, L., Loureiro, S.O., Reis, K.P., De Lima, B.O., Zamboni, F., Gandolfi, T., Narvaes, R., Da Rocha, J.B., Pessoa-Pureur, R. Cross-talk among intracellular signaling pathways mediates the diphenyl ditelluride actions on the hippocampal cytoskeleton of young rats. *Chem. Res. Toxicol.* 24, 1754-1764, 2011.

Heimfarth, L., Loureiro, S.O., Reis, K.P., De Lima, B.O., Zamboni, F., Lacerda, S., Soska, A.K., Wild, L., Da Rocha, J.B., Pessoa-Pureur, R.. Diphenyl ditelluride

induces hypophosphorylation of intermediate filaments through modulation of DARPP-32-dependent pathways in cerebral cortex of young rats. *Arch. Toxicol*. 86, 217-230, 2012.

Heimfarth, L., Loureiro, S.O., Zamoner, A., Pelaez, P. L., Nogueira, C.W., Rocha, J. B., Pessoa-Pureur, R. Effects of in vivo treatment with diphenyl ditelluride on the phosphorylation of cytoskeletal proteins in cerebral cortex and hippocampus of rats. *Neurotoxicol*. 29, 40-47, 2008

Helfand B.T., Chou,Y-H., Shumaker D.K. And Goldman R.D. Intermediate filament proteins participate in signal transduction. *TRENDS Cell Biol.* 15, 568-570, 2005.

Hirano, A., Donnenfeld, H., Sasaki, S., Nakano, I. Fine structural observations of neurofilamentous changes in amyotrophic lateral sclerosis. *J Neuropathol. Exp. Neurol.* 43, 461-470, 1984.

Inagaki M., Nishi Y., Nishizawa K., Matsuyama M., Sato C. Site-specific phosphorylation induces disassembly of vimentin filaments in vitro. *Nature.* 328: 649–652, 1987.

Krebs, E.G.. Beavo, J.A. Phosphorylation-dephosphorylation of enzymes, *Annu Rev. Biochem*. 48, 923-959, 1979.

Laden B.P. & Porter T.D. Inhibition of human squalene monooxygenase by tellurium compounds: evidence of interaction with vicinal sulfhydryls. *J. Lipid Res*. 42:235-40, 2001.

Lara J., Kusano K., House S., Gainer H. Interactions of cyclic adenosine monophosphate, brain-derived neurotrophic factor, and glial cell line-derived neurotrophic factor treatment on the survival and growth of postnatal mesencephalic dopamine neurons in vitro. *Exp. Neurol*. 180(1):32-45, 2003.

Lariviere R.C., Julien J.P. Functions of intermediate filaments in neuronal development and disease. *J. Neurobiol*. 58(1):131-48. Review, 2004.

Ledig M., Ciesielski L., Simler S., Lorentz J.G., Mandel P. Effect of pre- and postnatal alcohol consumption on GABA levels of various brain regions in the rat offspring. *Alcohol Alcohol.* 23(1):63-7, 1988.

Li, R., Messing, A., Goldman, J.E., Brenner, M. GFAP mutations in Alexander disease. *Int. J. Dev. Neurosci.* 20, 259-268, 2002.

Liu A.Y.C (1982). Diferentiation-specific increase of cAMP-dependent protein kinase in 3T3 L1 cells. *J. Biol. Chem*. 257, 298-306, 1982.

Liu, Y.; Peterson, D.A.; Kimura, H; Schubert, D. (1997). Mechanism of cellular 3-(4,5-dimethylthiazol-2yl)-2,5-diphenyltetrazolium bromide (MTT) reduction. *J..Neurochem*., 69, 581-593.

Loureiro S.O., Heimfarth L., Pelaez P.L., Vanzin C.S., Viana L., Wyse A.T., Pessoa-Pureur R. (2008) Homocysteine activates calcium-mediated cell signaling mechanisms targeting the cytoskeleton in rat hippocampus. *Int. J. Dev. Neurosci.* 26(5):447-55.

Lugokenski T.H., Müller L.G., Taube P.S., Rocha J.B., Pereira M.E (2011). Inhibitory effect of ebselen on lactate dehydrogenase activity from mammals: a comparative study with diphenyl diselenide and diphenyl ditelluride. Drug Chem *Toxicol.* 34(1),66-76.

Maciel E.N., Bolzan R.C., Braga A.L., Rocha J.B. (2000). Diphenyl diselenide and diphenyl ditelluride differentially affect delta-aminolevulinate dehydratase from liver, kidney, and brain of mice. *J. Biochem. Mol. Toxicol*. 14:310-309, 2000.

Mccubrey, M.M. Lahair, R.A Franklin (2006). Reactive oxygen species-induced activation of the MAP kinase signaling pathwaysAntioxid. *Redox Signal.,* 8, pp. 1775–1789

Meotti F.C., Borges V.C., Zeni G., Rocha J.B., Nogueira C.W. (2003). Potential renal and hepatic toxicity of diphenyl diselenide, diphenyl ditelluride and Ebselen for rats and mice. *Toxicol Lett.* 5;143(1):9-16, 2003.

Moretto M.B, Funchal C., Zeni G., Rocha J.B., Pessoa-Pureur R. Organoselenium compounds prevent hyperphosphorylation of cytoskeletal proteins induced by the neurotoxic agent diphenyl ditelluride in cerebral cortex of young rats. *Toxicol*. 210:213-222, 2005.

Mosmann, T. Rapid colorimetric assay for cellular growth and survival: application to proliferation and cytotoxicity assays. *J. Immunol. Met*., 65 55-63, 1983.

Nestler Ej, Greengard P. Protein phosphorylation and the regulation of neuronal function In Siegel GJ, Albers RW, Agranoff BW, Molinoff P (eds). Basic neurochemistry: molecular, cellular, and medical aspects. Boston: Little Brown p 449–74, 1994.

Nixon R.A. E Sihag R.K. Neurofilament phosphorylation: a new look at regulation and function. *Trends Neurosci*. 14(11):501-6. Review, 1991.

Nogueira, C.W., Rotta, L.N., Perry, M.L., Souza, D.O., And Da Rocha, J.B. Diphenyl diselenide and diphenyl ditelluride affect the rat glutamatergic system in vitro and in vivo. *Brain Res. 906*, 157-163, 2001.

Omary, M.B., Coulombe, P.A., Mclean, W.H. Intermediate filament proteins and their associated diseases. *N. Engl. J. Med*. 351, 2087-2100, 2004.

Othman T., Legare D., Sadri P., Lautt W.W., Parkinson F.E. A preliminary investigation of the effects of maternal ethanol intake during gestation and lactation on brain adenosine A(1) receptor expression in rat offspring. *Neurotoxico*l, 24(2):275-9, 2002.

Peng, S., Zhang., J. Wang, H, Ren, B. ERK in learning and memory: a review of recent research. Int J Mol Sci. 13;11(1):222-32, 2010

Pierozan P., Zamoner A., Soska A.K., De Lima B.O., Reis K.P., Zamboni F., Wajner M., Pessoa-Pureur R. Signaling mechanisms downstream of quinolinic acid targeting the cytoskeleton of rat striatal neurons and astrocytes. *Exp Neurol*. 2012.

Pinton S., Luchese C., Stangherlin E.C., Nogueira C.W. Acute exposure to diphenyl ditelluride causes oxidative damage in rat lungs. *Ecotoxicol Environ Saf*. 74(3):521-6, 2011.

Riccio A., Ahn S., Davenport C.M., Blendy J.A., Ginty D.D. Mediation by a CREB family transcription factor of NGF-dependent survival of sympathetic neurons. *Science*, 286:2358–61, 1999.

Rice, D., Barone, S. Critical periods of vulnerability for the developing nervous system: evidence from humans and animal models. *Environ. Health Perspect*. 108, 511–533, 2000.

Rigon A.P., Cordova F.M., Oliveira C.S., Posser T., Costa A.P., Silva I.G., Santos D.A., Rossi F.M., Rocha J.B., Leal R.B. Neurotoxicity of cadmium on immature hippocampus and a neuroprotective role for p38 MAPK. *Neurotoxicol.* 29(4):727-34, 2008.

Rockwell P., Martinez J., Papa L , Gomes E. Redox regulates COX-2 upregulation and cell death in the neuronal response tocadmium. *Cell. Signal*. 16, 343–353, 2004.

Saijoh K., Fukunaga T., Katsuyama H., Lee M.J., Sumino K. Effects of methylmercury on protein kinase A and protein kinase C in the mouse brain. *Environ Res*. 63(2):264-73, 1993.

Schmidt, M.L., Martin, J.A., Lee, V.M., Trojanowski, J.Q. Convergence of Lewy bodies and neurofibrillary tangles in amygdala neurons of Alzheimer's disease and Lewy body disorders. *Acta Neuropathol.* 91, 475-481, 1996.

Schmidt, R.E., Beaudet, L.N., Plurad, S.B., Dorsey, D.A. Axonal cytoskeletal pathology in aged and diabetic human sympathetic autonomic ganglia. *Brain Res* 769, 375-383, 1997.

Shepherd, C.E., Mccann, H., Thiel, E., Halliday, G.M. Neurofilament immunoreactive neurons in Alzheimer's disease and dementia with Lewy bodies. *Neurobiol Dis* 9, 249-257, 2002.

Sihag R.K., Inagaki M., Yamaguchi T., Shea T.B., Pant H.C. Role of phosphorylation on the structural dynamics and function of types III and IV intermediate filaments. *Exp Cell Res*. 10;313(10):2098-109. Review, 2007.

Sihag, R.K., Nixon, R.A. Identification of Ser-55 as a major protein kinase A phosphorylation site on the 70-kDa subunit of neurofilaments. Early turnover during axonal transport. *J. Biol. Chem*. 266(28), 18861-18867, 1991.

Souza A.C., Stangherlin E.C., Ardais A.P., Nogueira C.W. Diphenyl diselenide and diphenyl ditelluride: neurotoxic effect in brain of young rats, in vitro. *Mol Cell Biochem.* 340(1-2):179-85, 2010.

Squire, L.R., Berg, D., Bloom, F.E, Lac, S.D., Ghosh, A., Spitzer, N.C. Synapses Elimination. In: *Fundamental Neuroscience*, 3 ed. London. Elsevier, pp 469-491, 2008

Stangherlin E.C., Ardais A.P., Rocha J.B., Nogueira C.W. Exposure to diphenyl ditelluride, via maternal milk, causes oxidative stress in cerebral cortex, hippocampus and striatum of young rats. *Arch Toxicol*. 83(5):485-91. 2009b

Stangherlin E.C., Favero A.M., Zeni G., Rocha J.B., Nogueira C.W. Exposure of mothers to diphenyl ditelluride during the suckling period changes behavioral tendencies in their offspring. *Brain Res Bull*. 14;69(3):311-7, 2006.

Stangherlin E.C., Favero A.M., Zeni G., Rocha J.B., Nogueira C.W. Teratogenic vulnerability of Wistar rats to diphenyl ditelluride. *Toxicol*. 14;207(2):231-9, 2005.

Stangherlin E.C., Rocha J.B., Nogueira C.W. Diphenyl ditelluride impairs short-term memory and alters neurochemical parameters in young rats. *Pharmacol. Biochem. Behav*. 91(3):430-5, 2009a.

Sulkowski Z.L., Chen T., Midha S., Zavacki A.M., Sajdel-Sulkowska E.M. Maternal Thimerosal Exposure Results in Aberrant Cerebellar Oxidative Stress, Thyroid Hormone Metabolism, and Motor Behavior in Rat Pups; Sex- and Strain-Dependent Effects. *Cerebellum.* 2011

Taylor, A. Biochemistry of tellurium. *Biol. Trace Elem. Res.* 55: 231-239, 1996.

Tidyman W.E, Rauen K.A. The RASopathies: developmental syndromes of Ras/MAPK pathway dysregulation. *Curr. Opin. Genet. Dev*. 19(3):230-6, 2009.

Torii S., Yamamoto T., Tsuchiya Y., Nishida E. ERK MAP kinase in G cell cycle progression and cancer. *Cancer Sci., 97* pp. 697–702, 2006.

Veeranna, K.T, Boland B., Odrljin T., Mohan P., Basavarajappa B.S., Peterhoff C., Cataldo A., Rudnicki A., Amin N., Li B.S., Pant H.C., Hungund B.L., Arancio O.,

Nixon R.A. Calpain mediates calcium-induced activation of the erk1,2 MAPK pathway and cytoskeletal phosphorylation in neurons: relevance to Alzheimer's disease. *Am J Pathol*. 165: 795-805, 2004.

Wagner-Recio, M., Toews, A.D., Morell P. Tellurium blocks cholesterol synthesis by inhibiting squalene metabolism: preferential vulnerability to this metabolic block leads to peripheral nervous system demyelination. *J. Neurochem.* 57:1891-901, 1991.

Walbran, B.B., Robins, E. Effects of central nervous system accumulation of tellurium on behavior in rats. *Pharmacol. Biochem. Behav*. 9: 297-300, 1978.

Watson, D.F., Nachtman, F.N., Kuncl, R.W., Griffin, J.W. Altered neurofilament phosphorylation and beta tubulin isotypes in Charcot-Marie-Tooth disease type 1. *Neurol.* 44, 2383-2387, 1994.

Widy-Tyszkiewicz, E., Piechal, A., Gajkowska, B., Smialek, M. Tellurium-induced cognitive deficits in rats are related to neuropathological changes in the central nervous system. *Toxicol. Lett*. 131: 203-214, 2002.

Yarema M.C., Curry S.C. Acute tellurium toxicity from ingestion of metal-oxidizing solutions. *Pediat.* 116:319–21, 2005.

Zamoner A., Heimfarth L., Loureiro S.O., Royer C., Mena Barreto Silva F.R, Pessoa-Pureur R. Nongenomic actions of thyroxine modulate intermediate filament phosphorylation in cerebral cortex of rats. Neurosci. 15;156(3):640-52, 2008.

Capítulo 4

DIPHENYL DITELLURIDE INDUCES HYPOPHOSPHORYLATION OF INTERMEDIATE FILAMENTS THROUGH MODULATION OF DARPP-32-DEPENDENT PATHWAYS IN CEREBRAL CORTEX OF YOUNG RATS.

Luana Heimfarth, Samanta Oliveira Loureiro, Karina Pires Reis , Bárbara Ortiz de Lima, Fernanda Zamboni, Sabrina Lacerda, Ângela Kronbauer Soska. Luisa Wild, João Batista Teixeira da Rocha, Regina Pessoa-Pureur

Artigo publicado na revista Archives of Toxicology

Arch Toxicol (2012) 86:217–230
DOI 10.1007/s00204-011-0746-6

MOLECULAR TOXICOLOGY

Diphenyl ditelluride induces hypophosphorylation of intermediate filaments through modulation of DARPP-32-dependent pathways in cerebral cortex of young rats

Luana Heimfarth · Samanta Oliveira Loureiro · Karina Pires Reis · Bárbara Ortiz de Lima · Fernanda Zamboni · Sabrina Lacerda · Ângela Kronbauer Soska · Luisa Wild · João Batista Teixeira da Rocha · Regina Pessoa-Pureur

Received: 23 June 2011 / Accepted: 11 August 2011 / Published online: 24 August 2011

Abstract We studied the effect of different concentrations of diphenyl ditelluride $(PhTe)_2$ on the in vitro phosphorylation of glial fibrillary acidic protein (GFAP) and neurofilament (NF) subunits from cerebral cortex and hippocampus of rats during development. $(PhTe)_2$-induced hypophosphorylation of GFAP and NF subunits only in cerebral cortex of 9- and 15-day-old animals but not in hippocampus. Hypophosphorylation was dependent on ionotropic glutamate receptors, as demonstrated by the specific inhibitors 10 μM DL-AP5 and 50 μM MK801, 100 μM CNQX and 100 μM DNQX. Also, 10 μM verapamil and 10 μM nifedipine, two L-voltage-dependent Ca^{2+} channels (L-VDCC) blockers; 50 μM dantrolene, a ryanodine channel blocker, and the intracellular Ca^{2+} chelator Bapta-AM (50 μM) totally prevented this effect. Results obtained with 0.2 μM calyculin A (PP1 and PP2A inhibitor), 1 μM Fostriecin a potent protein phosphatase 2A (PP2A) inhibitor, 100 μM FK-506 or 100 μM cyclosporine A, specific protein phosphatase 2B inhibitors, pointed to PP1 as the protein phosphatase directly involved in the hypophosphorylating effect of $(PhTe)_2$. Finally, we examined the activity of DARPP-32, an important endogenous Ca^{2+}-mediated inhibitor of PP1 activity. Western blot assay using anti-DARPP-32, anti-pThr34DARPP-32, and anti-pThr75DARPP-32 antibodies showed a decreased phosphorylation level of the inhibitor at Thr34, compatible with inactivation of protein kinase A (PKA) by pThr75 DARPP-32. Decreased cAMP and catalytic subunit of PKA support that $(PhTe)_2$ acted on neuron and astrocyte cytoskeletal proteins through PKA-mediated inactivation of DARPP-32, promoting PP1 release and hypophosphorylation of IF proteins of those neural cells. Moreover, in the presence of Bapta, the level of the PKA catalytic subunit was not decreased by $(PhTe)_2$, suggesting that intracellular Ca^{2+} levels could be upstream the signaling pathway elicited by this neurotoxicant and targeting the cytoskeleton.

Keywords Diphenyl ditelluride · Cytoskeleton · Calcium · Protein phosphatase 1 · Protein kinase A · DARPP-32

Introduction

Tellurium, a rare element, used as an industrial component of many alloys and in the electronic industry, can cause poisoning which leads to neurotoxic symptoms such as significant impairment of learning and spatial memory (Walbran and Robins 1978; Widy-Tyszkiewicz et al. 2002). Otherwise, the organic compound of tellurium, diphenyl ditelluride $(PhTe)_2$ has been described to possess very interesting biological activities. While some studies provide evidence for anticonvulsant and antioxidant properties of $(PhTe)_2$, which indicate neuroprotective activities of this compound (Brito et al. 2009; Hassan et al. 2009), other evidence has pointed on deformations in the brain of rat fetuses during development (Stangherlin et al. 2005), alterations in glutamate homeostasis (Souza et al. 2010),

L. Heimfarth · S. O. Loureiro · K. P. Reis · B. O. de Lima · F. Zamboni · S. Lacerda · Â. K. Soska · L. Wild · R. Pessoa-Pureur (✉)
Departamento de Bioquímica, Instituto de Ciências Básicas da Saúde, Universidade Federal do Rio Grande do Sul, Rua Ramiro Barcelos 2600 anexo, Porto Alegre, RS 90035-003, Brazil
e-mail: rpureur@ufrgs.br

J. B. T. da Rocha
Departamento de Química, Centro de Ciências Naturais e Exatas, Universidade Federal de Santa Maria, Santa Maria, RS, Brazil

and ansiolitic-like behavior induced by $(PhTe)_2$. In addition, organotellurium compounds, including $(PhTe)_2$, can inhibit thiol-containing enzymes, such as aminolevulinate dehydratase (ALA-D; Barbosa et al. 1998; Farina et al. 2002; Nogueira et al. 2001, 2003, 2004), Na^+, K^+ ATPase, (Borges et al. 2005), catepsin B (Cunha et al. 2005), and squalene monooxygenase (Laden and Porter 2001). Taken together, these findings highlight the complexity of the actions of this organocalcogen and indicate that the brain is an important target for the action of this compound.

Human exposure to tellurium is rare. However, accidental exposure to this element has been reported in the literature (Taylor 1996; Yarema and Curry 2005), and the industrial and laboratorial use of inorganic and organic forms of tellurium indicates that exposure to toxic levels of tellurium is conceivable in the work-place. Additionally, the antioxidant properties and low toxicity of different organotellurium compounds have been demonstrated by different laboratories and have been exploited to support their potential therapeutic use in pathologies associated with oxidative stress (Kanski et al. 2001; Giles et al. 2003; de Avila et al. 2006, 2010). Tellurium is also found in relatively large amounts in the human body (Schroeder et al. 1967), and Larner (1995) has hypothesized that tellurium can be an important factor in the etiology of neurodegenerative diseases in man.

Intermediate filaments (IFs) are cytoskeletal structures formed by the members of a family of related proteins (Herrmann et al. 2003; Herrmann and Aebi 2004). The IF proteins can self-assemble into flexible and nonpolar filaments. Based on the gene structure and amino acid sequence, IFs have been classified into five types. Acidic and basic keratins (types I and II) are typically expressed in epithelial cells. Vimentin (mesenchymal cells), desmin (muscle cells), glial fibrillary acidic protein (GFAP) expressed in astrocytes, and peripherin found in neurons of the peripheral nervous system are classified as type III IF proteins. Type IV IF proteins are expressed in the neurons of the central nervous system and include the neurofilament (NF) triplet proteins of low (NF-L), medium (NF-M), and high (NF-H) molecular weight, as well as α-internexin (Sihag et al. 2007). The nuclear lamins are type V intermediate filament proteins that form meshworks at the inner aspect of the nuclear envelope and are also present throughout the nuclear interior. Through these meshwork structures, lamins regulate the shape, size, and mechanical properties of the nucleus (Shimi et al. 2010).

Phosphorylation of IF proteins is a dynamic process mediated by the combined action of several protein kinases and phosphatases controlling their physiological role in response to extracellular signals. Phosphorylation of the amino-terminal head domain sites on GFAP and NF proteins plays a key role in the assembly/disassembly of the IF subunits into 10 nm filaments (Sihag et al. 2007). Otherwise, the phosphorylation level of carboxyl terminal sites on NFs is correlated with the interactions of NFs with each other and with other cytoskeletal structures, and consequently, mediate the formation of a cytoskeletal lattice that supports the mature axon (Grant and Pant 2000). Also, there is evidence that phosphorylation of specific sites at tail domains of NF subunits regulates the axonal transport of these proteins (Yabe et al. 2000; Motil et al. 2006) and is correlated with axon caliber (Gou et al. 1998).

The importance of GFAP and NF subunits on cellular function is evident from the fact that perturbation of their function accounts for several genetically determined protein misfolding/aggregation diseases (Arbustini et al. 2006; Green et al. 2005). Also, perikaryal accumulations/aggregations of NF proteins have been correlated with aberrantly phosphorylated NF in several neurodegenerative diseases, such as Alzheimer's disease, motor neuron diseases, and Parkinson's disease (Grant and Pant 2000; Lariviere and Julien 2004; Nixon 1993; Nixon and Sihag 1991). Otherwise, nerve biopsies from patients with Charcot-Marie-Tooth 1 exhibited marked hypophosphorylation of NF proteins (Watson et al. 1994) corroborating the evidence that deregulation of NF phosphorylation correlates with the pathology characteristic of several neurodegenerative disorders.

We have previously reported that the phosphorylating system associated with the IF proteins is responsive to the metabolites accumulating in genetic disorders (Loureiro et al. 2010; Pessoa-Pureur and Wajner 2007; Pierozan et al. 2010) as well as to hormonal signals (Zamoner et al. 2008). These actions can be initiated by the activation of N-methyl-D-aspartate (NMDA)-, voltage-dependent Ca^{2+} channels type L (L-VDCC) or G protein-coupled receptors, and the signal is transduced downstream Ca^{2+} mobilization or monomeric GTPase activation through different kinase/phosphatase pathways, regulating the dynamics of the cytoskeleton (Loureiro et al. 2008; Zamoner et al. 2008). Besides the physiological and pathological responses to metabolites, the phosphorylating system associated with the IF proteins has been shown to be targeted by $(PhTe)_2$. Recently, we have reported in vivo actions of this neurotoxicant on the cytoskeleton (Heimfarth et al. 2008). Accordingly, previous results from our group have described the in vitro effects of $(PhTe)_2$ on the phosphorylation level of IFs of neural cells from cerebral cortex of 17-day-old rats (Moretto et al. 2005). However, the potential intracellular pathways involved in $(PhTe)_2$ neurotoxicity related to cytoskeleton are unknown. Therefore, the aim of the present study was to extend our investigation analyzing the in vitro effects of $(PhTe)_2$ in cerebral cortex and hippocampus during

development, in 9- and 15-day-old animals, providing an insight into the participation of Ca^{2+}-mediated mechanisms in this action.

Materials and methods

Radiochemical and compounds

[^{32}P]Na_2HPO_4 was purchased from CNEN, São Paulo, Brazil. *N*,*N*,*N*′,*N*′-tetraacetic acid tetrakis (acetoxymethyl ester; BAPTA-AM), dantrolene, benzamidine, leupeptin, antipain, pepstatin, chymostatin, verapamil hydrochloride, acrylamide and bis-acrylamide, calyculin A, FK-506, CNQX, D-2-amino-5-phosphonopentanoic acid (DL-AP5), 6,7-dinitroquinoxaline-2,3(1H,4H)-dione (DNQX), (±)-α-methyl-(4-carboxyphenyl)glycine (MCPG), (+)-MK-801 hydrogen maleate (MK-801), apamin, nifedipine, and cyclosporin A were obtained from Sigma (St. Louis, MO, USA). Fostriecin was obtained from Tocris Biosciences, UK. The chemiluminescence ECL kit peroxidase and the conjugated anti-rabbit IgG were obtained from Amersham (Oakville, ON, Canada). Anti-DARPP-32, anti-pThr34D ARPP-32, anti-pThr75DARPP-32, and anti-PKAc-α antibodies were obtained from Cell Signaling Technology (USA). The organochalcogenide $(PhTe)_2$ was synthesized using the method described by Petragnani (1994). Analysis of the 1H NMR and 13C NMR spectra showed that the compound obtained presented analytical and spectroscopic data in full agreement with their assigned structures. The purity of the compounds was assayed by high-resonance mass spectroscopy (HRMS) and was higher that 99.9%. $(PhTe)_2$ was dissolved in dimethylsulfoxide (DMSO) just before use. The final concentration of DMSO was adjusted to 0.1%. Solvent controls attested that at this concentration, DMSO did not interfere with the phosphorylation measurement. All other chemicals were of analytical grade and were purchased from standard commercial supplier.

Animals

Nine- and fifteen-day-old Wistar rats were obtained from our breeding stock. Rats were maintained on a 12-h light/12-h dark cycle in a constant temperature (22°C) colony room. On the day of birth, the litter size was culled to seven pups. Litters smaller than seven pups were not included into the experiments. Water and a 20% (w/w) protein commercial chow were provided ad libitum. The experimental protocol followed the "Principles of Laboratory Animal Care" (NIH publication 85-23, revised 1985) and was approved by the Ethics Committee for Animal Research of the Federal University of Rio Grande do Sul.

Preparation and labeling of slices

Rats were killed by decapitation, and the cerebral cortex and hippocampus were dissected onto the Petri dishes placed on ice and cut into 400-μm-thick slices with a McIlwain chopper.

Preincubation

Tissue slices were initially preincubated at 30°C for 20 min in a Krebs-Hepes medium containing 124 mM NaCl, 4 mM KCl, 1.2 mM $MgSO_4$, 25 mM Na-HEPES (pH 7.4), 12 mM glucose, 1 mM $CaCl_2$, and the following protease inhibitors: 1 mM benzamidine, 0.1 μM leupeptin, 0.7 μM antipain, 0.7 μM pepstatin, and 0.7 μM chymostatin in the presence or absence of 10 μM verapamil, 10 μM nifedipine, 50 μM dantrolene, 50 μM Bapta-AM, 10 μM DL-AP-5, 100 μM CNQX, 50 μM MK-801, 100 μM DNQX, 100 μM FK-506, 0.2 μM calyculin A, 100 μM cyclosporin A, and 1 μM Fostriecin.

Incubation

After preincubation, the medium was changed and incubation was carried out at 30°C with 100 μl of the basic medium containing 80 μCi of [^{32}P] orthophosphate with or without addition of 10 μM verapamil, 10 μM nifedipine, 50 μM dantrolene, 50 μM Bapta-AM, 100 μM DL-AP-5, 100 μM MCPG, 50 μM CNQX, 50 μM MK-801, 100 μM DNQX, 100 μM FK-506, 0.2 μM calyculin A, 100 μM cyclosporin, and 1 μM Fostriecin in the presence or absence of $(PhTe)_2$, when indicated. The labeling reaction was normally allowed to proceed for 30 min at 30°C and stopped with 1 ml of cold stop buffer (150 mM NaF, 5 mM EDTA, 5 mM EGTA, 50 mM Tris–HCl, pH 6.5, and the protease inhibitors described above). Slices were then washed twice with stop buffer to remove excess radioactivity.

Preparation of the high salt-Triton insoluble cytoskeletal fraction from tissue slices

After treatment, IF-enriched cytoskeletal fractions were obtained from cerebral cortex and hippocampus of 9- or 15-day-old rats as described by Funchal et al. (2003). Briefly, after the labeling reaction, slices were homogenized in 400 μl of ice-cold high salt buffer containing 5 mM KH_2PO_4 (pH 7.1), 600 mM KCl, 10 mM $MgCl_2$, 2 mM EGTA, 1 mM EDTA, 1% Triton X-100, and the protease inhibitors described above. The homogenate was centrifuged at 14,000×*g* for 10 min at 4°C, in Eppendorf centrifuge, the supernatant was discarded and the pellet homogenized with the same volume of the high-salt

medium. The suspended pellet was centrifuged as described and the supernatant was discarded. The final Triton-insoluble IF-enriched pellet, containing NF subunits, vimentin, and GFAP, was dissolved in 1% SDS and protein concentration was determined (Lowry et al. 1951).

Polyacrylamide gel electrophoresis (SDS-PAGE)

The cytoskeletal fraction was prepared as described above. Equal protein amount (50 μg) was loaded onto 10% polyacrylamide gels and analyzed by SDS-PAGE according to the discontinuous system of Laemmli (1970). After drying, the gels were exposed to X-ray films (Kodak T-Mat) at −70°C with intensifying screens, and finally, the autoradiograph was obtained. Cytoskeletal proteins were quantified from Coomassie-stained gels by scanning the gels with a Hewlett-Packard Scanjet 6100C scanner and determining optical densities with an Optiquant version 02.00 software (Packard Instrument Company). Phosphorylation level of the proteins studied was obtained by scanning the corresponding bands on the autoradiograph. Density values were obtained for the studied proteins.

Preparation of total protein homogenate

Tissue slices were initially preincubated at 30°C for 20 min with or without addition of 50 μM BAPTA-AM or 100 μM FK-506 in a Krebs-Hepes medium. After preincubation, the medium was changed, and incubation was carried out at 30°C with 100 μl of the basic medium in the presence or absence of 50 μM Bapta-AM, 100 μM FK-506 and/or 50 or 100 μM $(PhTe)_2$. Tissues slices were then homogenized in 100 μl of a lysis solution containing 2 mM EDTA, 50 mM Tris–HCL, pH 6.8, 4% (w/v) SDS. For electrophoresis analysis, samples were dissolved in 25% (v/v) of a solution containing 40% glycerol, 5% mercaptoethanol, 50 mM Tris–HCl, pH 6.8 and boiled for 3 min.

Western blot analysis

Protein homogenate (80 μg) was analyzed by SDS-PAGE and transferred to PVDF membranes (Trans-blot SD semi-dry transfer cell, BioRad) for 1 h at 15 V in transfer buffer (48 mM Trizma, 39 mM glycine, 20% methanol and 0.25% SDS). The PVDF membranes were washed for 10 min in Tris-buffered saline (TBS; 0.5 M NaCl, 20 mM Trizma, pH 7.5), followed by 2 h incubation in blocking solution (TBS plus 5% bovine serum albumin and 0.1% Tween 20). After incubation, the blot was washed twice for 5 min with TBS plus 0.05% Tween-20 (T-TBS) and then incubated overnight at 4°C in blocking solution containing the following monoclonal antibodies: anti-DARPP-32 diluted 1:600, anti-pThr34DARPP-32 diluted 1:600, anti-pThr75DARPP-32 diluted 1:600, and anti-PKAc-α diluted 1:1,000. The blot was then washed twice for 5 min with T-TBS and incubated for 2 h in blocking solution containing peroxidase-conjugated donkey anti-rabbit IgG diluted 1:1,000. The blot was washed twice again for 5 min with T-TBS and twice for 5 min with TBS. The blot was then developed using a chemiluminescence ECL kit. Immunoblots were quantified by scanning the films as described above. Optical density values were obtained for the studied proteins.

Measurement of cyclic AMP levels in slices of cerebral cortex

Two tissue slices placed into Eppendorf tubes were preincubated in 500 μl of Krebs buffer at 37°C for 60 min. The buffer was changed twice during this period. After preincubation, the medium was changed, and incubation was carried out at 37°C for 30 min in the presence or absence of $(PhTe)_2$, when indicated. Incubation was stopped by placing the tubes in an ice-cold bath, and samples were processed as described (Tasca et al. 1998). In brief, incubation medium was replaced by 0.5 N perchloric acid, slices were homogenized, and an aliquot was used for protein measurement (Lowry et al. 1951) using bovine serum albumin as standard. The homogenate was centrifuged for 2 min (12,800×*g*), and the supernatant was neutralized with 2 M KOH and 1 M Tris/HCl to pH 7.4. The pellet was removed by centrifugation for 3 min (12,800×*g*), and an aliquot from the supernatant was evaporated under a stream of air in a 50°C bath, according to the procedure of Baba et al. (1982) modified. Residues were dissolved in 50 mM Tris–HCl, pH 7.4, containing 4 mM EDTA. Cyclic AMP content was measured by the protein-binding method of Tovey et al. (1974), using [^{3}H] cyclic AMP (23 Ci/mmol) and protein kinase 3′,5′ cyclic AMP dependent as the binding protein. Radioactivity was counted by liquid scintillation.

Statistical analysis

Data were statistically analyzed by one-way analysis of variance (ANOVA) followed by the Tukey–Kramer multiple comparison test when the *F* test was significant and necessary. All analyses were performed using the SPSS software program on an IBM-PC compatible computer.

Results

The effect of different concentrations of $(PhTe)_2$ on the in vitro phosphorylation of IF-enriched cytoskeletal fraction

from cerebral cortex and hippocampus of 9- and 15-day-old rats was tested. Results showed a developmentally regulated dose-dependent action of this neurotoxicant on the phosphorylation of NF subunits (NF-M and NF-L), vimentin, and GFAP. In cerebral cortex of 9-day-old animals, 15 and 50 μM $(PhTe)_2$ significantly decreased the IF phosphorylation, while 100 μM $(PhTe)_2$ failed in altering this parameter (Fig. 1a), while in 15-day-old animals, only the higher concentration (100 μM) induced hypophosphorylation (Fig. 1b). In contrast with cortex, $(PhTe)_2$ did not alter hippocampal phosphorylation level of these cytoskeletal proteins in both ages studied (Fig. 1c, d). Therefore, we have chosen the concentrations of 50 and 100 μM $(PhTe)_2$ for subsequent experiments with the cerebral cortex of 9- and 15-day-old rats, respectively. All the subsequent results concerning the mechanism of action of $(PhTe)_2$ obtained in the present study were similar for 9- and 15-day-old-rats; therefore, we have chosen to present only data from cerebral cortex of 15-day-old animals.

Considering that it has been previously described glutamate-mediated actions of $(PhTe)_2$ in brain (Nogueira et al. 2001; Souza et al. 2010), in the present study, we used ionotropic and metabotropic glutamate antatogonists to investigate the involvement of this neurotransmitter in the cytoskeletal phosphorylation of IF proteins from cerebral cortex of young rats. Results showed that the NMDA receptor antatogonists DL-AP5 (100 μM) and MK801 (noncompetitive NMDA antagonist, 50 μM) prevented the

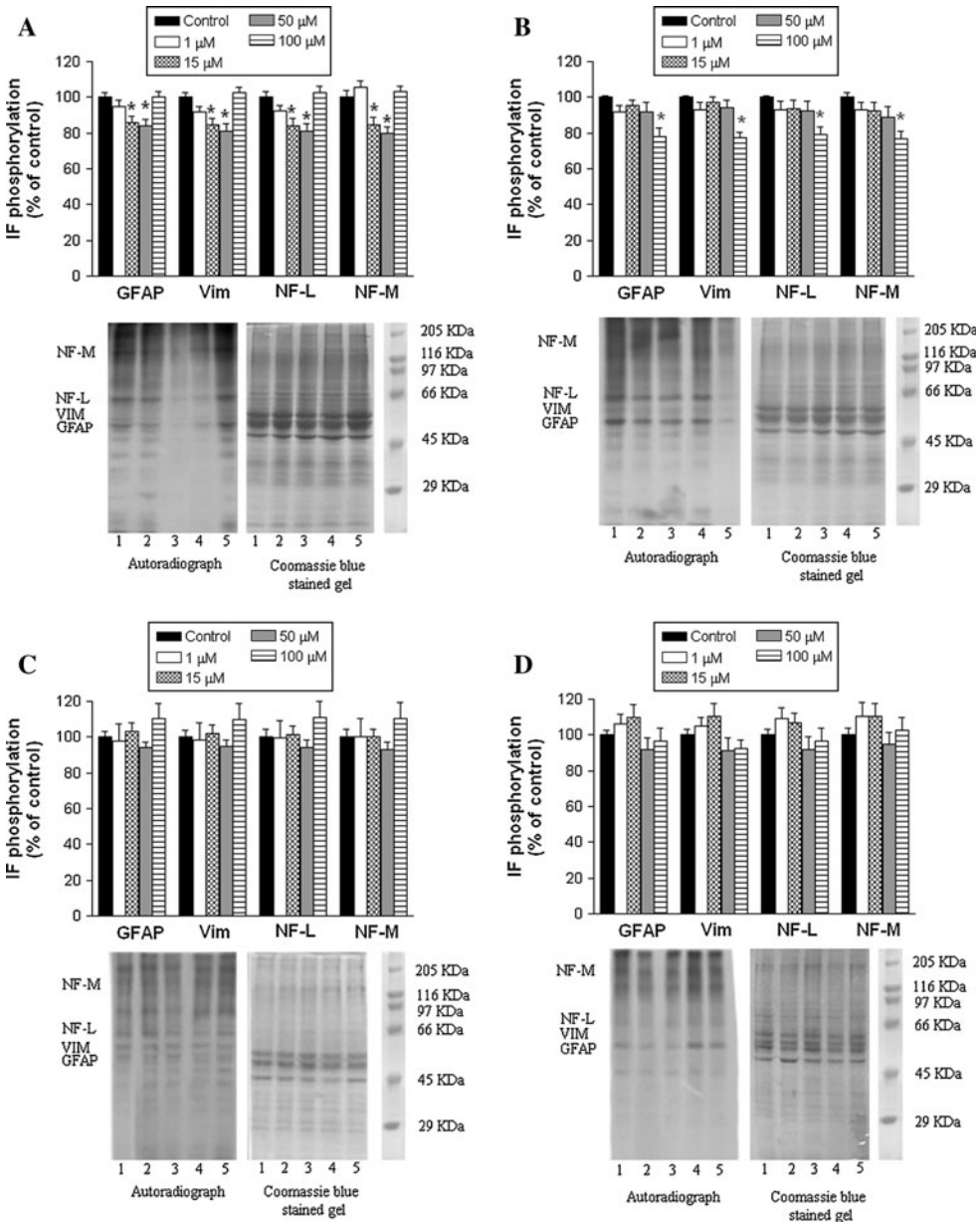

Fig. 1 Effect of different concentrations of $(PhTe)_2$ on IF phosphorylation in cerebral cortex (**a**, **b**) and hippocampus (**c**, **d**). Slices of cerebral cortex were incubated with ^{32}P-orthophosphate in the absence or presence of 1, 15, 50 and 100 μM $(PhTe)_2$, as described in "Materials and methods". The cytoskeletal fraction was extracted, and the radioactivity incorporated into GFAP, vimentin, NF-L and NF-M was measured. Representative stained gel and autoradiographs of the proteins studied are shown (*line 1* control, *line 2* 1 μM $(PhTe)_2$, *line 3* 15 μM $(PhTe)_2$, *line 4* 50 μM $(PhTe)_2$, *line 5* 100 μM $(PhTe)_2$). (**a**, **c**, 9-day-old rats; **b**, **d**, 15-day-old rats). Data are reported as mean ± SEM of 16 animals in each group and expressed as % of control. Statistically significant differences from controls, as determined by one-way ANOVA followed by Tukey–Kramer multiple comparison test are indicated: $*P < 0.05$

hypophosphorylation elicited by the neurotoxicant. Similarly, CNQX (100 μM) and DNQX (100 μM), both AMPA/kainate-specific antatogonists were effective in preventing this effect (Fig. 2a). In contrast, the metabotropic glutamate antagonist, MCPG (group I/II metabotropic glutamate receptor antagonist, 100 μM) did not prevent the action of $(PhTe)_2$ on the phosphorylating system associated with the IF proteins both in 9 (data not shown) and 15-day-old animals (Fig. 2b). Since Ca^{2+}-mediated mechanisms are frequently involved in the activity of the phosphorylating system modulating the cytoskeleton (Loureiro et al. 2008; Zamoner et al. 2008), we next investigated the participation of the L-VDCC and Ca^{2+} from intracellular stores on $(PhTe)_2$-induced hypophosphorylation of IF proteins. In this context, the two L-VDCC blockers used, verapamil (10 μM) and nifedipine (10 μM), prevented the hypophosphorylating effect, suggesting that Ca^{2+} influx via L-VDCC is involved in the ability of this neurotoxicant to induce IF hypophosphorylation. Similarly, dantrolene (50 μM), a ryanodine channel

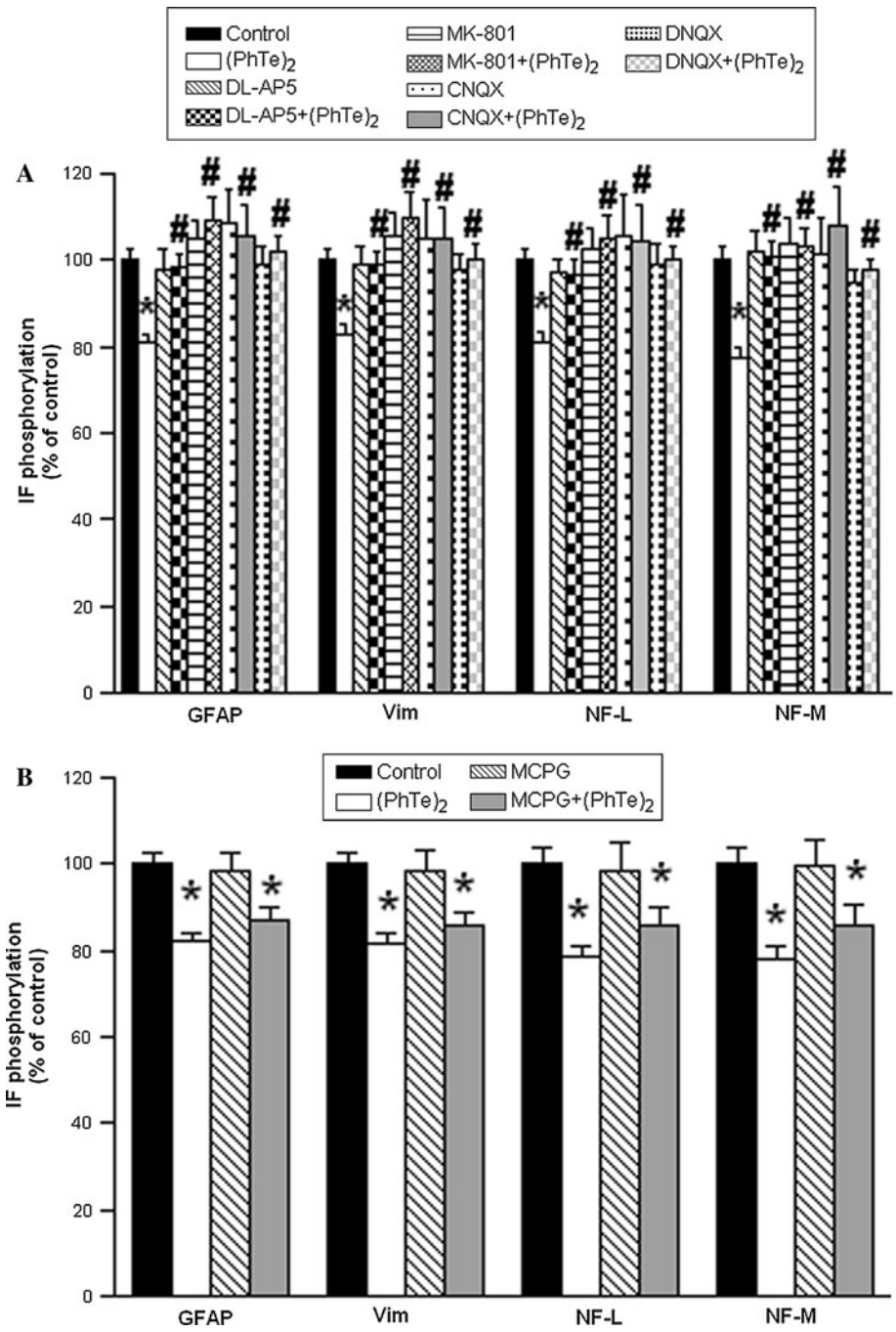

Fig. 2 Effect of the NMDA, AMPA, kainate and metabotropic glutamate receptor antagonists on $(PhTe)_2$-induced IF hypophosphorylation in cerebral cortex of 15-day-old. Slices were preincubated for 20 min in the presence or absence of 10 μM DL-AP5, or 50 μM MK-801 (NMDA antagonist), or 50 μM CNQX (nonNMDA antagonist), or 100 μM DNQX (kainate antagonist) (**a**); or 100 μM MCPG (metabotropic glutamate receptor antagonist) (**b**); as described in "Materials and methods". Preincubation was followed by incubation with ^{32}P orthophosphate in the presence or absence of the glutamate antagonists and 100 μM $(PhTe)_2$, as described in 2.5. The cytoskeletal fraction was extracted, and the radioactivity incorporated into NF-M, NF-L, vimentin (VIM) and GFAP was measured. Data are reported as means ± SEM of 15 animals in each group and expressed as % of control. Statistically significant differences as determined by one-way ANOVA followed by Tukey–Kramer multiple comparison test are indicated. $^{*}P < 0.05$ compared with control group; $^{\#}P < 0.05$ compared with $(PhTe)_2$ group

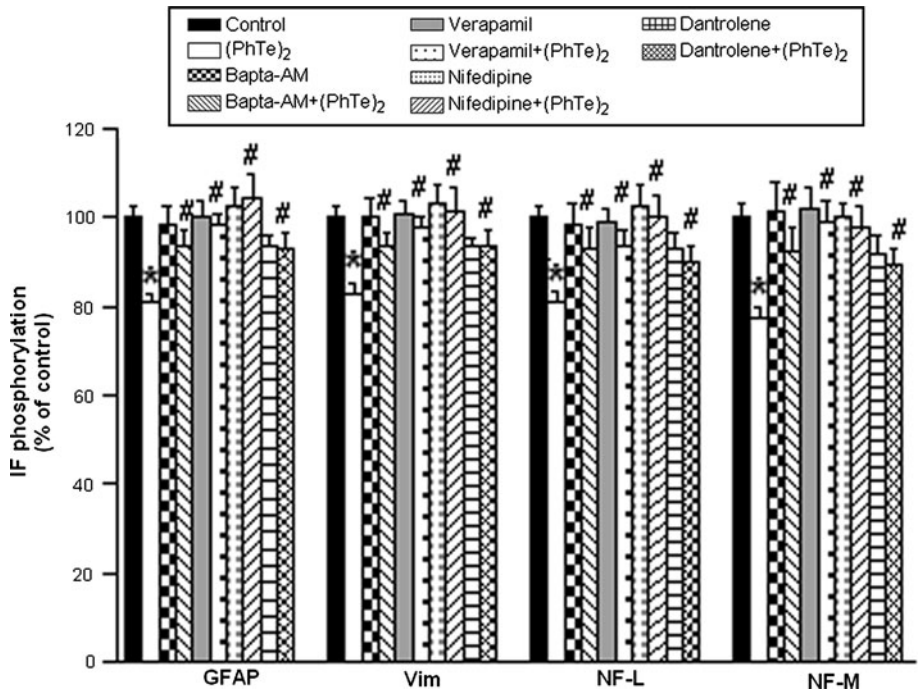

Fig. 3 Involvement of intracellular Ca^{2+} levels on $(PhTe)_2$ induced IF hypophosphorylation. Slices of cerebral cortex of 15-day-old rats were preincubated for 20 min in the presence or absence of 50 μM BAPTA-AM (intracellular Ca^{2+} chelator), 10 μM verapamil or nifedipine (L-type voltage-dependent Ca^{2+} channel blockers) or 50 μM dantrolene (ryanodine channel blocker). Preincubation was followed by incubation with ^{32}P orthophosphate in the presence or absence of the Ca^{2+} blockers and 100 μM $(PhTe)_2$, as described in "Materials and methods". The cytoskeletal fraction was extracted and the radioactivity incorporated into NF-M, NF-L, vimentin (VIM) and GFAP was measured. Data are reported as mean ± SEM of 15 animals in each group and expressed as % of control. Statistically significant differences as determined by one-way ANOVA followed by Tukey–Kramer multiple comparison test are indicated: $^{*}P < 0.05$ compared with control group; $^{\#}P < 0.05$ compared with $(PhTe)_2$ group

blocker impaired the hypophosphorylating effect of the neurotoxicant. The importance of increased cytosolic Ca^{2+} levels in eliciting this effect was reinforced with the data obtained using the intracellular Ca^{2+} chelator Bapta-AM (50 μM), which totally prevented the action of the neurotoxicant on the phosphorylating system, emphasizing the role of intracellular Ca^{2+} levels in such effect (Fig. 3).

Hypophosphorylation in response to a cellular signal is frequently associated with protein phosphatase activation and/or protein kinase inhibition. Therefore, we investigated the potential participation of the most frequent Ser–Thr phosphatases involved in the modulation of phosphorylating level of IF cytoskeletal proteins: protein phosphatase 1 (PP1), 2A (PP2A), and 2B (PP2B) (de Almeida et al. 2003; Funchal et al. 2005; de Mattos-Dutra et al. 1997) in the action of $(PhTe)_2$. In order to identify the protein phosphatases involved in such effect, we used specific protein phosphatase inhibitors. Therefore, results from calyculin A (0.2 μM) a potent PP1and PP2A inhibitor showed total reversion of the $(PhTe)_2$-induced hypophosphorylation. To further distinguish between PP1 and PP2A activities, Fostriecin (1 μM), a specific PP2A inhibitor, was used and results showed that this inhibitor was not able to prevent hypophosphorylation, suggesting, therefore, that the effect was mediated by PP1 rather than PP2A. In addition, FK506 (100 μM) and cyclosporine A (100 μM), specific PP2B inhibitors, were ineffective in preventing this effect (Fig. 4).

In order to better understand the molecular mechanisms underlying the hypophosphorylation of IF proteins by PP1, we examined the activity of the 32-kDa dopamine- and adenosine 3′,5′-monophosphate-regulated phosphoprotein (DARPP-32), an important endogenous regulator of PP1 activity. Depending on the site of phosphorylation, DARPP-32 is able to produce opposing biochemical effects, i.e., inhibition of PP1 activity or inhibition of protein kinase A (PKA) activity. Phosphorylation of DARPP-32 at Thr34 by PKA constitutes an important mechanism to activate DARPP-32 blocking PP1. Conversely, when pThr34DARPP-32 is dephosphorylated by PP2B, it is itself inhibited, promoting the release of PP1 activity. Moreover, phosphorylation of Thr75DARP-32 by Cdk-5 inhibits PKA, reinforcing the relase of PP1 activity (Håkansson et al. 2004).

Western blot assay using anti-pThr34DARPP-32 antibody showed that $(PhTe)_2$ decreased phosphorylation level at pThr34DARPP-32 and this effect was not prevented by FK506, suggesting that hypophosphorylation of

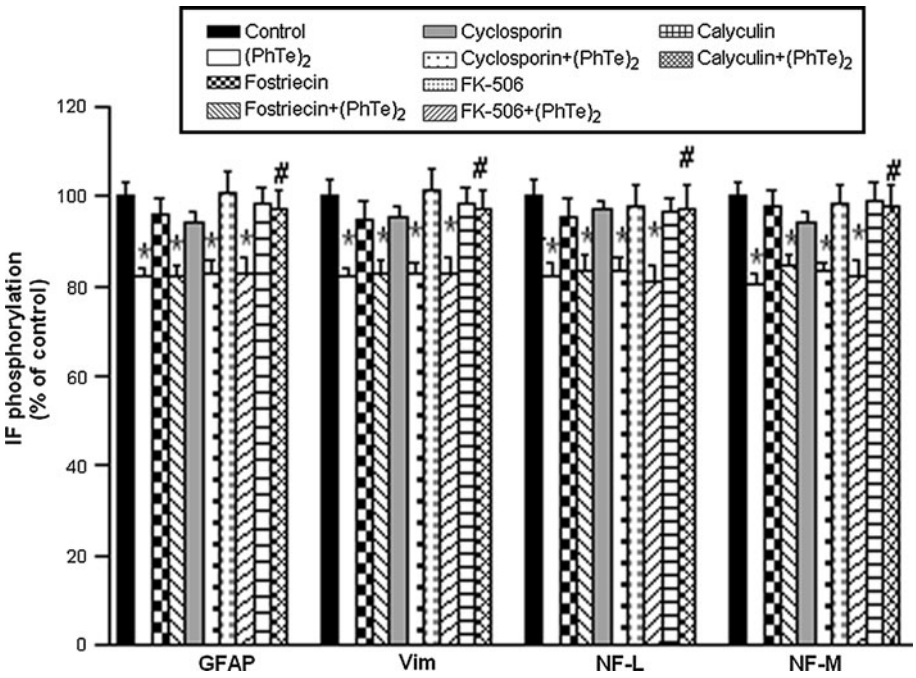

Fig. 4 Involvement of PP2A, PP2B and PP1 on IF hypophosphorylation induced by $(PhTe)_2$. Slices of cerebral cortex of 15-day-old rats were preincubated in the presence or absence of 100 μM FK-506 or 100 μM cyclosporine (PP2B inhibitors); 0.2 μM Calyculin A (PP1 and PP2A inhibitor) or 1 μM Fostriecin (PP2A inhibitor). Preincubation was followed by incubation with ^{32}P orthophosphate in the presence or absence of the phosphatase inhibitors and 100 μM $(PhTe)_2$, as described in "Materials and methods". The cytoskeletal fraction was extracted, and the radioactivity incorporated into NF-M, NF-L, vimentin (VIM) and GFAP was measured. Data are reported as mean ± SEM of 15 animals in each group and expressed as % of control. Statistically significant differences as determined by one-way ANOVA followed by Tukey–Kramer multiple comparison test are indicated: $^{*}P < 0.05$ compared with control group; $^{\#}P < 0.05$ compared with $(PhTe)_2$ group

Thr34DARPP-32 was not directly dependent on PP2B (Fig. 5a). Conversely, $(PhTe)_2$ elicited hyperphosphorylation of Thr75DARPP-32 (Fig. 5b), known to intensify the decreased levels of phosphoTh34DARPP-32, via inhibition of PKA (Bibb et al. 1999; Nishi et al. 2000).

Therefore, in order to demonstrate the involvement of the cAMP/PKA/DARPP-32 cascade in the $(PhTe)_2$-mediated regulation of the phosphorylating system associated with the cytoskeleton in young rats, we measured cAMP levels. Results showed that the neurotoxicant significantly decreased cAMP levels (Fig. 6a). Similarly, the Western blot analysis using the anti-PKAcα antibody showed reduced levels of PKAcα catalytic subunit in $(PhTe)_2$-treated tissue slices. Moreover, when the slices were treated with $(PhTe)_2$ in the presence of the intracellular Ca^{2+} chelator Bapta, at the concentration that prevented IF hypophosphorylation, the level of the PKA catalytic subunit was not decreased, remaining similar to controls (Fig. 6b).

Discussion

Previously, we have demonstrated that $(PhTe)_2$ can modulate the IF phosphorylation after in vivo or in vitro exposure (Heimfarth et al. 2008; Moretto et al. 2005). However, little is known about the system(s) and mechanism(s) which underlie the alterations caused by $(PhTe)_2$ on the phosphorylation of IF proteins.

In the present work, we show that 15–100 μM $(PhTe)_2$ induced hypophosphorylation of both neuronal (light and medium neurofilament subunits) and glial (vimentin and GFAP) IF cytoskeletal proteins in slices of cerebral cortex of 9- and 15-day-old rats. Moreover, the dose able to provoke hypophosphorylation in the 15-day-old rats was higher (100 μM) than those able to induce a similar effect in 9-day-old animals (15 and 50 μM). In this context, it is important to note that in the younger animals, hypophosphorylation was observed at intermediate, but not at high $(PhTe)_2$ concentrations. Although at present we are not able to establish the molecular basis underlying these differential susceptibilities, we could speculate that different intensities of signal elicit different signaling mechanisms, so that $(PhTe)_2$ at higher concentrations probably stimulate signaling pathways other than those targeted to the phosphorylating system associated with the cytoskeleton.

Similarly, our previously described data showed that $(PhTe)_2$ induces hyperphosphorylation rather than hypophosphorylation in 17-day-old rats (Moretto et al. 2005).

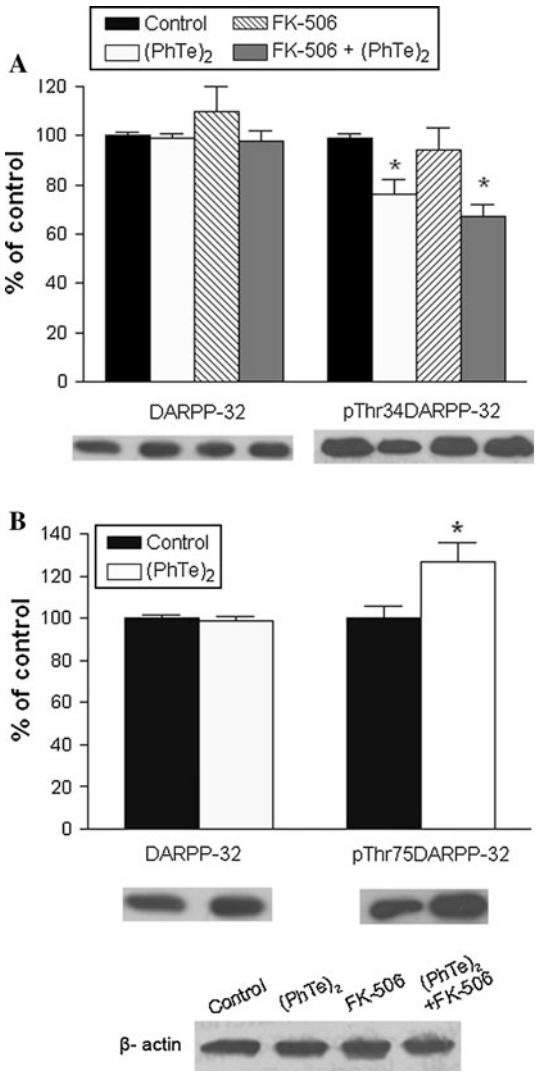

Fig. 5 Effect of $(PhTe)_2$ on DARPP-32 phosphorylation on Thr-34 (**a**) and Thr-75 (**b**) in cerebral cortex of 15-day-old rats. **a** Slices of cerebral cortex were incubated in the presence or absence of 100 μM FK-506 (PP2b inhibitor) and/or $(PhTe)_2$ as described in "Materials and methods". Tissue was lysed and prepared to Western blot analysis. The total and phospho levels of Thr34DARPP-32 were measured. **b** Slices of cerebral cortex were incubated in the presence or absence of $(PhTe)_2$ as described in "Materials and methods". Tissue was lysed and prepared to Western blot analysis. The total and phospho levels of Thr75DARPP-32 were measured. Western blot of β-actin was used as loading control. Data are reported as mean ± SEM of 8 animals in each group and expressed as % of control. Statistically significant differences as determined by one-way ANOVA followed by Tukey–Kramer are indicated: $^{*}P < 0.05$ compared with control group; $^{\#}P < 0.05$ compared with $(PhTe)_2$ group

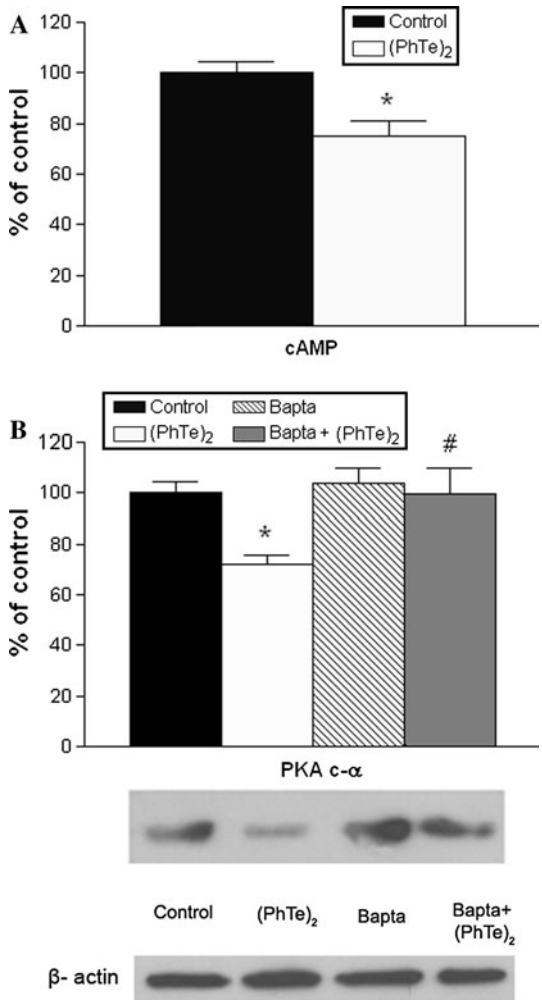

Fig. 6 Effect of $(PhTe)_2$ on cAMP levels and in total imunocontent of PKA C-α in cerebral cortex of 15-day-old rats. The levels of cAMP (**a**) and PKA c-α (**b**) were measured as described in "Materials and methods" representative Western blot of the proteins studied are shown (**b**). Western blot of β-actin was used as loading control. Data are reported as mean ± SEM of 8 animals in each group and expressed as % of control. Statistically significant differences as determined by one-way ANOVA followed by Tukey–Kramer are indicated: $^{*}P < 0.05$ compared with control group; $^{\#}P < 0.05$ compared with $(PhTe)_2$ group

These findings provide an interesting insight into the differential susceptibility of cortical IF cytoskeleton to the in vitro exposure to this neurotoxicant and could reflect the existence of different vulnerabilities of the cytoskeleton of cortical cells during development based on the temporal maturation mediated through a multitude of developmental processes and signaling pathways (Rice and Barone 2000). Moreover, our present findings are in agreement with previous results from our group demonstrating that α-keto-isocaproic acid affects the in vitro ^{32}P incorporation into the IF proteins from cerebral cortex of young rats inducing hypophosphorylation in 9- and 12-day-old rats and hyperphosphorylation in 17-day-old animals (Funchal et al. 2002).

The effects observed in the present work on the phosphorylating system were about 20%, which is close to the maximal changes we have been observing in the last decade with different in vitro and in vivo systems of neurotoxicity (de Mattos-Dutra et al. 1997; Funchal et al. 2002,

2005; de Almeida et al. 2003; Moretto et al. 2005; Heimfarth et al. 2008; Zamoner et al. 2008; Loureiro et al. 2008, 2010; Pierozan et al. 2010). However, the impact of these changes can be of neurotoxicological significance. Importantly, we have observed that in vivo exposure of young rats can cause lasting changes on brain phosphorylating system determined ex vivo (Heimfarth et al. 2008; Pierozan et al. 2010). Consequently, we can suppose that in vitro changes on the cerebral phosphorylating system of this magnitude can be a predictor of the potencial in vivo neurotoxicity of diphenyl ditelluride. Although the focus of our study is on the actions of $(PhTe)_2$ on the IF-associated phosphorylating system, it is noteworthy that IFs are not the only targets of serine/threonine kinases and phosphatases, so a signal able to disrupt the homeostasis of the IF subunits can also alter the phosphorylation level of a wide range of phosphoproteins present in the cytoskeletal fraction and elsewhere.

The present work also shows that the phosphorylating system associated with the cytoskeleton of hippocampus neural cells was not responsive to the concentrations of $(PhTe)_2$ used. Although we do not know the reasons underlying this different susceptibilities, they are probably related to the differential physiological responses of cortical and hippocampus neurons and astrocytes to the insult.

The action of the neurotoxicant in cortical cells was dependent on ionotropic glutamate receptors NMDA, AMPA, and kainate, but was independent on metabotropic receptors. These results support previous evidence that $(PhTe)_2$ can inhibit glutamate uptake by cortical brain slices in vitro (Moretto et al. 2007a) and can alter glutamate metabolism in brain (Nogueira et al. 2001; Souza et al. 2010) in age- and concentration-dependent manner. In this context, Souza et al. (2010) have described that sensitivity of the glutamatergic system to $(PhTe)_2$ decreased with aging of the suckling rats. Therefore, taking into account that the actions of $(PhTe)_2$ on the cytoskeleton are also dependent on the glutamatergic system, these could explain the developmentally increased resistance of the phosphorylating system to the action of the neurotoxicant.

Considering that we have previously described increased $^{45}Ca^{2+}$ uptake into synaptosomes provoked by $(PhTe)_2$ (Moretto et al. 2007b), we have chosen to study the involvement of Ca^{2+}-mediated mechanisms on the effects of $(PhTe)_2$ on the IF cytoskeleton of cortical cells. In this context, verapamil and nifedipine, specific L-VDCC blockers, (Rinker et al. 2010) as well as intracellular Ca^{2+} chelation by Bapta-AM totally prevented the effect of $(PhTe)_2$ on IF phosphorylation. Similarly, dantrolene-induced inhibition of Ca^{2+} release from the endoplasmic reticulum through ryanodine receptors also prevented this effect. It is interesting to note that besides Ca^{2+}, the Na^+ influx through AMPA receptors seems to play a role in the signaling cascade targeting the cytoskeleton, although the molecular mechanisms involved in these actions need further investigation.

Evidence in the literature points to a reciprocal regulation of ionic channel, receptor activities, and cytoskeleton equilibrium through phosphorylation/dephosphorylation mechanisms. Ryanodine receptors are regulated by PKA-mediated phosphorylation and PP1-/PP2A-mediated dephosphorylation (Marx et al. 2000). In addition, PP1 has been linked to the regulation of NMDA and AMPA receptors (Feng et al. 2000), otherwise NMDA receptors physiologically modulate the phosphorylation level of NF-M (Fiumelli et al. 2008). Therefore, we could propose that $(PhTe)_2$-activated PP1/inactivated PKA could modulate the receptor-mediated Ca^{2+} conductance.

IF hypophosphorylation is in agreement with previous evidence showing that protein phosphatases are highly concentrated in the mammalian brain (Strack et al. 1997a, b; Yoshimura et al. 1999) and pointing the cytoskeleton as a preferential target of the action of phosphatases both in physiological and pathological conditions (Liu et al. 2008; Saito et al. 1995). In this context, increased levels of astrocyte PP2A and PP2B were identified in Alzheimer's disease cerebral cortex and were considered as part of the astrogliosis seen in this disorder (Pei et al. 1997). Also, patients with Charcot-Marie-Tooth disease type 1 (CMT1) present NF hypophosphorylation (Watson et al. 1994).

In order to characterize the protein phosphatase activities responsible for the hypophosphorylating effect of $(PhTe)_2$ on neural and glial IF proteins, we used different phosphatase inhibitors, and we concluded that hypophosphorylation was mediated by PP1 in both 9- and 15-day-old rats. PP1 is a major eukaryotic protein serine/threonine phosphatase that regulates an enormous variety of cellular functions through the interaction of its catalytic subunit (PP1c) with over fifty different established or putative regulatory subunits. Regulation of PP1c in response to extra and intracellular signals occurs mostly through changes in the levels, conformation or phosphorylation status of targeting subunits (Cohen 2002). In addition, a critical integrative role is played by DARPP-32 (PP1 Inhibitor 1B), which is an isoform of the Inhibitor 1 typically expressed in brain (Cohen 2002).

DARPP-32 has the unique property of being a dual-function protein, acting as an inhibitor of either PP1 or PKA. In this context, it becomes a potent inhibitor of PP1 when phosphorylated at Thr34 by PKA (D'Addario et al. 2007; Viggiano et al. 2003). Otherwise, dephosphorylation of Thr34 mediated by PP2B, upon activation of the Ca^{2+} pathway, releases PP1 inhibition (Fernandez et al. 2006). In addition, the concomitant increase in Thr75 phosphorylation by Cdk5 would convert DARPP-32 into an inhibitor of

PKA, further reducing phosphorylation of target proteins. The DARPP-32/PP1 pathway integrates information from a variety of inputs and produces a coordinated response involving numerous downstream physiological effectors (Souza et al. 2006; Svenningsson et al. 2004).

Our results show that $(PhTe)_2$ induced PP1-mediated IF hypophosphorylation by regulating DARPP-32 activity. PP1 release was a consequence of Thr34 dephosphorylation, and this action was mediated by inhibition of PKA- rather than PP2B-mediated mechanisms. In this signaling cascade, Ca^{2+} influx through L-VDCC and ionotropic glutamate receptors would inhibit the cAMP/PKA pathway which is central in maintaining nonphosphorylated Thr34DARPP-32, inactivating this PP1 inhibitor. A question to be clarified concerns the mechanism by which Ca^{2+} would inhibit cAMP synthesis; however, it is known that all adenylyl cyclase (AC) activities are inhibited by high, nonphysiological concentrations of Ca^{2+} in the submillimolar range (Defer et al. 2000). This appears to be a special feature of the two closely related cyclase isoforms, AC5 and AC6, (Cooper et al. 1994, 1998; Mons and Cooper 1994). Whether Ca^{2+} modulates AC5 and AC6 activities directly or via a Ca^{2+}-binding protein remains to be determined. Therefore, taking together our experimental evidence, a proposed signaling pathway of $(PhTe)_2$ eliciting PP1-mediated hypophosphorylation of IF cytoskeletal proteins is depicted in Fig. 7. In this mechanism, $(PhTe)_2$ would induce cdk5-mediated hyperphosphorylation of Thr75DARPP-32 leading to PKA inhibition. Ca^{2+} influx through L-VDCC and ionotropic glutamate receptors would further inhibit the cAMP/PKA pathway. Decreased PKA activity is central in maintaining nonphosphorylated Thr34DARPP-32, therefore releasing the PP1-mediated hypophosphorylation of downstream IF proteins.

IF proteins are known to be phosphorylated on their head and tail domains, and the dynamics of their phosphorylation/dephosphorylation plays a major role in regulating the structural organization and function of IFs in a cell- and tissue-specific manner (Helfand et al. 2004; Nixon and Sihag 1991; Omary et al. 2006). On the other hand, appropriate phosphorylation of NF subunits appears to be correlated to synaptogenesis and myelination, as the mature axonal cytoskeleton begins to be established (Grant et al. 2001). Also, it has been suggested that regulation of phosphorylation of specific sites on the tail domain on NF-H and NF-M might play a role in NF spacing and thus

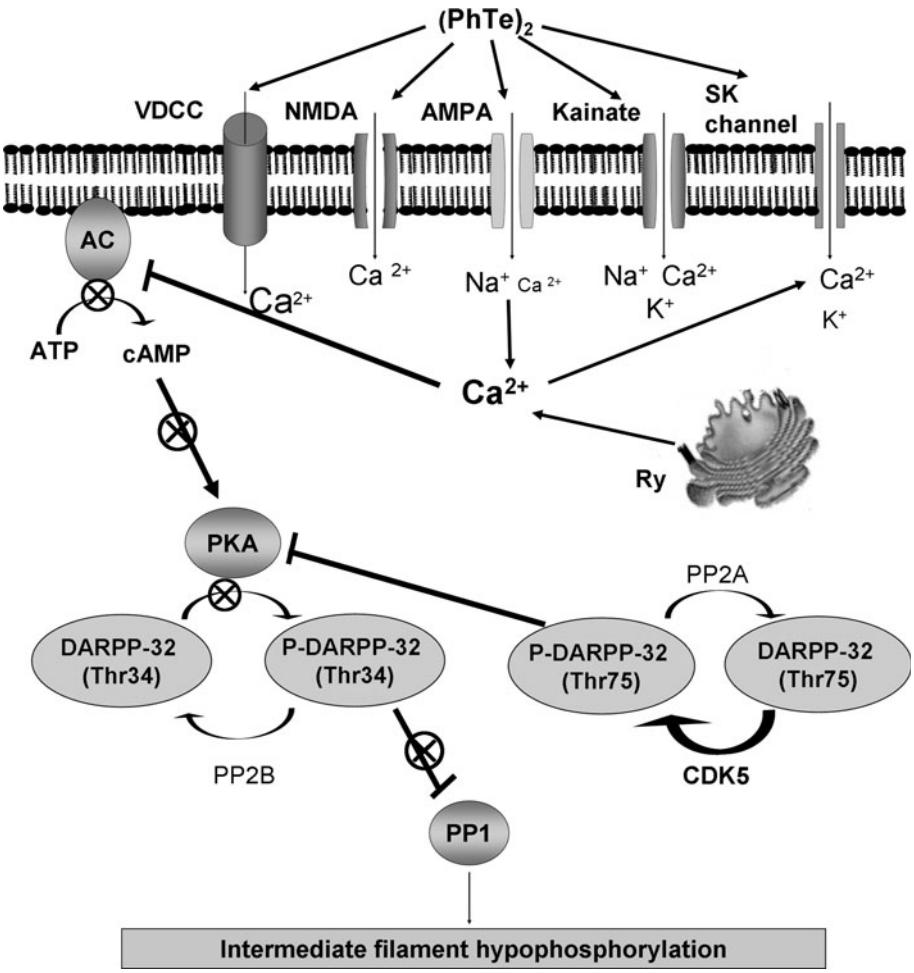

Fig. 7 Proposed mechanism of $(PhTe)_2$ induced IF hypophosphorylation in cerebral cortex of 9- and 15-day-old rats. $(PhTe)_2$ induces cdk5-mediated hyperphosphorylation of Thr75DARPP-32 leading to PKA inhibition. Ca^{2+} influx through L-VDCC and ionotropic glutamate receptors would further inhibit the cAMP/PKA pathway. Decreased PKA activity is central in maintaining nonphosphorylated Thr34DARPP-32, therefore releasing the PP1-mediated hypophosphorylation of downstream IF proteins

the axon caliber (Fuchs and Cleveland 1998; Inagaki et al. 1996; Lee et al. 1987).

We conclude that in vitro exposure to $(PhTe)_2$ induces PP1-mediated hypophosphorylation of neuronal and glial IF proteins in cerebral cortex of young rats. We presume that the action of $(PhTe)_2$ is upstream increased Ca^{2+} influx and may involve dysregulation of the cAMP signaling cascade by changes in the state of phosphorylation of DARPP-32, inhibiting PKA and releasing PP1 activity.

It must be emphasized that misregulation of the IF-associated phosphorylation system is assumed to have an important role in neurodegeneration. Thus, cytoskeleton may represent a target in $(PhTe)_2$ neurotoxicity, and cytoskeletal dysfunction might underlie the deleterious action of $(PhTe)_2$ on the brain, a fact that might explain at least in part the neurotoxicity of this compound.

Acknowledgments This work was supported by Conselho Nacional de Desenvolvimento Científico e Tecnológico (CNPq), FINEP research grant "Rede Instituto Brasileiro de Neurociência" (IBN-Net) #01.06.0842-00, Fundação de Amparo à Pesquisa do Estado do Rio Grande do Sul (FAPERGS), PRONEX and Propesq-UFRGS.

References

Arbustini E, Pasotti M, Pilotto A, Pellegrini C, Grasso M, Previtali S, Repetto A, Bellini O, Azan G, Scaffino M, Campana C, Piccolo G, Vigano M, Tavazzi L (2006) Desmin accumulation restrictive cardiomyopathy and atrioventricular block associated with desmin gene defects. Eur J Heart Fail 8:477–483

Avila DS, Colle D, Gubert P, Palma AS, Puntel G, Manarin F, Noremberg S, Nascimento PC, Aschner M, Rocha JB, Soares FA (2010) A possible neuroprotective action of a vinylic telluride against Mn-induced neurotoxicity. Toxicol Sci 115:194–201

Baba A, Lee E, Tatsuno T, Iwata H (1982) Cysteine sulfinic acid in the central nervous system: antagonistic effect of taurine on cysteine sulfinic acid-stimulated formation of cyclic AMP in guinea pig hippocampal slices. J Neurochem 38:1280–1285

Barbosa NBV, Rocha JBT, Zeni G, Emanuelli T, Beque MC, Braga AL (1998) Effect of organic forms of selenium on delta-aminolevulinate dehydratase from liver, kidney and brain of adult rats. Toxicol Appl Pharmacol 149:243–253

Bibb J, Snyder GL, Nishi A, Yan Z, Meijer L, Fienberg AA, Tsai L-H, Kwon YT, Girault J-A, Czernik AJ, Huganir RL, Hemmings HC, Nairn AC, Greengard P (1999) Phosphorylation of DARPP-32 by Cdk5 modulates dopamine signalling in neurons. Nature 402:669–671

Borges VC, Rocha JBT, Nogueira CW (2005) Effect of diphenyl diselenide, diphenyl ditelluride and ebselen on cerebral Na+, K+ ATPase activity in rats. Toxicology 215:191–197

Brito VB, Rocha JB, Folmer V, Erthal F (2009) Diphenyl diselenide and diphenyl ditelluride increase the latency for 4-aminopyridine-induced chemical seizure and prevent death in mice. Acta Biochim Pol 56:125–134

Cohen PTW (2002) Protein phosphatase 1-targeted in many directions. J Cell Sci 115:241–256

Cooper DM, Mons N, Fagan K (1994) Ca21-sensitive adenylyl cyclases. Cell Signal 6:823–840

Cooper DM, Karpen JW, Fagan KA, Mons NE (1998) Ca(21)-sensitive adenylyl cyclases. Adv Second Messenger Phosphoprot Res 32:23–51

Cunha LOR, Urano ME, Chagas JR, Almeida PC, Bincoletto C, Tersariol ILS, Comasseto JV (2005) Tellurium-based cysteine protease inhibitors: evaluation of novel organotellurium (IV) compounds as inhibitors of human Cathepsin B. Bioorg Med Chem Lett 15:755–760

D'Addario C, Di Benedetto M, Candeletti S, Romualdi P (2007) The kappa-opioid receptor agonist U-69593 prevents cocaine-induced phosphorylation of DARPP-32 at Thr(34) in the rat brain. Brain Res Bull 73:34–39

de Almeida LM, Funchal C, Pelaez PL, Pessutto FD, Loureiro SO, Vivian L, Wajner M, Pessoa-Pureur R (2003) Effect of propionic and methylmalonic acids on the in vitro phosphorylation of intermediate filaments from cerebral cortex of rats during development. Metab Brain Dis 18:207–219

de Avila DS, Beque MC, Folmer V, Braga AL, Zeni G, Nogueira CW, Soares FA, Rocha JB (2006) Diethyl 2-phenyl-2 tellurophenyl vinylphosphonate: an organotellurium compound with low toxicity. Toxicology 224:100–107

de Mattos-Dutra A, Sampaio de Freitas M, Schröder N, Fogaça Lisboa CS, Pessoa-Pureur R, Wajner M (1997) In vitro phosphorylation of cytoskeletal proteins in the rat cerebral cortex is decreased by propionic acid. Exp Neurol 147:238–247

Defer N, Best-Belpomme M, Hanoune J (2000) Tissue specificity and physiological relevance of various isoforms of adenylyl cyclase. Am J Physiol Renal Physiol 279:F400–F416

Farina M, Barbosa NB, Nogueira CW, Folmer V, Zeni G, Andrade LH, Braga AL, Rocha JBT (2002) Reaction of diphenyl diselenide with hydrogen peroxide and inhibition of delta-aminolevulinate dehydratase from rat liver and cucumber leaves. Braz J Med Biol Res 35:623–631

Feng J, Yan Z, Ferreira A, Tomizawa K, Liauw JA, Zhuo M, Allen PB, Ouimet CC, Greengard P (2000) Spinophilin regulates the formation and function of dendritic spines. Proc Natl Acad Sci USA 97:9287–9292

Fernandez E, Schiappa R, Girault JA, Le Novère N (2006) DARPP-32 is a robust integrator of dopamine and glutamate signals. PLoS Comput Biol 2:e176

Fiumelli H, Riederer IM, Martin JL, Riederer BM (2008) Phosphorylation of neurofilament subunit NF-M is regulated by activation of NMDA receptors and modulates cytoskeleton stability and neuronal shape. Cell Motil Cytoskel 65:495–504

Fuchs E, Cleveland DW (1998) A structural scaffolding of intermediate filaments in health and disease. Science 279:514–519

Funchal C, de Lima Pelaez P, Loureiro SO, Vivian L, Dall Bello Pessutto F, de Almeida LM, Tchernin Wofchuk S, Wajner M, Pessoa Pureur R (2002) α-Ketoisocaproic acid regulates phosphorylation of intermediate filaments in postnatal rat cortical slices through ionotropic glutamatergic receptors. Brain Res Dev Brain Res 139:267–276

Funchal C, de Almeida LM, Oliveira Loureiro S, Vivian L, de Lima Pelaez P, Dall Bello Pessutto F, Rosa AM, Wajner M, Pessoa-Pureur R (2003) In vitro phosphorylation of cytoskeletal proteins from cerebral cortex of rats. Brain Res Prot 11:111–118

Funchal C, Zamoner A, dos Santos AQ, Moretto MB, Rocha JB, Wajner M, Pessoa-Pureur R (2005) Evidence that intracellular Ca2+ mediates the effect of alpha-ketoisocaproic acid on the phosphorylating system of cytoskeletal proteins from cerebral cortex of immature rats. J Neurol Sci 238:75–82

Giles GI, Fry FH, Tasker KM, Holme AL, Peers C, Green KN, Klotz LO, Sies H, Jacob C (2003) Evaluation of sulfur, selenium and tellurium catalysts with antioxidant potential. Org Biomol Chem 1:4317–4322

Gou JP, Gotow T, Janmey PA, Leterrier JF (1998) Regulation of neurofilament interactions in vitro by natural and synthetic polypeptides sharing Lys-Ser-Pro sequences with the heavy neurofilament subunit NF-H: neurofilament crossbridging by antiparallel sidearm overlapping. Med Biol Eng Comput 36:371–387

Grant P, Pant HC (2000) Neurofilament protein synthesis and phosphorylation. J Neurocytol 29:843–872

Grant P, Sharma P, Pant HC (2001) Cyclin-dependent protein kinase 5 (Cdk5) and the regulation of neurofilament metabolism. Eur J Biochem 268:1534–1546

Green SL, Westendorf JM, Jaffe H, Pant HC, Cork LC, Ostrander EA, Vignaux F, Ferrell JE Jr (2005) Allelic variants of the canine heavy neurofilament (NFH) subunit and extensive phosphorylation in dogs with motor neuron disease. J Comp Pathol 132:33–50

Håkansson K, Lindskog M, Pozzi L, Usiello A, Fisone G (2004) DARPP-32 and modulation of cAMP signaling: involvement in motor control and levodopa-induced dyskinesia. Parkinsonism Relat Disord 10:281–286

Hassan W, Ibrahim M, Nogueira CW, Braga AL, Deobald AM, Mohammadzai IU, Rocha JB (2009) Influence of pH on the reactivity of diphenyl ditelluride with thiols and anti-oxidant potential in rat brain. Chem Biol Interact 180:47–53

Heimfarth L, Oliveira Loureiro S, Zamoner A, de Lima Pelaez P, Nogueira CW, Rocha JBT, Pessoa-Pureur R (2008) Effects of in vivo treatment with diphenyl ditelluride on the phosphorylation of cytoskeletal proteins in cerebral cortex and hippocampus of rats. Neurotoxicology 29:40–47

Helfand BT, Chang L, Goldman RD (2004) Intermediate filaments are dynamic and motile elements of cellular architecture. J Cell Sci 117:133–141

Herrmann H, Aebi U (2004) Intermediate filaments: molecular structure, assembly mechanism, and integration into functionally distinct intracellular scaffolds. Annu Rev Biochem 73:749–789

Herrmann H, Hesse M, Reichenzeller M, Aebi U (2003) Functional complexity of intermediate filament cytoskeletons: from structure to assembly to gene ablation. Int Rev Cytol 223:83–175

Inagaki M, Matsuoka Y, Tsujimura K, Ando S, Tokui T, Takahashi T, Inagaki N (1996) Dynamic property of intermediate filaments: regulation by phosphorylation. Bioessays 18:481–487

Kanski J, Drake J, Aksenova M, Engman L, Butterfield DA (2001) Antioxidant activity of the organotellurium compound 3-[4-(N, N-dimethylamino)benzenetellurenyl]propanesulfonic acid against oxidative stress in synaptosomal membrane systems and neuronal cultures. Brain Res 911:12–21

Laden BP, Porter TD (2001) Inhibition oh human squalene monooxigenase by tellurium compounds: evidence of interaction with vicinal sulfhydryls. J Lipid Res 42:235–240

Laemmli UK (1970) Cleavage of structural proteins during the assembly of the head of bacteriophage T4. Nature 277:680–685

Lariviere RC, Julien JP (2004) Functions of intermediate filaments in neuronal development and disease. J Neurobiol 58:131–148

Larner AJ (1995) How does garlic exert its hypocholesterolaemic action? The tellurium hypothesis. Med Hypotheses 44:295–297

Lee VM, Carden MJ, Schlaepfer WW, Trojanowski JQ (1987) Monoclonal antibodies distinguish several differentially phosphorylated states of the two largest rat neurofilament subunits (NF-H and NF-M) and demonstrate their existence in the normal nervous system of adult rats. J Neurosci 7:3474–3488

Liu R, Zhou XW, Tanila H, Bjorkdahl C, Wang JZ, Guan ZZ, Cao Y, Gustafsson JA, Winblad B, Pei JJ (2008) Phosphorylated PP2A (tyrosine 307) is associated with Alzheimer neurofibrillary pathology. J Cell Mol Med 12:241–257

Loureiro SO, Heimfarth L, de Lima Pelaez P, Simioni Vanzin C, Viana L, Wyse ATS, Pessoa-Pureur R (2008) Homocysteine activates calcium-mediated cell signaling mechanisms targeting the cytoskeleton in rat hippocampus. Int J Dev Neurosci 26:447–455

Loureiro SO, Heimfarth L, Lacerda BA, Vidal LF, Soska A, dos Santos NG, de Souza Wyse AT, Pessoa-Pureur R (2010) Homocysteine induces hypophosphorylation of intermediate filaments and reorganization of actin cytoskeleton in C6 glioma cells. Cell Mol Neurobiol 30:557–568

Lowry OH, Rosebrough NJ, Farr AL, Randall RJ (1951) Protein measurement with the Folin phenol reagent. J Biol Chem 193:265–275

Marx SO, Reiken S, Hisamatsu Y, Jayaraman T, Burkhoff D, Rosemblit N, Marks AR (2000) PKA phosphorylation dissociates FKBP12.6 from the calcium release channel (ryanodine receptor): defective regulation in failing hearts. Cell 101:365–376

Mons N, Cooper DM (1994) Adenylyl cyclase mRNA expression does not reflect the predominant Ca21/calmodulin-stimulated activity in the hypothalamus. J Neuroendocrinol 6:665–671

Moretto MB, Funchal C, Zeni G, Rocha JBT, Pessoa-Pureur R (2005) Organoselenium compounds prevent hyperphosphorylation of cytoskeletal proteins induced by the neurotoxic agent diphenyl ditelluride in cerebral córtex of young rats. Toxicology 210:213–222

Moretto MB, Thomazi AP, Godinho G, Roessler TM, Nogueira CW, Souza DO, Wofchuk S, Rocha JB (2007a) Ebselen and diorganylchalcogenides decrease in vitro glutamate uptake by rat brain slices: prevention by DTT and GSH. Toxicol In Vitro 21:639–645

Moretto MB, Boff B, Franco J, Posser T, Roessler TM, Souza DO, Nogueira CW, Wofchuk S, Rocha JB (2007b) (45)Ca(2+) influx in rat brain: effect of diorganylchalcogenides compounds. Toxicol Sci 99:566–571

Motil J, Chan WK, Dubey M, Chaudhury P, Pimenta A, Chylinski TM, Ortiz DT, Shea TB (2006) Dynein mediates retrograde neurofilament transport within axonal neurites and anterograde delivery of NFs from perikarya into axons: regulation by multiple phosphorylation events. Cell Motil Cytoskel 63:266–286

Nishi A, Bibb JA, Snyder GL, Higashi H, Nairn AC, Greengard P (2000) Amplification of dopaminergic signaling by a positive feedback loop. Proc Natl Acad Sci USA 97:12840–12845

Nixon RA (1993) The regulation of neurofilament protein dynamics by phosphorylation: clues to neurofibrillary pathology. Brain Pathol 3:29–38

Nixon RA, Sihag RK (1991) Neurofilament phosphorylation: a new look at regulation and function. Trends Neurosci 14:501–506

Nogueira CW, Rotta LN, Perry ML, Souza DO, da Rocha JB (2001) Diphenyl diselenide and diphenyl ditelluride affect the rat glutamatergic system in vitro and in vivo. Brain Res 906:157–163

Nogueira CW, Borges VC, Zeni G, Rocha JBT (2003) Organochalcogens effects on ð-aminolevilinate dehydratase activity from human erythrocytic cells in vitro. Toxicology 191:169–178

Nogueira CW, Zeni G, Rocha JBT (2004) Organoselenium and organotellurium compounds: toxicology and pharmacology. Chem Rev 104:6255–6285

Omary MB, Ku NO, Tao GZ, Toivola DM, Liao J (2006) Heads and tails of intermediate filament phosphorylation: multiple sites and functional insights. Trends Biochem Sci 31:383–394

Pei JJ, Grundke-Iqbal I, Iqbal K, Bogdanovic N, Winblad B, Cowburn RF (1997) Elevated protein levels of protein phosphatases PP-2A and PP-2B in astrocytes of Alzheimer's disease temporal cortex. J Neural Transm 104:1329–1338

Pessoa-Pureur R, Wajner M (2007) Cytoskeleton as a potential target in the neuropathology of maple syrup urine disease: insight from animal studies. J Inher Metab Dis 30:664–672

Petragnani N (1994) Preparation of the principal classes of organic tellurium compounds. In: Katritzky AR, Meth-Cohn O, Rees CW (eds) Tellurium in organic synthesis. Academic Press, London, pp 9–88

Pierozan P, Zamoner A, Soska Â, Silvestrin R, Loureiro SO, Heimfarth L, Souza T, Wajner M, Pessoa-Pureur R (2010) Acute intrastriatal administration of quinolinic acid provokes hyperphosphorylation of cytoskeletal intermediate filament proteins in astrocytes and neurons of rats. Exp Neurol 224:188–196

Rice D, Barone S Jr (2000) Critical periods of vulnerability for the developing nervous system: evidence from humans and animal models. Environ Health Perspect 108:511–533

Rinker B, Fink BF, Barry NG, Fife JA, Milan ME (2010) The effect of calcium channel blockers on smoking-induced skin flap necrosis. Plast Reconstr Surg 125:866–871

Saito T, Shima H, Osawa Y, Nagao M, Hemmings BA, Kishimoto T, Hisanaga S (1995) Neurofilament-associated protein phosphatase 2A: its possible role in preserving neurofilaments in filamentous states. Biochemistry 34:7376–7384

Schroeder HA, Buckman J, Balassa JJ (1967) Abnormal trace elements in man: tellurium. J Chronic Dis 20:147–161

Shimi T, Butin-Israeli V, Adam SA, Goldman RD (2010) Nuclear lamins in cell regulation and disease. Cold Spring Harb Symp Quant Biol 75:525–531

Sihag RK, Inagaki M, Yamaguchi T, Shea TB, Pant HC (2007) Role of phosphorylation on the structural dynamics and function of types III and IV intermediate filaments. Exp Cell Res 313:2098–2109

Souza RP, Rosa DV, Souza BR, Romano-Silva MA (2006) DARPP-32. AFCS Signal. Gateway. doi:10.1038/mp.a000752.01

Souza AC, Stangherlin EC, Ardais AP, Nogueira CW (2010) Diphenyl diselenide and diphenyl ditelluride: neurotoxic effect in brain of young rats, in vitro. Mol Cell Biochem 340:179–185

Stangherlin EC, Favero AM, Zeni G, Rocha JBT, Nogueira CW (2005) Teratogenic vulnerability of Wistar rats to diphenyl ditelluride. Toxicology 207:231–239

Strack S, Barban MA, Wadzinski BE, Colbran RJ (1997a) Differential inactivation of postsynaptic density-associated and soluble Ca2+/calmodulin-dependent protein kinase II by protein phosphatases 1 and 2A. J Neurochem 68:2119–2128

Strack S, Westphal RS, Colbran RJ, Ebner FF, Wadzinski BE (1997b) Protein serine/threonine phosphatase 1 and 2A associate with and dephosphorylate neurofilaments. Brain Res Mol Brain Res 49:15–28

Svenningsson P, Nishi A, Fisone G, Girault J-A, Nairn AC, Greengard P (2004) DARPP-32: an integrator of neurotransmission. Annu Rev Pharmacol Toxicol 44:269–296

Tasca CI, Cardoso LF, Martini LH, Ramírez G, Souza DO (1998) Guanine nucleotides inhibit cAMP accumulation induced by metabotropic glutamate receptors activation. Neurochem Res 23:183–188

Taylor A (1996) Biochemistry of tellurium. Biol Trace Elem Res 55:231–239

Tovey KC, Oldham KG, Whelan JA (1974) A simple direct assay for cyclic AMP in plasma and other biological samples using an improved competitive protein binding technique. Clin Chim Acta 56:221–234

Viggiano D, Ruocco LA, Sadile AG (2003) Dopamine phenotype and behaviour in animal models: in relation to attention deficit hyperactivity disorder. Neurosci Biobehav Rev 27:623–637

Walbran BB, Robins E (1978) Effects of central nervous system accumulation of tellurium on behavior in rats. Pharmacol Biochem Behav 9:297–300

Watson DF, Nachtman FN, Kuncl RW, Griffin JW (1994) Altered neurofilament phosphorylation and beta tubulin isotypes in Charcot-Marie-Tooth disease type 1. Neurology 44:2383–2387

Widy-Tyszkiewicz E, Piechal A, Gajkowska B, Smialek M (2002) Tellurium-induced cognitive deficits in rats are related to neuropathological changes in the central nervous system. Toxicol Lett 131:203–214

Yabe JT, Jung C, Chan W, Shea TB (2000) Phospho-dependent association of neurofilament proteins with kinesin in situ. Cell Motil Cytoskel 45:249–262

Yarema MC, Curry SC (2005) Acute tellurium toxicity from ingestion of metal-oxidizing solutions. Pediatrics 116:e319–e321

Yoshimura Y, Sogawa Y, Yamauchi T (1999) Protein phosphatase 1 is involved in the dissociation of Ca2+/calmodulin-dependent protein kinase II from postsynaptic densities. FEBS Lett 446:239–242

Zamoner A, Heimfarth L, Oliveira Loureiro S, Royer C, Mena Barreto Silva FR, Pessoa-Pureur R (2008) Nongenomic actions of thyroxine modulate intermediate filament phosphorylation in cerebral cortex of rats. Neuroscience 156:640–652

Capítulo 5

CROSS-TALK AMONG INTRACELLULAR SIGNALING PATHWAYS MEDIATE THE DIPHENYL DITELLURIDE ACTIONS ON THE HIPPOCAMPAL CYTOSKELETON OF YOUNG RATS

Luana Heimfarth, Samanta Oliveira Loureiro, Karina Pires Reis, Bárbara Ortiz de Lima, Fernanda Zamboni, Talita Gandolfi, Rodrigo Narvaes, João Batista Teixeira da Rocha and Regina Pessoa-Pureur

Artigo publicado na revista Chemical Research in Toxicology

Chemical Research in Toxicology

ARTICLE

pubs.acs.org/crt

Cross-Talk among Intracellular Signaling Pathways Mediates the Diphenyl Ditelluride Actions on the Hippocampal Cytoskeleton of Young Rats

Luana Heimfarth,[‡] Samanta Oliveira Loureiro,[‡] Karina Pires Reis,[‡] Bárbara Ortiz de Lima,[‡] Fernanda Zamboni,[‡] Talita Gandolfi,[‡] Rodrigo Narvaes,[‡] João Batista Teixeira da Rocha,[§] and Regina Pessoa-Pureur*[,‡]

[‡]Departamento de Bioquímica, Instituto de Ciências Básicas da Saúde, UFRGS, Porto Alegre, RS, Brasil

[§]Departamento de Química, Centro de Ciências Naturais e Exatas, Universidade Federal de Santa Maria, RS Brasil

ABSTRACT: In the present report, we showed that diphenyl ditelluride $(PhTe)_2$ induced in vitro hyperphosphorylation of glial fibrillary acidic protein (GFAP), vimentin and neurofilament (NF) subunits in hippocampus of 21 day-old rats. Hyperphosphorylation was dependent on L-voltage dependent Ca^{2+} channels (L-VDCC), *N*-methyl-D-aspartate (NMDA) and metabotropic glutamate receptors, as demonstrated by the specific inhibitors verapamil, DL-AP5 and MCPG, respectively. Also, dantrolene, a ryanodine channel blocker, EGTA and Bapta-AM, extra and intracellular Ca^{2+} chelators respectively, totally prevented this effect. Activation of metabotropic glutamate receptors by $(PhTe)_2$ upregulates phospholipase C (PLC), producing inositol 1, 4, 5-trisphosphate (IP_3) and diacylglycerol (DAG). Therefore, high Ca^{2+} levels and DAG directly activate Ca^{2+}/calmodulin-dependent protein kinase (PKCaMII) and protein kinase C (PCK), resulting in the hyperphosphorylation of Ser-57 in the carboxyl-terminal tail domain of the low molecular weight NF subunit (NF-L). Also, the activation of Erk1/2, and p38MAPK resulted in hyperphosphorylation of KSP repeats of the medium molecular weight NF subunit (NF-M). It is noteworthy that PKCaMII and PKC inhibitors prevented $(PhTe)_2$-induced Erk1/2MAPK and p38MAPK activation as well as hyperphosphorylation of KSP repeats on NF-M, suggesting that PKCaMII and PKC could be upstream of this activation. Taken together, our results highlight the role of Ca^{2+} as a mediator of the $(PhTe)_2$-elicited signaling targeting specific phosphorylation sites on IF proteins of neural cells of rat hippocampus. Interestingly, this action shows a significant cross-talk among signaling pathways elicited by $(PhTe)_2$, connecting glutamate metabotropic cascade with activation of Ca^{2+} channels. The extensively phosphorylated amino- and carboxyl- terminal sites could explain, at least in part, the neural dysfunction associated with $(PhTe)_2$ exposure

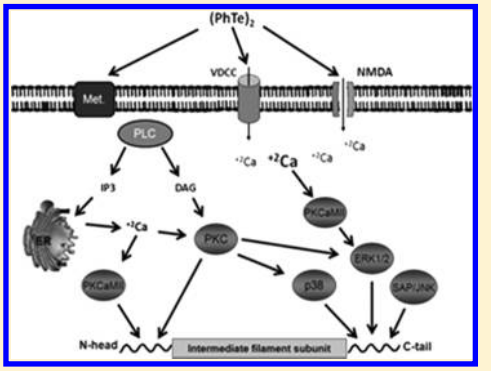

INTRODUCTION

Tellurium, a rare element, used as an industrial component of many alloys and in the electronic industry, can cause poisoning which leads to neurotoxic symptoms, such as significant impairment of learning and spatial memory.[1,2] Otherwise, the organic compound of tellurium, diphenyl ditelluride $(PhTe)_2$ has been described to possess very contrasting and interesting biological activities,[3−6] including actions on the cytoskeleton in rat brain.[7,8] In effect, organotellurium compounds, namely the simplest of the diaryl ditelluride $(PhTe)_2$, can have profound neurotoxic effects in rodents and can cause symptoms similar to those associated with disruption of axonal transport.[9,10] These neurotoxic properties can be related to changes in the dynamics of intermediate filaments (IFs)[11] via interaction with neural targets that are not completely identified. Taken together, these findings indicate that the brain is an important target for the action of this compound.

Human exposure to tellurium is rare. However, accidental exposure to this element has been reported in the literature,[12,13] and the industrial and laboratorial use of inorganic and organic forms of tellurium indicates that exposure to toxic levels of tellurium is conceivable in the work-place. Furthermore, the exposure of immature humans via mother contamination is also possible. This is of particular concern in view of the extreme sensitivity of developing brain to neurotoxic chemicals,[14] including $(PhTe)_2$.[4,15−17] Additionally, the antioxidant properties and low toxicity of different organotellurium compounds have been demonstrated by different laboratories and have been exploited to support their potential therapeutic use in pathologies associated with oxidative stress.[18−22] Tellurium is also found in relatively large amounts in the human body,[23] and Larner[24] has hypothesized that tellurium can be an important factor in the etiology of neurodegenerative diseases in man.

IFs are major components of the cytoskeleton and nuclear envelope in most types of eukaryotic cells. They are expressed in cell-type-specific patterns and play an important structural or tension-bearing role in the cell. Evidence is now emerging that

Received: July 26, 2011
Published: August 31, 2011

IFs also act as an important framework for the modulation and control of essential cell processes, in particular, signal transduction events.[25,26] The neuronal cytoskeleton comprises a protein network formed mainly by microtubules (MT) and neurofilaments (NF), the neuronal IFs. NF are composed of three different polypeptides whose approximate molecular weights are 200, 160, and 68 kDa, and are commonly referred to as heavy (NF-H), medium (NF-M), and light (NF-L) NF subunits.[27] Glial fibrillary acidic protein (GFAP) is the IF of mature astrocytes [28] and vimentin is the IF of cells of mesenchimal origin.[29]

IFs are important phosphoproteins whose phosphorylation/dephosphorylation is a dynamic process mediated by the combined action of several protein kinases and phosphatases. The phosphorylation/dephosphorylation of IFs has a profound effect on IF physiology, controlling the cytoskeletal role in response to extracellular signals. In this context, the phosphorylation of the amino-terminal head domain sites on GFAP and NF proteins plays a key role in the assembly/disassembly of IF subunits into 10 nm filaments and influences the phosphorylation of sites on the carboxyl terminal tail domain.[30] These phosphorylation events are largely under the control of second messenger-dependent protein kinases that provide the cells a mechanism to reorganize the IFs in response to the changes in second messenger levels.[31]

Accordingly, in vitro studies have identified Ca^{2+}/calmodulin-dependent protein kinase (CaMK) as the main protein kinase targeting NF-L subunit on Ser-57,[32] protein kinase C (PKC) targeting Ser-12, Ser-27, Ser-33 and Ser-51 [33] while cAMP-dependent protein kinase (PKA) was shown to phosphorylate NF-L Ser-55.[34,35]

Otherwise, most of the NF phosphorylation sites on the carboxyl-terminal tail domain of NF-M and NF-H subunits are located on the multiple Lys-Ser-Pro (KSP) repeat motifs.[36−38] Phosphorylation of these carboxyl-terminal sites regulates the interactions of NFs with each other and with other cytoskeletal structures, mediating the formation of a cytoskeletal lattice that supports the mature axon, regulates axonal transport and axon caliber.[31] There is evidence that phosphorylation of KSP motif rich tail domains on NF-M and NFH might be regulated by the activation of proline-directed kinases (ERK1/2, Cdk5, p38 MAP kinase or SAPK/JNK) by signal transduction cascades triggered by several signals,[39−42] including Ca^{2+} influx.[40]

Ca^{2+} levels in neurons are regulated by influx through Ca^{2+} channels as well as by release of Ca^{2+} from intracellular stores. Ca^{2+} influx can be mediated mainly by voltage-dependent Ca^{2+} channels (VDCC) and N-methyl-D-astartate (NMDA) receptors. Release from stores mainly involves Ca^{2+}-induced Ca^{2+} release (CICR) or activation by ligands that lead to the production of inositol-3-phosphate (IP3), which mobilizes Ca^{2+} from the endoplasmic reticulum IP3-sensitive pools. Upon Ca^{2+} entry via VDCC or NMDA Ca^{2+} channels, Ca^{2+}-binding proteins, such as calmodulin, bind multiple Ca^{2+} ions and can activate various intracellular effectors. The most prominent kinases include CaMKs and mitogen-activated protein kinases (MAPK) [43] which mediate many of the responses to Ca^{2+} signals in animal cells.

The importance of IFs, on cellular function is evident from the fact that perturbation of their function accounts for the protein misfolding/aggregation, such as the accumulation of GFAP, in astrocytes of Alexander disease.[44] Also, perikaryal accumulations/aggregations of NF proteins has been correlated with aberrantly phosphorylated NF in several neurodegenerative diseases, such as Alzheimer's disease, motor neuron diseases and Parkinson's disease.[45−48]

We have previously demonstrated that the low stoichiometry of IF phosphorylation under basal conditions increases about 30% in rat brain slices exposed to toxic levels of metabolites [49,50] or toxins.[7,8,51] Conversely, hypophosphorylation has also been observed, reflecting misregulation of the phosphorylating system in response to different signals.[52−55] In this context, different concentrations of $(PhTe)_2$, from 5 to 100 μM, induced hypophosphorylation of GFAP and NF subunits mediated by activation of protein phosphatase 1 (PP1) in cerebral cortex of 9 and 15 day-old animals.[11] Also, intracellular Ca^{2+} levels were identified to be upstream of the signaling pathways targeting the cytoskeleton. Interestingly, in these young animals the phosphorylating system associated with the IFs of neural cells from hippocampus was not misregulated by the exposure to this neurotoxicant.

Taking into account these recent findings, and considering that the signaling pathways are spatially and temporally regulated, the aim of the present study was to extend our investigation to cerebral cortex and hippocampus 21 day-old rats, analyzing the in vitro effects of $(PhTe)_2$, emphasizing the complexity of the mechanisms elicited by this neurotoxicant on the cytoskeleton and the role of Ca^2 in this action.

EXPERIMENTAL PROCEDURES

Radiochemical and Compounds. [^{32}P]Na_2HPO_4 was purchased from CNEN, São Paulo, Brazil. *N*,*N*,*N*′,*N*′-tetraacetic acid tetrakis (acetoxymethyl ester) (BAPTA-AM), EGTA, dantrolene, benzamidine, leupeptin, antipain, pepstatin, chymostatin, verapamil hydrochloride, SP600125, p38 inhibitor, staurosporine, acrylamide and bis-acrylamide, D-2-amino-5-phosphonopentanoic acid (DL-AP5) and MCPG, were obtained from Sigma (St. Louis, MO, U.S.A.). KN-93, PD98059, and U73122 were obtained from Calbiochem (La Jolla, CA, U.S.A.). The chemiluminescence ECL kit peroxidase and the conjugated antirabbit IgG were obtained from Amersham (Oakville, Ontario, Canada). Anti-ERK/MAPK, anti-phosphoERK/MAPK, anti-JNK/MAPK, anti-phosphoJNK/MAPK, anti-phosphoSer-55NF-L, anti-phosphoSer-57NF-L antibodies were obtained from Cell Signaling Technology (U.S.A.) and anti-NF-M/NF-H KSP repeats were obtained from Millipore. The monoclonal antibodies anti-p38/MAPK (A-12) and anti-phosphop38/MAPK were obtained from Santa Cruz biotechnology and the monoclonal antibodies anti GFAP (clone G-A-5), anti vimentin (clone VIM-13.2), anti-NF-L (clone NR4), anti-NF-M (clone NN18) were from Sigma (St. Lous, MO, U.S.A.). The organochalcogenide $(PhTe)_2$ was synthesized using the method described by Petragnami.[56] Analysis of the ^{1}H NMR and ^{13}C NMR spectra showed that the compound obtained presented analytical and spectroscopic data in full agreement with its assigned structure. The purity of the compound was assayed by high ressonance mass spectroscopy (HRMS) and was higher than 99.9%. All other chemicals were of analytical grade and were purchased from standard commercial supplier.

Animals. Twenty-one day-old Wistar rats were obtained from our breeding stock. Rats were maintained on a 12-h light/12-h dark cycle in a constant temperature (22 °C) colony room. On the day of birth the litter size was culled to seven pups. Litters smaller than seven pups were not included in the experiments. Water and a 20% (w/w) protein commercial chow were provided ad libitum. The experimental protocol followed the "Principles of Laboratory Animal Care" (NIH publication 85−23, revised 1985) and was approved by the Ethics Committee for Animal Research of the Federal University of Rio Grande do Sul.

Preparation and Labeling of Slices. Rats were killed by decapitation, the cerebral cortex and hippocampus were dissected onto

Petri dishes placed on ice and cut into 400 μm thick slices with a McIlwain chopper.

Preincubation. Tissue slices were initially preincubated at 30 °C for 20 min in a Krebs−Hepes medium containing 124 mM NaCl, 4 mM KCl, 1.2 mM $MgSO_4$, 25 mM Na-HEPES (pH 7.4), 12 mM glucose, 1 mM $CaCl_2$, and the following protease inhibitors: 1 μM benzamidine, 0.1 μM leupeptin, 0.7 μM antipain, 0.7 μM pepstatin, and 0.7 μM chymostatin in the presence or absence of 10 μM verapamil (L-VDCC channel blocker),[49,50] 50 μM dantrolene (ryanodine channel blocker),[49,50] 50 μM Bapta-AM plus 1 mM EGTA (intra- and extracellular Ca^{2+} chelators, respectively),[49,50,57] 100 μM DL-AP-5 (NMDA antagonist),[50] 1 μM staurosporine (PKC inhibitor),[50] 10 μM U7322 (phospholipase C inhibitor),[49] 30 μM SP600125 (SAP/JNK inhibitor),[58] 10 μM KN-93 (PKCaMII inhibitor),[49,50] 10 μM p38 inhibitor (p38MAPK inhibitor),[59] 10 μM H-89 (PKA inhibitor),[49,50] 30 μM PD98059 (MEK inhibitor).[49]

Incubation. After preincubation, the medium was changed and incubation was carried out at 30 °C with 100 μL of the basic medium containing 80 μCi of [^{32}P] orthophosphate with or without addition of 10 μM verapamil, 50 μM dantrolene, 50 μM Bapta-AM plus 1 mM EGTA, 100 μM DL-AP-5, 1 μM staurosporine, 10 μM U7322, 30 μM SP600125, 10 μM KN-93, 10 μM p38 inhibitor, 10 μM H-89, 30 μM PD98059 in the presence or absence of $(PhTe)_2$, when indicated. $(PhTe)_2$ was dissolved in dimethylsulfoxide (DMSO) just before use. In the experiments using the Ca^{2+} chelators Bapta-AM plus EGTA, the incubation medium was free of Ca^{2+}. The final concentration of DMSO was adjusted to 0.1%. Solvent controls attested that at this concentration DMSO did not interfere with the phosphorylation measurement. The labeling reaction was normally allowed to proceed for 30 min at 30 °C and stopped with 1 mL of cold stop buffer containing 150 mM NaF, 5 mM EDTA, 5 mM EGTA, 50 mM Tris-HCl, pH 6.5, and the protease inhibitors described above. Slices were then washed twice with stop buffer to remove excess radioactivity.

Preparation of the High Salt-Triton Insoluble Cytoskeletal Fraction from Tissue Slices. After treatment, IF-enriched cytoskeletal fractions were obtained from cerebral cortex and hippocampus of 21-day-old rats, as described by our group.[60] Briefly, after the labeling reaction, slices were homogenized in 400 μL of ice-cold high salt buffer containing 5 mM KH_2PO_4 (pH 7.1), 600 mM KCl, 10 mM $MgCl_2$, 2 mM EGTA, 1 mM EDTA, 1% Triton X-100, and the protease inhibitors described above. The homogenate was centrifuged at 14000*g* for 10 min at 4 °C, in an Eppendorf centrifuge, the supernatant was discarded and the pellet homogenized with the same volume of the high salt medium. The suspended pellet was centrifuged as described and the supernatant was discarded. The final Triton-insoluble IF-enriched pellet, containing NF subunits, vimentin and GFAP, was dissolved in 1% SDS and protein concentration was determined.[61]

Polyacrylamide Gel Electrophoresis (SDS-PAGE). The cytoskeletal fraction was prepared as described above. Equal protein concentrations were loaded onto 10% polyacrylamide gels and analyzed by SDS-PAGE according to the discontinuous system of Laemmli.[62] After drying, the gels were exposed to X-ray films (Kodak T-Mat) at −70 °C with intensifying screens and finally the autoradiograph was obtained. Cytoskeletal proteins were quantified by scanning the films with a Hewlett-Packard Scanjet 6100C scanner and determining optical densities with an Optiquant version 02.00 software (Packard Instrument Company). Density values were obtained for the studied proteins.

Preparation of Total Protein Homogenate. Tissue slices were initially preincubated at 30 °C for 20 min with or without addition of 10 μM KN-93, 10 μM p38 inhibitor, 1 μM staurosporine or 30 μM PD98059 in a Krebs−Hepes medium. After preincubation, the medium was changed and incubation was carried out at 30 °C with 100 μL of the basic medium in the presence or absence of the above-mentioned inhibitors and/or 100 μM $(PhTe)_2$. Tissues slices were then homogenized in 100 μL of a lysis solution containing 2 mM EDTA, 50 mM Tris-HCl, pH 6.8, 4% (w/v) SDS. For electrophoresis analysis, samples were dissolved to 25% (v/v) of a solution containing 40% glycerol, 5% mercaptoethanol, 50 mM Tris-HCl, pH 6.8, and boiled for 3 min.

Western Blot Analysis. Protein homogenate (80 μg) was analyzed by SDS-PAGE and transferred to PVDF or nitrocellulose membranes (Trans-blot SD semidry transfer cell, BioRad) for 1 h at 15 V in transfer buffer (48 mM Trizma, 39 mM glycine, 20% methanol and 0.25% SDS). The membranes were washed for 10 min in Tris-buffered saline (TBS; 0.5 M NaCl, 20 mM Trizma, pH 7.5), followed by 2 h incubation in blocking solution (TBS plus 5% bovine serum albumin and 0.1% Tween 20). After incubation, the blot was washed twice for 5 min with TBS plus 0.05% Tween-20 (T-TBS), and then incubated overnight at 4 °C in blocking solution containing the following monoclonal antibodies: anti-GFAP diluted 1:500, antivimentin diluted 1:400, anti-NF-L diluted 1:1000, anti-NF-M diluted 1:400, anti-ERK/MAPK diluted 1:1000, anti-phosphoERK/MAPK diluted 1:1000, anti-JNK/MAPK diluted 1:1000, anti-phosphoJNK/MAPK diluted 1:1000, anti-p38/MAPK diluted 1:1000, anti-phosphop38/MAPK diluted 1:1000, anti-NF-M/NF-H KSP repeats diluted 1:1000, anti-phosphoSer-57NF-L diluted 1:800 or anti-phosphoSer-55NF-L diluted 1:800. The blot was then washed twice for 5 min with T-TBS and incubated for 2 h in blocking solution containing peroxidase conjugated antirabbit IgG diluted 1:2000 or peroxidase conjugated antimouse IgG diluted 1:2000. The blot was washed twice again for 5 min with T-TBS and twice for 5 min with TBS. The blot was then developed using a chemiluminescence ECL kit. Immunoblots were quantified by scanning the films as described above. Optical density values were obtained for the studied proteins.

Statistical Analysis. Data were statistically analyzed by one-way analysis of variance (ANOVA) followed by the Tukey−Kramer multiple comparison test when the F-test was significant. All analyses were performed using the SPSS software program on an IBM-PC compatible computer.

RESULTS

Diphenylditelluride Induces Hyperphosphorylation of Neuronal and Glial Intermediate Filament Subunits. We initially tested the effect of different concentrations of $(PhTe)_2$ (1, 15 50 and 100 μM) on the in vitro phosphorylation of IF-enriched cytoskeletal fraction from cerebral cortex and hippocampus of 21-day old rats. Results showed that 100 μM $(PhTe)_2$ significantly increased the phosphorylation level of NF subunits studied (NF-M and NF-L), vimentin and GFAP in hippocampus (Figure 1A and B). In contrast, the neurotoxicant did not alter the phosphorylation level of these cytoskeletal proteins in cerebral cortex of rats at the age studied (Figure 1C and D). Therefore, we have chosen the hippocampus of rats to further studies on the molecular aspects of the action of $(PhTe)_2$ (100 μM) on the endogenous phosphorylating system associated with the IFs.

To verify whether $(PhTe)_2$ elicited signaling pathways targeting the phosphorylating system independently of protein synthesis and degradation, we evaluated protein levels by Western blot analysis, and results showed unaltered levels of both astrocyte and neuron IF subunits (Figure 2).

Next, we investigated the kinases potentially involved in the $(PhTe)_2$-induced hyperphosphorylation of the IF proteins using specific inhibitors of second messenger dependent protein kinases known to phosphorylate sites located on the amino-terminal head domain of the IF subunits [63] and second messenger independent protein kinases described to target residues on the carboxyl-terminal tail domains.[64−67] Results showed that

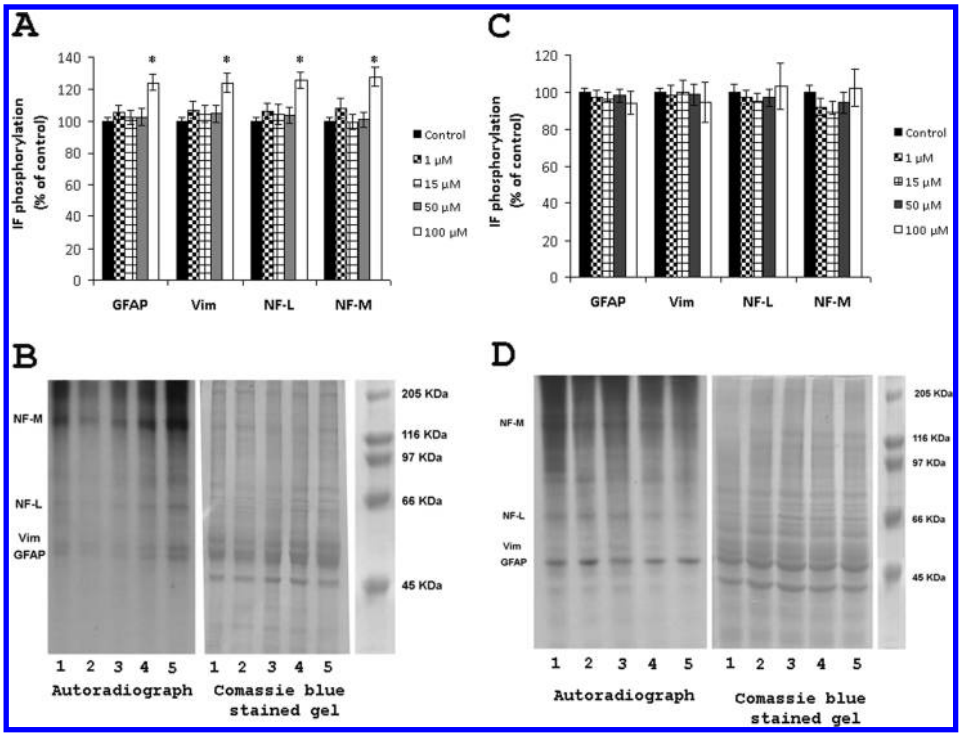

Figure 1. Effect of different concentrations of $(PhTe)_2$ on IF phosphorylation in hippocampus (A) and cerebral cortex (C). Slices of cerebral cortex or hippocampus were incubated with ^{32}P-orthophosphate in the absence or presence of 1, 15, 50, and 100 μM $(PhTe)_2$. The cytoskeletal fraction was extracted and the radioactivity incorporated into GFAP, vimentin, NF-L and NF-M was measured, as described in the Experimental Procedures section. Representative stained gel and autoradiographs of the proteins studied are shown (B = hippocampus; D = cerebral cortex) (lane 1 = control; lane 2 = 1 μM $(PhTe)_2$; lane 3 = 15 μM $(PhTe)_2$; lane 4 = 50 μM $(PhTe)_2$; lane 5 = 100 μM $(PhTe)_2$). Data are reported as mean ± SEM of 16 animals in each group and expressed as % of control. Statistically significant differences from controls, as determined by one-way ANOVA followed by Tukey−Kramer multiple comparison test are indicated: *$P < 0.05$.

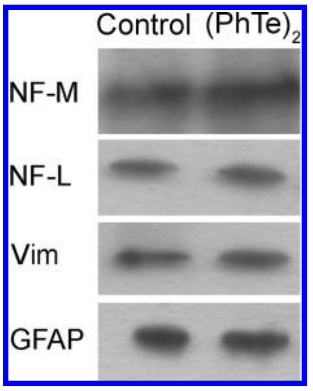

Figure 2. Representative Western blot assay of IF proteins from cytoskeletal fraction of hippocampus exposed to $(PhTe)_2$. Incubations were carried out in the presence or absence of 100 μM $(PhTe)_2$ for 30 min. The cytoskeletal fraction was extracted as described in the Experimental Procedures section and analyzed by SDS-PAGE. All lanes received an equivalent amount of protein (60 μg). Nitrocellulose membranes were treated with the antibodies anti-NF-M, anti-NF-L, antivimentin and anti-GFAP. The blots were developed using an ECL kit.

KN93 (10 μM), a specific PKCaMII inhibitor, and staurosporine (1 μM), a specific PKC inhibitor, prevented $(PhTe)_2$-induced GFAP, vimentin, NF-L, and NF-M hyperphosphorylation. Interestingly, the PKA inhibitor, H-89 (10 μM), was ineffective in preventing such effect (Figure 3A). We also investigated the involvement of MAPK pathway on the hyperphosphorylation of IF proteins. Results showed that 30 μM PD98059, a MEK inhibitor and 10 μM p38 inhibitor (p38/MAPK inhibitor) totally prevented the IF hyperphosphorylation induced by $(PhTe)_2$, while 30 μM SP600125, a SAP/JNK inhibitor, did not prevent the effect of the organotelluride on the phosphorylating system (Figure 3B).

Roles of Ca^{2+} Influx through L-Type Voltage-Dependent Calcium Channel and Ca^{2+} Release from Intracellular Stores in the IF Hyperphosphorylation Induced by $(PhTe)_2$. Taking into account the importance of Ca^{2+} in a plethora of intracellular events that result in the regulation of cell physiology, particularly the cytoskeletal roles,[68] and that PKC and PKCaMII activities are regulated by intracellular Ca^{2+} levels, we examined the involvement of Ca^{2+} in the $(PhTe)_2$-mediated IF hyperphosphorylation. Figure 4 shows that verapamil (10 μM), a L-type voltage-dependent Ca^{2+} channel (L-VDCC) blocker, prevented IF hyperphosphorylation. Similarly, dantrolene (50 μM), a ryanodine channel blocker impaired the effect of the neurotoxicant, indicating a role of Ca^{2+} released from the intracellular stores in this action. The importance of increased cytosolic Ca^{2+} levels in eliciting this effect was reinforced by coincubating tissue slices with the neurotoxicant in the presence of both the intracellular Ca^{2+} chelator Bapta-AM (50 μM) and the extracellular Ca^{2+} chelator EGTA (1 mM) in a Ca^{2+}-free medium. Results showed that the action of the neurotoxicant on the phosphorylating system was totally prevented, emphasizing the role of intracellular Ca^{2+} levels in such effect.

dx.doi.org/10.1021/tx200307u |*Chem. Res. Toxicol.* 2011, 24, 1754–1764

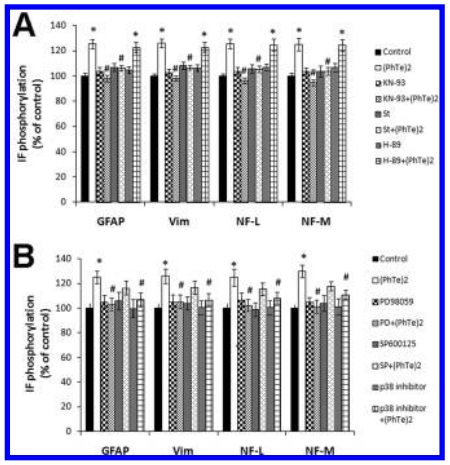

Figure 3. Involvement of PKA, PKC, PKCaMII (A), MEK, SAP/JNK, and p38/MAPK (B) on IF hyperphosphorylation induced by $(PhTe)_2$. Slices of hippocampus of 21 day-old rats were preincubated in the presence or absence 10 μM H-89 (PKA inhibitor), 1 μM staurosporine (St) (PKC inhibitor) or 10 μM KN-93 (PKCaMII inhibitor) (A), or 30 μM PD98059 (MEK inhibitor), or 30 μM SP600125 (SAP/JNK inhibitor), or 10 μM p38 inhibitor (B). Preincubation was followed by incubation with ^{32}P orthophosphate in the presence or absence of the kinase inhibitors and 100 μM $(PhTe)_2$, as described in Experimental Procedures section. The cytoskeletal fraction was extracted and the radioactivity incorporated into NF-M, NF-L, vimentin (VIM) and GFAP was measured. Data are reported as mean ± SEM of 15 animals in each group and expressed as % of control. Statistically significant differences as determined by one-way ANOVA followed by Tukey-Kramer multiple comparison test are indicated: $^{*}p < 0.05$ compared with control group; $^{\#}p < 0.05$ compared with $(PhTe)_2$ group.

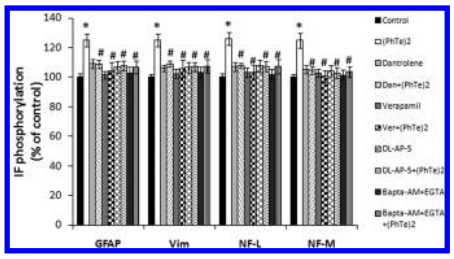

Figure 4. Involvement of intracellular Ca^{2+} levels on $(PhTe)_2$ induced IF hyperphosphorylation. Slices of hippocampus of 21 day-old rats were preincubated for 20 min in the presence or absence of 50 μM BAPTA-AM (intracellular Ca^{2+} quelator) plus 1 mM EGTA (extracellular Ca^{2+} quelator), 10 μM verapamil (L-type voltage-dependent Ca^{2+} channel blockers), 50 μM dantrolene (ryanodine channel blocker) or 100 μM DL-AP5 (NMDA antagonist). Preincubation was followed by incubation with ^{32}P orthophosphate in the presence or absence of the Ca^{2+} blockers and 100 μM $(PhTe)_2$, as described in the Experimental Procedures section. The cytoskeletal fraction was extracted and the radioactivity incorporated into NF-M, NF-L, vimentin (VIM) and GFAP was measured. Data are reported as mean ± SEM of 15 animals in each group and expressed as % of control. Statistically significant differences as determined by one-way ANOVA followed by Tukey-Kramer multiple comparison test are indicated: $^{*}p < 0.05$ compared with control group; $^{\#}p < 0.05$ compared with $(PhTe)_2$ group.

Glutamate Receptors Are Involved in the $(PhTe)_2$-Mediated Intermediate Filament Hyperphosphorylation. To further investigate the relevance of Ca^{2+} in the action mediated by $(PhTe)_2$, we tested the participation of Ca^{2+} influx through the

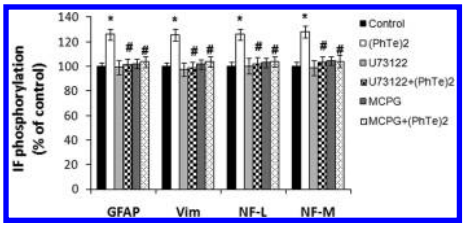

Figure 5. Effect of the metabotropic glutamate receptor antagonist and the PLC inhibitor on $(PhTe)_2$ induced IF hyperphosphorylation in hippocampus of 21 days old rats. Slices were preincubated for 20 min in the presence or absence of 100 μM MCPG (mGluR antagonist) or 10 μM U7322 (PLC inhibitor). Preincubation was followed by incubation with ^{32}P orthophosphate in the presence or absence of the glutamate antagonist or PLC inhibitor and 100 μM $(PhTe)_2$. The cytoskeletal fraction was extracted and the radioactivity incorporated into NF-M, NF-L, vimentin (VIM) and GFAP was measured as described in the Experimental Procedures section. Data are reported as means ± SEM of 15 animals in each group and expressed as % of control. Statistically significant differences as determined by one-way ANOVA followed by Tukey-Kramer multiple comparison test are indicated. $^{*}p < 0.05$ compared with control group; $^{\#}p < 0.05$ compared with $(PhTe)_2$ group.

N-methyl-D-aspartate (NMDA) glutamate receptors on IF hyperphoshorylation. Results showed that 100 μM DL-AP5, a competitive NMDA ionotropic antagonist totally prevented GFAP, vimentin, NF-L and NF-M hyperphosphorylation (Figure 4).

The role of glutamatergic metabotropic receptors (mGluR) and phospholipase C (PLC) mediating the effect of $(PhTe)_2$ was verified using 100 μM MCPG, a group I/II mGluR antagonist and 10 μM U7322, a PLC inhibitor. Results showed that both inhibitors prevented $(PhTe)_2$-induced IF hyperphosphorylation (Figure 5).

Parallel Intracellular Signaling Pathways Activated by $(PhTe)_2$ Mediate Activation of MAPK Pathway and Phosphorylation of KSP Repeats on the Medium Molecular Weight Neurofilament Subunit. The role of MAPK pathway on the IF hyperphosphorylation provoked by $(PhTe)_2$ was tested measuring total and phosphorylated ERK1/2, JNK/MAPK, and p38/MAPK levels. Western blot assays using specific phosphorylation-independent and phosphorylation-dependent antibodies showed that MAPK total levels were unaltered, whereas phosphoERK1/2, phosphoJNK/MAPK and phosphop38/MAPK levels significantly increased at 30 min of exposure to $(PhTe)_2$. (Figure 6A, B, and C). It is important to note that the results of the experiments shown in (Figure 3) have indicated that inhibition of PKCaMII and PKC, which are known to phosphorylate N-terminal sites of NF-L, GFAP, and vimentin, also prevented the phosphorylation of NF-M, whose main phosphorylating sites are localized on the carboxyl terminal domain. To determine a possible cross-talk among the Ca^{2+}-dependent protein kinases and MAPK pathway, we used specific PKC and PKCaMII inhibitors followed by Western blot analysis of phosphoERK 1/2, phosphop38/MAPK and phosphoJNK/MAPK levels .

Results showed that staurosporine (1 μM) and KN-93 (10 μM), specific PKC and PKCaMII inhibitors, respectively, totally prevented the neurotoxicant effect on ERK1/2 phosphorylation (Figure 6A). On the other hand, phosphorylation of JNK/MAPK, was not prevented by the specific PKC and PKCaMII inhibitors (Figure 6B). Finally, p38/MAPK activation was blocked only by staurosporine, demonstrating a PKC-dependent activation of this MAP kinase (Figure 6C).

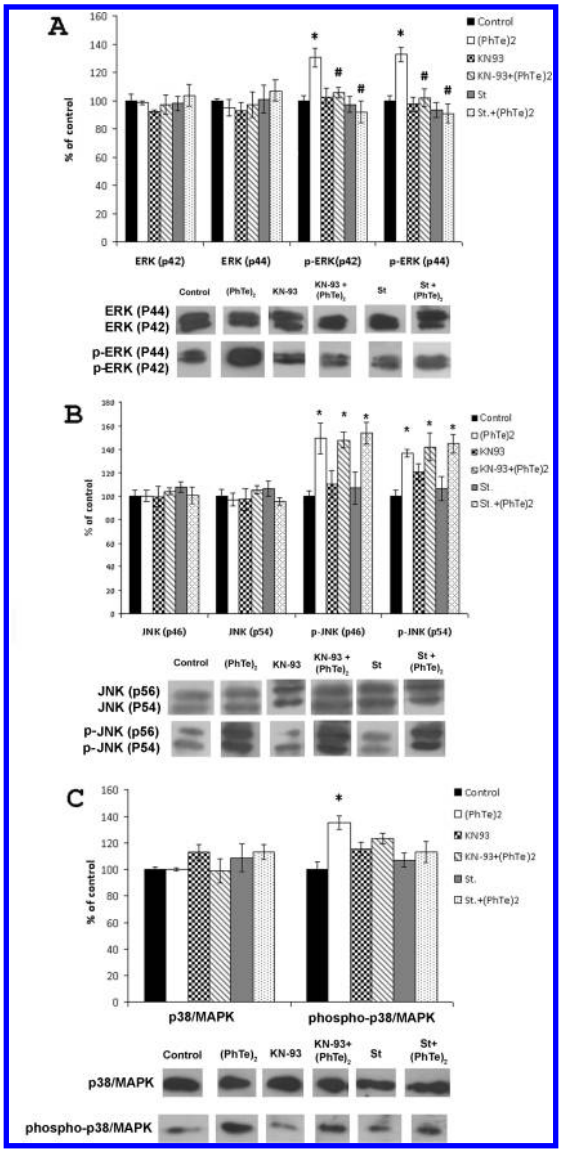

Figure 6. Involvement of PKC and PKCaMII on ERK1/2 (A), JNK/SAP (B), and p38/MAPK (C) activation induced by $(PhTe)_2$ in hippocampus of rats. Slices of hippocampus of 21 day-old rats were preincubated in the presence or absence 1 μM staurosporine (St) (PKC inhibitor) or 10 μM KN-93 (PKCaMII inhibitor). Tissue was lysed and prepared for immunoblotting analysis. The total and phosphorylated levels of ERK1/2, JNK/SAP, and p38/MAPK were measured, as described in the Experimental Procedures section. Data are reported as means ± SEM of 10 animals in each group and expressed as % of control. Statistically significant differences as determined by one-way ANOVA followed by Tukey-Kramer multiple comparison test are indicated. $^{*}p < 0.05$ compared with control group; $^{\#}p < 0.05$ compared with $(PhTe)_2$ group. The representative blots are shown.

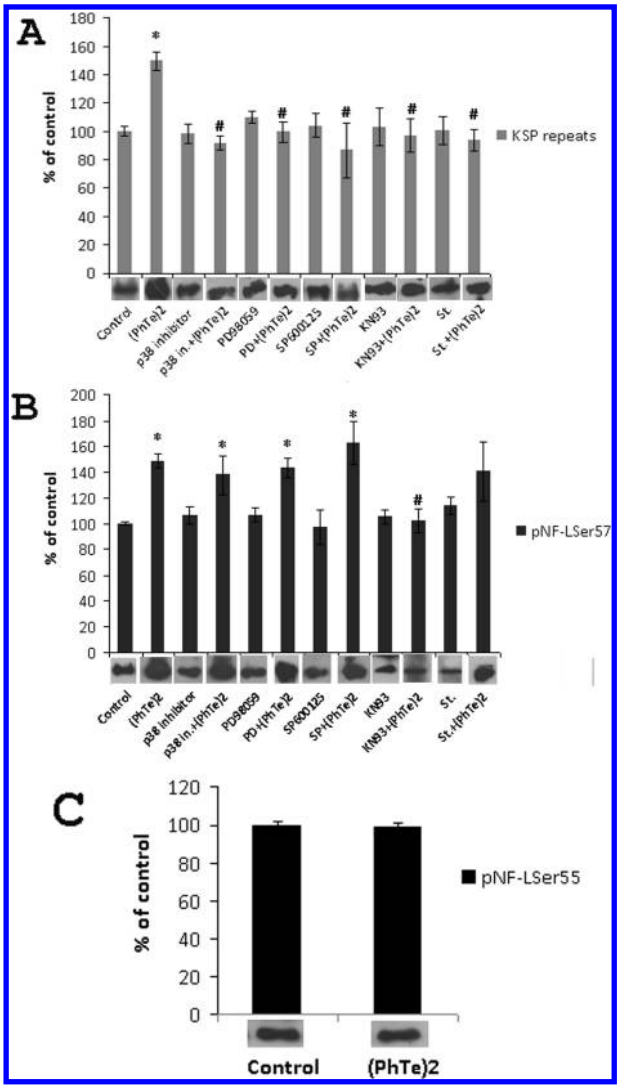

Figure 7. Effect of $(PhTe)_2$ on cytoskeletal-associated intermediate filament subunits NF-M/NF-H KSP repeats (A), phosphoNF-L Ser-57 (B), and phosphoNF-L Ser-55 (C) of in hippocampus of rats. Involvement of PKC, PKCaMII (A), MEK, SAP/JNK and p38/MAPK on IF hyperphosphorylation induced by $(PhTe)_2$. Slices of hippocampus of 21 day-old rats were preincubated in the presence or absence 1 μM staurosporine (PKC inhibitor), 10 μM KN-93 (PKCaMII inhibitor), 30 μM PD98059 (MEK inhibitor), 30 μM SP600125 (SAP/JNK inhibitor), or 10 μM p38 inhibitor. Preincubation was followed by incubation with or without the kinases inhibitors and 100 μM $(PhTe)_2$, as described in the Experimental Procedures section. The cytoskeletal fraction was extracted and the immunocontent of NF-M/NF-H KSP repeats (A), phosphoNF-L Ser-57 (B) and phosphoNF-L Ser-55 (C) was measured. Data are reported as means ± SEM of 10 animals in each group and expressed as % of control. Statistically significant differences as determined by one-way ANOVA followed by Tukey-Kramer multiple comparison test are indicated. $^{*}p < 0.05$ compared with control group; $^{\#}p < 0.05$ compared with $(PhTe)_2$ group. The representative blots are shown.

In an attempt to identify the phosphorylating sites targeted by the protein kinases PKC, PKCaMII and MAPK, we assayed NF-L Ser-57 and NF-L Ser-55 on NF-L head domain as well as KSP repeats on NF-M tail domain, respectively. Western blot assay using anti-phosphoSer-57 antibody and anti-NF-M/NF-H KSP repeats showed that the phosphorylation level of NF-L Ser-57 and NF-M KSP repeats was increased following treatment with $(PhTe)_2$ (Figures 7A and B). However, phosphorylation of NF-L Ser-57 was totally prevented by 10 μM KN-93 (PKCaMII inhibitor) and partially prevented by 1 μM staurosporine (PKC inhibitor), while 30 μM PD98059 (MEK inhibitor), 30 μM SP600125 (JNK/MAPK inhibitor) and 10 μM p38 inhibitor (p38/MAPK inhibitor) were ineffective in preventing such effect (Figure 7A). Otherwise, the phosphorylation level of NF-M KSP repeats induced by the neurotoxicant was prevented by all the

inhibitors used (Figure 7B). Finally, we investigated the phosphorylating level of NF-L Ser-55, the main phosphorylating site targeted by PKA on NF-L,[45] and results showed that $(PhTe)_2$ did not induce phosphorylation of this site (Figure 7C), corroborating our results showing that PKA is not involved in the action of $(PhTe)_2$.

The results of these experiments are consistent with the argument that Ca^{2+} influx induced by $(PhTe)_2$ in the hippocampus of 21 day old rats activates PKC and PKCaMII which, in turn, activate Erk1/2 and p38MAPK, specifically phosphorylating KSP sites in the NF-M tail domain.

DISCUSSION

In the present Article, we show experimental evidence that $(PhTe)_2$ disrupts the dynamic equilibrium of the phosphorylating system associated with glial and neuronal cytoskeletal proteins from hippocampus of 21 day-old rats leading to hyperphosphorylation of the IF proteins from astrocytes and neurons. Interestingly, results of the present work show that $(PhTe)_2$ did not modify cortical IF phosphorylation of 21 day-old rats, whereas we have recently described that in 9 and 15 day-old rats, the cerebral cortex, rather than hippocampus, was responsive to this neurotoxicant. Moreover, it is remarkable that in the cerebral cortex $(PhTe)_2$ has provoked IF hypophosphorylation.[11]

Our present findings provide an interesting insight on the differential susceptibility of cortical and hippocampal IF cytoskeleton to the in vitro exposure to $(PhTe)_2$ and could reflect the vulnerability of the cytoskeleton of hippocampal cells in 21 day old rats. Accordingly, a single subcutaneous injection of $(PhTe)_2$ in 15 day-old rats induced hyperphosphorylation of IF proteins in cerebral cortex 3 days after injection, while in hippocampus this effect was evidenced only 6 days after injection, corresponding to 21 days of age.[51] In this context, it is assumed that the various parts of the brain develop at different times and have different windows of vulnerability, both prenatally and postnatally, based on the temporal and regional maturation mediated through a multitude of developmental processes.[69] Here we have observed a quite different response of brain areas to the neurotoxicant $(PhTe)_2$ in a very narrow period of postnatal life. The developmental changes which are associated with these phenomena can be related to changes in the regulation of the pathways that control IF phosphorylation/dephosphorylation.

Interestingly, our previous results and the present data, suggest that $(PhTe)_2$ acts as an upstream signal disrupting cerebral Ca^{2+} homeostasis. The increase in intracellular Ca^{2+}, elicits the activation of complex signaling pathways targeting the cytoskeleton in a spatially and temporally regulated manner. Although, here we can not decipher the exact molecular mechanisms involved in the $(PhTe)_2$ effects, it must be considered that the level of intracellular Ca^{2+} is fundamental to its response profile following excitation. Of particular importance, local microdomains of Ca^{2+} influx can activate distinct signaling pathways [70,71] and the magnitude of the change can determine the activation of kinases versus phosphatases.[72,73]

Ca^{2+} is an almost universal intracellular messenger, controlling a diverse range of cellular processes, such as gene transcription, muscle contraction and cell proliferation. The diversity of Ca^{2+} mechanisms underlies the huge variability in the characteristics of Ca^{2+} signals recorded in different cell types.[74] In this context, the rise in intracellular Ca^{2+} concentrations in response to a stimulus could originate from a Ca^{2+} influx pathway, from release of Ca^{2+} from an internal store, or through a combination of these.[75] The central role of Ca^{2+} in the actions of $(PhTe)_2$ was evidenced by results showing that prevention of Ca^{2+} influx by DL-AP5, a specific NMDA antagonist or verapamil, a L-VDCC blocker; inhibition of Ca^{2+} release from ryanodine-sensitive intracellular stores, as well as chelation of intra/extracellular Ca^{2+}, totally prevented the hyperphosphorylation provoked by $(PhTe)_2$.

Increased Ca^{2+} levels in $(PhTe)_2$-treated hippocampal slices are upstream of the activation of PKCaMII which hyperphosphorylated the residue Ser-57 localized in the middle of the amino-terminal head domain of NF-L, which are known to be important in filament assembly.[34,35] This is consistent with our previous reports demonstrating that this protein kinase is associated with the cytoskeletal fraction.[49,76,77] In addition, the increase in the intracellular Ca^{2+} provoked by $(PhTe)_2$ is upstream of the activation of MAPK cascade. The role of Ca^{2+} as mediator of a signal targeting kinase cascades is consistent with our previous findings, showing that different metabolites in toxic concentrations modulate the cytoskeleton through Ca^{2+}-mediated mechanisms leading to a cell response.[49,50,76−81]

The complexity of the mechanisms of action of $(PhTe)_2$ was also evidenced by the activation of mGluRs. On the basis of our experimental approach, we could propose that the binding of the neurotoxicant to specific metabotropic receptors in the plasma membrane could be upstream of the activation of PLC. This signaling pathway is consistent with the hydrolysis of phosphatidylinositol 4,5-bisphosphate (PIP2) to produce the intracellular messengers IP3 and diacylglycerol (DAG). The IP3 encounters specific receptors (IP3Rs) on the endoplasmic reticulum releasing Ca^{2+} stores, otherwise, DAG and the high Ca^{2+} levels are able to activate PKC.[82] Furthermore, our results demonstrated that staurosporine, an inhibitor of PKC activity, prevented the action of $(PhTe)_2$ on GFAP, vimentin, NF-L and NF-M phosphorylation. Although PKC is described to phosphorylate Ser-51 in the amino-terminal domain of NF-L,[34,35] our results showed that this protein kinase is partially involved in the phosphorylation of NF-L Ser-57 together with PKCaMII, further supporting a role of $(PhTe)_2$ misregulating the dynamics of neurofilament assembly and therefore neural function.

It is known that NF-M/NF-H are mainly phosphorylated at Ser residues on KSP repeat motifs located on the head domain of these subunits by the proline-directed kinases Cdk5 and MAPK.[66,83] It is noteworthy that staurosporine and KN-93 prevented $(PhTe)_2$-induced hyperphosphorylation of KSP repeats. Moreover, PKCaMII and PKC inhibitors prevented $(PhTe)_2$-induced Erk1/2 and p38MAPK activation, suggesting that $(PhTe)_2$ activated MAPK cascade and that PKCaMII and PKC could be upstream of this activation. Supporting these findings, we have previously described that PKC is upstream of Erk1/2 activation, which in turn, phosphorylated IF proteins.[49] Furthermore, according to Ji and Strichartzan,[84] increased intracellular Ca^{2+} activated PKC and PKCaMII, which could activate Erk1/2, and p38MAPK. It is important to emphasize that phosphorylation of KSP repeats by MAPKs might be influenced by Ca^{2+}-dependent kinases, acting on sites localized in the amino terminal domain of the NF-M subunit. This supports the idea that phosphorylation of N-terminal sites not only regulates the NF assembly/disassembly, they might play a role in determining the phosphorylation state of specific carboxyl-terminal tail domain phosphorylation sites in NF-M.[31]

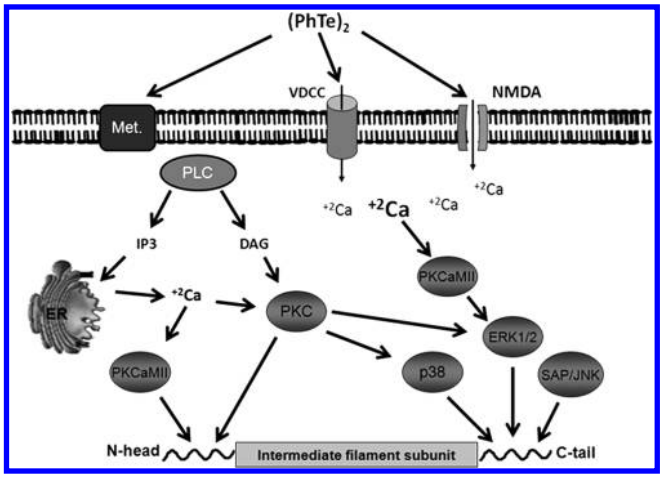

Figure 8. Proposed mechanism by which $(PhTe)_2$ induces IF hyperphosphorylation in hippocampus of 21 day-old rats. Extracellular Ca^{2+} enters the cytosol through either IP3 and ryanodine receptors. High Ca^{2+} levels directly activate PKCaMII. Otherwise, the increased intracellular Ca^{2+} levels and DAG activate PKC. Both second messenger-dependent kinases phosphorylate the amino-terminal domain on the astrocyte IF proteins GFAP and vimentin as well as the residue Ser-57 on the neurofilament subunit NF-L. In addition, MAPK activation is downstream to PKC and PKCaMII, which, in turn, phosphorylate KSP repeats on carboxyl-terminal domain of NF-M. Met. = metabotropic receptor.

Taking together all the above-discussed signaling pathways, here we have proposed the scheme depicted in Figure 8 to illustrate the complexity of the signaling mechanisms elicited by $(PhTe)_2$. The final consequence of these events is the disruption of the cytoskeleton dynamic, which is triggered by the combined activation of mGlu and NMDA receptors together with L-VDCC. Extracellular Ca^{2+} enters the cytosol through Ca^{2+} channels and the Ca^{2+} from the endoplasmic reticulum is released into the cytosol through either IP3 and ryanodine receptors. IP_3 and DAG are downstream of mGluR and PLC activity. Ryanodine receptors are activated by Ca^{2+} binding in a Ca^{2+}-induced Ca^{2+} release mechanism. High Ca^{2+} levels directly activate PKCaMII. Otherwise, the increased intracellular Ca^{2+} levels and DAG activate PCK. Both second messenger-dependent kinases phosphorylate the amino-terminal domain on the astrocyte IF proteins GFAP and vimentin, as well as the residue Ser-57 on NF-L. In addition, PKC and PKCaMII are upstream of MAPK activation, which, in turn, phosphorylate KSP repeats on the carboxyl-terminal domain of NF-M.

It has been determined that the majority of the phosphate groups incorporated in the carboxyl-terminal tail domain are added in polymerized NFs after they enter the axon, and when phosphorylated, these tail regions of NF-H and NF-M protrude laterally from the filament backbone to form sidearms.[31,39] Hyperphosphorylation of tail KSP repeats on NF-M/NF-H progressively restricts association of NFs with kinesin, the axonal anterograde motor protein, and stimulates its interaction with dynein, the axonal retrograde motor protein. This event could represent one of the mechanisms by which carboxyl-terminal phosphorylation would slow neurofilament axonal transport.[85]

In effect, here we have observed that the neurotoxic effects of $(PhTe)_2$ can be linked to disruption of IF phosphorylation/dephosphorylation homeostasis via a complex hierarchical cascade of events. The primary targets of $(PhTe)_2$ in the hippocampus of 21-day-old rats are proteins involved in the regulation of Ca^{2+} movement, namely metabotrobic and NMDA glutamate receptors and L-VDCC. The Ca^{2+} entry via these proteins activates the cross-talk among different intracellular signaling pathways that ultimately will disrupt the dynamics of IF phosphosphorylation/dephosphorylation, which can be involved in the neural toxicity of $(PhTe)_2$.[9,86]

AUTHOR INFORMATION

Corresponding Author

*Fax: 5551 3308 5535. Tel: 5551 3308 5565. E-mail: rpureur@ufrgs.br.

Funding Sources

This work was supported by Conselho Nacional de Desenvolvimento Científico e Tecnológico (CNPq), Fundação de Amparo à Pesquisa do Estado do Rio Grande do Sul (FAPERGS) and (PROPESq-UFRGS)

REFERENCES

(1) Walbran, B. B., and Robins, E. (1978) Effects of central nervous system accumulation of tellurium on behavior in rats. *Pharmacol., Biochem. Behav. 9*, 297–300.

(2) Widy-Tyszkiewicz, E., Piechal, A., Gajkowska, B., and Smialek, M. (2002) Tellurium-induced cognitive deficits in rats are related to neuropathological changes in the central nervous system. *Toxicol. Lett. 131*, 203–214.

(3) Brito, V. B., Rocha, J. B., Folmer, V., and Erthal, F. (2009) Diphenyl diselenide and diphenyl ditelluride increase the latency for 4-aminopyridine-induced chemical seizure and prevent death in mice. *Acta Biochim. Pol. 56*, 125–134.

(4) Stangherlin, E. C., Favero, A. M., Zeni, G., Rocha, J. B. T., and Nogueira, C. W. (2005) Teratogenic vulnerability of Wistar rats to diphenyl ditelluride. *Toxicology 207*, 231–239.

(5) Barbosa, N. B. V., Rocha, J. B. T., Zeni, G., Emanuelli, T., Beque, M. C., and Braga, A. L. (1998) Effect of organic forms of selenium on delta-aminolevulinate dehydratase from liver, kidney and brain of adult rats. *Toxicol. Appl. Pharmacol. 149*, 243–253.

(6) Laden, B. P., and Porter, T. D. (2001) Inhibition oh human squalene monooxigenase by tellurium compounds: Evidence of interaction with vicinal sulfhydryls. *J. Lipid Res. 42*, 235–240.

(7) Moretto, M. B., Funchal, C., Zeni, G., Rocha, J. B. T., and Pessoa-Pureur, R. (2005) Organoselenium compounds prevent hyperphosphorylation of cytoskeletal proteins induced by the neurotoxic agent diphenyl ditelluride in cerebral córtex of young rats. *Toxicology 210*, 213–222.

(8) Funchal, C., Moretto, M. B., Vivian, L., Zeni, G., Rocha, J. B. T., and Pessoa-Pureur, R. (2006) Diphenyl ditelluride- and methylmercury-induced hyperphosphorylation of the high molecular weight neurofilament subunit is prevented by organoselenium compounds in cerebral cortex of young rats. *Toxicology 222*, 143–153.

(9) Nogueira, C. W., Zeni, G., and Rocha, J. B. T. (2004) Organoselenium and organotellurium compounds: Toxicology and pharmacology. *Chem. Rev. 104*, 6255–6285.

(10) Maciel, E. N., Bolzan, R. C., Braga, A. L., and Rocha, J. B. (2000) Diphenyl diselenide and diphenyl ditelluride differentially affect delta-aminolevulinate dehydratase from liver, kidney, and brain of mice. *J. Biochem. Mol. Toxicol. 14*, 310–319.

(11) Heimfarth, L., Loureiro, S. O., Reis, K. P., de Lima, B. O., Zamboni, F., Lacerda, S., Soska, A. K., Wild, L., da Rocha, J. B., and Pessoa-Pureur, R. (2011) Diphenyl ditelluride induces hypophosphorylation of intermediate filaments through modulation of DARPP-32-dependent pathways in cerebral cortex of young rats. *Arch. Toxicol.*, DOI: 10.1007/s00204-011-0746-6.

(12) Taylor, A. (1996) Biochemistry of tellurium. *Biol. Trace Elem. Res. 55*, 231–239.
(13) Yarema, M. C., and Curry, S. C. (2005) Acute tellurium toxicity from ingestion of metal-oxidizing solutions. *Pediatrics 116*, e319–321.
(14) Farina, M., Aschner, M., and Rocha, J. B. (2011) Oxidative stress in MeHg-induced neurotoxicity. *Toxicol. Appl. Pharmacol.*, DOI: 10.1016/j.taap.2011.05.001.
(15) Stangherlin, E. C., Favero, A. M., Zeni, G., Rocha, J. B., and Nogueira, C. W. (2006) Exposure of mothers to diphenyl ditelluride during the suckling period changes behavioral tendencies in their offspring. *Brain Res. Bull. 69*, 311–317.
(16) Stangherlin, E. C., Ardais, A. P., Rocha, J. B., and Nogueira, C. W. (2009a) Exposure to diphenyl ditelluride, via maternal milk, causes oxidative stress in cerebral cortex, hippocampus and striatum of young rats. *Arch. Toxicol. 83*, 485–491.
(17) Stangherlin, E. C., Rocha, J. B., and Nogueira, C. W. (2009b) Diphenyl ditelluride impairs short-term memory and alters neurochemical parameters in young rats. *Pharmacol., Biochem. Behav. 91*, 430–435.
(18) Kanski, J., Drake, J., Aksenova, M., Engman, L., and Butterfield, D. A. (2001) Antioxidant activity of the organotellurium compound 3-[4-(*N*,*N*-dimethylamino)benzenetellurenyl]propanesulfonic acid against oxidative stress in synaptosomal membrane systems and neuronal cultures. *Brain Res. 911*, 12–21.
(19) Giles, G. I., Fry, F. H., Tasker, K. M., Holme, A. L., Peers, C., Green, K. N., Klotz, L. O., Sies, H., and Jacob, C. (2003) Evaluation of sulfur, selenium, and tellurium catalysts with antioxidant potential. *Org. Biomol. Chem. 1*, 4317–4322.
(20) Avila, D. S., de, Beque, M. C., Folmer, V., Braga, A. L., Zeni, G., Nogueira, C. W., Soares, F. A., and Rocha, J. B. (2006) Diethyl 2-phenyl-2 tellurophenyl vinylphosphonate: an organotellurium compound with low toxicity. *Toxicology 224*, 100–107.
(21) Avila, D. S., Colle, D., Gubert, P., Palma, A. S., Puntel, G., Manarin, F., Noremberg, S., Nascimento, P. C., Aschner, M., Rocha, J. B., and Soares, F. A. (2010) A possible neuroprotective action of a vinylic telluride against Mn-induced neurotoxicity. *Toxicol. Sci. 115*, 194–201.
(22) Ávila, D. S., Palm, A. S., Colle, D., Scolari, R., Manarin, F., da Silveira, A. F., Nogueira, C. W., Rocha, J. B., and Soares, F. A. (2011) Hepatoprotective activity of a vinylic telluride against acute exposure to acetaminophen. *Eur. J. Pharmacol. 661*, 92–101.
(23) Schroeder, H. A., Buckman, J., and Balassa, J. J. (1967) Abnormal trace elements in man: Tellurium. *J. Chronic Dis. 20*, 147–161.
(24) Larner, A. J. (1995) How does garlic exert its hypocholesterolaemic action? The tellurium hypothesis. *Med. Hypotheses 44*, 295–297.
(25) Paramio, J. M., and Jorcano, J. L. (2002) Beyond structure: Do intermediate filaments modulate cell signalling? *Bioessays 24*, 836–844.
(26) Kim, S., and Coulombe, P. A. (2007) Intermediate filament scaffolds fulfill mechanical, organizational, and signaling functions in the cytoplasm. *Genes Dev. 21*, 1581–1597.
(27) Ackerley, S., Grierson, A. J., Brownlees, J., Thornhiel, P., Anderton, B. H., Leight, P. N., Shew, C. E., and Mielerc, C. J. (2000) Glutamate slow axonal transport of neurofilaments in transfected neurons. *J. Cell Biol. 150*, 165–175.
(28) Eng, L. F., Ghirnikar, R. S., and Lee, Y. L. (2000) Glial fibrillary acidic protein: GFAP-thirty-one years (1969−2000). *Neurochem. Res. 25*, 1439–1451.
(29) Alberts, B., Johnson, A., Lewis, J., Raff, M., Roberts, K., Walter, P. (2008). The cytoskeleton. In Alberts, B., Johnson, A., Lewis, J., Raff, M., Roberts, K., Walter, P. (eds.), *Mol. Biol. Cell*, Garland Science, New York, pp 965−982.
(30) Zheng, Y. L., Li, B. S., Veeranna, and Pant, H. C. (2003) Phosphorylation of the head domain of neurofilament protein (NF-M): A factor regulating topographic phosphorylation of NF-M tail domain KSP sites in neurons. *J. Biol. Chem. 278*, 24026–24032.
(31) Sihag, R. K., Inagaki, M., Yamaguchi, T., Shea, T. B., and Pant, H. C. (2007) Role of phosphorylation on the structural dynamics and function of types III and IV intermediate filaments. *Exp. Cell Res. 313*, 2098–2109.
(32) Hashimoto, R., Nakamura, Y., Komai, S., Kashiwagi, Y., Tamura, K., Goto, T., Aimoto, S., Kaibuchi, K., Shiosaka, S., and Takeda, M. (2000) Site-specific phosphorylation of neurofilament-L is mediated by calcium/calmodulin-dependent protein kinase II in the apical dendrites during long-term potentiation. *J. Neurochem. 75*, 373–382.
(33) Gonda, Y., Nishizawa, K., Ando, S., Kitamura, S., Minoura, Y., Nishi, Y., and Inagaki, M. (1990) Involvement of protein kinase C in the regulation of assembly-disassembly of neurofilaments in vitro. *Biochem. Biophys. Res. Commun. 167*, 1316–1325.
(34) Heins, S., Wong, P. C., Muller, S., Goldie, K., Cleveland, D. W., and Aebi, U. (1993) The rod domain of NF-L determines neurofilament architecture, whereas the end domains specify filament assembly and network formation. *J. Cell Biol. 123*, 1517–1533.
(35) Gill, S. R., Wong, P. C., Monteiro, M. J., and Cleveland, D. W. (1990) Assembly properties of dominant and recessive mutations in the small mouse neurofilament (NF-L) subunit. *J. Cell Biol. 111*, 2005–2019.
(36) Geisler, N., Vandekerckhove, J., and Weber, K. (1987) Location and sequence characterization of the major phosphorylation sites of the high molecular mass neurofilament proteins M and H. *FEBS Lett. 221*, 403–407.
(37) Lee, V. M., Otvos, L., Jr., Carden, M. J., Hollosi, M., Dietzschold, B., and Lazzarini, R. A. (1988) Identification of the major multiphosphorylation site in mammalian neurofilaments. *Proc. Natl. Acad. Sci. U.S. A. 85*, 1998–2002.
(38) Xu, Z. S., Liu, W. S., and Willard, M. B. (1992) Identification of six phosphorylation sites in the COOH-terminal tail region of the rat neurofilament protein M. *J. Biol. Chem. 267*, 4467–4471.
(39) Li, B. S., Veeranna, Gu, J., Grant, P., and Pant, H. C. (1999) Activation of mitogen-activated protein kinases (Erk1 and Erk2) cascade results in phosphorylation of NF-M tail domains in transfected NIH 3T3 cells. *Eur. J. Biochem. 262*, 211–217.
(40) Li, B. S., Veeranna, Gu, J., Grant, P., and Pant, H. C. (1999) Calcium influx and membrane depolarization induce phosphorylation of neurofilament (NF-M) KSP repeats in PC12 cells. *Brain Res. Mol. Brain Res. 70*, 84–91.
(41) Li, B. S., Zhang, L., Gu, J., Amin, N. D., and Pant, H. C. (2000) Integrin alpha(1) beta(1)-mediated activation of cyclindependent kinase 5 activity is involved in neurite outgrowth and human neurofilament protein H Lys- Ser-Pro tail domain phosphorylation. *J. Neurosci. 20*, 6055–6062.
(42) Dashiell, S. M., Tanner, S. L., Pant, H. C., and Quarles, R. H. (2002) Myelin-associated glycoprotein modulates expression and phosphorylation of neuronal cytoskeletal elements and their associated kinases. *J. Neurochem. 81*, 1263–1272.
(43) Ghosh, A., and Greenberg, M. E. (1995) Calcium signaling in neurons: molecular mechanisms and cellular consequences. *Science 268*, 239–247.
(44) Tang, G., Perng, M. D., Wilk, S., Quinlan, R, and Goldman, J. E. (2010) Oligomers of mutant glial fibrillary acidic protein (GFAP) Inhibit the proteasome system in Alexander disease astrocytes, and the small heat shock protein alphaB-Crystallin reverses the inhibition. *J. Biol. Chem. 285*, 10527–10537.
(45) Grant, P, and Pant, H. C. (2000) Neurofilament protein synthesis and phosphorylation. *J. Neurocytol. 29*, 843–872.
(46) Lariviere, R. C., and Julien, J. P. (2004) Functions of intermediate filaments in neuronal development and disease. *J. Neurobiol. 58*, 131–148.
(47) Nixon, R. A. (1993) The regulation of neurofilament protein dynamics by phosphorylation: clues to neurofibrillary pathology. *Brain Pathol. 3*, 29–38.
(48) Nixon, R. A., and Sihag, R. K. (1991) Neurofilament phosphorylation: A new look at regulation and function. *Trends Neurosci. 14*, 501–506.
(49) Zamoner, A., Heimfarth, L., Oliveira Loureiro, S., Royer, C., Mena Barreto Silva, F. R., and Pessoa-Pureur, R. (2008) Nongenomic actions of thyroxine modulate intermediate filament phosphorylation in cerebral cortex of rats. *Neuroscience 156*, 640–652.
(50) Loureiro, S. O., Heimfarth, L., Pelaez, P., de, L., Vanzin, C. S., Viana, L., Wyse, A. T., and Pessoa-Pureur, R. (2008) Homocysteine activates calcium-mediated cell signaling mechanisms targeting the cytoskeleton in rat hippocampus. *Int. J. Dev. Neurosci. 26*, 447–455.

(51) Heimfarth, L., Oliveira Loureiro, S., Zamoner, A., de Lima Pelaez, P., Nogueira, C. W., Rocha, J. B. T., and Pessoa-Pureur, R. (2008) Effects of in vivo treatment with diphenyl ditelluride on the phosphorylation of cytoskeletal proteins in cerebral cortex and hippocampus of rats. *Neurotoxicology 29*, 40–47.

(52) de Mattos-Dutra, A ., de Freitas, M. S., Schroder, N., Lisboa, C. S. F., Pessoa-Pureur, R., and Wajner, M. (1997) In vitro phosphorylation of cytoskeletal proteins in the rat cerebral cortex is decreased by propionic acid. *Exp. Neurol. 147*, 238–247.

(53) de Mattos-Dutra, A., Sampaio de Freitas, M., and Pessoa-Pureur, R. (1998) Calcineurin dephosphorylates NF-M and β-tubulin of the cytoskeletal fraction from rat cerebelum. *Med. Sci. Res. 26*, 111–114.

(54) Carreras, A. L., de Mattos-Dutra, A., Meirelles, R., Bevilaqua da Rocha, B., Wannmacher, C. M. D., and Pessoa-Pureur, R. (2000) Phenylalanine inhibition of the phosphorylation of cytoskeletal proteins from cerebral cortex of young rats is prevented by alanine. *Eur. J. Clin. Invest. 30*, 536–542.

(55) Loureiro, S. O., Heimfarth, L., Lacerda, B. A., Vidal, L. F., Soska, A., dos Santos, N. G., de Souza Wyse, A. T., and Pessoa-Pureur, R. (2010) Homocysteine induces hypophosphorylation of intermediate filaments and reorganization of actin cytoskeleton in C6 glioma cells. *Cell. Mol. Neurobiol. 30*, 557–568.

(56) Petragnani, N. (1994) Preparation of the principal classes of organic tellurium compounds. In *Tellurium in Organic Synthesis*, Academic Press, London, pp 9−88.

(57) Hou, X., Wang, O., Li, Z., Mou, H., Chen, J., Deng, B., Qian, L., Liu, X., and Le, Y. (2011) Upregulation of pancreatic derived factor (FAM3B) expression in pancreatic β-cells by MCP-1 (CCL2). *Mol. Cell. Endocrinol. 343*, 18–24.

(58) Katayama, T., Tanaka, H., Yoshida, T., Uehara, T., and Minami, M. (2009) Neuronal injury induces cytokine-induced neutrophil chemoattractant-1 (CINC-1) production in astrocytes. *J. Pharmacol. Sci. 109*, 88–93.

(59) Rigon, A. P., Cordova, F. M., Oliveira, C. S., Posser, T., Costa, A. P., Silva, I. G., Santos, D. A., Rossi, F. M., Rocha, J. B. T., and Leal, R. B. (2008) Neurotoxicity of cadmium on immature hippocampus and a neuroprotective role for p38MAPK. *NeuroToxicology 29*, 727–734.

(60) Funchal, C., de Almeida, L. M., Oliveira Loureiro, S., Vivian, L., de Lima Pelaez, P., Dall Bello Pessutto, F., Rosa, A. M., Wajner, M., and Pessoa-Pureur, R. (2003) In vitro phosphorylation of cytoskeletal proteins from cerebral cortex of rats. *Brain Res. Prot. 11*, 111–118.

(61) Lowry, O. H., Rosebrough, N. J., Farr, A. L., and Randall, R. J. (1951) Protein measurement with the Folin phenol reagent. *J. Biol. Chem. 193*, 265–275.

(62) Laemmli, U. K. (1970) Cleavage of structural proteins during the assembly of the head of bacteriophage T4. *Nature 277*, 680–685.

(63) Sihag, R. K., and Nixon, R. A. (1990) Phosphorylation of the amino terminal head domain of the middle molecular mass 145 kDa subunit of neurofilaments. *J. Biol. Chem. 265*, 4166–4171.

(64) Shetty, K. T., Kink, W. T., and Pant, H. C. (1993) Cdc-like kinase from rat spinal cord specifically phosphorylates KSPXK motifs in neurofilament proteins: Isolation and characterization. *Proc. Natl. Acad. Sci. U.S.A. 90*, 6844–6848.

(65) Guidato, S., Tsai, L. H., Woodgett, J., and Miller, C. C. (1996) Differential cellular phosphorylation of neurofilament heavy side arms by glycogen synthase kinase-3 and cyclin-dependent kinase-5. *J. Neurochem. 66*, 1698–1706.

(66) Sun, D., Leung, C. L., and Liem, R. K. (1996) Phosphorylation of the high molecular weight neurofilament protein (NF-H) by Cdk5 and p35. *J. Biol. Chem. 271*, 14245–14251.

(67) Veeranna, Amin, N. D., Ahn, N. G., Jaffe, H., Winters, C. A., Grant, P., and Pant, H. C. (1998) Mitogen-activated protein kinases (Erk1, 2) phosphorylate Lys−Ser−Pro (KSP) repeats in neurofilament proteins NF-H and NF-M. *J. Neurosci. 18*, 4008–4021.

(68) Stull, J. T. (2001) Ca2+-dependent cell signaling through calmodulin-activated protein phosphatase and protein kinases minireview series. *J. Biol. Chem. 276*, 2311–2312.

(69) Rice, D., and Barone, S., Jr. (2000) Critical periods of vulnerability for the developing nervous system: evidence from humans and animal models. *Environ. Health Perspect. 108*, 511–533.

(70) Bito, H., Deisseroth, K., and Tsien, R. W. (1996) CREB phosphorylation and dephosphorylation: A Ca2+ and stimulus duration-dependent switch for hippocampal gene expression. *Cell 87*, 1203–1214.

(71) Deisseroth, K., Heist, E. K., and Tsien, R. W. (1998) Translocation of calmodulin to the nucleus supports CREB phosphorylation in hippocampal neurons. *Nature 392*, 198–202.

(72) Dolmetsch, R. E., Pajvani, U., Fife, K., Spotts, J. M., and Greenberg, M. E. (2001) Signaling to the nucleus by an L-type calcium channel-calmodulin complex through the MAP kinase pathway. *Science 294*, 333–339.

(73) Mermelstein, P. G., Bito, K., Deisseroth, K., and Tsien, R. W. (2000) Critical dependence of cAMP response element binding protein phosphorylation on L-type calcium channels supports a selective response to EPSPs in preference to action potentials. *J. Neurosci. 20*, 266–273.

(74) Bootman, M. D., Collins, T. J., Peppiatt, C. M., Prothero, L. S., MacKenzie, L., De Smet, P., Travers, M., Tovey, S. C., Seo, J. T., Berridge, M. J., Ciccolini, F., and Lipp, P. (2001) Calcium signalling—An overview. *Semin. Cell Dev. Biol. 12*, 3–10.

(75) Peuchen, S., Clark, J. B., and Duchen, M. R. (1996) Mechanisms of intracellular calcium regulation in adult astrocytes. *Neuroscience 71*, 871–883.

(76) Zamoner, A., Funchal, C., Heimfarth, L., Silva, F. R., and Pessoa-Pureur, R. (2006) Short-term effects of thyroid hormones on cytoskeletal proteins are mediated by GABAergic mechanisms in slices of cerebral cortex from young rats. *Cell. Mol. Neurobiol. 26*, 209–224.

(77) Funchal, C., Zamoner, A., dos Santos, A. Q., Loureiro, S. O., Wajner, M., and Pessoa-Pureur, R. (2005) Alpha-ketoisocaproic acid increases phosphorylation of intermediate filament proteins from rat cerebral cortex by mechanisms involving Ca2+ and cAMP. *Neurochem. Res. 30*, 1139–1146.

(78) de Freitas, M. S., de Mattos-Dutra, A., Wannmacher, C. M., and Pessoa-Pureur, R. (1996) Ca(2+)-mediated phosphorylation and proteolysis activity associated with the cytoskeletal fraction from cerebral cortex of rats. *Neurochem. Res. 21*, 1489–1495.

(79) de Mattos-Dutra, A., Meirelles, R., Bevilaqua da Rocha, B., Kommers, T., Wofchuk, S. T., Wajner, M., and Pessoa-Pureur, R. (2000) Methylmalonic and propionic acids increase the in vitro incorporation of 32P into cytoskeletal proteins from cerebral cortex of young rats through NMDA glutamate receptors. *Brain Res. 856*, 111–118.

(80) Funchal, C., de Lima Pelaez, P., Loureiro, S. O., Vivian, L., Dall Bello Pessutto, F., de Almeida, L. M., Tchernin Wofchuk, S., Wajner, M., and Pessoa Pureur, R. (2002) alpha-Ketoisocaproic acid regulates phosphorylation of intermediate filaments in postnatal rat cortical slices through ionotropic glutamatergic receptors. *Brain Res. Dev. Brain Res. 139*, 267–276.

(81) Funchal, C., Zamoner, A., dos Santos, A. Q., Moretto, M. B., Rocha, J. B., Wajner, M., and Pessoa-Pureur, R. (2005) Evidence that intracellular Ca2+ mediates the effect of alpha-ketoisocaproic acid on the phosphorylating system of cytoskeletal proteins from cerebral cortex of immature rats. *J. Neurol. Sci. 238*, 75–82.

(82) Slater, S. J., Ho, C., and Stubbs, C. D. (2002) The use of fluorescent phorbol esters in studies of protein kinase C-membrane interactions. *Chem. Phys. Lipids. 116*, 75–91.

(83) Jaffe, H., Veeranna, Shetty, K. T., and Pant, H. C. (1998) Characterization of the phosphorylation sites of human high molecular weight neurofilament protein by electrospray ionization tandem mass spectrometry and database searching. *Biochemistry 37*, 3931–3940.

(84) Ji, R.-R., and Strichartz1, G. (2004) Cell signaling and the genesis of neuropathic pain. *Sci. STKE 252*, No. re14, DOI: 10.1126/stke.2522004re14].

(85) Motil, J., Chan, W. K., Dubey, M., Chaudhury, P., Pimenta, A., Chylinski, T. M., Ortiz, D. T., and Shea, T. B. (2006) Dynein mediates

retrograde neurofilament transport within axons and anterograde delivery of NFs from perikarya into axons: regulation by multiple phosphorylation events. *Cell Motil. Cytoskeleton* 63, 266–286.

(86) Moretto, M. B., Boff, B., Franco, J., Posser, T., Roessler, T. M., Souza, D. O., Nogueira, C. W., Wofchuk, S., and Rocha, J. B. (2007) (45)Ca(2+) influx in rat brain: effect of diorganylchalcogenides compounds. *Toxicol. Sci.* 99, 566–571.

PARTE 3

5. DISCUSSÃO

O telúrio é um elemento traço usado como componente industrial de muitas ligas e na indústria eletrônica. Na forma de telureto de hidrogênio (H_2Te) pode estar ligado a proteínas (por exemplo, proteínas da pele e do cabelo) e apresentar uma taxa de eliminação muito lenta (Russel, 1992). O telúrio é uma substância tóxica, a qual pode produzir além de sintomas neurotóxicos como diminuição do aprendizado e da memória espacial (Walbran and Robins, 1978; Widy-Tyszkiewicz et al., 2002) e desmielinização do sistema nervoso periférico (Wagner-Recio et al., 1991; Laden e Porter, 2001), toxicidade reprodutiva, caracterizada por teratogênese (Stangherlin et al., 2006).

A importância da exposição ocupacional a compostos contendo telúrio tem crescido nos últimos anos, entretanto a clínica e a bioquímica dessa exposição são fracamente compreendidas. O contato com o telúrio nas suas diferentes formas pode afetar o desenvolvimento e a função cerebral causando hidrocefalia, hipomielinização ou desmielinização (Peres-D`Gregório e Miller, 1988; Taylor; 1996).

O composto orgânico de telúrio $(PhTe)_2$ pode afetar o sistema glutamatérgico (Nogueira et al., 2001; Borges et al., 2004; Souza et al., 2010) e alterar atividade de enzimas, como a delta-aminolevulinato dehidratase (Maciel *et al*., 2000; Nogueira *et al*, 2003) e Na^+-K^+-ATPase (Borges *et al*., 2005). Estudos em cultura de astrócitos mostraram que o $(PhTe)_2$ é citotóxico para esse tipo celular (Roy e Hardej, 2011). Os danos neurotóxicos causados pelo composto orgânico do telúrio podem estar relacionados, pelo menos em parte, a alterações na função dos canais de cálcio, levando à alteração na homeostase desse segundo mensageiro celular (Moretto et al. 2007).

Estudos prévios de nosso laboratório já demonstraram que o citoesqueleto é alvo do $(PhTe)_2$ e que a ação desse composto sobre essa rede complexa de filamentos proteicos é dependente da estrutura cerebral (Heimfarth et al., 2008). O rompimento da homeostase do citoesqueleto neural tem sido relacionado à neurodegeneração (O'Callaghan, 1994) e modificações no nível de fosforilação de proteínas do citoesqueleto são consideradas eventos críticos na patologia do sistema nervoso central (Koliatsos *et al.*, 1989), podendo levar as células neuronais à morte, causando disfunção neurológica. Várias doenças neurodegenerativas humanas, como Doença de Alzheimer, Parkinson, Huntington, Pick e Demência com corpos de Lewy, são caracterizadas pelo acúmulo de agregados de FI relativamente insolúveis no corpo celular (Goedert, 1998; Julien e Mushynski, 1998; Julien, 1999; Diprospero *et al.*, 2004).

O desenvolvimento do sistema nervoso central é um ponto chave na ação do composto orgânico de telúrio. Desordens do desenvolvimento podem envolver lesões por um agente tóxicos, resultando em processos destrutivos com rápido crescimento cerebral e diferenciação (Morgane et al., 2002). Além disso, a via de administração da droga, bem como a estrutura cerebral afetada também interferem nas características neurotóxicas de um composto.

Com base no que foi exposto acima, esse trabalho teve como objetivo principal verificar o efeito do $(PhTe)_2$ sobre o citoesqueleto cerebral do estriado, cerebelo, hipocampo e córtex cerebral. Além disso, teve como objetivo também tentar compreender como essa droga neurotóxica poderia causar o quadro de neurodegeneração verificado em animais expostos a essa substância. Para isso, utilizamos 3 modelos de administração do $(PhTe)_2$, tentando entender a relação entre o tipo de exposição ao neurotoxicante e os efeitos desencadeados pela mesma. O primeiro modelo é uma injeção subcutânea de $(PhTe)_2$ em ratos jovens, mimetizando o contato

direto, ou *in vivo*, com o organotelureto e a influência de todo o organismo em sua ação sobre o citoesqueleto cerebral. O segundo modelo, também considerado um modelo *in vivo*, é o da transmissão vertical, ou seja, mãe-filhote, através do leite materno. O terceiro modelo tem como objetivo verificar o efeito dessa droga adicionada diretamente sobre a fatia da estrutura cerebral estudada, caracterizando um modelo *in vitro*. O modelo *in vitro* nos permite investigar mais profundamente as vias de sinalização que participam da ação da toxina.

5.1. Modelo 1: Efeito *in vivo* da administração subcutânea do $(PhTe)_2$ sobre o citoequeleto de ratos jovens

Nesse trabalho estudamos o efeito de uma única administração subcutânea de $(PhTe)_2$ sobre o citoesqueleto de ratos jovens. Animais de 15 dias de idade foram submetidos a uma única administração de 0,3 µMol de $(PhTe)_2$ /Kg de peso corporal e os parâmetros analisados foram determinados no estriado e cerebelo 3 e 6 dias após a administração da droga. Estudos prévios de nosso grupo já haviam demonstrado a toxicidade do organotelureto quando administrado por essa via, utilizando como parâmetro a diminuição do peso corporal dos animais (Heimfarth et al., 2008). Além disso, a suscetibilidade do citoesqueleto a esta toxina manifestada através do desequilíbrio do sistema fosforilante associado aos FIs gliais e neuronais foi também descrita por nós em córtex cerebral e hipocampo de ratos jovens, onde verificamos um aumento de fosforilação dessas proteínas do citoesqueleto (Heimfarth et al. 2008).

No presente trabalho, os resultados mostraram que o $(PhTe)_2$ administrado subcutaneamente (0,3 µmol/kg) em animais de 15 dias causa hiperfosforilação dos FIs neuronais e gliais no cerebelo e estriado. Esses achados estão de acordo os resultados

obtidos anteriormente para o córtex cerebral e hipocampo. No córtex cerebral (Heimfarth et al., 2008) e estriado essa modificação no citoesqueleto ocorre 3 (figura11, resultados suplementares) e 6 dias após a injeção da droga. Já o cerebelo apresenta seus FIs hiperfosforilados 3 dias após o contato com o composto orgânico de telúrio, não se verificando alteração alguma 6 dias após. O hipocampo, como demonstrado Heimfarth et al., 2008, só responde à ação da toxina 6 dias após a injeção subcutânea da mesma e apenas nas proteínas gliais (GFAP e vimentina), mostrando que nestas condições apenas o citoesqueleto dos astrócitos, não dos neurônios, foi responsivo à droga. O conjunto desses resultados mostra que cada estrutura cerebral responde de maneira diferente ao mesmo insulto com esse neurotoxicante e que pode existir janelas de suscetibilidade do sistema fosforilante associado ao citoequeleto nas diferentes estruturas cerebrais. Entretanto, em todas elas ocorre um aumento na incorporação de fosfato aos resíduos de serina, treonina ou tirosina de suas proteínas.

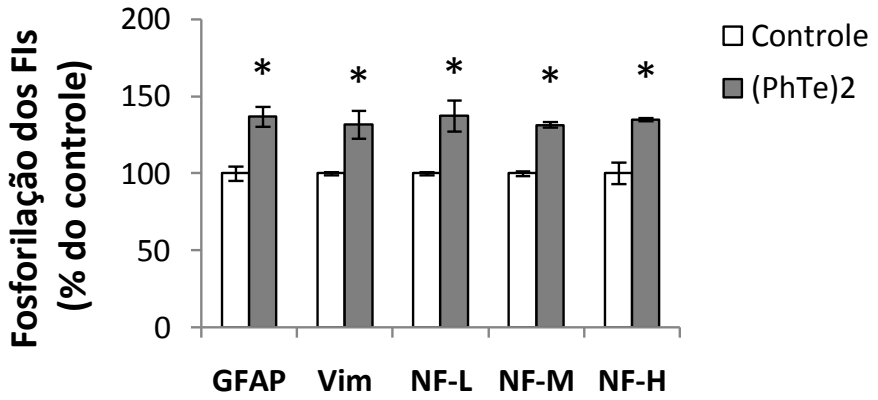

Figura 11: Efeito do $(PhTe)_2$ administrado subcutaneamente em ratos de 15 dias sobre a fosforilação dos FIs gliais e neuronais 3 dias após o contato com a droga. NF-H, neurofilamento de alto peso molecular; NF-M, neurofilamento de médio peso molecular; NF-L, neurofilamento de baixo peso molecular; GFAP, proteína glial fibrilar

ácida. Dados são descritos como média ±E.P.M de 8 animais e expressos como % do controle. Diferenças estatisticamente significativas comparadas com os animais controle, que receberam óleo de canola, foram determinadas por ANOVA de uma via, seguida pelo pós-teste Tukey-Kramer e são indicadas por: $p<0,05$.

Um ponto importante a salientar é que estruturas relacionadas com a motricidade, como córtex cerebral, estriado e cerebelo (Squire et al., 2008), são afetadas na mesma janela de suscetibilidade, ou seja, quando o animal atinge 18 dias de idade (3 dias após a injeção); enquanto que o hipocampo, estrutura cerebral relacionada ao aprendizado e memória (Bear et al., 2008) apresenta outra janela de suscetibilidade, aos 21 dias de idade, ou 6 dias após a injeção. As ações do $(PhTe)_2$ nas estruturas motoras, que estamos demonstrando, podem estar relacionadas com achados anteriores que mostram que a exposição a compostos de telúrio pode conduzir a deficiências motoras em modelos experimentais, especialmente por causa de suas propriedades desmielinizantes (Rawlins e Smith, 1971, Said e Duckett, 1981, Said et al., 1981, Wagner-Recio *et al*., 1991, Laden e Porter, 2001).

A fosforilação dos FIs envolve um complexo balanço entre as atividades de quinases e fosfatases associadas ao citoesqueleto (Nixon, 1994; Pant et al., 2000). A hiperfosforilação das subunidades dos FIs neuronais, NF-L, NF-M e NF-H, bem como da GFAP e vimentina dos astrócitos refletem uma alteração na atividade do sistema fosforilante associado ao citoesqueleto. A importância fisiológica da fosforilação dos NFs não é completamente compreendida, entretanto sabe-se que uma alteração no estado de fosforialação da NF-L está relacionada com a associação da estrutura do FI propriamente dito (Sihag et al 2007). Resultados *in vitro* mostram que a fosforilação dos

domínios carboxi-terminais da NF-M e NF-H organiza os NFs individuais e promove o alinhamento dos feixes (Leterrier et al 1996). Por outro lado, vários autores demonstraram que a fosforilação dessas subunidades está associada com um aumento no espaço entre os NFs *in vivo* (Hsieh et al 1994) e relacionada com a interação dessas proteínas com outros elementos do citoesqueleto (Gotow et al 1994). Além disso, alteração no estado de fosforilação da NF-M e NF-H pode modificar o transporte axonal (Sihag et al., 1991; 2007).

Para tentar compreender melhor como o $(PhTe)_2$ age sobre a homeostase do sistema de fosforilação dos NFs, GFAP e vimentina, estudamos importantes vias de sinalização envolvidas com essa modificação pós-traducional dos FIs.

Nossos resultados mostraram que o composto orgânico de telúrio quando administrado por via subcutânea em animais de 15 dias de idade é capaz de ativar a PKA no estriado e no cerebelo, e causar hiperfosforilação do resíduo serina 55 da NF-L. A PKA é uma importante enzima envolvida em várias vias de sinalização, sendo que um dos seus alvos é o citoesqueleto neural. Ela está envolvida com a fosforilação da GFAP (Funchal et al., 2005), bem como com o resíduo Ser23 da NF-M e Ser55 da NF-L na região amino-terminal (Ram et al., 1991; Sihag et al., 1999). É importante notar que a fosforilação de subunidades dos FIs mediada por serina-treonina quinases dependentes de segundos mensageiros como a PKA (Ser-55), a PKC (Ser-51) e a PKCaMII (Ser-57) é relevante para a polimerização/associação do filamento propriamente dito. Além disso, o fosfato adicionado na subunidade NF-L durante a polimerização/associação do NF é rapidamente removido, sugerindo um possível papel de bloqueio na associação dos NFs antes deles serem transportados para os neuritos (Sihag e Nixon, 1991). Podemos propor, então, que o $(PhTe)_2$ esteja causando uma

alteração no equilíbrio de associação/desassociação dos FIs, levando a um aumento das subunidades solúveis livres no citoplasma.

Além da ativação de quinases dependentes de segundos mensageiros, uma administração subcutânea de $(PhTe)_2$ causa, também, ativação da via das MAPK tanto no estriado, quanto no cerebelo. Provavelmente esse aumento da forma fosforilada da ERK1/2, JNK ou p38MAPK, que é a forma ativa dessas enzimas, esteja relacionado com a hiperfosforilação da NF-M e da NF-H nos sítios KSP. Os sítios de fosforilação de quinases independentes de segundos mensageiros como as MAPK e a CDK5 nos FIs estão localizados nas sequências de repetição dos aminoácidos lisina, serina e prolina (KSP) na região carboxi-terminal das subunidades NF-M e NF-H dos NFs (Geisler et al., 1987, Xu et al., 1992).

Alteração de fosforilação na região carboxi-terminal leva a uma modificação no transporte axonal (Strack *et al*., 1997, Motil et al., 2006, Sihag et al. 2007). Isso pode estar acontecendo, pois o aumento das cargas negativas dos grupos fosfato restringe a associação dos NFs com a quinesina, a proteína axonal motora anterógrada, bem como demonstra uma afinidade com a dineína, a proteína motora retrógrada (Motil et al., 2006). Além disso, a fosforilação dos NFs na região carboxi-terminal promove a associação entre eles, conduzindo a formação de aglomerados de NFs (Yabe et al., 2001a,b). Essas duas características levam provavelmente a uma alteração no transporte axonal, podendo contribuir, em parte, pelos danos neuronais provocados pelo neurotoxicante.

A fosforilação anormal dos NFs pode também estar envolvida com a excitotoxicidade glutamatérgica. O tratamento de culturas primárias de neurônios com glutamato em concentração descrita por provocar excitoxicidade ativa membros da

família das MAPK, os quais fosforilam os NFs, levando a um transporte axonal mais lento (Ackerley, 2000). O glutamato também conduz à ativação da proteína quinase N1 (PKN1), uma enzima que fosforila os NFs na região amino-terminal. A PKN1 rompe a organização dos NFs e altera o transporte axonal (Manser et al., 2008). A excitotoxicidade mediada por receptores NMDA também está associada com a co-localização aberrante das proteínas de NFs, tanto fosforiladas quanto desfosforildas (King et al., 2007). Além disso, estudos têm demonstrado que o riluzole, inibidor da liberação de glutamato, protege contra a alteração do transporte axonal por diminuir a fosforilação dos NFs, provavelmente através da diminuição da atividade da ERK e da p38MAPK (Stevenson et al., 2009). Agregados de NFs também levam ao aumento dos níveis intracelulares de cálcio e à morte celular induzida pela ativação do receptor NMDA, sugerindo, portanto que agregados de NFs deixam os neurônios mais susceptíveis a excitotocicidade glutamatérgica (Sanelli et al., 2007). Podemos propor, então, que o quadro de neurodegeneração visto em animais tratados com $(PhTe)_2$ pode estar relacionado a uma excitotoxicidade glutamatérgica, levando a ativação de quinases, que por sua vez hiperfoforilam os FIs neuronais, causando um acúmulo dos mesmos no corpo celular, o que provocaria uma diminuição do transporte axonal e morte celular. Os resultados obtidos para o cerebelo nesse trabalho e outros estudos com $(PhTe)_2$ demonstraram que esse composto é capaz de inibir a captação de glutamato, levando a um quadro de excitotoxicidade glutamatérgica (Moretto et al., 2007). Além disso, o sistema glutamatérgico está envolvido com alterações de fosforilação dos FIs induzidas por outros metabólitos em diferentes estruturas cerebrais (Loureiro et al., 2010, Pierozan et al., 2012).

Os astrócitos são células importantes para manter a homeostase do glutamato, pois retiram o mesmo da fenda sináptica, impedindo assim um aumento dos seus níveis,

o que é prejudicial à célula (Rothstein et al, 1996). Estudos têm mostrado que distúrbios na captação de glutamato por essas células estão diretamente envolvidos com desordens neurodegenerativas (revisado por Seifert et al., 2006). Portanto, alterações na fisiologia dos astrócitos também podem contribuir para uma excitotoxicidade glutamatérgica, levando à neurodegeneração.

Para melhor entender os mecanismos moleculares que levam ao quadro de neurodegeneração visto nos animais submetidos a uma administração de $(PhTe)_2$ analisamos vias de morte celular. Para isso, medimos a ativação da caspase 3 e encontramos que essa enzima está ativa 6 dias após a injeção tanto no estriado, quanto no cerebelo. A ativação de caspases, e a caspase 3 em particular, parece ser o maior fator que leva a apoptose neuronal (Yakovlev e Faden 2001). Levando em consideração que o $(PhTe)_2$ altera a homeostase do glutamato, pode-se propor que a excitotoxicidade glutamatérgica está envolvida com a ativação da caspase 3. Relatos da literatura tem mostrado que o glutamato estimula a clivagem da pró-caspase 3 em caspase ativa (Hassanzadeh et al., 2011), levando à ativação das vias apoptóticas. Além disso, é bem conhecido que a JNK/SAP e a p38 MAPK medeiam a morte neuronal induzida por glutamato (Schwarzschild et al., 1997; Segura-Torres et al., 2006). Ramin et al., 2011 mostraram que uma inibição da JNK/SAP provoca uma diminuição na ativação da caspase 3 induzida pelo peptídeo β-amilóide, bem como uma redução no imunoconteúdo do fator Bax e um aumento do imunoconteúdo do fator Bcl-2, proteínas pró-apoptóticas e anti-apoptóticas respectivamente. Portanto, podemos propor que o $(PhTe)_2$ esteja causando uma excitotoxicidade glutamatérgica, que acarretaria na ativação da via das MAPK, que por sua vez ativas estariam agindo sobre as caspases, ativando as mesmas e provocando o quadro de neurodegeneração verificado em animais expostos a esse elemento.

Outra importante via de sobrevivência celular é a via da fosfatidil-inositol-3-quinase/AKT (PI3K/AKT) (Datta et al., 1999). A identificação de vários substratos para essa serina/treonina quinase sugerem que ela bloqueia a morte celular por agir sobre a maquinaria de morte celular citoplasmática, bem como regular a expressão de genes envolvidos com a morte e sobrevivência celular (Koh et al 2004). A AKT inibe a liberação do citocromo c da mitocôndria, impedindo assim a ativação da via intrínseca das caspases (Cardone et al 1998). Nossos resultados mostraram que uma administração subcutânea de $(PhTe)_2$ diminui a forma fosforilada da AKT, que é a sua forma ativa, no estriado e no cerebelo, deixando a enzima inativa e consequentemente ativando vias de morte celular, uma vez que ela não consegue mais agir sobre os fatores anti-apoptóticos. Esse resultado corrobora os dados anteriores que mostraram que esse organocalcogênio está ativando vias de morte celular, levando à neurodegeneração.

Então, levando em consideração tudo o que já foi discutido até o presente momento, podemos propor que o quadro de neurodegeneração causado pelo $(PhTe)_2$ tanto em estriado, quanto no cerebelo possa estar associado tanto a uma alteração no citoesqueleto neural, quanto à ativação de vias de morte celular, sendo as células neuronais muito susceptíveis à ação dessa droga. É importante salientar, entretanto, que, no estriado, uma alteração de fosforilação dos FIs está acompanhada de morte celular, enquanto no cerebelo isso não ocorre. Verifica-se que os FIs estão hiperfosforilados nas células cerebelares 3 dias após a injeção e seu estado de fosforilação volta ao normal 6 dias após o contato com a droga. Já a morte neuronal ocorre 6 dias após, mostrando que, nessa estrutura, uma alteração de fosforilação precede a morte neuronal. .

Danos ao sistema nervoso central decorrentes de um trauma mecânico, de uma doença ou por ação de uma neurotoxina podem desencadear um processo denominado astrogliose, ou seja, os astrócitos se tornam reativos (Pekny e Nilsson, 2005). A

astrogliose pode ser considerada como um processo desencadeado para restaurar a homeostase cerebral no processo de injúria. Isso ocorre através de importantes funções que incluem a formação de cicatrizes gliais, regulação da resposta imune, modulação da sobrevivência neuronal e crescimento dos neuritos (Sofroniew, 2009). Morfologicamente a astrogliose é caracterizada por mudanças que incluem hipertrofia, estrelação e proliferação dos astrócitos, além de numerosas mudanças bioquímicas que incluem a superexpressão da GFAP, as quais alteram as funções e a viabilidade neuronal (Pekny e Nilsson, 2005). A astrogliose reativa induz a expressão de proteínas capazes de serem benéficas ou prejudiciais aos neurônios, sendo que as consequências dependem de outros fatores, tais como, a idade do organismo, o tipo e a extensão da lesão (Sofroniew, 2009). Além disso, também é descrita a ativação de caspases, principalmente as caspases 3 e 11 em astrócitos em processo de gliose reativa, mostrando um papel não apoptótico para essa enzima (Aras et al., 2012). Similarmente às caspases, a p38/MAPK, que é comumentemente ativada em processos de morte celular, e a ERK também contribuem para o processo de astrogliose (Che et al., 2001 a,b; Ito et al 2009).

Resultados obtidos nesse trabalho demonstraram que o $(PhTe)_2$ injetado subcutaneamente em ratos jovens causa reatividade astrocitária. Essa conclusão baseia-se no fato de que esse composto é capaz de aumentar a expressão da proteína GFAP, um marcador astrocitário, bem como aumentar a quantidade de células GFAP positivas. Esse processo de astrogliose é verificado tanto no estriado, quanto no cerebelo e pode estar ocorrendo, inicialmente, para tentar proteger os neurônios da ação do neurotoxicante, sendo que, com o passar do tempo, pode se tornar prejudicial às células neuronais. Tanto no estriado, quanto no cerebelo verificamos morte neuronal associada à proliferação de astrócitos 6 dias após a administração da droga, indicando que,

provavelmente, nessa etapa da intoxicação os astrócitos reativos estejam secretando fatores tóxicos para os neurônios. No estriado, entretanto, verificou-se também uma ativação da via das MAPK 6 dias após o insulto, mostrando que provavelmente essa rota esteja envolvida tanto com a morte neuronal, quanto com o processo de astrogliose. Portanto, podemos propor que a via das MAPK pode ter papel duplo, agindo de diferentes maneiras nos diferentes tipos celulares: em neurônios ativam vias de morte celular e em astrócitos desencadeiam a proliferação.

No cerebelo não temos ativação da via das MAPK 6 dias após a injeção da droga, entretanto, verificamos ativação da ERK1/2 e da p38/MAPK e um aumento da quantidade de GFAP em animais expostos ao $(PhTe)_2$ 3 dias após a administração do telúrio, mostrando que já existe um fenômeno de astrogliose em tempos mais curtos nessa estrutura cerebral. Surpreendentemente, não se verificou morte celular nos animais de 18 dias (3 dias após a administração do $(PhTe)_2$), somente quando eles completavam 21 dias (6 dias após a administração do $(PhTe)_2$), indicando que o processo de astrogliose precedeu a morte, provavelmente para tentar proteger os neurônios da ação desse neurotoxicante. No entanto, não podemos descartar a hipótese de que a astrogliose tenha sido um fator desencadeante da morte neuronal. De acordo com Sofroniew, 2009 a astrogliose pode ser tanto um fator de morte neuronal quanto de neuroproteção. Podemos também supor que a ativação da via das MAPK, além de regular a homeostase do citoesqueleto neuronal atuando sobre o nível de fosforilação dos NFs, esteja envolvida com o desenvolvimento da astrogliose nos animais mais jovens.

Podemos concluir, portanto, que uma injeção subcutânea de $(PhTe)_2$ em animais de 15 dias afeta o citoesqueleto, bem como a rota das MAPK, AKT e PKA no estriado e cerebelo, sendo que essas alterações podem estar relacionadas com o quadro de

neurodegeneração verificado nos animais. Entretanto, a alteração no citoesqueleto é diferente nas duas estruturas cerebrais, sendo que o efeito no estriado é mais persistente, pois começa 3 dias após a injeção e permanece até 6 dias após a administração da droga, sendo concomitante com a ativação de vias de morte celular. Já no cerebelo, alteração de fosforilação nos FIs é vista apenas em tempos curtos, não persistindo até o sexto dia, quando ocorre a morte celular. Não podemos, entretanto, descartar a possibilidade de no cerebelo termos alteração de fosforilação dos FIs juntamente com a ativação das vias de morte celular nos dias intermediários, ou seja, 4 ou 5 dias após a injeção. Além disso, também não podemos descartar a possibilidade de que o nível de fosforilação dos FIs volte aos valores dos animais controle no estriado de animais mais velhos, porém ainda persista a ativação das vias de apoptose e necrose.

5.2. Modelo 2: Efeito do $(PhTe)_2$ transmitido verticalmente (através do leite materno) sobre o citoequeleto de ratos jovens

As consequências, sobre o sistema nervoso central, da exposição a uma toxina durante o período de lactação não são bem compreendidas. Além disso, a barreira hematoencefálica não está completamente formada nesse período pós-natal, portanto drogas presentes no leite materno podem alcançar o sistema nervoso central da prole, interferindo no seu desenvolvimento (Favero et al., 2006), por essa razão estudos utilizando essa via de transmissão são extremamente relevantes.

Relatos da literatura têm demonstrado que o $(PhTe)_2$ administrado em ratas adultas durante o período de lactação causa alteração nos filhotes (Stangherlin et al, 2009 a, b). Nesse trabalho, portanto, investigamos o efeito da administração subcutânea do composto orgânico do telúrio (0,01 mg/kg de peso corporal) nas mães durantes os

primeiros 14 dias de lactação (P0-P13) sobre parâmetros bioquímicos no córtex cerebral, hipocampo, estriado e cerebelo dos filhotes, quando esses tinham 15, 21, 30 ou 45 dias. O alvo principal desse estudo foi alterações no citoesqueleto cerebral, usando como foco a fosforilação dos FIs gliais e neuronais. Além disso, também analisamos a influência desse tratamento na atividade de importantes enzimas do sistema fosforilante associados ao citoesqueleto.

Inicialmente foi determinado se esse tipo de exposição causava toxicidade aparente nas mães e nos filhotes. Nós verificamos anteriormente (Heimfarth et al., 2008) que ratos jovens submetidos a uma injeção subcutânea de $(PhTe)_2$ apresentam diminuição do peso corporal. Os resultados desse estudo, entretanto, mostraram que esse tipo de exposição não provoca alteração nesse parâmetro nas mães. Além disso, não ocorre alteração no desenvolvimento ou no ganho de peso corporal nos filhotes. Isso está de acordo com outros relatos da literatura que também não viram alteração no peso corporal das mães, nem dos filhotes nesse modelo de exposição ao $(PhTe)_2$ (Stangherlin et al, 2009 a, b).

O $(PhTe)_2$ administrado nas mães causa alteração no sistema fosforilante associado ao citoesqueleto dos filhotes. Esses efeitos são tempo e estrutura dependentes, ou seja, o desenvolvimento do animal, bem como as características individuais de cada estrutura são fundamentais para a ação desse composto. Isso pode ser explicado, pois as várias partes do cérebro se desenvolvem em tempos diferentes e apresentam diferentes janelas de vulnerabilidade a neurotoxicantes, tanto quando no estágio pré-natal, quanto pós-natal. Isso é baseado na maturação regional e temporal, através de múltiplos processos de desenvolvimento (Rice e Barone, 2000). Os roedores possuem, no período pós-natal, um considerável desenvolvimento do cérebro, caracterizado por uma intensa síntese de proteínas (Gottlieb et al., 1977). De fato, a maturação ocorre por diversas

semanas após o nascimento, durante as quais o cérebro é extremamente sensível a agentes químicos ou ambientais que podem induzir o aparecimento de alterações nos animais (Favero el al., 2006). Além disso, durante o desenvolvimento as sinapses formadas geram algumas conexões que existem apenas transientemente, ou seja, há eliminação de conexões sinápticas durante o amadurecimento (Squire et al., 2008). Essa alteração na quantidade de sinapses do SNC pode influenciar na resposta de uma estrutura cerebral ao contato com uma substância tóxica. Além disso, outro estudo já demonstrou que a toxicidade induzida por esse organotelureto é dependente da idade do animal e consequentemente do estágio de desenvolvimento do cérebro (Souza et al., 2010). Esse neurotoxicante induz mudanças na homeostase do glutamato de uma maneira dependente da idade do animal (Souza et al., 2010).

Outro ponto importante a salientar é que o contato com neurotoxinas durante o período pré e/ou pós natal pode alterar a expressão de receptores, neurotransmissores e proteínas importantes para a transmissão normal dos sinais. Wang et al., 2012 mostraram que uma exposição a baixas doses de chumbo durante a gestação e a lactação altera a expressão dos receptores glutamatérgicos, sendo que os receptores ionotrópicos alteram no córtex cerebral e hipocampo e os metabotrópicos apenas no hipocampo. Liu et al., 2009 demonstraram que o Perfluorooctanesulfonato (PFOS) administrado durante o período de lactação altera a expressão do subtipo 2B do receptor NMDA (NR2B), das proteínas dependentes de cálcio, calmodulina e PKCaM, bem como do fator de ligação responsivo ao AMPc (CREB) durante o desenvolvimento do hipocampo. Além disso, o contato durante a gravidez e a lactação a compostos contendo cádmio, uma metal considerado neurotóxico, induz mudanças no desenvolvimento do sistema de neurotransmissores em diferentes estruturas. Os autores mostraram que uma intoxicação com esse metal causa alteração no sistema serotoninérgico no hipocampo e modifica

diferentemente as concentrações de glutamato no hipotálamo e hipocampo e do GABA no córtex cerebral (Antônio et al., 2010). A suscetibilidade das diferentes áreas cerebrais à exposição a uma toxina pode estar relacionada com as diferenças locais no desenvolvimento de sistemas de neurotransmissores (Antonio et al., 1998, 1999; Leret et al., 2003).

Não existem estudos, entretanto, mostrando que o $(PhTe)_2$ altera a expressão de receptores glutamatérgicos, proteínas dependentes de cálcio ou neurotransmissores. Porém, podemos propor, que essa seria uma hipótese plausível para a ação desse neurotoxicante, uma vez que ela é capaz de afetar a maquinaria de síntese proteica e alterar a homeostase do glutamato e do cálcio. Alterações nos receptores glutamatérgicos, proteínas que respondem ao cálcio, bem como no conteúdo de neurotransmissores durante o desenvolvimento do córtex cerebral, hipocampo, estriado e cerebelo poderiam explicar, em parte, as diferentes respostas observadas em cada estrutura cerebral nos filhotes após a administração do $(PhTe)_2$ na mãe durante o período de lactação.

O cálcio é um mensageiro intracelular que controla numerosos processos celulares incluindo proliferação, diferenciação, sobrevivência e morte celular (Clapham, 2007). Estudos têm demonstrado que o $(PhTe)_2$ altera a homeostase do cálcio no SNC (Heimfarth et al., 2011, Moretto et al., 2007) e induz a morte neuronal, a qual está implicada em várias desordens neurodegenerativas (Gibbons et al., 1993; Mattson, 2007). Como segundo mensageiro, esse íon media respostas fisiológicas dos neurônios ao estímulo de um neurotransmissor ou de um fator neurotrófico (Neher e Sakaba, 2008; Surmeier et al., 2010). É descrito também que uma elevação citoplasmática de cálcio pode ativar a via das MAPK (Son et al., 2010). Essa via é central em várias rotas de transdução de sinal e sua desregulação está associada a doenças como câncer (Robert

et al., 2007), diabete (Hirosumi et al., 2002) e doença de Alzheimer (Giovannini et al., 2008), bem como é alvo de neurotoxicantes como o cádmio (Chen et al. 2011) e o próprio telúrio (Sredni-Kenigsbuch et al., 2008). Nesse trabalho verificamos que o $(PhTe)_2$, ou algum metabólito dele, transmitido através do leite materno, é capaz de ativar ou inibir a rota das MAPK durante o período de lactação nas diferentes estruturas cerebrais estudadas, sendo que cada uma delas apresentou uma resposta diferente, mostrando novamente a relevância da estrutura cerebral, bem como do seu estado de maturação para a ação do $(PhTe)_2$.

Há trabalhos interligando além da via das MAPK, a rota PKA com alterações na homeostase do cálcio (Bugrin et al., 1999, Bruce et al., 2003, Borodinsky et al., 2006), do glutamato (Zheng e Keifer, 2009), bem como do citoesqueleto (Pierozan et al., 2010, Eriksson et al., 2003). A ativação da PKA regula um vasto número de processos biológicos, entre eles o metabolismo (Krebs et al., 1979), crescimento, divisão e diferenciação celular (Boynton et al., 1983, Liu et al., 1982, Schwartzet al., 1983, Lara et al 2003), conduvividade de canais (Li et al., 1993), liberação de neurotransmissores, dessensibilização de receptores, plasticidade sináptica e transcrição gênica (Borrelli et al 1992; Nestler e Greengard 1994; Riccio et al 1999). Além disso, essa enzima está envolvida em mecanismos de neurotoxicidade induzida por metais (Saijoh et al., 1993). Analisando os efeitos do neurotoxicante sobre essa importante enzima, nossos resultados mostraram que uma administração subcutânea de $(PhTe)_2$ em ratas durante a lactação pode afetar diferentemente a atividade da PKA no SNC dos filhotes. A imunorreatividade da subunidade cataliticamente ativa da PKA apresenta-se diminuída no córtex cerebral e aumentada no hipocampo, estriado e cerebelo dos filhotes de mães tratadas com $(PhTe)_2$ com relação aos filhotes de mães tratadas apenas com óleo de

canola. Esses resultados sugerem um papel importante da via AMPc/PKA nos efeitos desencadeados pela neurotoxicante através do leite materno.

Analisando cada estrutura cerebral separadamente, observamos que o estriado e o cerebelo respondem a esse insulto durante o período de lactação, ou seja, nos animais de 15 e 21 dias através de um aumento de fosforilação dos FIs gliais e neuronais, sendo que nos animais de 30 e 45 dias a homeostase do sistema fosforilante associado ao citoesqueleto volta aos valores basais. É difícil avaliar os mecanismos moleculares que conduzem a alteração na homeostase do citoesqueleto até o 21º dia pós-natal, entretanto isso pode estar relacionado com o programa de maturação dessas duas estruturas cerebrais. Nesse contexto, Tepper et al., 1998 mostraram que na terceira semana pós natal existe um período de intensas mudanças eletrofisiológicas e morfológicas no estriado. Por outro lado, o cerebelo pode ter sua maior suscetibilidade ao $(PhTe)_2$ nesse período atribuída ao aparecimento das células granulares (Fonnum e Lock 2000). Além disso, nos ratos, a última semana pré-natal e as primeiras três semanas pós-natal são o período de maior vulnerabilidade dos neurotransmissores aos metais pesados (Antonio et al., 1999), portanto, uma intoxicação nesse período pode levar a uma alteração nos neurotransmissores e a uma ativação ou inibição de várias vias de sinalização celular, entre elas a rota das MAPK e da PKA, que tem como um dos seus principais alvos o citoesqueleto cerebral.

Já no hipocampo, a alteração da fosforilação das proteínas do citoesqueleto ocorreu apenas nos animais de 30 dias. Entretanto, nos ratos de 21 dias temos um aumento no imunoconteúdo de todos os FIs estudados, portanto, provavelmente a atividade do sistema fosforilante já esteja diminuída no 21º dia pós-natal. Isso está de acordo com nossos trabalhos anteriores, mostrando que em animais de 21 dias há alteração nas proteínas do citoesqueleto no hipocampo (Heimfarth et al., 2008). Além

disso, estes achados corroboram com a hipótese de que essa estrutura é afetada mais tardiamente numa intoxicação com esse organotelureto. Isso pode estar relacionado com as características de desenvolvimento do hipocampo, cuja maturação é completada no período pós-natal. Relatos da literatura mostram que os neurônios hipocampais presentes nas regiões CA alcançam o seu destino já no nascimento, porém células imaturas ainda existem no giro denteado nas etapas iniciais da vida. Além disso, em humanos um contínuo remodelamento dos dendritos é observado nos primeiros anos após o nascimento e essas mudanças são acompanhadas de um aumento do volume do hipocampo durante o início do desenvolvimento (Squire et al., 2008).

Estudos têm mostrado que o contato com neurotoxinas durante o período de gravidez e/ou lactação pode provocar alterações nos receptores glutamatérgicos presentes no hipocampo dos filhotes. A exposição de ratas ao alumínio ou ao PFOS provoca mudança na proporção dos receptores NMDA da prole (Liu et al., 2009, Jin et al., 2011). Apesar de não existirem relatos na literatura mostrando que o telúrio afeta a expressão dos receptores NMDA, pode-se propor que esteja ocorrendo uma alteração na expressão ou na atividade dessas proteínas durante o desenvolvimento do hipocampo, levando a uma resposta diferente nessa estrutura. Os receptores NMDA medeiam a transmissão sináptica lenta e estão envolvidos com eventos de plasticidade sináptica e excitotoxicidade (Rang et al., 2008; Lau e Zukin, 2007). Qualquer disfunção nos mecanismos moleculares que controlam a expressão dessas proteínas na membrana plasmática pode resultar em desordens neurodegenerativas (Cull-Candy et al., 2001). Além disso, esses receptores glutamatérgicos tem um papel fundamental no ajuste de padrões anatômicos das conexões sinápticas durante o desenvolvimento do sistema nervoso central (Alberts et al., 2008).

Quando analisamos os FIs e sua modificação pós-traducional no córtex cerebral verificamos que essa estrutura apresentou-se como a mais resistente, pois não se observou alteração na fosforilação dos FIs. Esse resultado do córtex cerebral é surpreendente, pois outros trabalhos de nosso grupo mostraram que o $(PhTe)_2$ administrado subcutaneamente ou adicionado diretamente sobre a fatia de córtex cerebral de ratos jovens causa alteração no estado de fosforilação dos NFs e da GFAP (Moretto et al., 2005; Heimfarth et al., 2008). Entretanto, Stangerling et al. (2009), já haviam mostrado que a injeção desse organutelureto em ratas durante a lactação causa alteração no estado redox principalmente no estriado e hipocampo dos filhotes, sendo o córtex cerebral a estrutura menos afetada. O $(PhTe)_2$ transmitido via leite materno inibe a rota das MAPK e a atividade da PKA no córtex cerebral, mostrando, entretanto, que essa estrutura é alvo desse neurotoxicante nesse modelo. A inibição da via das MAPK pode ser um mecanismo de proteção, pois é bem descrito que a ativação da p38MAPK e da JNK/SAP está envolvida com mecanismos de morte celular (Rockwell et al. 2004). Além disso, no córtex cerebral essa inibição na rota das MAPK e na PKA provavelmente não está afetando o citoesqueleto neural, uma vez que não há alteração na fosforilação dos FIs.

Os resultados desse trabalho mostraram, portanto, que o $(PhTe)_2$ administrado subcutaneamente em ratas durante os primeiros 14 dias de lactação causa alteração em diversos parâmetros bioquímicos no SNC da prole, sendo o citoesqueleto, a rota das MAPK e da PKA importantes alvos deste neurotoxicante. A fosforilação anormal das proteínas do citoesqueleto pode estar relacionada com danos neuronais e formação de agregados de elementos do citoesqueleto em diferentes compartimentos celulares, o qual é uma característica comum a várias desordens neurodegenerativas (Petzold, 2005).

Portanto, levando em consideração a relevância do citoesqueleto como alvo de muitos mecanismos de sinalização durante os primeiros dias do desenvolvimento pós-natal (Guardiola-Diaz et al 2012; Riederer 1992), presume-se que essa desregulação da homeostase do citoesqueleto observada nos filhotes possa provavelmente estar contribuindo para as ações deletérias do $(PhTe)_2$ durante o desenvolvimento e no cérebro do animal adulto. De fato, isso pode explicar pelo menos em parte, a neurotoxicidade desse composto.

5.3. Modelo 3: Efeitos *in vitro* do ditelureto de fenila sobre o citoequeleto de ratos jovens

Considerando que o $(PhTe)_2$ rompe o equilíbrio do citoesqueleto neural de ratos jovens *in vivo* e que esse efeito pode causar neurodegeneração, procuramos entender um pouco melhor como o organotelureto age no SNC, estudando para isso as principais vias de sinalização envolvidas na ação da droga. Nesse trabalho, portanto, verificamos o efeito de uma exposição *in vitro* ao $(PhTe)_2$ sobre a fosforilação dos FIs neuronais e gliais no córtex cerebral e hipocampo de ratos jovens. Além disso, determinamos também os mecanismos de ação pelos quais essa droga altera a homeostase do citoesqueleto.

Os resultados mostraram que o $(PhTe)_2$ adicionado diretamente sobre uma fatia de córtex cerebral ou hipocampo é capaz de alterar a fosforilação da GFAP, Vim e das subunidades dos NFs, de uma maneira dependente da idade do animal e da estrutura cerebral. Como descrito anteriormente, essa diferente suscetibilidade verificada entre as estruturas cerebrais pode estar relacionada a características individuais, como receptores, transportadores e regulação do sistema fosforilante associados aos FIs gliais

e neuronais de cada região cerebral, bem como do desenvolvimento pós-natal de cada uma delas.

No córtex cerebral observou-se que o $(PhTe)_2$ causou hipofosforilação dos FIs neuronais e gliais em animais de 9 e 15 dias, não alterando o sistema fosforilante associado ao citoesqueleto em animais de 21 dias. Já no hipocampo, verificamos um aumento de fosforilação dos FIs em animais de 21 dias, não apresentando alteração desse parâmetro em ratos mais jovens. Isso está de acordo com nossos estudos *in vivo* que mostraram que o hipocampo só responde a ação desse neurotoxicante a partir do 21º dia pós-natal.

É importante salientar que no córtex cerebral apenas as concentrações de 15 µM e 50 µM agiram sobre o citoesqueleto cerebral. Já o hipocampo necessitou de um insulto mais forte (100 µM) para causar alteração de fosforilação dos FIs. A resposta do sistema fosforilante a uma toxina é muito dependente da concentração utilizada, ou seja, a via de sinalização ativada vai depender da intensidade do insulto. De acordo com esta observação, Loureiro et al. (2008, 2010) mostraram que a homocisteína é capaz de causar hiperfosforilação dos FIs na concentração de 100 µM e hipofosforilação na concentração de 500 µM em hipocampo de animais de 17 dias.

A ação do organotelureto nas células corticais foi dependente dos receptores glutamatérgicos ionotrópicos, mas independentes dos metabotrópicos. No hipocampo, entretanto, verificamos que os receptores glutamatérgicos metabotrópicos desempenharam um papel fundamental na ação desse composto orgânico do telúrio. Esses achados sustentam a hipótese de que o telúrio age em diferentes vias de sinalização nas diversas estruturas cerebrais estudas. Os receptores glutamatérgicos metabotrópicos estão muito envolvidos com a fisiologia do hipocampo. É descrito que o

mGluR5 é extremamente importante para a plasticidade sináptica, bem como para o desenvolvimento do aprendizado e memória (Balschun and Wetzel, 2002; Grassi et al., 2002; Balschun et al., 2006; Ayala et al., 2009; Xu et al., 2009). Além disso, Xu et al., (2007, 2009) demonstraram o envolvimento dos mGluR na neurotoxicidade induzida por chumbo nessa estrutura.

Os receptores NMDA estão envolvidos nos efeitos desencadeados pelo $(PhTe)_2$ tanto no córtex cerebral, quanto no hipocampo, mostrando a importância deste receptor glutamatérgico ionotrópico para a toxicidade desse composto. Vários trabalhos do nosso grupo e de outros têm demonstrado que a ativação dos receptores NMDA está envolvida com alteração do estado de fosforilação dos FIs gliais e neuronais em diferentes estruturas cerebrais (Doroudchi e Durham, 1997; Loureiro et al., 2008, Pierozan et al., 2012). A ativação dos receptores NMDA leva a um aumento no influxo do íon cálcio, provocando uma alteração na homeostase desse importante segundo mensageiro e ativando e inibindo quinases e fosfatases. Resultados usando os quelantes de cálcio intra e extracelular, Bapta-AM e EGTA respectivamente, mostraram que esse segundo mensageiro está envolvido nos efeitos desencadeados pelo $(PhTe)_2$ sobre o citoesqueleto celular tanto no córtex cerebral, como no hipocampo. Esses achados reforçam a importância de uma ativação glutamatérgica para a ação do organotelureto, bem como o envolvimento de mecanismos regulados por cálcio. Durante a atividade fisiológica normal, a concentração intracelular de cálcio aumenta apenas transientemente e não desencadeia efeitos adversos nos neurônios. Entretanto, em processos patológicos, a habilidade dos neurônios em controlar o influxo de cálcio e restaurar os níveis basais desse segundo mensageiro está comprometida, levando a um rompimento da homeostase desse íon e em muitos casos à morte celular (Revisado por Mattson, 2007), a qual está implicada em várias desordens neurodegenerativas (Gibbons

et al., 1993; Mattson, 2007). Estudos recentes têm indicado que o cálcio citosólico também participa de processos de autofagia, degradação lisossomal e eliminação celular de proteínas e organelas (Høyer-Hansen et al., 2007, Criollo et al., 2007, Sarkar et al. 2009).

Além dos receptores NMDA, outros canais de cálcio estão envolvidos na modulação dos níveis intracelulares desse íon, entre eles temos os canais de cálcio dependentes de voltagem (CCDV) e os receptores rianodina e IP3, presentes no retículo endoplasmático. Nosso trabalho mostrou que o $(PhTe)_2$ causou alteração nos níveis intracelulares de cálcio através da ativação dos receptores CCDV presentes na membrana plasmática, e receptores rianodina, do retículo endoplasmático no córtex cerebral e no hipocampo. Os CCDV regulam a atividade elétrica neuronal, modulam a abertura de outros canais e controlam numerosos processos celulares, como a liberação de neurotransmissores, sobrevivência neuronal, ativação de quinases, crescimento de neuritos e transcrição gênica através do influxo de cálcio extracelular, seguido de despolarização da membrana, ou pela liberação dos estoques de cálcio intracelular. (Dolmetsch et al., 2001; Lipscombe et al., 2004). Além disso, Shcheglovitov et al. (2012) demonstraram que metais traços, bem como o glutamato podem modular os CCDV, e esses, por sua vez, também estão envolvidos com a ativação ou inibição dos receptores rianodina (Revisado por Lanner et al., 2010). Já os receptores rianodina, no sistema SNC, contribuem para a plasticidade sináptica, no aprendizado e memória e nos processos de apoptose (Chavis et al. 1996; Schwab et al. 2001, Galleoti et al., 2008).

Outro ponto importante a considerar é que o cálcio pode tanto ativar quinases, como visto no hipocampo, como inibir essa classe de enzimas, como observado no córtex cerebral. Esses efeitos antagônicos do íon cálcio podem ser explicados pelos diferentes estímulos sofridos pelas células, que geram oscilações na concentração

intracelular de cálcio, que por sua vez são importantes para a regulação da função celular. Essa geração das ondas de cálcio intracelular envolve dois diferentes mecanismos: a geração de picos basais, que são caracterizados por um aumento transiente e rápido da concentração intracelular de cálcio a partir do nível basal, sempre voltando à concentração de repouso; e as oscilações ou ondas sinusoidais, que apresentam uma frequência maior que os picos basais e uma oscilação simétrica sobreposta a uma concentração de cálcio intracelular sustentada, que é em alguns casos acima do estímulo basal (Bird e Putney Jr., 2006). Imagens representativas desses dois tipos de ondas de cálcio são mostradas na figura 11.

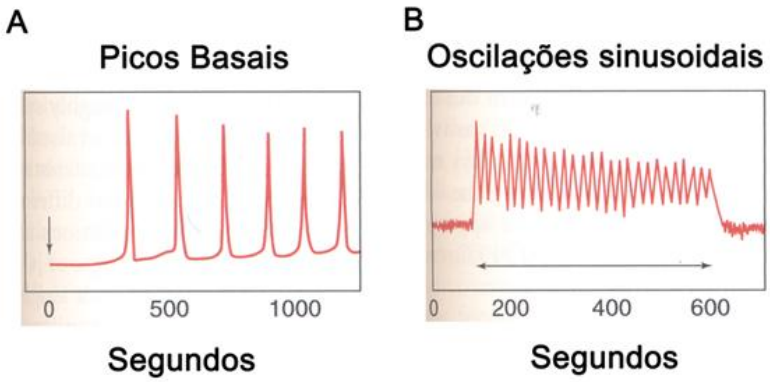

Figura 12: Padrões dos maiores tipos de oscilações das concentrações intracelulares de cálcio, ou seja, diferentes tipos de ondas de cálcio gerandas por um sinal extracelular. Adaptada de Bird e Putney, 2006.

Esses dois mecanismos envolvidos na geração de ondas de cálcio após uma alteração na homeostase desse íon diferem em vários pontos, sendo que a ativação de cada um deles pode acarretar respostas celulares diferentes. A geração de picos basais pode continuar por prolongados períodos de estimulação, enquanto as oscilações

sinusoidais da concentração do íon cálcio tendem a diminuir em poucos minutos. Além disso, uma importante diferença entre esses dois tipos de ondas de cálcio é a relação entre a amplitude de oscilação e a frequência de estímulo ou a concentração do agonista, sendo que nos picos basais um aumento na concentração do agonista, aumenta a frequência dos picos, mas afeta muito pouco a média da quantidade de cálcio intracelular. Já nas ondas sinusoidais, um aumento da concentração do agonista aumenta o cálcio intracelular, mas não interfere na frequência das oscilações (Bird e Putney Jr., 2006).

Portanto, podemos propor que as diferentes ações desencadeadas por um mesmo segundo mensageiro podem estar relacionadas ao tipo de onda de cálcio gerada na estrutura cerebral após um estímulo externo. Ou seja, o $(PhTe)_2$ pode estar alterando a homeostase do cálcio de diferentes maneiras no córtex cerebral e hipocampo, podendo em uma estrutura esse estímulo desencadear ondas sinusoidais e na outra desencadear a formação de picos basais, levando a respostas celulares diversas e nesse caso, antagônicas.

Uma alteração na homeostase do cálcio e do glutamato leva à ativação direta ou indireta de quinases e fosfatases, que, por sua vez, regulam o equilíbrio de fosforilação/desfosforilação dos FIs gliais e neuronais. Os estudos *in vitro* com $(PhTe)_2$ mostraram que esse composto é capaz de ativar a PKC, PKCaMII e a via das MAPK no hipocampo e inibir a PKA no córtex cerebral. É importante salientar que o organotelureto teve efeitos opostos nessas duas estruturas, ou seja, ele aumenta a fosforilação das subunidades dos NFs, GFAP e vimentina no hipocampo e diminui o estado de fosforilação dessas mesmas proteínas no córtex cerebral. Entretanto, surpreendentemente, em ambos os casos verificou-se o envolvimento de quinases.

Analisando separadamente cada uma das estruturas cerebrais, verificamos que no córtex cerebral, além da PKA, a PP1 e a proteína DARPP-32 estão envolvidas com a ação do $(PhTe)_2$. A DARPP-32 é uma fosfoproteína regulada por AMPc e dopamina, que desempenha um papel crítico no córtex cerebral e no estriado em resposta a estímulos glutamatérgicos, GABAérgicos, dopaminérgicos, bem como por ação de drogas (Fienberg et al., 1998, Schiffmann et al., 1998). Ela age como um inibidor da PP1, mas isso vai depender do seu estado de fosforilação e do resíduo envolvido. A DARPP-32 é fosforilada no resíduo treonina 34 pela PKA e quando fosforilada nesse resíduo age como um inibidor da PP1. Entretanto, quando fosforilada no resíduo treonina 75 pela CDK5, inibe a PKA, que por sua vez não fosforila o resíduo treonina 34 da própria DARPP-32, liberando a PP1 para desencadear sua ação (Huag et al., 1999, Fernadez et al., 2006). Uma imagem representativa da ativação/inibição da DARPP-32 é mostrada na figura 13.

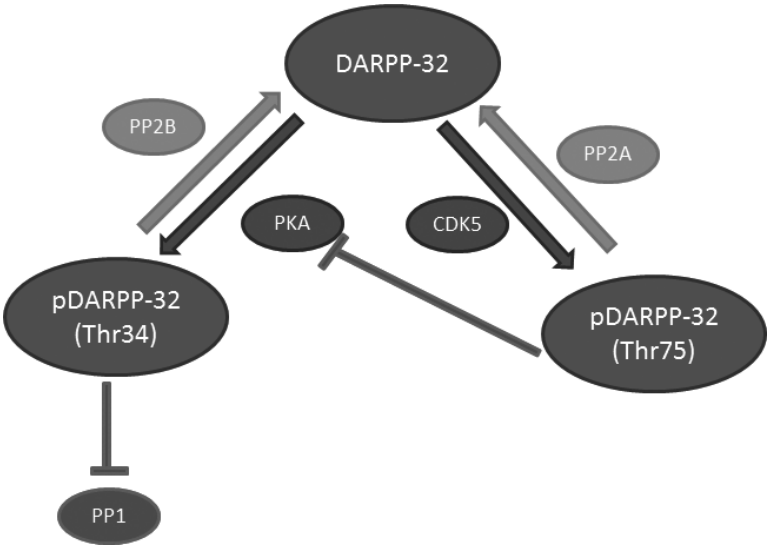

Figura 13: Figura representativa da ativação/inibição da DARPP-32. Adaptada de Nishi et al., 2002.

É descrito que o glutamato, liberado no terminal nervoso glutamatérgico, ativa os receptores AMPA e NMDA, conduzindo a um decréscimo na fosforilação da DARPP-32 (treonina 34) através de mecanismos dependentes de cálcio (Halpain et al., 1999, Nishi et al., 2002), mostrando o envolvimento do sistema glutamatérgico, bem como do cálcio com a regulação da DARPP-32. Nosso estudo também mostrou que a ação do $(PhTe)_2$ sobre a fosforilação da DARPP-32 é dependente do íon cálcio, reforçando a importância desse segundo mensageiro para as ações da droga. Entretanto, no presente trabalho foi mostrado uma via alternativa para a diminuição da fosforilação da DARPP-32 (treonina 34) induzida por cálcio, não envolvendo a ativação da calcineurina. Uma alteração na homeostase do cálcio causaria a inibição de uma isoforma da enzima adenilato ciclase, sensível a esse íon, levando à diminuição nos níveis intracelulares de AMPc e consequentemente não ocorreria a ativação da PKA, a quinase responsável pela fosforilação da DARPP-32 no resíduo treonina 34, deixando essa proteína na sua forma desfosforilada. A DARPP-32 desfosforilada no resíduo treonina-34 não consegue atuar como um inibidor da PP1, deixando essa enzima livre para desencadear sua ação.

Alteração no estado de fosforilação da DARPP-32 nos resíduos treonina 34 e/ou treonina 75 está implicado em respostas motoras, como a observada com psicoestimulantes, que modulam a rota AMPc/PKA (Polissidis et al., 2010) e com canabinóides, onde a fosforilação dessa proteína suprime os efeitos de aumento da atividade motora induzidas por essa substância (Andersson et al., 2005, Borgkvist et al., 2007, Borgkvist et al. 2008). Além disso, Cordova et al., 2012 verificaram o envolvimento da DARPP-32 na intoxicação provocada por manganês. Levando em consideração tudo isso, podemos propor que as alterações do estado de fosforilação dessa proteína possam estar envolvidas com a toxicidade do $(PhTe)_2$ *in vitro*, e podemos

supor que também estejam relacionadas com as alterações observadas nos animais após um tratamento *in vivo*.

Como visto anteriormente, a principal fosfatase envolvida com as ações do $(PhTe)_2$ no córtex cerebral sobre o citoesqueleto neural é a PP1. Essa enzima é a mais abundante serina/treonina fosfatase dos eucariotos e está envolvida com muitos processos biológicos. A PP1 regula o transporte axonal (Morfint et al., 2004), a plasticidade estrutural e sináptica (Munton et al., 2004) e a resposta dos receptores de neurotransmissores, como o AMPA (Yan et al., 1999). Além disso, está envolvida com a reorganização do citoesqueleto, sendo uma das principais fosfatases associadas à desfosforilação dos NFs, bem como da GFAP e vimentina (Strack et al., 1997; Oguri et al., 2006; Loureiro et al., 2010; Cantuti-Castelvetri et al., 2012).

Então, podemos concluir que no córtex cerebral o $(PhTe)_2$ causa uma ativação dos receptores ionotrópicos glutamatérgicos, bem como do CCVD e rianoidina, alterando a concentração intracelular de cálcio. Esse por sua vez, inibe uma isoforma adenilato ciclase, fazendo com que ocorra uma diminuição dos níveis intracelulares de AMPc e consequentemente uma diminuição da ativação da PKA. Essa enzima menos ativa não fosforila a proteína DARPP-32 no resíduo treonina 34, não agindo dessa forma como um inibidor da PP1, liberando essa fosfatase para desencadear sua ação sobre os FIs neurais. Além disso, o $(PhTe)_2$ também aumenta a fosforilação da DARPP-32, no resíduo treonina 75, inibindo ainda mais a PKA. Como consequência há uma diminuição da fosforilação dos FIs corticais.

No hipocampo, o $(PhTe)_2$ induz hiperfosforilação dos FIs neuronais e gliais através da ativação dos receptores metabotrópicos e do íon cálcio como descrito anteriormente. As principais enzimas envolvidas com essa alteração no estado de

fosforilação dessas proteínas são a PKC, PKCaMII e a via das MAPK. Esses resultados mostram a importância, bem como a integração de diversas vias de sinalização para as ações desencadeadas pelo composto orgânico do telúrio no cérebro.

O aumento dos níveis intracelulares de cálcio no hipocampo ativa a PKCaMII, a qual hiperfosforila o resíduo serina 57 localizado na região amino-terminal da NF-L, o qual é importante para a polimerização dos FIs (Heins et al., 1993, Gill et al., 1990). Isso está de acordo com outros estudos que mostram que essa proteína quinase está associada com a fração citoesquelética e está envolvida com a alteração de fosforilação dos FIs em vários modelos de desordens neurodegenerativas (Funchal et al., 2005, Zamoner et al., 2008, Pierozan et al., 2012). Além disso, RamaRao et al. (2011a) verificaram um aumento na atividade dessa enzima em várias regiões cerebrais após uma exposição ao soman, um pesticida organofosforado, levando a um aumento da fosforilação de várias proteínas neurais, entre elas os NFs, GFAP e vimentina. A PKCaMII também está envolvida com a plasticidade neuronal, aprendizado e memória, sendo o maior mediador fisiológico do glutamato nesses eventos (Malenka et al., 1999, Lisman et al., 2002, Hudman et al., 2002). Além disso, essa enzima pode participar da regulação tanto da morte neuronal, através do aumento da condutância do receptor AMPA (Oh et al., 2005), quanto da sobrevivência neuronal, através da inibição da óxido nítrico sintase neuronal, reduzindo a produção de óxido nítrico, que pode ser neurotóxico (Komeima et al., 2000, Osuka et al., 2002, Rameau et al., 2004).

A PKC, outra proteína quinase ativada pelo $(PhTe)_2$, regula muitas funções no cérebro, incluindo eventos de curta duração, como o fluxo de íons e liberação de neurotransmissores; de média duração, como a modulação de receptores; e longa duração, como o remodelamento sináptico e a expressão gênica (revisado em RamRao e Bhattacharya, 2011). Vários estudos tem indicado a importância da PKC em injúrias

neuronais. Krieger et al. (1996) descreveu um aumento da atividade dessa enzima em pacientes com Esclerose Lateral Amiotrófica e sugeriu que a PKC possa estar envolvida com a patogênese da doença. Uma diminuição da atividade desta quinase protege culturas de neurônios da morte induzida por aminoácidos excitatórios (Felipo et al., 1993) e metais neurotóxicos (Pavlakovic et al., 1995). Assim como a PKCaMII, a PKC também está envolvida com a fosforilação das proteínas dos NFs, GFAP e vimentina. Inibidores da PKC previnem a hiperfosforilação dos FIs induzida pela homocisteína (Loureiro et al., 2010), pelo ácido quinolínico (Pierozan et al., 2012) e pelos hormônios da tireóide (Zamoner et al., 2008). Além disso, RamaRao et al. (2011b) verificaram o envolvimento da PKC no aumento da fosforilação de várias proteínas neurais, entre elas os NFs, GFAP e vimentina, em várias regiões cerebrais após uma exposição ao soman.

Outra via de sinalização envolvida com a ação do $(PhTe)_2$ sobre o citoesqueleto neural do hipocampo é a rota das MAPK. Essa via regula vários processos biológicos como proliferação, diferenciação, sobrevivência, morte e transformação celular (McCubrey e Lahair, 2006, Torii et al. 2006, Dhillon et al., 2007) além de processos patológicos, como processos inflamatórios (Beyaert et al, 1996), doenças neurodegenerativas (Kim e Choi, 2010), distúrbios do desenvolvimento (Tidyman e Rauen, 2009), diabetes (Tanti e Jager, 2009) e câncer (Dhillon et al., 2007). Além disso, essas proteínas podem estar envolvidas com a reorganização do citoesqueleto neuronal (Loureiro et al., 2008). Estudos *in vitro* desse trabalho mostraram que esse organotelureto é capaz da ativar a ERK e a p38MAPK no hipocampo, estando essas duas enzimas envolvidas principalmente com a fosforilação dos sítios KSP da NF-M e da NF-H. Isso está de acordo com relatos da literatura que mostram que as MAPK atuam sobre os sítios KSP dessas duas subunidades dos NFs (Veerana et al., 1998), bem como com os resultados dos estudos *in vivo* desse trabalho.

Vários estudos têm sugerido a existência de uma conexão entre a sinalização mediada por cálcio e a rota das MAPK, sendo a PKCaMII e a PKC importantes quinases envolvidas com essa integração de sinais. Segundo Illario et al., 2003, a ativação da ERK mediada pela fibronectina, um ativador de integrina, é dependente da PKCaMII. Chen et al., 2012 relatou que a ativação da ERK por agonistas mGLUR5 foi bloqueada por inibidores da PKC, mostrando que a ativação da ERK é dependente dessa proteína quinase. Além disso, a PKC também está envolvida com a ativação da p38MAPK (Galeotti e Ghelardini, 2011). Esses relatos estão de acordo com os resultados do presente estudo que mostraram uma integração das vias de sinalização da PKC, PKCaMII e MAPK, uma vez que o aumento de fosforilação dos sítios KSP da NF-M e da NF-H, bem como a ativação da ERK e/ou da p38MAPK podem ser prevenidas pelos inibidores da PKC (staurosporina) e PKCaMII (KN-93), no hipocampo de ratos jovens. O $(PhTe)_2$, portanto, ativa uma complexa cadeia de sinais, integrando várias vias de sinalização e enzimas, que levam a uma alteração dos FIs e rompimento da homeostase do citoesqueleto.

Portanto, podemos concluir que no hipocampo, o $(PhTe)_2$ age sobre os receptores glutamatérgicos metabotrópicos, levando a uma ativação da PLC e consequentemente ativação da PKC e liberação de cálcio do retículo endoplasmático. Além disso, há o envolvimento dos receptores NMDA e CCVD, que são canais de cálcio. Essa alteração na homeostase do cálcio acarreta na ativação da PKCaMII, bem como está envolvida indiretamente com o aumento da atividade das enzimas da via das MAPK. A PKC e a PKCaMII vão fosforilar a região amino-terminal dos NFs, bem como a GFAP e a vimentina. Já as MAPK estão envolvidas com a fosforilação da região carboxi-terminal dos FIs.

Analisando os resultados obtidos tanto em córtex cerebral como em hipocampo, podemos concluir que o $(PhTe)_2$ age sobre o sistema glutamatérgico, e altera a homeostase do cálcio de uma maneira independente da estrutura estudada, mostrando a importância do glutamato e do cálcio para a neurotoxicidade desse composto orgânico do telúrio. Isso está de acordo com a proposta de excitotoxicidade glutamatérgica induzindo neurodegeneração em animais expostos a essa droga. Além disso, esse organocalcogênio ativa diferentes vias de sinalização no SNC, sendo as proteínas quinases importantes alvos desse neurotoxicante.

5.4. Efeito do tipo de exposição ao $(PhTe)_2$ sobre a fosforilação dos FIs neuronais e gliais em diferentes estruturas cerebrais

Como visto anteriormente, o $(PhTe)_2$ é um composto neurotóxico para o SNC de roedores, sendo que ele é capaz de afetar diferentes estruturas cerebrais como o córtex cerebral, estriado, hipocampo e cerebelo. Entretanto, os seus efeitos sobre o citoesqueleto vão depender das características individuais de cada estrutura, bem como do estágio de desenvolvimento do animal e do tipo de exposição. Um resumo os efeitos do $(PhTe)_2$ sobre a fosforilação dos FIs está descrito nas tabelas 1, 2 e 3.

Tabela 1: Efeito administração subcutânea de $(PhTe)_2$ em ratos de 15 dias sobre a fosforilação dos FIs neuronais (NF-H, NF-M e NF-L) e gliais (GFAP e vimentina) em diferentes estruturas cerebrais 3 ou 6 dias após a injeção.

Estrutura cerebral	Idade do animal	
	18 dias (3 dias após a injeção)	21 dias (6 dias após a injeção)
Córtex cerebral	Aumenta a fosforilação dos FIs neuronais e gliais	Aumenta a fosforilação dos FIs neuronais e gliais
Hipocampo	Não altera a fosforilação dos FIs neuronais e gliais	Aumenta a fosforilação dos FIs gliais
Estriado	Aumenta a fosforilação dos FIs neuronais e gliais	Aumenta a fosforilação dos FIs neuronais e gliais
Cerebelo	Aumenta a fosforilação dos FIs neuronais e gliais	Não altera a fosforilação dos FIs neuronais e gliais

Tabela 2: Efeito da administração subcutânea de $(PhTe)_2$ nas mães durante os primeiros 14 dias de lactação (P0-P13) sobre a fosforilação dos FIs neuronais (NF-H, NF-M e NF-L) e gliais (GFAP e vimentina) em diferentes estruturas cerebrais, nos filhotes de 15, 21, 30 ou 45 dias de idade.

Estrutura cerebral	Idade do animal			
	15 dias	**21 dias**	**30 dias**	**45 dias**
Córtex cerebral	Não altera a fosforilação dos FIs neuronais e gliais	Não altera a fosforilação dos FIs neuronais e gliais	Não altera a fosforilação dos FIs neuronais e gliais	Não altera a fosforilação dos FIs neuronais e gliais
Hipocampo	Não altera a fosforilação dos FIs neuronais e gliais	Diminui a fosforilação dos FIs neuronais e	Diminui a fosforilação dos FIs neuronais e	Não altera a fosforilação dos FIs neuronais e

		gliais	gliais	gliais
Estriado	Aumenta a fosforilação dos FI neuronais e gliais	Aumenta a fosforilação dos FIs neuronais e gliais	Não altera a fosforilação dos FIs neuronais e gliais	Não altera a fosforilação dos FIs neuronais e gliais
Cerebelo	Aumenta a fosforilação dos FIs neuronais e gliais	Aumenta a fosforilação dos FIs neuronais e gliais	Não altera a fosforilação dos FIs neuronais e gliais	Não altera a fosforilação dos FIs neuronais e gliais

Tabela 3: Efeito do tratamento *in vitro* $(PhTe)_2$ sobre a fosforilação dos FIs neuronais (NF-H, NF-M e NF-L) e gliais (GFAP e vimentina) no córtex cerebral e hipocampo de animais de 9, 15 e 21 dias de idade.

Estrutura cerebral	**Idade do animal**		
	9 dias	**15 dias**	**21 dias**
Córtex cerebral	Diminui a fosforilação dos FIs neuronais e gliais	Diminui a fosforilação dos FIs neuronais e gliais	Não altera a fosforilação dos FIs neuronais e gliais
Hipocampo	Não altera a fosforilação dos FIs neuronais e gliais	Não altera a fosforilação dos FIs neuronais e gliais	Aumenta a fosforilação dos FIs neuronais e gliais

Analisando os resultados das tabelas acima podemos propor que a via de contato (injeção s.c., transmissão pelo leite materno ou tratamento *in vitro*) com o $(PhTe)_2$ pode estar influenciando também a ação dessa droga neurotóxica, uma vez que uma mesma

estrutura cerebral responde diferentemente aos 3 modelos estudados, como podemos ver para o hipocampo e córtex cerebral em animais de 21 dias. Entretanto, mais estudos são necessários para compreender melhor a relação entre a maneira como ocorre o contato com o organocalcogênio e a ação dessa droga neurotóxica. Uma importante possibilidade a ser considerada é o $(PhTe)_2$ ser transformado no seu intermediário reduzido, feniltelurol no organismo, o qual é um potente agente nucleofílico (Zeni et al., 2000, 2003, 2004). Portanto, podemos propor que esse composto reduzido do $(PhTe)_2$ possa estar agindo no SNC nos experimentos *in vivo*, levando a respostas diferentes de uma mesma estrutura em função do tipo de exposição em animais da mesma idade. Entretanto, alterações sistêmicas podem também estar envolvidas com as modificações de fosforilação nos modelos *in vivo*, uma vez que o $(PhTe)_2$ é provocar alterações sistêmicas (Borges et al., 2007, Schiar et al.,2007).

6. CONCLUSÃO

6.1. Conclusão Geral

Células neurais do córtex cerebral, hipocampo, estriado e cerebelo são alvos de neurotoxicantes, entre eles o $(PhTe)_2$. Os resultados do presente trabalho mostraram que esse organocalcogênio é um importante modulador da dinâmica do citoesqueleto neural, alterando a homeostase dos FIs através de mecanismos dependentes de cálcio e glutamato e através de diferentes vias de sinalizações. Além disso, esse efeito sobre os FIs é dependente da estrutura cerebral, do desenvolvimento do animal, bem como do tipo de exposição. Portanto, as alterações do citoesqueleto cerebral podem estar envolvidas, pelo menos em parte, com a neurotoxicidade do composto orgânico de telúrio.

6.2. Conclusões Específicas

6.2.1. Modelo 1

6.2.1.1 Uma administração *in vivo* do $(PhTe)_2$ causa hiperfosforilação dos FIs neuronais (NF-L, NF-M e NF-H) e gliais (GFAP e vimentina) no estriado e cerebelo de ratos jovens.

6.2.1.1.1. O $(PhTe)_2$ injetado por via subcutânea em ratos de 15 dias provoca um aumento na fosforilação dos sítios KSP *repeats* da NF-M e NF-H e do resíduo Serina 55 da NF-L.

6.2.1.2 O $(PhTe)_2$ administrado subcutaneamente em ratos jovens altera o imunoconteúdo, bem como a expressão da GFAP e vimentina no estriado e cerebelo.

6.2.1.3. A administração subcutânea de $(PhTe)_2$ em ratos jovens ativa as vias das MAPK e da PKA e inibe a AKT/PKB no estriado e cerebelo.

6.2.1.4. O $(PhTe)_2$ injetado por via subcutânea em ratos de 15 dias causa astrogliose e morte neuronal.

6.2.2. Modelo 2

6.2.2.1. A administração subcutânea de $(PhTe)_2$ nas ratas mães durante os primeiros 14 dias de lactação altera a fosforilação da GFAP e subunidades dos NFs (NF-L, NF-M, NF-H) do hipocampo, estriado e cerebelo dos filhotes de uma maneira tempo e estrutura dependente.

6.2.2.1.1. A administração subcutânea de $(PhTe)_2$ nas ratas mães durante a lactação provoca um aumento na fosforilação dos sítios KSP *repeats* da NF-M e NF-H e do resíduo Serina 55 da NF-L do estriado e do cerebelo.

6.2.2.2. O $(PhTe)_2$ administrado nas mães durante os 14 primeiros dias de lactação provocou alteração no imunoconteúdo dos FIs no córtex cerebral, hipocampo e cerebelo.

6.2.2.3. A administração subcutânea de $(PhTe)_2$ nas ratas mães durante períodos iniciais de lactação ativa a via das MAPKs e da PKA no estriado e cerebelo dos filhotes e inibe no córtex cerebral. No hipocampo temos uma inibição da via das MAPK e uma ativação da PKA.

6.2.2.4. O $(PhSe)_2$ administrado concomitante com o $(PhTe)_2$ nas ratas mães durante a lactação previne os efeitos desencadeados pelo $(PhTe)_2$ sobre o sistema fosforilante associado ao citoesqueleto no estriado dos filhotes.

6.2.3. Modelo 3

6.2.3.1. O $(PhTe)_2$ adicionado diretamente sobre as fatias causa hipofosforilação dos FIs neuronais (NF-L, NF-M e NF_H) e gliais (GFAP e vimentina) no córtex

cerebral de animais de 9 e 15 dias, não alterando o estado de fosforilação dessas proteínas em animais de 21 dias. Já no hipocampo, os estudos *in vitro* mostraram que esse organotelureto induz a um aumento de incorporação de ortofosfato radioativo nos FIs gliais e neuronais dos animais de 21 dias, não afetando a fosforilação dessas proteínas em ratos mais jovens (9 ou 15 dias).

6.2.3.2. A hipofosforilação causada pelo $(PhTe)_2$ no córtex cerebral foi mediada por alteração homeostase do cálcio e glutamato, bem como pela inibição da PKA, alteração da fosforilação da proteína DARPP-32(Thr34) e liberação da PP1.

No hipocampo temos uma ativação dos receptores glutamatérgicos ionotrópicos e metabotrópicos, acarretando uma alteração na homeostase do cálcio e ativação da PKC, PKCaMII e via das MAPK, conduzindo a um aumento de fosforilação dos FIs neuronais e gliais.

8. PERSPECTIVAS

Os resultados obtidos nesse trabalho abrem novas possibilidades de estudo a fim de compreender melhor a neurotoxicidade do $(PhTe)_2$. Dessa maneira nossas perspectivas são:

8.1. Realizar um estudo ontogenético dos efeitos do $(PhTe)_2$ sobre a fosforilação *in vitro* dos FIs de estriado e cerebelo.

8.2. Identificar as vias de sinalização envolvidas nesses efeitos, com ênfase especial nas proteínas quinases e fosfatases, bem como mecanismos envolvendo o glutamato e o cálcio.

8.3. Estabelecer modelos de exposição ao $(PhTe)_2$ em cultura primária de astrócitos e neurônios corticais, estriatais e hipocampais de ratos.

8.4. Estudar o efeito do tratamento com $(PhTe)_2$ sobre a fosforilação dos FIs neuronais e gliais em culturas primárias de astrócitos e neurônios.

8.5. Verificar o efeito da exposição ao $(PhTe)_2$ em co-culturas de astrócitos e neurônios corticais de ratos.

8.6. Determinar o efeito dos fatores solúveis derivados dos astrócitos expostos ao $(PhTe)_2$ sobre os neurônios corticais

8.5. Determinar o efeito dos fatores solúveis derivados dos neurônios expostos ao $(PhTe)_2$ sobre os astrócitos corticais

9. BIBLIOGRAFIA

Alberts B., Johnson A., Lewis J., Raff M., Roberts K., Walter P.O. (2008). Citoesqueleto. In: Alberts B., Johnson A., Lewis J., Raff M, Roberts K, Walter P. (Eds) Biologia Molecular da Célula. 6. ed. New York: Garland Science, 907-982 .

Ackerley, S., Grierson, A.J., Brownlees, J., Thornhill, P., Anderton, B.H., Leigh, P.N., Shaw, C.E., and Miller, C.C. (2000). Glutamate slows axonal transport of neurofilaments in transfected neurons. J Cell Biol 150, 165-176.

Al-Chalabi, A., and Miller, C.C. (2003). Neurofilaments and neurological disease. Bioessays 25, 346-355.

Andersson M., Usiello A., Borgkvist A., Pozzi L.,Dominguez C., Fienberg A.A., Svenningsson P., Fredholm B.B., Borrelli E., Greengard P., Fisone G. (2005). Cannabinoid action depends on phosphorylation of dopamine- and cAMP-regulated phosphoprotein of 32 kDa at the protein kinase. A site in striatal projection neurons. J Neurosci, 25:8432–8438.

Antonio, M.T., Benito, M.J., Leret, M.L., Corpas, I. (1998). Gestational administrationof cadmium alters the neurotransmitter levels in newborn rat brains. J. Appl.Toxicol. 18, 83–88.

Antonio, M.T., Corpas, I., Leret, M.L. (1999) Neurochemical changes in newborn rat's brain after gestational cadmium and lead exposure. Toxicol. Lett. 104, 1–9.

Aras R, Barron AM, Pike CJ. (2012). Caspase activation contributes to astrogliosis. Brain Res. 23,1450:102-15. .

Arbustini, E., Pasotti, M., Pilotto, A., Pellegrini, C., Grasso, M., Previtali, S., Repetto, A., Bellini, O., Azan, G., Scaffino, M., et al. (2006). Desmin accumulation restrictive cardiomyopathy and atrioventricular block associated with desmin gene defects. Eur J Heart Fail 8, 477-483.

Ayala, J.E., Chen, Y., Banko, J.L., Sheffler, D.J., Williams, R., Telk, A.N., Watson, N.L.,Xiang, Z., Zhang, Y., Jones, P.J., Lindsley, C.W., Olive, M.F., Conn, P.J., (2009). mGluR5positive allosteric modulators facilitate both hippocampal LTP and LTD an enhance spatial learning. Neuropsychopharmacology 34, 2057–2071.

Ba, L.A., Doring, M., Jamier, V., and Jacob, C. (2010). Tellurium: an element with great biological potency and potential. Org Biomol Chem 8, 4203-4216.

Balschun, D., Wetzel, W. (2002). Inhibition of mGluR5 blocks hippocampal LTP in vivoand spatial learning in rats. Pharmacol. Biochem. Behav. 73, 375–380.

Baude A, Nusser Z, Roberts JDB, Mulvihill E, McIlhinney RAJ, Somogyi P. (1993) The metabotropic glutamate receptor (mGluR1) is concentrated at perisynaptic membrane of Neronal subpopulations as detected by immunogold reaction. Neuron 1993, 11,771–87.

Baude A, Nusser Z, Roberts JDB, Mulvihill E, McIlhinney RAJ, Somogyi P. (2003). The metabotropic glutamate receptor (mGluR1) is concentrated at perisynaptic membrane of Neronal subpopulations as detected by immunogold reaction. Neuron. 11, 771–87.

Bear, M.F.; Connors, B.W. e Paradiso, M.A. (2008) Neurociência: desvendando o Sistema Nervoso. 3.ed. Porto Alegre: Artmed, , pp. 143-157. cap. 6. Sistema de neurotransmissores.

Bear, M.F.; Connors, B.W., Paradiso, M.A. (2008) Neurociências. Desvendando o Sistema Nervoso. ed. Porto Alegre, Artmed p 761. Mecanismo Moleculares de Aprendizado e memória.

Beaulieu, J.M., Nguyen, M.D., and Julien, J.P. (1999a). Late onset of motor neurons in mice overexpressing wild-type peripherin. J Cell Biol 147, 531-544.

Beaulieu, J.M., Robertson, J., and Julien, J.P. (1999b). Interactions between peripherin and neurofilaments in cultured cells: disruption of peripherin assembly by the NF-M and NF-H subunits. Biochem Cell Biol 77, 41-45.

Berridge, M. J., Bootman, M. D., and Roderick, H. L. (2003) Calcium signalling: dynamics, homeostasis and remodeling. Nat. Rev. Mol. Cell Biol. 4, 517–529.

Beyaert R, Cuenda A, Vanden Berghe W, Plaisance S, Lee JC, Haegeman G, Cohen P, Fiers W. (1996). The p38/RK mitogen-activated protein kinase pathway regulates interleukin-6 synthesis response to tumor necrosis factor. EMBO J., 15, pp. 1914–1923

Bezprozvanny. (2005) The inositol 1,4,5-trisphosphate receptors Cell. Calcium, 38, pp. 261–272.

Bibb, J., Nestler, E.J. (2006). Serine and Threonine Phosphorylation, pg. 391-413 capítulo 23. In Siegel G J., Albers R.W.; Brady S.T. and Price D.L.(Ed), Basic Neurochemistry Molecular, Cellular, and Medical Aspect. 7 ed.

Bird, G.S., Putney J.W. (2006) Calcium. In: Siegel. G.J., Albers, R.W., Brady S.T., Price, D.L. Basic Neurochemistry Molecular, Cellular, and Medical Aspect. 7ed, p379.

Borges, V.C., Nogueira, C.W., Zeni, G., and Rocha, J.B. (2004). Organochalcogens affect the glutamatergic neurotransmission in human platelets. Neurochem Res 29, 1505-1509.

Borges, V.C., Rocha, J.B., and Nogueira, C.W. (2005). Effect of diphenyl diselenide, diphenyl ditelluride and ebselen on cerebral Na(+), K(+)-ATPase activity in rats. Toxicology 215, 191-197.

Borges, V.C., Rocha, J.B., Savegnago, L., and Nogueira, C.W. (2007). Repeated administration of diphenyl ditelluride induces hematological disorders in rats. Food Chem Toxicol 45, 1453-1458.

Borgkvist A, Fisone G. (2007). Psychoactive drugs and regulation of the cAMP/PKA/DARPP-32 cascade in striatal medium spiny neurons. Neurosci Biobehav Rev.31, 79–88.

Borgkvist A, Marcellino D, Fuxe K, Greengard P, Fisone G. (2008). Regulation of DARPP-32 phosphorylation by Delta9-tetrahydrocannabinol. Neuropharmacology. 2008;54:31–35

Borodinsky LN, Spitzer NC (2006). Second messenger pas de deux: the coordinated dance between calcium and cAMP. 23, (336):pe22.

Borrelli E, Montmayeur JP, Foulkes NS, Sassone-Corsi P. (1992). Signal transduction and gene control: The cAMP pathway. Crit Rev Oncog, 3, 321–38.

Boynton A.L., Whitreld, J.F. (1983). The role of cAMP in cell pro-liferation: A critical assessment of the evidence, Adv. Cyclic. Nucleotide Res. 15, 193-294.

Braitenberg, V. e Schüz, A (ed). (1998) Cortex: Statistic and geometric of neural connectivity, 2nd, Berlin, springer.

Bruce J.I., Straub S.V., Yule D.I. (2003). Crosstalk between cAMP and Ca2+ signaling in non-excitable cells. Cell Calcium 2003, 34:431-444.

Bugrim A.E. (1999) Regulation of Ca2+ release by cAMP-dependent protein kinase. A mechanism for agonist-specific calcium signaling? Cell Calcium, 25:219-226.

Camins A, Verdaguer E, Folch J, Pallàs M. (2006) Involvement of calpain activation in neurodegenerative processes. CNS Drug Rev. Summer;12(2):135-48. Review.

Cantuti-Castelvetri L., Zhu H., Givogri M.I., Chidavaenzi R.L., Lopez-Rosas A., Bongarzone E.R. (2012) Psychosine induces the dephosphorylation of neurofilaments by deregulation of PP1 and PP2A phosphatases. Neurobiol Dis. 46(2), 325-35.

Cardone M.H., Roy N., Stennicke H.R., Salvesen G.S., Franke T.F., Stanbridge E., Frisch S, Reed J.C. (1998). Regulation of cell death protease caspase-9 by phosphorylation. Science. 13,282(5392):1318-21.

Cargnello M., Roux P.P. (2011) Activation and function of the MAPKs and their substrates, the MAPK-activated protein kinases. Microbiol Mol Biol Rev. 75(1),50-83.

Carmignoto, G. (2000) Reciprocal communication system between astrocytes and neurones. Progress Neurobiol., v.62, pp. 561-581.

Carraway, C.A.C. (2000) The cytoskeleton in transduction of signal and regulation of cellular function. In: Carraway, K.L. and Carraway, C.A.C. Cytoskeleton: signaling and cellular regulation. New York, Oxford University Press, p 1-7.

Celsi F, Pizzo P, Brini M, Leo S, Fotino C, Pinton P, Rizzuto R. (2009) Mitochondria, calcium and cell death: a deadly triad in neurodegeneration. Biochim Biophys Acta 1787,335–44.

Chang, L., Goldman, R.D. (2004). Intermediate filaments mediate cytoskeletal crosstalk. Nat Rev Mol Cell Biol 5, 601-613.

Chavis P, Fagni L, Lansman JB, Bockaert J. (1996). Functional coupling between ryanodine receptors and L-type calcium channels in neurons. Nature 382: 719–722.

Che, Y., Piao, C.S., Han, P.L., Lee, J.K. (2001a). Delayed induction of alpha B-crystallin in activated glia cells of hippocampus in kainic acid-treated mouse brain. J. Neurosci. Res. 65, 425–431.

Che, Y., Yu, Y., Han, P., Lee, J. (2001b). Delayed induction of p38 MAPKs in reactive astrocytes in the brain of mice after KA-induced seizure. Mol. Brain Res. 94, 157–165.

Chen S., Xu Y., Xu B., Guo M., Zhang Z., Liu L., Ma H., Chen Z., Luo Y., Huang S., Chen L. (2011). CaMKII is involved in cadmium activation of MAPK and mTOR pathways leading to neuronal cell death. J Neurochem. 119(5), 1108-18.

Chen T., Cao L., Dong W., Luo P., Liu W., Qu Y., Fei Z. (2012). Protective Effects of mGluR5 Positive Modulators Against Traumatic Neuronal Injury Through PKC-Dependent Activation of MEK/ERK Pathway. Neurochem Res. 37, 983–990.

Chen, Z. T. B., Gibson, F. Robinson, L. Silvestro, G. Pearson, B. Xu, A.Wright, C. Vanderbilt, and M. H. Cobb. (2001). MAP kinases. Chem. Rev. 101:2449–2476.

Choi D.W. (1987). Ionic dependence of glutamate neurotoxicity. J Neurosci 7, 369–79.

Chou, Y.H., Skalli, O., and Goldman, R.D. (1997). Intermediate filaments and cytoplasmic networking: new connections and more functions. Curr Opin Cell Biol 9, 49-53.

Clapham DE (2007) Calcium signaling. Cell 131: 1047–1058.

Clayton, G.D. e Clayton, F.E (1981). Patty`s Industrial Hygiene and Toxicology. Wiley, Chichester..

Cooper W.C. (1971). Tellurium. Van Nostrand Reinhod Co.: New York.

Cooper, G.M.O (2001) Citoesqueleto e o Movimento Celular. In: Cooper, Geoffrey M.A Célula: uma abordagem molecular. 2.ed.. Porto Alegre: Artmed, pp. 445-489.

Cordova F.M., Aguiar A.S. Jr, Peres T.V., Lopes M.W., Gonçalves F.M., Remor A.P., Lopes S.C., Pilati C., Latini A.S., Prediger R.D., Erikson K.M., Aschner M., Leal R.B (2012). In vivo manganese exposure modulates Erk, Akt and Darpp-32 in the striatum of developing rats, and impairs their motor function. PLoS One. 7(3):e33057

Cotman C.W., Foster A, Lanthorn T. (1981). An overview of glutamate as a neurotransmitter.. Adv Biochem Psychopharmacol. 27,1-27. Review.

Coulombe, P.A., Bousquet, O., Ma, L., Yamada, S., and Wirtz, D. (2000). The 'ins' and 'outs' of intermediate filament organization. Trends Cell Biol 10, 420-428.

Criollo A., Vicencio J.M., Tasdemir E., Maiuri M.C., Lavandero S., Kroemer G. (2007). The inositol trisphosphate receptor in the control of autophagy. Autophagy. 3(4),350-3.

Cull-Candy S., Brickley, S. Farrant M. (2001). NMDA receptor subunits: diversity, development and disease, Curr Opin Neurobiol 11, 327-35.

Datta, S.R., Brunet, A., Greenberg, M.E. (1999). Cellular survival: a play in three Akts. Genes Dev. 13, 2905–2927.

DePianto, D., and Coulombe, P.A. (2004). Intermediate filaments and tissue repair. Exp Cell Res 301, 68-76.

Dhillon A.S., Hagan S., Rath O., Kolch W. (2007) MAP kinase signalling pathways in cancer. Oncogene. 26(22), 3279-90.

Diprospero, N.A.; Chen, E-Y.; Charles, V.; Plomann, M.; Kordower, J.H.; Tangle, D.A. (2004) Early changes in Huntington's disease patient brains involve alterations in cytoskeletal and synaptic elements. J Neurocytol 33: 517–533.

Dolmetsch, R. E., Pajvani, U., Fife, K., Spotts, J. M., & Greenberg, M. E. (2001). Signalingto the nucleus by an L-type calcium channel-calmodulin complex through the MAPkinase pathway. Science 294, 333–339.

Doroudchi M.M., Durham H.D (1997) Activation of NMDA receptors and Ca2+/calmodulin-dependent protein kinase participate in phosphorylation of neurofilaments induced by protein kinase C. J Neurosci Res.15;50(4),514-21.

Duckett, S., and White, R. (1974). Cerebral lipofucsinosis induced with tellurium: electron dispersive X-ray spectrophotometry analysis. Brain Res 73, 205-214.

Eckes, B., Dogic, D., Colucci-Guyon, E., Wang, N., Maniotis, A., Ingber, D., Merckling, A., Langa, F., Aumailley, M., Delouvee, A., et al. (1998). Impaired mechanical stability, migration and contractile capacity in vimentin-deficient fibroblasts. J Cell Sci 111 (Pt 13), 1897-1907.

Eddleston, M., Mucke, L. (1993). Molecular profile of reactive astrocytes--implications for their role in neurologic disease. Neuroscience 54, 15-36.

Elder, G.A., Friedrich, V.L., Margita, A. e Lazzarine, A. (1999) Age-related atrophy of motor axons in mice defidient in mid-sized neurofilament subunit. J. Cell Biol., 146, 181-192.

Eliasson, C., Sahlgren, C., Berthold, C.H., Stakeberg, J., Celis, J.E., Betsholtz, C., Eriksson, J.E., and Pekny, M. (1999). Intermediate filament protein partnership in astrocytes. J Biol Chem 274, 23996-24006.

Eng, L.F., Lee, Y.L., Kwan, H., Brenner, M., and Messing, A. (1998). Astrocytes cultured from transgenic mice carrying the added human glial fibrillary acidic protein gene contain Rosenthal fibers. J Neurosci Res 53, 353-360.

Engman L, Al-Maharik N, McNaughton M, Birmingham A, Powis G (2003) Thioredoxin reductase and cancer cells growth inhibition by organotellurium compounds that could be selectively incorporated intotumor cells. Bioorg Med Chem L ett 11:5091–5100

Engman, L., Kandra, T., Gallegos, A., Williams, R., and Powis, G. (2000). Water-soluble organotellurium compounds inhibit thioredoxin reductase and the growth of human cancer cells. Anticancer Drug Des 15, 323-330.

Eriksson, J.E., Goldman, R.D. (1993) Protein phosphatase inhibitors alter cytoskeletal structure and cellular morphology. Adv. Prot. Phosphtase 99, 104..

Eriksson J.E, He T., Trejo-Skalli A.V., Härmälä-Braskén A.S., Hellman J., Chou Y.H., Goldman R.D. (2004). Specific in vivo phosphorylation sites determine the assembly dynamics of vimentin intermediate filaments. J Cell Sci. 29,117(Pt 6):919-32.

Eriksson, J.E., He, T., Trejo-Skalli, A.V., Harmala-Brasken, A.S., Hellman, J., Chou, Y.H., and Goldman, R.D. (2004). Specific in vivo phosphorylation sites determine the assembly dynamics of vimentin intermediate filaments. J Cell Sci 117, 919-932.

Favero, A. M., Weis, S. N., Zeni, G., Rocha J. B., Nogueira, C. W. (2006). Diphenyl diselenide changes behavior in female pups. Neurotoxicol Teratol. 28, 607–616.

Felipo V., Miñana M.D., Grisolía S. (1993) Inhibitors of protein kinase C prevent the toxicity of glutamate in primary neuronal cultures. Brain Res. 26, 604(1-2):192-6.

Fernandez E., Schiappa R., Girault J.A., Le Novère N. (2006). DARPP-32 is a robust integrator of dopamine and glutamate signals. PLoS Comput Biol. 2006 Dec 22, 2(12)-e176.

Fienberg AA, Hiroi N, Mermelstein PG, Song W, Snyder GL, Nishi A, Cheramy A, O'Callaghan JP, Miller DB, Cole DG, Corbett R, Haile CN, Cooper DC, Onn SP, Grace AA, Ouimet CC, White FJ, Hyman SE, Surmeier DJ, Girault J, Nestler EJ, Greengard P.(1998) DARPP-32: Regulator of the efficacy of dopaminergic neurotransmission. Science. 281:838–842

Fonnum F, Lock EA. (2000). Cerebellum as a target for toxic substances. Toxicol Lett 112–113, 9–16.

Fuchs, E., and Cleveland, D.W. (1998). A structural scaffolding of intermediate filaments in health and disease. Science 279, 514-519.

Fuchs, E., and Weber, K. (1994). Intermediate filaments: structure, dynamics, function, and disease. Annu Rev Biochem 63, 345-382.

Funchal C, Zamoner A, dos Santos AQ, Loureiro SO, Wajner M, Pessoa-Pureur R. (2005) Alpha-ketoisocaproic acid increases phosphorylation of intermediate filament proteins from rat cerebral cortex by mechanisms involving Ca2+ and cAMP. Neurochem Res. 30(9),1139-46.

Funchal, C., Moretto, M.B., Vivian, L., Zeni, G., Rocha, J.B., and Pessoa-Pureur, R. (2006). Diphenyl ditelluride- and methylmercury-induced

hyperphosphorilation of the high molecular weight neurofilament subunit is prevented by organoselenium compounds in cerebral cortex of young rats. Toxicology 222, 143-153.

Galeotti N., Ghelardini C. (2011). Regionally selective activation and differential regulation of ERK, JNK and p38 MAP kinase signalling pathway by protein kinase C in mood modulation. Int J Neuropsychopharmacol.

Galeotti N., Quattrone A., Vivoli E., Norcini M., Bartolini A., Ghelardini C. (2008) Different involvement of type 1, 2, and 3 ryanodine receptors in memory processes.Learn Mem 15(5),315–23.

Geisler N., Vandekerckhove J., Weber K. (1987). Location and sequence characterization of the major phosphorylation sites of the high molecular mass neurofilament proteins M and H. FEBS Lett 221, 403–407.

Geisler, N., and Weber, K. (1981). Self-assembly in Vitro of the 68,000 molecular weight component of the mammalian neurofilament triplet proteins into intermediate-sized filaments. J Mol Biol 151, 565-571.

Gibbons S.J., Brorson JR, Bleakman D., Chard PS, Miller R.J. (1993) Calcium influx and neurodegeneration. Ann NY Acad Sci 679: 22–33.

Gibbons S.J., Brorson JR, Bleakman D., Chard PS, Miller R.J. (1993) Calcium influx and neurodegeneration. Ann NY Acad Sci 679: 22–33.

Gill, S. R., Wong, P. C., Monteiro, M. J., and Cleveland, D. W. (1990) Assembly properties of dominant and recessive mutations in the small mouse neurofilament (NF-L) subunit. J. Cell Biol. 111, 2005–2019.

Giovannini MG, Cerbai F, Bellucci A, Melani C, Grossi C, Bartolozzi C, Nosi D, Casamenti F. (2008). Differential activation of mitogen-activated protein kinase

signalling pathways in the hippocampus of CRND8 transgenic mouse, a model of Alzheimer's disease. Neuroscience 153,618–633.

Goedert, M. (1998) Filamentous nerve cell inclusions in neurodegenerative diseases. Curr Opin Neurobiol 8: 619–632.

Gohara, R., Tang, D., Inada, H., Inagaki, M., Takasaki, Y., Ando, S. (2001). Phosphorylation of vimentin head domain inhibits interaction with the carboxyl-terminal end of alpha-helical rod domain studied by surface plasmom resonance measurements. FEBS Lett., 489: 182-186.

Gonda Y., Nishizawa K., Ando S., Kitamura S., Minoura Y., Nishi Y., Inagaki M. (1990) Involvement of protein kinase C in the regulation of assembly-disassembly of neurofilaments in vitro. Biochem Biophys Res Commun, 167, 1316–1325.

Gonzales, M., Weksler, B., Tsuruta, D., Goldman, R.D., Yoon, K.J., Hopkinson, S.B., Flitney, F.W., and Jones, J.C. (2001). Structure and function of a vimentin-associated matrix adhesion in endothelial cells. Mol Biol Cell 12, 85-100.

Gotow, T., and Tanaka, J. (1994). Phosphorylation of neurofilament H subunit as related to arrangement of neurofilaments. J Neurosci Res 37, 691-713.

Gotow, T., Takeda, M., Tanaka, T., and Hashimoto, P.H. (1992). Macromolecular structure of reassembled neurofilaments as revealed by the quick-freeze deep-etch mica method: difference between NF-M and NF-H subunits in their ability to form cross-bridges. Eur J Cell Biol 58, 331-345.

Gotow, T., Tanaka, T., Nakamura, Y., and Takeda, M. (1994). Dephosphorylation of the largest neurofilament subunit protein influences the structure of crossbridges in reassembled neurofilaments. J Cell Sci 107 (Pt 7), 1949-1957.

Gottlieb, A., Keydar, I., Epstein, H.T. (1977) Rodent brain growth stages: an analytical review. Biol. Neonate. 32, 166–176.

Grant, P.,Pant, H.C. (2000). Neurofilament protein synthesis and phosphorylation. J Neurocytol 29, 843-872.

Grassi, S., Frondarolim, A., Pettorossi, V.E. (2002). Different metabotropic glutamate receptors play opposite roles in synaptic plasticity of the rat medial vestibular nuclei. J. Physiol. 543, 795–806

Green, S.L., Westendorf, J.M., Jaffe, H., Pant, H.C., Cork, L.C., Ostrander, E.A., Vignaux, F., and Ferrell, J.E., Jr. (2005). Allelic variants of the canine heavy neurofilament (NFH) subunit and extensive phosphorylation in dogs with motor neuron disease. J Comp Pathol 132, 33-50.

Guardiola-Diaz HM, Ishii A, Bansal R. (2012). Erk1/2 MAPK and mTOR signaling sequentially regulates progression through distinct stages of oligodendrocyte differentiation. Glia. 60(3):476-86.

Guo-Ross, S.X., Yang, E.Y., Walsh, T.J., and Bondy, S.C. (1999). Decrease of glial fibrillary acidic protein in rat frontal cortex following aluminum treatment. J Neurochem 73, 1609-1614.

Halpain S., Girault J.A., Greengard P (1990). Activation of NMDA receptors induces dephosphorylation of DARPP-32 in rat striatal slices. Nature 343, 369 - 372.

Hamilton S.L. (2005) Ryanodine receptors Cell Calcium, 38, 253–260.

Hanssel, B, Dingledine, R. Glutamate. Pg. 267-289. (2006) In: Siegel G J., Albers R.W.; Brady S.T. and Price D.L.(Ed), Basic Neurochemistry Molecular, Cellular, and Medical Aspect. 7 ed.

Hashimoto R., Nakamura Y., Komai S., Kashiwagi Y., Tamura K., Goto T, Aimoto S., Kaibuchi K., Shiosaka S., Takeda M. (2000) Site-specific phosphorylation

of neurofilament-L is mediated by calcium/ calmodulin-dependent protein kinase II in the apical dendrites during long-term potentiation. J Neurochem, 75:373–382.

Hassanzadeh K., Roshangar L., Habibi-asl B., Farajnia S., Izadpanah E., Nemati M., Arasteh M., Mohammadi S.(2011). Riluzole prevents morphine-induced apoptosis in rat cerebral cortex. Pharmacol Rep. 63(3), 697-707.

Heimfarth, L., Loureiro, S.O., Reis, K.P., De Lima, B.O., Zamboni, F., Gandolfi, T., Narvaes, R., Da Rocha, J.B., Pessoa-Pureur, R. (2011). Cross-talk among intracellular signaling pathways mediates the diphenyl ditelluride actions on the hippocampal cytoskeleton of young rats. Chem. Res. Toxicol. 24, 1754-1764.

Heimfarth, L., Loureiro, S.O., Zamoner, A., Pelaez Pde, L., Nogueira, C.W., Rocha, J.B., and Pessoa-Pureur, R. (2008). Effects of in vivo treatment with diphenyl ditelluride on the phosphorylation of cytoskeletal proteins in cerebral cortex and hippocampus of rats. Neurotoxicology 29, 40-47.

Heins, S., Wong, P. C., Muller, S., Goldie, K., Cleveland, D. W., Aebi, U. (1993) The rod domain of NF-L determines neurofilament architecture, whereas the end domains specify filament assembly and network formation. J. Cell Biol. 123, 1517–1533.

Helfand, B.T., Chang, L., and Goldman, R.D. (2003). The dynamic and motile properties of intermediate filaments. Annu Rev Cell Dev Biol 19, 445-467.

Helfand, B.T., Chou, Y.H., Shumaker, D.K., Goldman, R.D. (2005). Intermediate filament proteins participate in signal transduction. Trends Cell Biol 15, 568-570.

Herrmann, S., Aebi, U. (2000) Intermediate filaments and their associates: multi-talent structural elements specifying cytoarchitecture and cytodinamics. Curr. Opin. Cell. Biol., 12: 79-90, 2000.

Hesse, M., Magin, T.M., and Weber, K. (2001). Genes for intermediate filament proteins and the draft sequence of the human genome: novel keratin genes and a surprisingly high number of pseudogenes related to keratin genes 8 and 18. J Cell Sci 114, 2569-2575.

Hirosumi J., Tuncman G., Chang L., Gorgun C.Z., Uysal K.T., Maeda K., Karin M., Hotamisligil G.S. (2002) A central role for JNK in obesity and insulin resistance. Nature 420,333–336.

Hisanaga, S., Gonda, Y., Inagaki, M., Ikai, A., and Hirokawa, N. (1990). Effects of phosphorylation of the neurofilament L protein on filamentous structures. Cell Regul 1, 237-248.

Hisanaga, S., Matsuoka, Y., Nishizawa, K., Saito, T., Inagaki, M., and Hirokawa, N. (1994). Phosphorylation of native and reassembled neurofilaments composed of NF-L, NF-M, and NF-H by the catalytic subunit of cAMP-dependent protein kinase. Mol Biol Cell 5, 161-172.

Hisanga, S. & Hirokawa, N. (1088) Structure of peripheral domains of neurofilamets revealed by low angle rotary shadowing. J. Mol. Biol., 202: 1997-305.

Hollmann, M. and Heinemann, S. (1994) Cloned glutamate recep-tors. Ann. Rev. Neurosci. 17, 31-108.

Homan, S.M., Mercurio, A.M., and LaFlamme, S.E. (1998). Endothelial cells assemble two distinct alpha6beta4-containing vimentin-associated structures: roles for ligand binding and the beta4 cytoplasmic tail. J Cell Sci 111 ,2717-2728.

Høyer-Hansen M, Jäättelä M. (2007). AMP-activated protein kinase: a universal regulator of autophagy? Autophagy. 3(4),381-3.

Hsieh, S.T., Kidd, G.J., Crawforg, T.O., Xu, Z., Lin, W.M., Trapp, B.D., Cleveland, D.W., Griffin, J.W. (1994). Regional modulation of neurofilament organization by myelination in normal axons. J. Neurosci. 14, 6392-6401.

Huang, H.B., Horiuchi,A.,Goldberg, J.,Greengard,P, Nairn,A.C. (1997). Site-directed mutagenesis of amino aci dresidues of protein phosphatase 1involvedincatalysisand inhibitorbinding. Proc.Natl.Acad. Sci.U.S.A. 94, 3530–3535.

Hudmon A., Schulman H. (2002). Neuronal Ca2+/calmodulin-dependent protein kinase II: the role of structure and autoregulation in cellular function. Annu Rev Bioch 7.

Illario M., Cavallo A.L., Bayer K.U., Di Matola T., Fenzi G., Rossi G., Vitale M. (2003). Calcium/calmodulin-dependent protein kinase II binds to Raf-1 and modulates integrin-stimulated ERK activation.1: 473–510. J Biol Chem. 14, 278(46)-45101-8.

Inada, H., Nagata, K.I., Goto, H., Inagaki, M. (2000). Regulation of intermediate filament dynamicas: a novel approach using site and phosphorylation state specific antibodies. In: Carraway, K.L., Carraway, C.A.C. Cytoskeleton: signaling and cellular regulation. New York: Oxford University Press: pp. 183-207.

Inagaki M., Gonda Y., Nishizawa K., Kitamura S., Sato C., Ando S., Tanabe K., Kikuchi K., Tsuiki S., Nishi Y. (1990) Phosphorylation sites linked to glial filament disassembly in vitro locate in a non-alpha-helical head domain. J. Biol. Chem. 15,265(8):4722-9.

Inagaki M, Nishi Y, Nishizawa K, Matsuyama M, Sato C. (1987) Site-specific phosphorylation inducesdisassembly of vimentin filaments in vitro. Nature, 328: 649–652.

Isawa, I., Inagaki, M. (2006) Regulatory mechanism and function of intermediate filament: A study using site-and phosphorylation state-specific antibodies. Cancer Sci. 97(3), 167-74..

Ito M, Natsume A, Takeuchi H, Shimato S, Ohno M, Wakabayashi T, Yoshida. (2009). Type I interferon inhibits astrocytic gliosis and promotes functional recovery after spinal cord injury by deactivation of the MEK/ERK pathway. 26(1):41-53.

Ivaska J., Vuoriluoto, K., Huovinen, T., Izawa, I., Inagaki, M., Parker P.J. (2005) PKCepsilon-mediated phosphorylation of vimentin controls integrin recycling and motility. EMBO J. 24, 3834–3845

Ivaska, J., Pallari, H.M., Nevo, J., and Eriksson, J.E. (2007). Novel functions of vimentin in cell adhesion, migration, and signaling. Exp Cell Res 313, 2050-2062.

Ivaska, J., Vuoriluoto, K., Huovinen, T., Izawa, I., Inagaki, M., and Parker, P.J. (2005). PKCepsilon-mediated phosphorylation of vimentin controls integrin recycling and motility. EMBO J 24, 3834-3845.

Janosch, P., Kieser, A., Eulitz, M., Lovric, J., Sauer, G., Reichert, M., Gounari, F., Buscher, D., Baccarini, M., Mischak, H., and Kolch, W. (2000). The Raf-1 kinase associates with vimentin kinases and regulates the structure of vimentin filaments. FASEB J 14, 2008-2021.

Jin CH, Wu SW, Lu XB, Tang QS, Liu QF, Cai Y. (2011). The expression changes of N-methyl-D-aspartic acid receptor in hippocampus of offspring from female

rats exposed to aluminum in the pregnancy and lactation. Zhonghua Lao Dong Wei Sheng Zhi Ye Bing Za Zhi., 29(3), 198-201.

Johnson JW, Ascher P. (1992). Equilibrium and kinetic study of glycine action on the N-methyl-D-aspartate receptor in cultured mouse brain neurons. J Physiol. 55, 339-65.

Julien, J.P. (1999) Neurofilament functions in health and disease. Curr Opin Neurobiol 9: 554–560.

Julien, J.P., Mushynski, W.E. (1998) Neurofilaments in health and disease. Prog Nucleic Acid Res Mol Biol 61: 1–23.

Julien, J.P., Cote, F., and Collard, J.F. (1995). Mice overexpressing the human neurofilament heavy gene as a model of ALS. Neurobiol Aging 16, 487-490; discussion 490-482.

Jung, C., Yabe, J.T., and Shea, T.B. (2000). C-terminal phosphorylation of the high molecular weight neurofilament subunit correlates with decreased neurofilament axonal transport velocity. Brain Res 856, 12-19.

Kaneko, S., Satoh, Y., Ikemura, K., Konishi, T., Ohji, T., Karasaki, Y., Higashi, K., and Gotoh, S. (1995). Alterations of expression of the cytoskeleton after immortalization of human fibroblasts. Cell Struct Funct 20, 107-115.

Kanski, J., Drake, J., Aksenova, M., Engman, L., and Butterfield, D.A. (2001). Antioxidant activity of the organotellurium compound 3-[4-(N,N-dimethylamino)benzenetellurenyl]propanesulfonic acid against oxidative stress in synaptosomal membrane systems and neuronal cultures. Brain Res 911, 12-21.

Kawajiri A, Yasui Y., Goto H., Tatsuka M., Takahashi M., Nagata K., Inagaki M. (2003). Functional significance of the specific sites phosphorylated in desmin at cleavage furrow: Aurora-B may phosphorylate and regulate type III intermediate filaments during cytokinesis coordinatedly with Rho-kinase. Mol Biol Cell. 2003 14(4):1489-500.

Kim EK, Choi EJ.J.A. (2010). Pathological roles of MAPK signaling pathways in human diseases. Biochim Biophys Acta. 2010 1802(4), 396-405.

Kim, S., Coulombe, P.A. (2007). Intermediate filament scaffolds fulfill mechanical, organizational, and signaling functions in the cytoplasm. Genes Dev 21, 1581-1597.

King, A.E.. Dickson, T.C Blizzard, C.A.. Foster, S.S. Chung, R.S West, A.K..Chuah, M.I. Vickers, J.C. (2007). Excitotoxicity mediated by non-NMDA receptors causesdistal axonopathy inlong-termculturedspinalmotor neurons, Eur. J.Neurosci. 26, 2151–2159.

Kirkpatrick, L.L. E Brady, S.T. Cytoskelrton of neurons and glia. (1999) In Siegel, G.; Agranoff, B.W., Alberts, R.W., Fischer, S.K. & Ulher, M.D. (eds). Basic Neurochemistry-Molecular, cellular and medical aspects. 6 ed. New York, Lippincott – Raven Publishers,. p. 155-173.

Koh, S.H., Park Y., Song, C.W., Kim, J.G., Kim, K., Kim, J., Kim, M.H., Lee, S.R., Kim, D.W., Yu, H.J., Chang, D.I., Hwang, S.J., Kim, S.H. (2004). The effect of PARP inhibitor on ischaemic cell death, its related inflammation and survival signals. Eur. J. Neurosci. 20(6), 1461–1472.

Koliatsos, V.E., Applegate, M.D., Kitt, C.A., Walker, L.C., De Long, M.R., Price, D.L. (1989). Aberrant phosphorylation of neurofilaments accompanies

transmitter-related changes in rat septal neurons following transection of the fimbria-fornix. Brain Res 482: 205–218.

Komeima K, Hayashi Y, Naito Y, Watanabe Y. (2000) Inhibition of neuronal nitric-oxide synthase by calcium/calmodulin-dependent protein kinase II through Ser847 phosphorylation in NG108-15 neuronal cells. J Biol Chem 275, 28139 43.

Korolainen, M.A., Auriola, S., Nyman, T.A., Alafuzoff, I., Pirttila, T. (2005). Proteomic analysis of glial fibrillary acidic protein in Alzheimer's disease and aging brain. Neurobiol. Dis. 20, 858–870

Kosako, H., Amano, M., Yanagida, M., Tanabe, K., Nishi, Y., Kaibuchi, K., and Inagaki, M. (1997). Phosphorylation of glial fibrillary acidic protein at the same sites by cleavage furrow kinase and Rho-associated kinase. J Biol Chem 272, 10333-10336.

Krebs, E.G., Beavo, J.A. (1979) Phosphorylation-dephosphorylation of enzymes, Annu Rev. Biochem. 48 , 923-959.

Kreis, S., Schonfeld, H.J., Melchior, C., Steiner, B., and Kieffer, N. (2005). The intermediate filament protein vimentin binds specifically to a recombinant integrin alpha2/beta1 cytoplasmic tail complex and co-localizes with native alpha2/beta1 in endothelial cell focal adhesions. Exp Cell Res 305, 110-121.

Krieger C, Lanius RA, Pelech SL, Shaw CA. (1996). Amyotrophic lateral sclerosis: the involvement of intracellular Ca2+ and protein kinase C. Trends Pharmacol Sci.17(3),114-20. Review.

Kuchma, M.H., Kim, J.H., Muller, M.T., Arlen, P.A. (2012). Prostate cancer cell surface-associated keratin 8 and its implications for enhanced plasmin activity. Protein J 31, 195-205.

Kumar, N., Robidoux, J., Daniel, K.W., Guzman, G., Floering, L.M., and Collins, S. (2007). Requirement of vimentin filament assembly for beta3-adrenergic receptor activation of ERK MAP kinase and lipolysis. J Biol Chem 282, 9244-9250.

Kyriakis, J. M., and J. Avruch. (2001). Mammalian mitogen-activated proteinkinase signal transduction pathways activated by stress and inflammation.Physiol. Rev. 81, 807–869.

Laden B.P., Porter T.D. (2001) Inhibition of human squalene monooxygenase by tellurium compounds: evidence of interaction with vicinal sulfhydryls. J Lipid Res., 42:235-40.

Lanner J.T., Georgiou D.K., Joshi A.D., Hamilton S.L. (2010). Ryanodine receptors: structure, expression, molecular details, and function in calcium release. Cold Spring Harb Perspect Biol. 2(11):a003996.

Lara J, Kusano K, House S, Gainer H.. (2003). Interactions of cyclic adenosinemonophosphate, brain-derived neurotrophic factor, and glial cellline-derived neurotrophic factor treatment on the survival and growthof postnatal mesencephalic dopamine neurons in vitro. Exp Neurol,180, 32–45.

Lariviere, R.C., and Julien, J.P. (2004). Functions of intermediate filaments in neuronal development and disease. J Neurobiol 58, 131-148.

Lau, C.G., Zukin, R.S. (2007). NMDA receptor trafficking in synaptic plasticity andneuropsychiatric disorders. Nat. Rev. Neurosci. 8, 413–426.

Lee VM, Otvos L Jr, Carden MJ, Hollosi M, Dietzschold B, Lazzarini RA. (1988). Identification of the major multiphosphorylation site in mammalian neurofilaments. Proc. Natl. Acad. Sci .USA, 85:1998– 2002.

Leret, M.L., San Millán, J.A., Antonio, M.T. (2003). Perinatal exposure to lead and cadmium affects anxiety-like behaviour. Toxicology 186, 125–130.

Leterrier JF, Käs J, Hartwig J, Vegners R, Janmey PA. Mechanical effects of neurofilament cross-bridges. Modulation by phosphorylation, lipids, and interactions with F-actin. Biol Chem. 1996 Jun 28;271(26):15687-94.

Lewis, T. S., P. S. Shapiro, and N. G. Ahn. (1998). Signal transductionthrough MAP kinase cascades. Adv. Cancer Res. 74,49–139.

Li B.S., Veeranna, K.T. Gu J, Grant P, Pant HC. (1999)a Activation of mitogen-activated protein kinases (Erk1 and Erk2) cascade results in phosphorylation of NF-M tail domains in transfected NIH 3T3 cells. Eur. J. Biochem. 262:211–217, 1999a.

Li BS, Veeranna, K.T., Gu J, Grant P, Pant HC. (1999b). Calcium influx and membrane depolarization induce phosphorylation of neurofilament (NF-M) KSP repeats in PC12 cells. Brain Res Mol Brain Res. 70:84–91.

Li, M. West, J.W. Numann, R. Murphy, B.J. Scheuer, T. Catterall, W.A. (1993) Convergent regulation of sodium channels by protein kinase C and cAMP-dependent protein kinase,Science 261, 1439-1442.

Lipscombe, D., Helton, T. D., & Xu, W. (2004). L-type calcium channels: the low down. J Neurophysiol 92, 2633–2641.

Lipton S.A., Rosenberg P.A. (1994). Excitatory amino acids as a final common pathway for neurologic disorders.. N Engl J Med. 1994 Mar 3;330(9):613-22.

Lisman J, Schulman H, Cline H. (2002). The molecular basis of CaMKII functionin synaptic and behavioural memory. Nat Rev Neurosci 3, 75–90.

Liu X, Liu W, Jin Y, Yu W, Wang F, Liu L. (2010). Effect of gestational and lactational exposure to perfluorooctanesulfonate on calcium-dependent signaling molecules gene expression in rats' hippocampus. Arch Toxicol. 84(1),71-9.

Liu, A.Y.C. (1982). Diferentiation-specific increase of cAMP-dependent protein kinase in 3T3-L1 cells, J. Biol. Chem. 257, 298-306.

Liu, Q., Xie, F., Alvarado-Diaz, A., Smith, M.A., Moreira, P.I., Zhu, X., Perry, G. (1982). Neurofilamentopathy in neurodegenerative diseases. Open Neurol J 5, 58-62.

Liu, Q., Xie, F., Siedlak, S.L., Nunomura, A., Honda, K., Moreira, P.I., Zhua, X., Smith, M.A., and Perry, G. (2004). Neurofilament proteins in neurodegenerative diseases. Cell Mol Life Sci 61, 3057-3075.

Loureiro SO, Heimfarth L, Pelaez Pde L, Lacerda BA, Vidal LF, Soska A, Santos NG, Andrade C, Tagliari B, Scherer EB, Guma FT, Wyse AT, Pessoa-Pureur R. (2010). Hyperhomocysteinemia selectively alters expression and stoichiometry of intermediate filament and induces glutamate- and calcium-mediated mechanisms in rat brain during development. Int J Dev Neurosci. 2010 Feb;28(1):21-30.

Loureiro SO, Heimfarth L, Pelaez Pde L, Vanzin CS, Viana L, Wyse AT, Pessoa-Pureur R. (2008). Homocysteine activates calcium-mediated cell signaling mechanisms targeting the cytoskeleton in rat hippocampus. Int J Dev Neurosci./ 26(5),447-55.

Lujan R, Nusser Z, Roberts JD, Shigemoto R, Somogyi P. (1996). Perisynaptic location of metabotropic glutamate receptors mGluR1 and mGluR5 on dendrites and dendritic spines in the rat hippocampus. Eur J Neurosci. 8,1488–500.

Lujan R, Roberts JD, Shigemoto R, Ohishi H, Somogyi P. (1997). Differential plasma membrane distribution of metabotropic glutamate receptors mGluR1 alpha, mGluR2 and mGluR5, relative to neurotransmitter release sites. J Chem Neuroanat 13, 219–41.

Maciel, E.N., Bolzan, R.C., Braga, A.L., and Rocha, J.B. (2000). Diphenyl diselenide and diphenyl ditelluride differentially affect delta-aminolevulinate dehydratase from liver, kidney, and brain of mice. J Biochem Mol Toxicol 14, 310-319.

Malenka R.C. (1999) Nicoll RA. Long-term potentiation — a decade ofprogress? Science 285, 1870–4.

Manning, G., Plowman, G.D., Hunter, T., and Sudarsanam, S. (2002a). Evolution of protein kinase signaling from yeast to man. Trends Biochem Sci 27, 514-520.

Manning, G., Whyte, D.B., Martinez, R., Hunter, T., and Sudarsanam, S. (2002b). The protein kinase complement of the human genome. Science 298, 1912-1934.

Manser C, Stevenson A, Banner S, Davies J, Tudor EL, Ono Y, Leigh PN, McLoughlin DM, Shaw CE, Miller CC. (2008) Deregulation of PKN1 activity disrupts neurofilament organisation and axonal transport. FEBS Lett. 2008 25,582(15)-2303-8.

Mattson MP (2007) Calcium and neurodegeneration. Aging Cell 6: 337–350.

McCall, M.A., Gregg, R.G., Behringer, R.R., Brenner, M., Delaney, C.L., Galbreath, E.J., Zhang, C.L., Pearce, R.A., Chiu, S.Y., and Messing, A. (1996). Targeted deletion in astrocyte intermediate filament (Gfap) alters neuronal physiology. Proc Natl Acad Sci U S A 93, 6361-6366.

Mccubrey, M.M. Lahair, R.A. Franklin R.A. (2006). Reactive oxygen species-induced activation of the MAP kinase signaling pathwaysAntioxid. Redox Signal., 8. 1775–1789

McDonald J.W., Johnston M.V. (1990) Physiological and pathophysiological roles of excitatory amino acids during central nervous system development. Brain Res Brain Res Rev.15(1), 41-70. Review

McKinney, R.A. (2010) Excitatory amino acid involvement in dendritic spine formation, maintenance and remodeling. J Physiol 588.1 pp 107–116.

Meldrum BS. (2000) Glutamate as a neurotransmitter in the brain: review of physiology and pathology. J Nutr. 130(4S Suppl):1007S-15S.

Menet, V., Gimenez y Ribotta, M., Chauvet, N., Drian, M.J., Lannoy, J., Colucci-Guyon, E., and Privat, A. (2001). Inactivation of the glial fibrillary acidic protein gene, but not that of vimentin, improves neuronal survival and neurite growth by modifying adhesion molecule expression. J Neurosci 21, 6147-6158.

Meotti, F.C., Borges, V.C., Zeni, G., Rocha, J.B., and Nogueira, C.W. (2003). Potential renal and hepatic toxicity of diphenyl diselenide, diphenyl ditelluride and Ebselen for rats and mice. Toxicol Lett 143, 9-16.

Middeldorp, J., Hol, E.M. (2011). GFAP in health and disease. Prog Neurobiol 93, 421-443.

Mikoshiba, K. (2007) IP3 receptor/Ca2+ channel: from discovery to new signaling concepts J. Neurochem., 102, 1426–1446.

Moretto M.B., Boff B., Franco J. Posser T., Roessler T.M., Souza D.O., Nogueira C.W., Wofchuk S., Rocha J.B. (2007). (45)Ca(2+) influx in rat brain: effect of diorganylchalcogenides compounds. Toxicol Sci. 99(2), 566-71.

Moretto M.B., Funchal C., Zeni G., Rocha J.B., Pessoa-Pureur R. (2005) Organoselenium compounds prevent hyperphosphorylation of cytoskeletal proteins

induced by the neurotoxic agent diphenyl ditelluride in cerebral cortex of young rats. Toxicology. 1, 210(2-3):213-22.

Moretto M.B., Thomazi A.P., Godinho G., Roessler T.M., Nogueira C.W., Souza D.O., Wofchuk S, Rocha JB. (2007) Ebselen and diorganylchalcogenides decrease in vitro glutamate uptake by rat brain slices: prevention by DTT and GSH. Toxicol In Vitro. 21(4), 639-45.

Moretto, M.B., Funchal, C., Zeni, G., Rocha, J.B., and Pessoa-Pureur, R. (2005). Organoselenium compounds prevent hyperphosphorylation of cytoskeletal proteins induced by the neurotoxic agent diphenyl ditelluride in cerebral cortex of young rats. Toxicology 210, 213-222.

Morfini G., Szebenyi G., Brown H., Pant H.C., Pigino G., DeBoer S., Beffert U., Brady S.T. (2004). A novel CDK5-dependent pathway for regulating GSK3 activity and kinesin-driven motility in neurons. EMBO J. 2, 23(11):2235-45.

Morgane JP, Mokler JD, Galler RJ (2002) Effets of prenatal protein malnutrition on the hipocampal formation. Neurosci Biobehav Rev 26:471–483

Motil, J., Chan, W.K., Dubey, M., Chaudhury, P., Pimenta, A., Chylinski, T.M., Ortiz, D.T., and Shea, T.B. (2006). Dynein mediates retrograde neurofilament transport within axons and anterograde delivery of NFs from perikarya into axons: regulation by multiple phosphorylation events. Cell Motil Cytoskeleton 63, 266-286.

Munton RP, Vizi S, Mansuy IM. (2004). The role of protein phosphatase-1 in the modulation of synaptic and structural plasticity. FEBS Lett. 1;567(1):121-81999

Nakamura Y., Takeda M., Aimoto S., Hojo H., Takao T., Shimonishi Y., Hariguchi S., Nishimura T. (1992) Assembly regulatory domain of glial fibrillary acidic

protein. A single phosphorylation diminishes its assembly-accelerating property. J Biol Chem. 15, 267(32):23269-74.

Nakanishi, S. (1992) Molecular diversity of glutamate receptors and implications for brain function. Science (Wash. DC) 258, 597±603.

Ndozangue-Touriguine, O., Hamelin, J., Breard, J. (2008). Cytoskeleton and apoptosis. Biochem Pharmacol 76, 11-18.

Neher E, Sakaba T (2008) Multiple roles of calcium ions in the regulation ofneurotransmitter release. Neuron 59: 861–872.

Nestler EJ, Greengard P. (1994). Protein phosphorylation and the regulation of neuronal function In Siegel GJ, Albers RW, Agranoff BW, MolinoffP (eds). Basic neurochemistry: molecular, cellular, and medical aspects. Boston: Little Brown p 449–74.

Nestler, E.J. Greengard, P. (1999). Serine and threonine phosphorylation. In: Siegel, G., Agranoff, B.W., Alberts, R.W., Fisher, S.K. & Ulher, M.D. (eds). Basic Neurochemistry – Molecular, cellular and medical aspect. 6 ed. New York Lippincott – Raven Publishers, pp. 472-495.

Nieminen, M., Henttinen, T., Merinen, M., Marttila-Ichihara, F., Eriksson, J.E., and Jalkanen, S. (2006). Vimentin function in lymphocyte adhesion and transcellular migration. Nat Cell Biol 8, 156-162.

Nishi A, Bibb JA, Matsuyama S, Hamada M, Higashi H, Nairn AC, Greengard P.. (2002). Regulation of DARPP-32 dephosphorylation at PKA- and Cdk5-sites by NMDA and AMPA receptors: distinct roles of calcineurin and protein phosphatase-2A. J Neurochem . 2002 ; 81 : 832 - 841

Nixon, R.A. (1993). The regulation of neurofilament protein dynamics by phosphorylation: clues to neurofibrillary pathobiology. Brain Pathol 3, 29-38.

Nixon, R.A., and Shea, T.B. (1992). Dynamics of neuronal intermediate filaments: a developmental perspective. Cell Motil Cytoskeleton 22, 81-91.

Nixon, R.A.; Paskevich P.A.; Sihang, R.K. & Thayer, C.Y. (1994). Phosphorylation on COOH terminus domains of neurofilament protein in retinal ganglion cell neurons in vivo: influences on regional neurofilament accumulation, interneurofilament spacing and axonal caliber. J. Cell Biol., 126: 1031-1046.

Nogueira, C.W., Rotta, L.N., Perry, M.L., Souza, D.O., and da Rocha, J.B. (2001). Diphenyl diselenide and diphenyl ditelluride affect the rat glutamatergic system in vitro and in vivo. Brain Res 906, 157-163.

O'Callaghan, J.P. (1994) A potential role for altered protein phosphorylation in the mediation of developmental neurotoxicity. Neuro Toxicol 15: 29–40.

Oguri T, Inoko A, Shima H, Izawa I, Arimura N, Yamaguchi T, Inagaki N, Kaibuchi K, Kikuchi K, Inagaki M. (2006). Vimentin-Ser82 as a memory phosphorylation site in astrocytes. Genes Cells.

Olney, J.W. (1969) Brain Lesions, Obesity, and other disturbances in mice treated withmonosodium glutamate, Science 164, 719–721.

Omary M.B.; Ku N.O.; Tao G.Z.; Toivola D.M., Liao J. (2006). "Heads and Tails" of intermediate filament phosphorylation: multiple sites and functional insights. Trends Biochem Sci., 31:383-394, 2006.

Omary, M.B., and Ku, N.O. (1997). Intermediate filament proteins of the liver: emerging disease association and functions. Hepatology 25, 1043-1048.

Omary, M.B., Coulombe, P.A., and McLean, W.H. (2004). Intermediate filament proteins and their associated diseases. N Engl J Med 351, 2087-2100.

Omary, M.B., Ku, N.O., Tao, G.Z., Toivola, D.M., and Liao, J. (2006). "Heads and tails" of intermediate filament phosphorylation: multiple sites and functional insights. Trends Biochem Sci 31, 383-394.

Orrenius S, Zhivotovsky B, Nicotera P. (2003). Regulation of cell death: the calciumapoptosis link. Nat Rev Mol Cell Biol. 4:552–65.

Osuka K, Watanabe Y, Usuda N, Atsuzawa K, Aoshima C, Yamauchi K, Takayasu M, Yoshida J. (2007) Phosphorylation of neuronal nitric oxide synthase at Ser847 in the nucleus intermediolateralis after spinal cord injury in mice. Neuroscience. 2,145(1):241-7.

Ozawa, H.K., Keisuke T. (1998) Glutamate Receptors in the Mammalian Central Nervous System, Progress in Neurobiology 3-39-22 Gunma, Japan 371. 54, pp. 581 to 618.

Pallari, H.M., Eriksson, J.E. (2006). Intermediate filaments as signaling platforms. Sci STKE, pe53.

Pant, H.C., Veeranna, K., Grant, P. (2000). Regulation of axonal neurofilament phosphorylation. Curr. Top. Cell Regul. 36, 133–150.

Paramio, J.M., and Jorcano, J.L. (2002). Beyond structure: do intermediate filaments modulate cell signalling? Bioessays 24, 836-844.

Pavlaković G, Kane MD, Eyer CL, Kanthasamy A, Isom GE. (1995) Activation of protein kinase C by trimethyltin: relevance to neurotoxicity. J Neurochem. Nov;65(5):2338-43.

Pearson G, Robinson F, Beers Gibson T, Xu BE, Karandikar M, Berman K, Cobb MH. (2001) Mitogen-activated protein (MAP) kinase pathways: regulation and physiological functions. Endocr Rev. 22(2):153-83.

Pekny, M., Johansson, C.B., Eliasson, C., Stakeberg, J., Wallen, A., Perlmann, T., Lendahl, U., Betsholtz, C., Berthold, C.H., and Frisen, J. (1999). Abnormal reaction to central nervous system injury in mice lacking glial fibrillary acidic protein and vimentin. J Cell Biol 145, 503-514.

Pekny, M., Nilsson, M. (2005). Astrocyte activation and reactive gliosis. Glia 50, 427–434.

Peng J, Liang G, Inan S, Wu Z, Joseph DJ, Meng Q, Peng Y, Eckenhoff MF, Wei H. (2012) Dantrolene ameliorates cognitive decline and neuropathology in Alzheimer triple transgenic mice. Neurosci Lett. 16;516(2):274-9.

Peng, S., Zhang., J. Wang, H, Ren, B. (2010). ERK in learning and memory: a review of recent research. Int J Mol Sci 13,11(1):222-32.

Perez-D'Gregorio RE, Miller RK (1988) Teratogenicity of tellurium dioxide: prenatal assessment. Teratology 37:307–316

Perlson, E., Hanz, S., Ben-Yaakov, K., Segal-Ruder, Y., Seger, R., and Fainzilber, M. (2005). Vimentin-dependent spatial translocation of an activated MAP kinase in injured nerve. Neuron 45, 715-726.

Petralia RS, Wang YX, Singh S, Wu C, Shi L, Wei J, Wenthold RJ. (1997). A monoconal antibody shows discrete cellular and subcellular localizations of mGluR1 alpha metabotropic glutamate receptors. J Chem Neuroanat 13:77–93.

Petzold A. (2005). Neurofilament phosphoforms: surrogate markers for for axonal injury, degeneration and loss. J Neurol Sci. 15, 233(1-2):183-98

Pierozan P, Zamoner A, Soska AK, De Lima BO, Reis KP, Zamboni F, Wajner M, Pessoa-Pureur R. (2012) Signaling mechanisms downstream of quinolinic acid

targeting the cytoskeleton of rat striatal neurons and astrocytes. Exp Neurol. 233(1):391-9.

Pierozan P, Zamoner A, Soska AK, Silvestrin RB, Loureiro SO, Heimfarth L, Mello e Souza T, Wajner M, Pessoa-Pureur R. (2010). Acute intrastriatal administration of quinolinic acid provokes hyperphosphorylation of cytoskeletal intermediate filament proteins in astrocytes and neurons of rats. Exp Neurol. 224(1):188-96

Pin JP, Duvoisin R. (1995) The metabotropic glutamate receptors: structure and functions. Neuropharmacology. 34(1):1-26.

Pinton, S., Luchese, C., and Nogueira, C.W. (2011a). Comparison of the antioxidant properties and the toxicity of p,p'-dichlorodiphenyl ditelluride with the parent compound, diphenyl ditelluride. Biol Trace Elem Res 139, 204-216.

Pinton, S., Luchese, C., Stangherlin, E.C., and Nogueira, C.W. (2011b). Acute exposure to diphenyl ditelluride causes oxidative damage in rat lungs. Ecotoxicol Environ Saf 74, 521-526.

Polissidis A., Chouliara O., Galanopoulos A., Rentesi G., Dosi M., Hyphantis T., Marselos M., Papadopoulou-Daifoti Z., Nomikos G.G., Spyraki C., Tzavara E.T., Antoniou K. (2010). Individual differences in the effects of cannabinoids on motor activity, dopaminergic activity and DARPP-32 phosphorylation in distinct regions of the brain. Int J Neuropsychopharmacol. 13,1175–1191

Puntel, R.L., Roos, D.H., Paixao, M.W., Braga, A.L., Zeni, G., Nogueira, C.W., and Rocha, J.B. (2007). Oxalate modulates thiobarbituric acid reactive species (TBARS) production in supernatants of homogenates from rat brain, liver and kidney: effect of diphenyl diselenide and diphenyl ditelluride. Chem Biol Interact 165, 87-98.

Purves, D.; Augustine, G.J.; Fitzpatrick, D.; Katz, L.C.; Lamantia, A.S.; Mcnamara, J.O., Williams, S.M. (2005) Transdução intracelular de sinal. In: Purves, D., Augustine, G.J., Fitzpatrick, D., Katz, L.C., LaMantia, A.S. & McNamara, J.O. Neurociências. 2.ed. Porto Alegre: Artmed, pp 165-185.

Ralton JE, Lu X, Hutcheson AM, Quinlan RA. (1994). Identification of two N-terminal non-alpha-helical domain motifs important in the assembly of glial fibrillary acidic protein. J Cell Sci. 107 (Pt 7):1935-48.

Ram K. Sihag, S., Ralph , Nixon S (1991). Identification of Ser-55 as a Major Protein Kinase A Phosphorylation Site on the 70-kDa Subunit of Neurofilaments. J Biol Chem. 5,266(28):18861-7.

RamaRao G, Bhattacharya BK. (2012) Multiple signal transduction pathways alterations during nerve agent toxicity. Toxicol Lett. 5;208(1):16-22. Review.

RamaRao, G., Waghmare, C., Srivastava, N., Bhattacharya, B.K. (2011a). Regional alterations of JNK3 and CaMKII alpha subunit expression in the rat brain after soman poisoning. Hum. Exp. Toxicol. 30 (6), 448–459.

RamaRao, G., Waghmare, C.K., Gupta, A.K., Bhattacharya, B.K. (2011b). Soman induced alterations of protein kinase C isozymes expression in five discrete areas of the rat brain. Drug Chem. Toxicol. 34 (3), 221–232.

Rameau GA, Chiu LY , Ziff EB. Bidirectional regulation of neuronal nitric-oxide synthase phosphorylation at Serine 847 by the N-methyl- D-aspartate receptor . J Biol Chem 2004; 279: 14307–14.

Ramin M, Azizi P, Motamedi F, Haghparast A, Khodagholi F (2011).. Inhibition of JNK phosphorylation reverses memory deficit induced by β-amyloid (1-42) associated with decrease of apoptotic factors. Behav Brain Res. 1;217(2):424-31

Rang, H. P., Dale, M. M, Ritter, J. M.,Flower R.J. (2008), Farmacologia. 6.ed. Rio de Janeiro: Guanabara Koogan S.A., 2008 p 284. cap. 33.

Rawlins, F.A. (1971) Smith M.E. Myelin synthesis in vitro: a comparative study of central and peripheral nervous tissue. J. Neurochem., 18, pp. 1861–1870.

Riccio A, Ahn S, Davenport CM, Blendy JA, Ginty DD. (1999). Mediation by a CREB family transcription factor of NGF-dependent survival of sympathetic neurons. Science, 286:2358–61.

Rice, D., Barone, S. (2000) Critical periods of vulnerability for the developing nervous system: evidence from humans and animal models. Environ. Health Perspect. 108, 511–533.

Riederer BM. (1992). Differential phosphorylation of some proteins of the neuronalcytoskeleton during brain development. Histochem J. 24:783-90.

Roberts PJ, Der CJ. (2007) Targeting the Raf-MEK-ERK mitogen-activated protein kinase cascade for the treatment of cancer. Oncogene 26:3291–3310.

Rockwell P., Martinez J., Papa L. and Gomes E. (2004) Redox regulates COX-2 upregulation and cell death in the neuronal response to cadmium. Cell. Signal. 16, 343–353.

Roman, S.S., Nava, A., Favero, A.M., Weis, S.N., Zeni, G., Rocha, J.B., and Nogueira, C.W. (2007). Diphenyl ditelluride effect on embryo/fetal development in mice: interspecies differences. Toxicology 231, 243-249.

Rossato, J.I., Ketzer, L.A., Centuriao, F.B., Silva, S.J., Ludtke, D.S., Zeni, G., Braga, A.L., Rubin, M.A., and Rocha, J.B. (2002). Antioxidant properties of new chalcogenides against lipid peroxidation in rat brain. Neurochem Res 27, 297-303.

Rossi, D. Sorrentino. V. (2002) Molecular genetics of ryanodine receptors Ca2+-release channels. Cell Calcium, 32, pp. 307–319

Rothstein, J.D. Dykes-Hoberg, M. Pardo, C.A. Bristol, L.A Jin, L.. Kuncl, R.W. Kanai, Y. Hediger, M.A.Wang, Y P. Schielke, J., Welty, D.F. (1996). Knockout of glutamate transporters reveals a major role for astroglial transport in excitotoxicity and clearance of glutamate. Neuron. 16(3):675-86.

Roy S, Hardej D. Tellurium tetrachloride and diphenyl ditelluride cause cytotoxicity in rat hippocampal astrocytes. Food Chem Toxicol. 2011, 49(10):2564-74

Russel, J.B. (1992) Química Geral. 2 ed. São Paulo: Makron Books, v. 2, pp. 1092.

Said G., Duckett S. (1981) Tellurium-induced myelinopathy in adult rats Muscle Nerve, 4 pp. 319–325

Said, G.. Duckett, S. Sauron B. (1981) Proliferation of Schwann cells in tellurium-induced demyelination in young rats. A radioautographic and teased nerve fiber study. Acta Neuropathol. (Berl.), 155, pp. 173–179

Saijoh K, Fukunaga T, Katsuyama H, Lee MJ, Sumino K. (1993) Effects of methylmercury on protein kinase A and protein kinase C in the mouse brain. Environ Res. 63(2):264-73.

Sanchez, C., Diaz-Nido, J., and Avila, J. (2000). Phosphorylation of microtubule-associated protein 2 (MAP2) and its relevance for the regulation of the neuronal cytoskeleton function. Prog Neurobiol 61, 133-168.

Sanelli,T.,. Ge, W. Leystra-Lantz C,. Strong M.J (2007) Calcium mediated excitotoxicity in neurofilament aggregate-bearing neurons in vitro is NMDA receptordependant, J. Neurol. Sci. 256, 39–51.

Sarkar S, Korolchuk V, Renna M, Winslow A, Rubinsztein DC (2009). Methodological considerations for assessing autophagy modulators: a study with calcium phosphate precipitates. Autophagy 5:307–13.

Sasaki, T., Gotow, T., Shiozaki, M., Sakaue, F., Saito, T., Julien, J.P., Uchiyama, Y., and Hisanaga, S. (2006). Aggregate formation and phosphorylation of neurofilament-L Pro22 Charcot-Marie-Tooth disease mutants. Hum Mol Genet 15, 943-952.

Savegnago, L., Borges, V.C., Alves, D., Jesse, C.R., Rocha, J.B., and Nogueira, C.W. (2006). Evaluation of antioxidant activity and potential toxicity of 1-buthyltelurenyl-2-methylthioheptene. Life Sci 79, 1546-1552.

Schaumburg, H.H., Powers, J.M., Raine, C.S., Suzuki, K., and Richardson, E.P., Jr. (1975). Adrenoleukodystrophy. A clinical and pathological study of 17 cases. Arch Neurol 32, 577-591.

Schiar VP, Dos Santos DB, Lüdtke DS, Vargas F, Paixão MW, Nogueira CW, Zeni G, Rocha JB. (2007). Screening of potentially toxic chalcogens in erythrocytes. Toxicol In Vitro. ;21(1):139-45.

Schiffmann SN, Desdouits F, Menu R, Greengard P, Vincent JD, Vanderhaeghen JJ, Girault JA. (1998). Modulation of the voltage-gated sodium current

in rat striatal neurons by DARPP-32, an inhibitor of protein phosphatase. Eur J Neurosci. 10:1312–1320

Schubert V, Da Silva JS, Dotti CG. (2006) Localized recruitment and activation of RhoA underlies dendritic spine morphology in a glutamate receptor-dependent manner. J Cell Biol. 30;172(3):453-67.

Schwab Y, Mouton J, Chasserot-Golaz S, Marty I, Maulet Y,Jover E. (2001). Calcium-dependent translocation of synaptotagmin to the plasma membrane in the dendrites of developing neurones. 30;96(1-2):1-13.

Schwartz, D.A.. Rubin, C.S. (1983) Regulation of cAMP-dependent protein kinase subunit levels in Friend erythroleukemic cells, J. Biol. Chem. 258, 777-784.

Schwarzschild, M.A., Cole, R.L., Hyman, S.E. (1997). Glutamate, but not dopamine, stimulates stress-activated protein kinase and AP-1-mediated transcription in striatal neurons. J. Neurosci. 17, 3455–3466.

Seaton G., Hogg E.L., Jo J., Whitcomb D.J., Cho K. (2011). Sensing change: the emerging role of calcium sensors in neuronal disease. Semin Cell Dev Biol. 22, 530-5.

Seeburg, P. H. (1993) The molecular biology of mammalian gluta-mate receptor channels. Trends Neurosci. 16, 359-365.

Segovia G, Porras A, Del Arco A, Mora F. (2001) Glutamatergic neurotransmission in aging: a critical perspective. Mech Ageing Dev. 122(1):1-29. Review.

Segura Torres, J.E., Chaparro-Huerta, V., Rivera Cervantres, M.C., Montes-Gonzalez, R., Flores Soto, M.E., Beas-Zarate, C. (2006). Neuronal cell death due to

glutamate excitotocity is mediated by p38 activation in the rat cerebral cortex. Neurosci. Lett. 403, 233–238.

Seifert, G.; Schilling, K; Steinhäuser, C. (2006). Astrocyte dysfunction in neurological disorders: a molecular perspective. Nature review/Naeuroscience V7 194-207.

Sekimata M, Tsujimura K, Tanaka J, Takeuchi Y, Inagaki N, Inagaki M. (1996). Detection of protein kinase activity specifically activated at metaphase-anaphase transition. J Cell Biol. 132(4):635-41.

Shcheglovitov A, Vitko I, Lazarenko RM, Orestes P, Todorovic SM, Perez-Reyes E. (2012). Molecular and biophysical basis of glutamate and trace metal modulation of voltage-gated Ca(v)2.3 calcium channels. J Gen Physiol. 139(3):219-34.

Sihag RK, Inagaki M, Yamaguchi T, Shea TB, Pant HC. (2007). Role of phosphorylation on the structural dynamics and function of types III and IV intermediate filaments. Exp Cell Res. 10;313(10):2098-109.

Sihag RK, Jaffe H, Nixon RA, Rong X. (1999). Serine-23 is a major protein kinase A phosphorylation site on the amino-terminal head domain of the middle molecular mass subunit of neurofilament proteins. J Neurochem. 72(2):491-9.

Sihag RK, Nixon RA. (1990) Phosphorylation of the amino-terminal head domain of the middle molecular mass 145-kDa subunit of neurofilaments. Evidence for regulation by second messenger-dependent protein kinases. J Biol Chem. 5, 265(7):4166-71.

Sihag, R.K., and Nixon, R.A. (1991). Identification of Ser-55 as a major protein kinase A phosphorylation site on the 70-kDa subunit of neurofilaments. Early turnover during axonal transport. J Biol Chem 266, 18861-18867.

Siman R, Noszek JC, Kegerise C. (1989) Calpain I activation is specifically related to excitatory amino acid induction of hippocampal damage. J Neurosci. 9:1579–90.

Sofroniew, M.V. (2009). Molecular dissection of reactive astrogliosis and glial scar formation. Trends Neurosci. 32, 638–647.

Son YO, Lee JC, Hitron JA, Pan J, Zhang Z, et al. (2010) Cadmium inducesintracellular Ca2+- and H2O2-dependent apoptosis through JNK- and p53-mediated pathways in skin epidermal cell line. Toxicol Sci 113: 127–137.

Souza A.C., Stangherlin E.C., Ardais A.P., Nogueira C.W. (2010). Diphenyl diselenide and diphenyl ditelluride: neurotoxic effect in brain of young rats, in vitro. Mol Cell Biochem. 340(1-2):179-85.

Squire, L.R., Berg, D., Bloom, F.E, Lac, S.D., Ghosh, A., Spitzer, N.C. (2008) Synapses Elimination. In: Fundamental Neuroscience, 3 ed. London. Elsevier, pp 469-491.

Squire, LR; Berg, D; Bloom, FE; Lac, Sd; Ghosh, A; Spitzer, NC. (200* Motor System. In: Fundamental Neuroscience, 3 ed. London. Elsevier, pp 666-770.

Sredni, B. (2011). Immunomodulating tellurium compounds as anti-cancer agents. Semin Cancer Biol 22, 60-69.

Sredni-Kenigsbuch D, Shohat M, Shohat B, Ben-Amitai D, Chan CC, David M.(2008). The novel tellurium immunomodulator AS101 inhibits interleukin-10 production and p38 MAPK expression in atopic dermatitis. J Dermatol Sci. 50(3):232-5.

Stangherlin E.C., Ardais A.P., Rocha J.B., Nogueira C.W. (2009b) Exposure to diphenyl ditelluride, via maternal milk, causes oxidative stress in cerebral cortex, hippocampus and striatum of young rats. Arch Toxicol. 83(5):485-91.

Stangherlin E.C., Favero A.M., Zeni G., Rocha J.B., Nogueira C.W. (2005) Teratogenic vulnerability of Wistar rats to diphenyl ditelluride. Toxicol. 14, 207:231-9.

Stangherlin E.C., Rocha J.B., Nogueira C.W. (2009a) Diphenyl ditelluride impairs short-term memory and alters neurochemical parameters in young rats. Pharmacol. Biochem. Behav. 91(3):430-5.

Stangherlin, E.C., Favero, A.M., Weis, S.N., Zeni, G., Rocha, J.B., and Nogueira, C.W. (2006). Assessment of reproductive toxicity in male rats following acute and sub-chronic exposures to diphenyl diselenide and diphenyl ditelluride. Food Chem Toxicol 44, 662-669.

Steinert, P.M., and Roop, D.R. (1988). Molecular and cellular biology of intermediate filaments. Annu Rev Biochem 57, 593-625.

Stevenson, A.. Yates D.M, Manser C.,. De Vos, K.J Vagnoni A., Leigh P.N. McLoughlin, , D.M., Miller C.C. (2009) Riluzole protects against glutamate-induced slowing of neurofilament axonal transport, Neurosci. Lett. 454 161–164.

Strack, S., Westphal, R.S., Colbran, R.J., Ebner, F.F., Wadzinski, B.E. (1997). Protein serine/threonine phosphatase 1 and 2A associate with and dephosphorylate neurofilaments. Brain Res Mol Brain Res 49, 15-28.

Strack, S., Westphal, R.S., Colbran, R.J., Ebner, F.F., and Wadzinski, B.E. (1997). Protein serine/threonine phosphatase 1 and 2A associate with and dephosphorylate neurofilaments. Brain Res Mol Brain Res 49, 15-28.

Su, W., Chen, H.B., Li, S.H., Wu, D.Y. (2012). Correlational study of the serum levels of the glial fibrillary acidic protein and neurofilament proteins in Parkinson's disease patients. Clin Neurol Neurosurg 114, 372-375.

Surmeier DJ, Guzman JN, Sanchez-Padilla J (2010) Calcium, cellular aging, andselective neuronal vulnerability in Parkinson's disease. Cell Calcium 47:175–182.

Takemura, M, Nishiyama, H, Itohara, S. (2002). Distribution of phosphorylated glial fibrillary acidic protein in the mouse central nervous system. Genes Cells 7, 295–307.

Tanti JF, Jager J. (2009) Cellular mechanisms of insulin resistance: role of stress-regulated serine kinases and insulin receptor substrates (IRS) serine phosphorylation. Curr Opin Pharmacol. 2009;9(6):753-62.

Taylor, A. (1996). Biochemistry of tellurium. Biol Trace Elem Res. 55: 231-239.

Tepper JM, Sharpe NA, Koós TZ, Trent F. (1998) Postnatal development of the rat neostriatum: electrophysiological, lightand electron-microscopic studies. Dev Neurosci 20:125– 45.

Tidyman W.E, Rauen K.A. The RASopathies: developmental syndromes of Ras/MAPK pathway dysregulation. Curr. Opin. Genet. Dev. 19(3):230-6, 2009.

Toivola, D.M., Tao, G.Z., Habtezion, A., Liao, J., and Omary, M.B. (2005). Cellular integrity plus: organelle-related and protein-targeting functions of intermediate filaments. Trends Cell Biol 15, 608-617.

Torii S., Yamamoto T., Tsuchiya Y., Nishida E. (2006) ERK MAP kinase in G cell cycle progression and cancer. Cancer Sci., 97 pp. 697–702.

Tsujimura K, Tanaka J, Ando S, Matsuoka Y, Kusubata M, Sugiura H, Yamauchi T, Inagaki M. (1994). Identification of phosphorylation sites on glial fibrillary acidic protein for cdc2 kinase and Ca(2+)-calmodulin-dependent protein kinase II. J Biochem. 116(2):426-34.

Tsuruta, D., Jones, J.C. (2003). The vimentin cytoskeleton regulates focal contact size and adhesion of endothelial cells subjected to shear stress. J Cell Sci 116, 4977-4984.

Tymianski M, Charlton MP, Carlen PL, Tator CH. (1993) Source specificity of earlycalcium neurotoxicity in cultured embryonic spinal neurons. J Neurosci 13:2085–104.

Veeranna, K.T, Boland B., Odrljin T., Mohan P., Basavarajappa B.S., Peterhoff C., Cataldo A., Rudnicki A., Amin N., Li B.S., Pant H.C., Hungund B.L., Arancio O., Nixon R.A. (2004). Calpain mediates calcium-induced activation of the erk1,2 MAPK pathway and cytoskeletal phosphorylation in neurons: relevance to Alzheimer's disease. Am J Pathol. 165: 795-805, 2004.

Wagner, O.I, Lifshitz, J., Janmey, P.A., Linden, M., Mcintosh, T.K., Leterrier, J.F. (2003) Mechanisms of mitochondria-neurofilament interactions. J. Neurosci., 23: 9046-58.

Wagner-Recio, M., Toews, A.D., and Morell, P. (1991). Tellurium blocks cholesterol synthesis by inhibiting squalene metabolism: preferential vulnerability to this metabolic block leads to peripheral nervous system demyelination. J Neurochem 57, 1891-1901.

Walbran, B.B., and Robins, E. (1978). Effects of central nervous system accumulation of tellurium on behavior in rats. Pharmacol Biochem Behav 9, 297-300.

Wang XM, Liu WJ, Zhang R, Zhou YK. (2012) Effects of exposure to low-level lead on spatial learning and memory and the expression of mGluR1, NMDA receptor in different developmental stages of rats Toxicol Ind Health. 2012 Feb 23..

Widmann, C., S. Gibson, M. B. Jarpe, and G. L. Johnson. (1999). Mitogen activated protein kinase: conservation of a three-kinase module from yeast. Physiol Rev. 1999 Jan;79(1):143-80.

Widy-Tyszkiewicz, E., Piechal, A., Gajkowska, B., and Smialek, M. (2002). Tellurium-induced cognitive deficits in rats are related to neuropathological changes in the central nervous system. Toxicol Lett 131, 203-214.

www.mie.utoronto.ca/labs/lcdlab/biopic, acessado em 23.02.2011.

Xu J., Yan C.H., Wu S.H., Yu X.D., Yu X.G., Shen X.M. (2007). Developmental lead exposure alters gene expression of metabotropic glutamate receptors in rat hippocampal neurons. Developmental lead exposure alters gene expression of metabotropic glutamate receptors in rat hippocampal neurons. Neurosci Lett. 21;413(3):222-6.

Xu J., Yan C.H., Yang B., Xie H.F., Zou X.Y., Zhong L., Gao Y., Tian Y., Shen X.M. (2009). The role of metabotropic glutamate receptor 5 in developmental lead neurotoxicity. Toxicol Lett. 15;191(2-3):223-30.

Xu Z.S., Liu W.S., Willard M.B. (1992). Identification of six phosphorylation sites in the COOH-terminal tail region of the rat neurofilament protein. M. J Biol Chem, 267:4467–4471.

Xu, B., Chen, S., Luo, Y., Chen, Z., Liu, L., Zhou, H., Chen, W., Shen, T., Han,X., Chen, L., Huang, S. (2011). Calcium Signaling Is Involved in Cadmium-

InducedvNeuronal Apoptosis via Induction of Reactive Oxygen Species and Activation of MAPK/mTOR Network . PLoS One. 22;6(4):e19052.

Xu, J., Zhu, Y., Contractor, A., Heinemann, S.F. (2009). mGluR5 has a critical role in inhibitory learning. J. Neurosci. 29, 3676–3684.

Yabe, J.T., Chylinski, T., Wang, F.-S., Pimenta, A., Kattar, S.D., Linsley, M.-D., Chan, W.K.-H. & Shea, T.B. (2001a) Neurofilaments consist of distinct populations that can be distinguished by C-terminal phosphorylation, bundling and axonal transport rate in growing axonal neurites. J. Neurosci., 21, 2195–2205.

Yabe, J.T., Wang, F.-S., Chylinski, T., Katchmar, T. & Shea, T.B. (2001b) Selective accumulation of the high molecular weight neurofilament subunit within the distal region of growing axonal neurites. Cell Motil. Cytoskel., 50, 1–12.

Yakovlev AG, Faden AI. (2001) Caspase-dependent apoptotic pathways in CNS injury. Mol Neurobiol. 24(1-3):131-44. Review.

Yan Z, Hsieh-Wilson L, Feng J, Tomizawa K, Allen PB, Fienberg AA, Nairn AC, Greengard P. (1999). Protein phosphatase 1 modulation of neostriatal AMPA channels: regulation by DARPP-32 and spinophilin .Nat Neurosci 2:13–17.

Yang, X., Wang, J., Liu, C., Grizzle, W.E., Yu, S., Zhang, S., Barnes, S., Koopman, W.J., Mountz, J.D., Kimberly, R.P., and Zhang, H.G. (2005). Cleavage of p53-vimentin complex enhances tumor necrosis factor-related apoptosis-inducing ligand-mediated apoptosis of rheumatoid arthritis synovial fibroblasts. Am J Pathol 167, 705-719.

Yarema, M.C., Curry, S.C. (2005). Acute tellurium toxicity from ingestion of metal-oxidizing solutions. Pediatrics 116, e319-321.

Yasui Y, Amano M, Nagata K, Inagaki N, Nakamura H, Saya H, Kaibuchi K, Inagaki M. (1998) Roles of Rho-associated kinase in cytokinesis; mutations in Rho-

associated kinase phosphorylation sites impair cytokinetic segregation of glial filaments. J Cell Biol. 30;143(5):1249-58.

Yuan, A., Rao, M.V., Sasaki, T., Chen, Y., Kumar, A., Veeranna, Liem, R.K., Eyer, J., Peterson, A.C., Julien, J.P., and Nixon, R.A. (2006). Alpha-internexin is structurally and functionally associated with the neurofilament triplet proteins in the mature CNS. J Neurosci 26, 10006-10019.

Zamoner, A., Heimfarth, L., Oliveira Loureiro, S., Royer, C., Mena Barreto Silva, F. R., and Pessoa-Pureur, R. (2008) Nongenomic actions of thyroxine modulate intermediate filament phosphorylation in cerebral cortex of rats. Neuroscience 156, 640–652

Zeni, G.R., Barros, O., Do Rego, S., Moro, A.V., Braga, A.L., Peppe, C. (2003). Hydroteluration of Aminoalkynes. Chem Commun (Camb). 7;(11):1258-9..

Zeni, G.R., Formiga, H., Comasseto, J.V. (2000). Improved procedure for the hydrotelluration of alkynes. Tetrahedron Lett. 41,

Zeni, G.R., Stracke, M.P., Nogueira, C.W., Braga, A.L., Menezes, P.H., Stefani, H.A. (2004). Hydroselenation of alkynes by lithium butylselenolate: an approach in the synthesis of vinylic selenides. 1;6(7):1135-8..

Zheng Z., Keifer J. (2009). PKA has a critical role in synaptic delivery of GluR1- and GluR4-containing AMPARs during initial stages of acquisition of in vitro classical conditioning. J Neurophysiol. 101(5):2539-49.